



REPORT NO. RP-SR-0002

PHOEBUS - 2 MATERIALS FINAL REPORT



NUCLEAR ROCKET OPERATIONS

CONTRACT SNPC-35

SEPTEMBER 1967

**CLASSIFICATION CATEGORY**

**UNCLASSIFIED**

*L. J. Glasier*  
CLASSIFYING OFFICER

*9-29-67*  
DATE

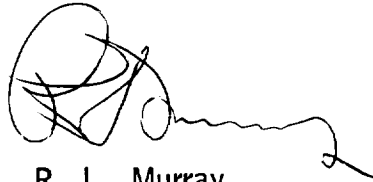
**AEROJET - GENERAL CORPORATION**  
A SUBSIDIARY OF THE GENERAL TIRE & RUBBER COMPANY



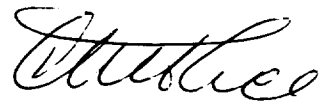
PRECEDING PAGE BLANK NOT FILMED.

REPORT NO. RP-SR-0002

PHOEBUS - 2 MATERIALS FINAL REPORT

A handwritten signature in black ink, appearing to read 'R. L. Murray', with a long, wavy tail extending to the right.

R. L. Murray  
Project Manager - Phoebus  
Nuclear Rocket Operations

A handwritten signature in black ink, appearing to read 'C. M. Rice', written in a cursive style.

C. M. Rice  
Program Manager  
Nuclear Rocket Operations

## ACKNOWLEDGEMENTS

The following participated in the Phoebus-2 materials development program and contributed to this report: F. J. Flens C. W. Fletcher, L. F. Glasier, D. M. Hamilton, I. M. Rehn, and H. W. Spaletta. Production and printing of this report was under the direction of R. L. Campbell.



## ABSTRACT

The report documents, in abbreviated form, all metallurgical testing conducted in support of the Phoebus 2 Nozzle Program.

The tensile properties of forgings, strip, weldments, and brazements are presented as individual test data and as statistical means with sigma limits through the temperature range of -423 to 1800°F. The mechanical properties of shear strength, bearing strength, low-cycle fatigue, and thermal cycling are also presented. In addition, the manufacturing and fabrication processes are presented from raw material melting through fabrication of individual hardware components. Metallurgical analysis of thermal treatments and processing are also provided.



CONTENTS (cont.)

	<u>Page</u>
5.4.6 Cleaning	36
5.4.7 Weld Equipment	36
5.4.8 Tooling	36
5.4.9 Heat Treatment	38
5.4.10 Schedule	38
5.5 Welding-Dissimilar Metals	39
5.6 Furnace Brazing	39
6.0 Specifications	40
7.0 Physical Properties	41
7.1 Moduli: Tension, Shear, and Tangent	41
7.2 Thermal Expansion	51
7.3 Thermal Diffusivity (Conductivity)	55
8.0 Mechanical Properties	63
8.1 Specimens - Location, Orientation and Configuration	69
8.2 Statistical Tensile Test Plans	69
8.2.1 Ring Forgings	76
8.2.2 Welded Ring Forgings	81
8.2.3 Coolant Tube Strip	83
8.3 Actual Tensile Properties	83
8.3.1 Ring Forgings	83
8.3.2 Welded Ring Forgings	94
8.3.3 Coolant Tube Strip	94
8.4 0.3% and 0.4% Offset Yield Strengths - Ring Forgings	94
8.5 Shear Strength	109
8.6 Bearing Strength	109
8.7 Compression Field Strength	114
8.8 Stress-Strain Curves	119
8.9 Low by C/P Fatigue Testing	123
9.0 Braze Joint Mechanical Properties	136
9.1 Tensile Tests	136

CONTENTS

	<u>Page</u>
1.0 Introduction	1
2.0 Physical Metallurgy	3
2.1 Chemistry	3
2.1.1 General	3
2.1.2 Aluminum/Titanium	4
2.1.3 Boron	4
2.1.4 Heat Analyses	5
2.2 Microstructure	8
2.3 Thermal Treatments	8
2.3.1 As Received	8
2.3.2 Post-Weld and Post-Forming	8
2.3.3 Brazing	9
3.0 Melting	12
4.0 Primary Fabrication	13
4.1 Nozzle Forgings	13
4.2 Development Program Forgings	13
4.3 Forgings of Improved Strength	23
4.4 Strip	23
4.5 Wire	23
5.0 Secondary Fabrication	25
5.1 Conventional Machining	25
5.1.1 Recommended Cutting Conditions	25
5.2 Electric Discharge Machining	28
5.3 Strip Forming and Welding	29
5.4 Welding of Nozzle and Development Forgings	32
5.4.1 Process	32
5.4.2 Joint Design	32
5.4.3 Wire	32
5.4.4 Operator Qualifications	35
5.4.5 Inspection Requirements	35

CONTENTS (cont.)

	<u>Page</u>
9.2 Shear Tests	150
9.3 Braze Alloy Tensile Tests	164
9.4 Braze-Alloy Diffusion	165
9.5 Grooved Specimen Tensile Testing	180
10.0 Effects of Various Thermal Treatments	183
10.1 Post-Weld Annealing	183
10.2 Cooling Rate and Time at Temperature	183
10.3 Intermediate Low Temperature Annealing	185
10.4 Effect of Extra Brazing Cycle	185
11.0 Thermal Fatigue Testing	188

APPENDIXES

- A Development of Improved Strength Large Hastelloy X Forgings
- B Hastelloy X Coolant Tube Investigation
- C Torus Dissimilar Metal Welding Evaluation
- D To Investigate the Capability of Hastelloy X Tubing to Withstand Thermal Cycling Between 1600°F and Cryogenic Temperature
- E Thermal Fatigue Analysis of a Cryogenically Cooled Rocket Nozzle

## TABLES

<u>Number</u>		<u>Page</u>
2.1	Hastelloy X Nominal Chemical Composition	3
2.2	Boron Analysis of Nickel Base Alloys	6
2.3	Chemical Analysis Data for Hastelloy X Forgings, Sheet, and Weld Wire	7
2.4	Summary of Average Tensile Properties of Post-Weld Annealed and Brazed Hastelloy X Forgings	10
2.5	Tensile Properties of Annealed and Brazed Hastelloy X Forgings	11
4.1	Summary of Average Tensile Properties of Annealed Forgings of Hastelloy X	17
4.2	Tensile Properties of Annealed Forgings of Hastelloy	19
7.1	Dynamic Moduli of Hastelloy X Ring Forging, Heat 261-5-4000	43
7.2	Modulus of Elasticity (Static) and Tangent Modulus (0.2% Offset) Hastelloy X, Heat 261-5-4000 (Braze Forging)	44
7.3	Modulus of Elasticity (Static) and Tangent Modulus (0.2% Offset) Hastelloy X, Heat 261-5-4001 (Braze Forging)	47
7.4	Mean Coefficient of Thermal Expansion, Braze Ring Forging (AGC 90056), Heat 261-5-4000	56
7.5	Thermal Conductivity, Diffusivity, and Specific Heat, Braze Forging, Heat 261-5-4000	58
8.1	Summary of Average Tensile Properties of Hastelloy X Annealed Plate and Strip (AGC 90057) Utilized in Developmental Programs	64
8.2	Tensile Properties of Annealed Plate, Sheet, and Strip (AGC 90057) and Bar (AGC 90056) Utilized in Developmental Programs	65
8.3	Summary of Average Tensile Properties of Annealed Weldments of Hastelloy X Forgings (AGC 90056) and Plate (AGC 90057)	67
8.4	Tensile Properties and Hardness of Annealed Weldments of Hastelloy X Forgings (AGC 90056) and Plate (AGC 90057)	68
8.5	Statistical Test Plans for Ring Forgings	74
8.6	Statistical Test Plan for Welded Ring Forging, Heat 261-5-4000	75
8.7	Hastelloy X Forging (AGC 90056) Statistical Tensile (Unnotched) Data Versus Temperature	78
8.8	Statistical Tensile (Unnotched) Properties and Test Variability vs Temperature for Axial and Tangential Properties of Hastelloy X Forgings, Heats 261-5-4000 and 261-5-4001	79

TABLES (cont.)

<u>Number</u>		<u>Page</u>
8.9	Statistical Unnotched and Notched Tensile Strength of Hastelloy X Forgings, Mean Values and Variability Versus Temperature, Heats 261-5-4000 and 261-5-4001	80
8.10	Hastelloy X Welded Forging Tensile Property Statistical Mean Values and Test Variability Versus Temperature, Unnotched and Notched	82
8.11	Hastelloy X Strip Tensile Property Statistical Mean Values and Test Variability Versus Temperature, Unnotched and Notched	84
8.12	Tensile Properties (Unnotched) from Hastelloy X Ring Forging, Heat 261-5-4000	85
8.13	Tensile Properties (Unnotched) from Hastelloy X Forging, Heat 261-5-4001	89
8.14	Tensile Properties (Notched) from Hastelloy X Ring Forgings (AGC 90056), Heats 261-5-4000 and 261-5-4001	93
8.15	Tensile Properties of Welded Hastelloy X Ring Forging, Heat 261-5-4000, Welded With Heat 260-5-2784 Wire	97
8.16	Tensile Properties of Welded Hastelloy X Ring Forging, Heat 261-5-4001, Welded With Heat 260-5-2783 Wire	97
8.17	Tensile Properties of Welded Hastelloy X Ring Forging, Heat 260-5-2813, Welded With Heat 261-5-4003 Wire	98
8.18	All-Weld Metal Tensile Properties of Hastelloy X Ring Forging, Heat 261-5-4000, Welded With Heat 260-5-2784 Wire	
8.19	All-Weld Metal Tensile Properties of Hastelloy X Ring Forging, Heat 261-5-4001, Welded With Heat 260-5-2783 Wire	100
8.20	Tensile Properties (Unnotched) for 0.012-Inch Thick Coolant Tube Strip	101
8.21	Tensile Properties (Notched) for 0.012-Inch Thick Coolant Tube Strip	102
8.22	0.3% and 0.4% Offset Yield Strength of Hastelloy X Ring Forging, Heat 261-5-4000	103
8.23	0.3% and 0.4% Offset Yield Strength of Hastelloy X Ring Forging, Heat No. 261-5-4001	106
8.24	Ultimate Shear Strength of Hastelloy X Ring Forging, Heat 261-5-4000	112
8.25	Bearing Strength of Sheet and Strip, Heat 261-5-4000	113
8.26	Compression Tests of Hastelloy X Ring Forgings, Heats 261-5-4000 and 260-5-2813	116

TABLES (cont.)

<u>Number</u>		<u>Page</u>
9.1	Tensile Test Results for 0.25-Inch Round Hastelloy X Bar Stock	137
9.2	Tensile Test Results for 0.250-Inch Round Hastelloy X Bar Stock Exposed to Braze Cycle per AGC 90169 (Forging Surfaces Nickel Plated)	142
9.3	Tensile Test Results for 0.012-Inch Thick Hastelloy X Strip Braze-Alloy Diffusion Specimens	145
9.4	Tensile Test Results for Simulated Seal-Joint Specimens Exposed to Multiple Braze Cycles	152
9.5	Tensile Test Results for Simulated Seal-Joint Specimens Exposed to Single Braze Cycle	154
9.6	Shear Test Results for Hastelloy X Brazed With Nioro, Palniro-7, and Nicoro-80	159
9.7	Tensile Strength of Braze Alloys Nioro, Palniro-7, and Nicoro-80	164
9.8	Braze-Alloy Diffusion Study Test Plan for Hastelloy X	167
10.1	Effect of Cooling Rate on Room Temperature Tensile Properties of Hastelloy X Ring Forgings	184
10.2	Effect of Intermediate Annealing on Hastelloy X Ring Forging, Room Temperature Tensile Properties	186
10.3	Effect of Brazing Cycles on Hastelloy X Tensile Properties	187
11.1	Thermal Fatigue Tests of Flat Tubular Hastelloy X Specimens, Heat 260-6-4002	189



## FIGURES

<u>Number</u>		<u>Page</u>
4.1	Forging Operations	14
4.2	Convergent Section Forging, P/N 1114856-7	15
4.3	Divergent Section Forging, P/N 1114856-11	16
5.1	Coolant Tube Forming	30
5.2	Coolant Tube Contour Forming	31
5.3	Coolant Tube End-Cap Welding	33
5.4	Typical Double U-Groove Utilized in Nozzle Jacket Welds	34
5.5	Welding Control Panel and Boom in Position for Outside Diameter, Aft-End Weld	37
7.1	Hastelloy X Brazed Forgings (AGC 90056) Design Tensile and Shear Moduli vs Temperature	42
7.2	Hastelloy X Brazed Forgings (AGC 90056) Modulus of Elasticity in Tension, Dynamic Versus Static	52
7.3	Hastelloy X Brazed Forgings (AGC 90056) Tangent Modulus at 0.2% Offset Versus Temperature	53
7.4	Hastelloy X Brazed Forgings (AGC 90056) Mean Coefficient of Thermal Expansion	54
7.5	Hastelloy X Brazed Forging Thermal Conductivity	60
7.6	Hastelloy X Brazed Forging Specific-Heat and Density Values	61
7.7	Hastelloy X Brazed Forging Thermal Diffusivity Values, Heat 261-5-4000 (Source: D. E. Baker and R. E. Nightingale, Battelle, Northwest)	62
8.1	Specimen Layout Plan, Forging Heat 261-5-4000	70
8.2	Tensile Test Specimens Used for Forging and Welded Ring Evaluation	71
8.3	Sample Plan Specimen Layout for Welded Ring Forging, Heat 261-5-4000	72
8.4	Notched and Unnotched Coolant Tube Strip Tensile Specimens	73
8.5	Hastelloy X Forging Design Tensile Strengths vs Temperature	77
8.6	Ultimate Bearing Strength Specimen	110
8.7	Tensile, Shear, and Bearing Strength of Hastelloy X	111
8.8	Bearing-Load Test Specimens from 0.052-Inch Thick Hastelloy X Sheet (Heat 261-5-4000) After Testing	115
8.9	Compression Test Specimens	117

FIGURES (cont.)

<u>Number</u>		<u>Page</u>
8.10	Hastelloy X Typical Stress Strain Curves	120
8.11	Hastelloy X Typical Stress Strain Curves, Partial Elastic Plastic Region	122
8.12	Low-Cycle Fatigue Specimen (Lower) and Original Test Method (Upper)	124
8.13	Low-Cycle Fatigue Test Assembly (Specimen is supported between pins eight inches apart and stressed in bending at the center in both tension and compression)	125
8.14	Unetched, Slightly Enlarged Specimen, Tested at Room Temperature, From Heat 260-5-4001 Showing Location of Fracture (The initial fracture was from the bottom surface. Note localized reduction of area which was present on four surfaces but greatest on edges.)	127
8.15	Typical Load-Deflection Curve, Low-Cycle Fatigue Testing	128
8.16	Hastelloy X Stress Strain Curves	130
8.17	Stress Cycles to Failure of Hastelloy X	131
8.18	Microhardness Profile, Room Temperature and Liquid Nitrogen Tests, Heat 260-5-4001	132
8.19	Microhardness Profile, Room Temperature Test, Heat 260-5-4000	133
8.20	Unetched, Slightly Enlarged Specimen Tested at 320°F, from Heat 260-5-4001 Showing Location of Fracture (Oblique view shows fracture location about 0.2 inch away from loading contact area. Strain gage shows as dark area on left. No significant reduction of area was observed. Initial fracture area was on top surface.)	135
9.1	Standard Round Tensile Specimen	141
9.2	Flat Tensile Specimen	149
9.3	Flat, Simulated Seal-Joint Specimen	151
9.4	Miller-Peaslee Shear Test Specimen	158
9.5	Miller-Peaslee Shear Stress-Strain for Hastelloy X Brazed with Nicro	161
9.6	Miller-Peaslee Shear Stress-Strain for Hastelloy X Brazed with Palniro-7	162
9.7	Miller-Peaslee Shear Stress-Strain for Hastelloy X Brazed with Nicoro-80	163

FIGURES (cont.)

<u>Number</u>		<u>Page</u>
9.8	Braze-Alloy Diffusion Specimen	166
9.9	Gross-Volume Diffusion of Braze Alloys into Hastelloy X Base	168
9.10	Braze-Alloy Diffusion, Palniro-1 Brazed at 2050°F	170
9.11	Braze-Alloy Diffusion, Copper Brazed at 2050°F	171
9.12	Braze-Alloy Diffusion, Palniro-7 Brazed at 1950°F	172
9.13	Braze-Alloy Diffusion, Nicoro Brazed at 2050°F	173
9.14	Braze-Alloy Diffusion, 60 Cu-40 Au Brazed at 1950°F	174
9.15	Braze-Alloy Diffusion, Nioro Brazed at 1800°F	175
9.16	Braze-Alloy Diffusion, Nicoro-80 Brazed at 1750°F	176
9.17	Braze-Alloy Diffusion, Nicoro-80 Brazed at 2050°F	177
9.18	Braze-Alloy Diffusion, Palniro-7 Brazed at 2150°F	178
9.19	Braze-Alloy Diffusion, Nioro Brazed at 2150°F	179
9.20	Grooved Tensile Specimen	181



## 1.0 INTRODUCTION

Hastelloy Alloy X\*, hereafter referred to as Hastelloy X, is a nickel-base alloy with exceptionally good corrosion and oxidation resistance at temperatures to 2100°F, superior strength (when compared to the AISI 300 series stainless steels), good resistance to a radiation environment ( $\alpha$  and n), good fabricative qualities (forming and welding), and good notch-toughness. However, specific and adequate data were not available for design use on large, heavy-wall forgings and thin strip. Also, the effect of the brazing cycle on properties and metallurgical properties was not well known. It was the purpose of the materials development task, therefore, to:

1. Provide mechanical and physical properties for design use on large forgings, thin strip, and weldments.
2. Develop welding procedures for large forgings.
3. Verify suitable brazing-cycle and braze-joint properties.
4. Monitor, guide, and assist in procurement and fabrication of materials and components.

All Hastelloy X for the program was melted by the Stellite Division of Union Carbide Corporation (UCCSD), Kokomo, Indiana. Plate, sheet, and bar stock were provided as mill products from UCCSD. Strip stock was converted by Ulbrich, Inc., Wallingford, Connecticut.\*\* The convergent/divergent nozzle-jacket forgings were produced by the Wyman-Gordon Company, Grafton, Massachusetts. Nozzle-jacket inlet rings were made by Standard Steel Company, Burnham, Pennsylvania, and procured through Wyman-Gordon. All materials were supplied in the solution heat-treated condition (2150°F followed by rapid cooling).

---

\*Trademark, Union Carbide Corporation, Stellite Division

\*\*To establish a second source, a small quantity of strip (Heat 261-5-2813) was produced by the W. B. Driver Co., Newark, New Jersey.

The overall manufacturing cycle required numerous thermal cycles: hence, it was necessary to evaluate their effects. Broadly, the sequence of manufacturing was:

1. Air- or vacuum-induction melted, followed by consumable electrode, vacuum-arc melting.
  
2. Primary Fabrication
  - a. Mill products: Ingot forged to billet, hot rolled/cold rolled and annealed at 2150°F.
  - b. Convergent/divergent/inlet ring: Ingot hot upset, die forged/ring rolled and annealed at 2150°F.
  
3. Secondary Fabrication
  - a. Strip: cold formed and brazed.
  - b. Plate: cold/hot formed, welded, annealed (2080°F), and brazed.
  - c. Forgings: machined, welded, annealed (2080°F), and brazed.

The brazing operation consisted of multiple cycles in a hydrogen atmosphere with controlled heat-up and cool-down at a maximum temperature range of 1725 to 1875°F.\* The process specification controlling the brazing operation is listed in Section 6.0.

---

\*Brazing operation details are classified and not included in this report.

## 2.0 PHYSICAL METALLURGY

### 2.1 CHEMISTRY

#### 2.1.1 General

The nominal chemical composition of commercial Hastelloy X, produced to Aeronautical Material Specifications (AMS), is presented in Table 2.1 with the nominal composition utilized for the Phoebus-2 program.

TABLE 2.1  
NOMINAL CHEMICAL COMPOSITION (%) HASTELLOY X

<u>Spec.</u>	<u>Mo</u>	<u>Cr</u>		<u>Fe</u>		<u>W</u>	<u>Co</u>		
AMS	8.00-10.00	20.50-23.00		17.00-20.00		0.20-1.00	0.50-2.50		
Phoebus	8.00-10.00	20.50-23.00		17.00-20.00		0.20-1.00	0.50-2.50		
	<u>C</u>	<u>Mn</u>	<u>Si</u>	<u>Al+Ti</u>	<u>Cu</u>	<u>P</u>	<u>S</u>	<u>B</u>	<u>V</u>
AMS	0.05-0.15	1.00x	1.00x	*	*	0.040x	0.030x	*	*
Phoebus	0.05-0.15	1.00x	1.00x	0.50x	0.35x	0.020x	0.015x	0.001x	0.50

x = maximum

\* not specified

Although the basic chemical composition was retained unchanged, additional control was introduced by the requirements for lower maximums for phosphorous and sulfur, as well as the establishment of maximum values for copper, boron and aluminum plus titanium. Control of these elements (an out-growth of the development of the Oak Ridge National Laboratory material denoted INOR-8) was incorporated into the Phoebus specification as an aid to improved weld-cracking resistance, radiation resistance, and precipitation-hardening stability. Specifically, boron content was controlled at a maximum of 0.001% (10 ppm) to minimize the boron-to-helium transmutation with the resultant elevated-temperature ductility degradation. UCCSD, however, would

not guarantee a known content less than 0.005% (50 ppm) in the heavy forgings (the actual range was 0.0006 to 0.0024% boron). Strip and sheet stock was produced to specification and the boron range obtained in practice was 0.0001 to 0.0009% (1 to 9 ppm).

### 2.1.2 Aluminum/Titanium

As a result of braze-alloy wetting and flow difficulties encountered on full-scale braze sectors (traced to aluminum-oxide deposits on the faying surfaces which were not reduced in the hydrogen cycle), it was necessary to lower the aluminum content.\* The chemistry was changed as follows (however, because of scheduling, only one heat of material was procured but not in time to be utilized):

<u>Original</u>	<u>Changed to</u>
Al+Ti = 0.5 w/o max	Al = 0.02 w/o max
Zr = not specified	Ti = 0.02 w/o max
	Zr = 0.02 w/o max

### 2.1.3 Boron

Boron analysis still remains a problem since values as low as 0.0001% (1 ppm) may be necessary to effectively minimize high-temperature embrittlement resulting from boron-to-helium transmutation. The determination of low-boron content in nickel-base alloys is difficult because of the lack of consistent laboratory findings and, occasionally, the inability of a laboratory to accurately repeat its findings. There are three major reasons for the difficulty:

1. The inhomogeneity of the boron as a result of grain-boundary precipitation.

---

\*The function of the aluminum is that of a de-oxidizer during the melting cycle.



2. The lack of complete dissolution of boron compounds in wet-chemical analyses (because of the insolubility of heavy metal-borides).

3. The problem of boron contamination (e.g., boron exists in substantial quantities in grinding media, solvents, cleaners and Pyrex glass).

One way to surmount the difficulty is to prepare the sample with a diamond cutoff wheel followed by spark-source mass spectrographic analyses\*. Another approach employed by commercial laboratories is the use of a wet-chemical process (with quartz equipment or special boron-free glassware) and highly sensitive colorimetric measurement of ethyl borate after distillation. Another procedure for determination of boron content in steels employs a solvent-extraction process followed by colorimetric procedures. The application to nickel-base alloys of procedures developed for steels proved to be unreliable (see Table 2.2).

Ledoux and Company was selected as the primary boron analysis source. It was the unanimous agreement of the analysts that the major contribution to the difficulties was the lack of suitable standards.

#### 2.1.4 Heat Analyses

The chemical analysis of all heats was prescribed in the material specifications and the certified analyses were rechecked on several occasions to assure that the values obtained were correct. The wet-chemical analyses, as well as Aerojet-General spectrographic analyses, consistently agreed within normal variations to vendor analyses for all elements but boron. Table 2.3 lists chemical-analyses data for Hastelloy X forgings, sheet, and weld wire employed in the design properties development program. All analyses

---

\*Franklin, J. C. and Griffin, E. B., Spark-Source Mass Spectrographic Analysis of Steels and Nickel Alloys, No. Y-1543, Oak Ridge Y-12 Report, July 6, 1966.

listed were performed by the suppliers except those otherwise indicated. There was no instance when the major elements were found to disagree with the original certified analysis.

TABLE 2.2

BORON ANALYSIS OF NICKEL BASE ALLOYS  
(Samples of the Same Bar were Prepared, Coded, and Submitted as "Unknowns" to the Three Laboratories)

<u>Laboratories</u>	<u>Procedure</u>	<u>Sample No.</u>	<u>Boron, ppm</u>	<u>Y-12 Predetermined<sup>(1)</sup> Boron on same Material, ppm</u>
Crobough Lab. Cleveland, Ohio	Emission	6	2	7.0
	Spectrographic Assay	14(3)	5	35
Hales Testing Lab. Oakland, Calif.	Solvent	2	4.1	7.0
	Extraction	5	3.6	7.0
	Colorimetric <sup>(2)</sup> (Standardized for boron in steel)	11(3)	4.3	35
		15(3)	4.0	35
Ledoux and Co. Teaneck, N. J.	Distillation-	3	8	7.0
	Photometric	4	8	7.0
	Curcumin	12(3)	14	35
	(Adapted from ASTM E 30-56)	13(3)	16	35

- (1) Predetermined values established by spark-source mass spectrographic analysis, and checked by wet chemical analysis at Oak Ridge-Y12 plant. Reference: ORNL Letter, 10/8/65, P. Patriarca to L. F. Glasier, Jr.
- (2) L. Pasztor, J. D. Bode, and Q. Fernando, Analytical Chemistry, Vol 32, No. 2 (Feb. 1960), pp 277-281.
- (3) Specimens 11 through 15 were Waspaloy. All others were Hastelloy N. However, the composition was not revealed other than to identify the samples as nickel-base alloys.

TABLE 2.3

CHEMICAL ANALYSIS DATA FOR HASTELLOY X FORGINGS, SHEET AND WELD WIRE

Specification AGC-90056B Chemical Composition, % (Single Values are Maximum)	FORGING			STRIP			WELD WIRE				
	HEAT 261-5-4000	HEAT 261-5-4001	HEAT 260-5-2813	HEAT 261-5-4000	HEAT 261-5-4001	HEAT 261-5-4002	HEAT 260-5-2735	HEAT 260-5-2783	HEAT 260-5-2784	HEAT 261-6-4003	
Nickel	Remainder	Balance	Balance	Balance	Balance	Balance	Balance	Balance	Balance	Balance	Balance
Carbon	0.05 to 0.15	0.12	0.10	0.07	0.15	0.12	0.11	0.11	0.08	0.08	0.12
Molybdenum	8.00 to 10.00	9.05	8.96	8.68	9.28	9.22	9.22	9.54	8.90	8.93	9.09
Chromium	20.50 to 23.00	21.77	21.53	22.23	21.15	21.42	21.56	21.61	21.57	21.42	21.76
Iron	17.00 to 20.00	18.22	17.53	17.85	18.20	18.00	18.20	17.50	18.09	18.36	18.69
Maganese	1.00	0.66	0.58	0.66	0.64	0.66	0.74	0.42	0.51	0.63	0.60
Silicon	1.00	0.32	0.27	0.60	0.26	0.27	0.31	0.28	0.32	0.37	0.31
Tungsten	0.20 to 1.00	0.48	0.54	0.54	0.44	0.46	0.54	0.87	0.38	0.61	0.38
Aluminum +	0.50	0.14	0.12	0.30	0.23	0.15	0.17	.09	0.21	0.22	0.15
Titanium		0.01	0.02	0.01	0.01	0.03	0.02	.02	0.02	0.03	0.02
Copper	0.35	0.03	0.02	0.04	0.01	0.02	0.02	0.005	0.02	0.03	0.01
Cobalt	0.50 to 2.50	1.59	1.55	2.05	1.54	1.59	1.46	2.16	1.40	1.93	1.51
Phosphorus	0.020	0.001	0.002	0.013	0.003	0.002	0.003	0.016	0.005	0.012	0.003
Sulfur	0.015	0.010	0.003	0.004	0.009	0.010	0.009	0.010	0.001	0.002	0.009
Boron	0.001	0.0007(c)	0.0007(c)	0.0007(b)	0.0002(c)	0.0002(c)	0.0002(c)	0.001(a)	0.00027(b)	0.0005(b)	0.00026(b)
										0.0006(c)	0.0008(c)
Vanadium	0.50	0.01	0.01	0.02	0.02	0.01	0.01	0.04	-	-	

NOTES: Boron values (a) were obtained from the Haynes Stellite Laboratory.  
 Boron values (b) were reported by Oak Ridge - Y12-Laboratory.  
 Boron values (c) were reported by Ledoux and Company.

## 2.2 MICROSTRUCTURE

The microstructure of Hastelloy X in the recommended solution-annealed condition (2150°F, followed by rapid cooling) consists of a single-phase matrix with randomly dispersed carbides of the  $M_6C$  type, and occasional clusters or stringers of a primary phase frequently termed  $M_6C$  prime which is stable and does not go into solution appreciably until a temperature of 2250°F is reached. Exposure of the alloy to temperatures between 1050 and 1800°F results in precipitation of the  $M_6C$  and  $M_{23}C_6$  carbides which are concentrated at the grain boundaries and sparsely present in the grain matrices. Exposure above 1800°F results in agglomeration of the grain-boundary carbides and increasing solution of the carbides into the matrix until at 2100°F all  $M_6C$  and  $M_{23}C_6$  carbides dissolve. At a temperature of 2290°F, all carbides (including  $M_6C$  prime) are in solution and incipient melting occurs.

## 2.3 THERMAL TREATMENT

### 2.3.1 As Received

All material was procured in the manufacturer's recommended full-solution-annealed condition to provide maximum dimensional stability and fabricative qualities. Plate, forgings, and other heavy sections were provided a 1/2-to-1 hour soak at 2150°F, while thin strip-stock was exposed only for minutes to retain an ASTM6-8 grain size consistent with the requirements for moderate forming. The grain size of the heavy sections and forged forms ranged from ASTM 1 to 4.

### 2.3.2 Post-Weld and Post-Forming

To retard further grain growth (but still provide solution of carbides formed in the weld heat-affected zone and adequate stress relief), a post-weld annealing temperature of 2080°F was selected with an exposure time of 30 to 45 minutes. Tensile testing and metallurgical investigation of

numerous nozzle forgings revealed that annealing at 2080°F was satisfactory. Grain growth did not occur, and strength and ductility properties were essentially unaffected by the double annealing cycle. Test results are presented in Tables 2.4 and 2.5.

### 2.3.3 Brazing

The exposure to the brazing cycle resulted in heavy grain-boundary carbide formation with some precipitation in the matrix. Control of the brazing cycle heat-up and cool-down (to minimize thermal differentials between the assembled components) resulted in many hours of exposure in the 1000 to 1800°F temperature range. The full-solution-annealed Hastelloy X responded to carbide precipitation in the grain boundaries throughout this temperature range, resulting in measurable property changes. The manifestations of carbide precipitation during the brazing cycle were the slight increases in ultimate tensile and yield strengths with decreases in elongation and reduction in area. Hardness also increased. The most significant effect was a reduction in ductility, especially at cryogenic temperatures. The following typical values indicate this effect:

<u>Material Condition</u>	<u>Tensile Elongation, % in 2-in</u>	
	<u>Room Temp.</u>	<u>-320°F</u>
Solution Annealed	46	45
Brazed (Phoebus Cycle)	25	13

The quantized test results for the brazed Hastelloy X forgings, weldments, and strip material are presented in Section 8.0.

TABLE 2.4

SUMMARY OF AVERAGE TENSILE PROPERTIES OF POST-WELD ANNEALED (2080°F)  
AND BRAZED\* HASTELLOY X FORGINGS (AGC 90056)

Temp. (°F)		UTS (ksi)	0.2% YS (ksi)	Elong (%)**	No.	
					Forgings	Heats
-320	Average	134.8	73.5	19	5	4
	Minimum	114.7	68.5	11		
	Maximum	158.6	79.0	34		
Room	Average	109.9	45.6	29	5	4
	Minimum	103.2	43.9	24.5		
	Maximum	115.2	48.4	38		
1200	Average	85.5	29.3	35	5	4
	Minimum	79.2	27.7	31		
	Maximum	90.5	31.1	38.5		

\*Includes (a) Solution heat-treat at 2150°F, fan-cool plus solution-anneal at 2080°F, and rapid-cool within one hour to 1200°F followed by braze cycle.

(b) Solution heat-treat at 2150°F and fan-cool followed by braze cycle.

\*\*All specimens R-3 with 1.0-inch gage length.

1. Strain rate 0.005-in./in./min to yield, then 0.05-in./in./min to failure.
2. All specimens oriented tangentially.

TABLE 2.5

TENSILE PROPERTIES OF ANNEALED AND BRAZED HASTELLOY X FORGINGS (AGC 90056)

Temp. (°F)	Thermal Condition*	Material Heat No.	Forging No. and S/N	UTS (ksi)	0.2% YS (ksi)	Elong. (%)**		
-320	SHT + SA + Braze	260-5-2793	1114856-13/880600	124.4	73.9	15		
		-2793	-13/880600	125.3	70.6	15		
		-2793	-13/880601	119.5	72.9	12.5		
		-2793	-13/880601	114.7	72.4	11		
		-2820	-15/880602	143.0	68.5	22		
		-2820	-15/880602	138.1	69.8	18		
		-2863	- 7/880601	144.8	75.8	23		
		-2863	- 7/880601	138.1	69.7	20		
		260-6-2901	-13/880603	158.6	70.5	34		
		260-6-2901	-13/880603	156.4	-	32		
		260-5-2793	-13/880601	128.1	79.0	13		
		260-5-2793	-13/880601	126.1	78.0	12.5		
		Room	SHT + SA + Braze	260-5-2793	1114856-13/880601	103.2	43.9	24.5
				-2793	-13/880601	103.3	44.6	25
				-2820	-15/880602	112.0	44.4	29.5
-2820	-15/880602			111.5	44.9	28.5		
-2863	- 7/880601			112.6	47.9	28		
-2863	- 7/880601			110.0	45.1	31		
260-6-2901	-13/880603			115.1	44.3	38		
260-6-2901	-13/880603			115.2	45.4	36.5		
260-5-2793	-13/880601			107.1	46.9	25		
260-5-2793	-13/880601			109.0	48.4	25		
1200	SHT + SA + Braze			260-5-2793	1114856-13/880601	80.1	27.7	35.5
				-2793	-13/880601	79.2	28.0	35
				-2820	-15/880602	87.2	29.3	38
				-2820	-15/880602	86.9	29.0	31
				-2863	- 7/880601	87.6	31.1	34
		-2863	- 7/880601	84.7	28.0	33.5		
		260-6-2901	-13/880603	90.5	30.0	38.5		
		260-6-2901	-13/880603	89.9	30.0	38.5		
		260-5-2793	-13/880601	83.4	30.7	33.5		
		SHT + Braze						

NOTES: \*SHT = Solution heat-treated one hour at 2150°F and fan cooled.  
 SA = Solution-annealed 30 to 45 minutes at 2080°F and cooled to 1200°F in less than 60 minutes.  
 \*\*All specimens R-3 with 1.0-inch gage length.  
 1. Strain rate 0.005-in./in./min to yield, then 0.05-in./in./min to failure.  
 2. All specimens oriented tangentially.

### 3.0 MELTING

All material for forgings was melted by the consumable-electrode, vacuum-arc process (Consarc) at the Kokomo, Indiana, facilities of UCCSD. The selected, virgin raw materials were arc-melted in air in a nominal 30,000-pound melt which, in turn, was cast into electrode molds. The electrodes were Consarc melted into three nominal 10,000 to 12,000 pound, 24-inch nominal diameter "as-cast" ingots.\* These ingots, "scalped" to a nominal 21 to 22-inch diameter, were utilized to produce the various bars, plates, sheets, and forgings. Fourteen heats of material were melted for these products.

The weld-wire and strip-stock materials were produced by vacuum-induction melting followed by Consarc melting.\*\* This method and careful control of melt stock and equipment were utilized to assure that boron content was below the desired 0.001% maximum. Four 10,000-pound heats of material were produced for these products.

A weldability test was required prior to release of a heat of material. All heats met this specification requirement, which involved a multipass, restrained plate, one-inch thick weldment (refer to Specification AGC 90059).

---

\*Heat Nos. 260-x-xxxx

\*\*Heat Nos. 261-x-xxxx



#### 4.0 PRIMARY FABRICATION

##### 4.1 NOZZLE FORGINGS

The nozzle was fabricated by welding three forgings together. The forgings consisted of the following:

<u>Forging</u>	<u>Approximate Size</u>
Inlet Ring, No. 1114856-13	Right cylinder with 65-inch diameter, 14 inches long by 3 inches thick
Convergent Section, No. 1114856-7	Cone with 72-inch maximum diameter, 33 inches long by 2.5 inches minimum thickness
Divergent Section, No. 1114856-11	Cone with 53-inch maximum diameter, 46 inches long by 3 inches minimum thickness

The inlet rings were produced from 14-inch octagonal billet stock (weighing 3000 pounds) made from nominal 24-inch diameter ingots. The 14-inch billet was forged to a pancake configuration, the center punched out, then ring rolled to the desired diameter.

The convergent and divergent sections were forged directly from the "scalped" 24-inch diameter ingots (weighing 8000 pounds) by upsetting, pancaking, then closed-die forging (see Figure 4.1). Locations of test specimens are shown in Figures 4.2 and 4.3. Test results are summarized by forging and heat number in Tables 4.1 and 4.2.

##### 4.2 DEVELOPMENT PROGRAM FORGINGS

Forgings for the materials properties testing and welding programs were procured as rings of the following dimensions:

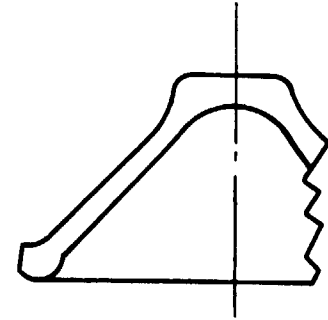
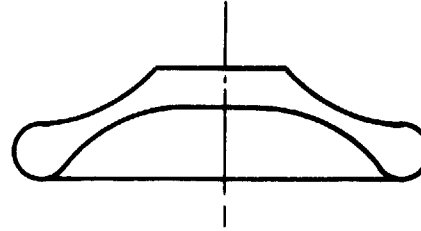
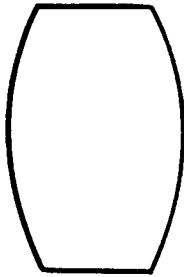
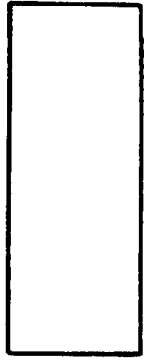
STOCK

UPSET

PANCAKE

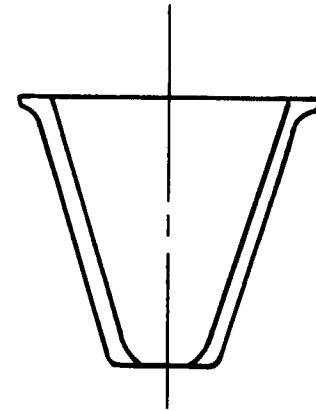
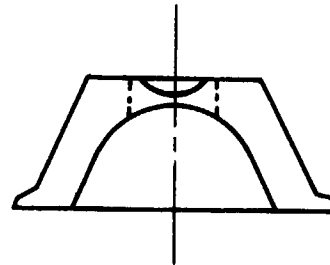
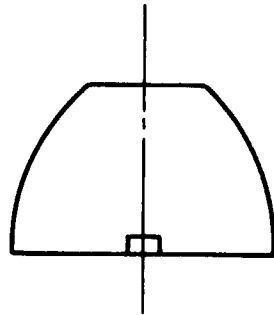
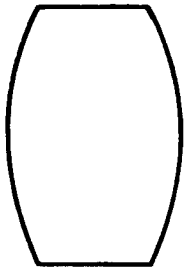
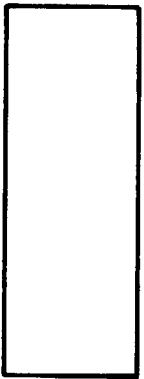
POT OR PRE-FORM

FINISH



CONVERGENT SECTION

14



DIVERGENT SECTION

Figure 4.1 - Forging Operations

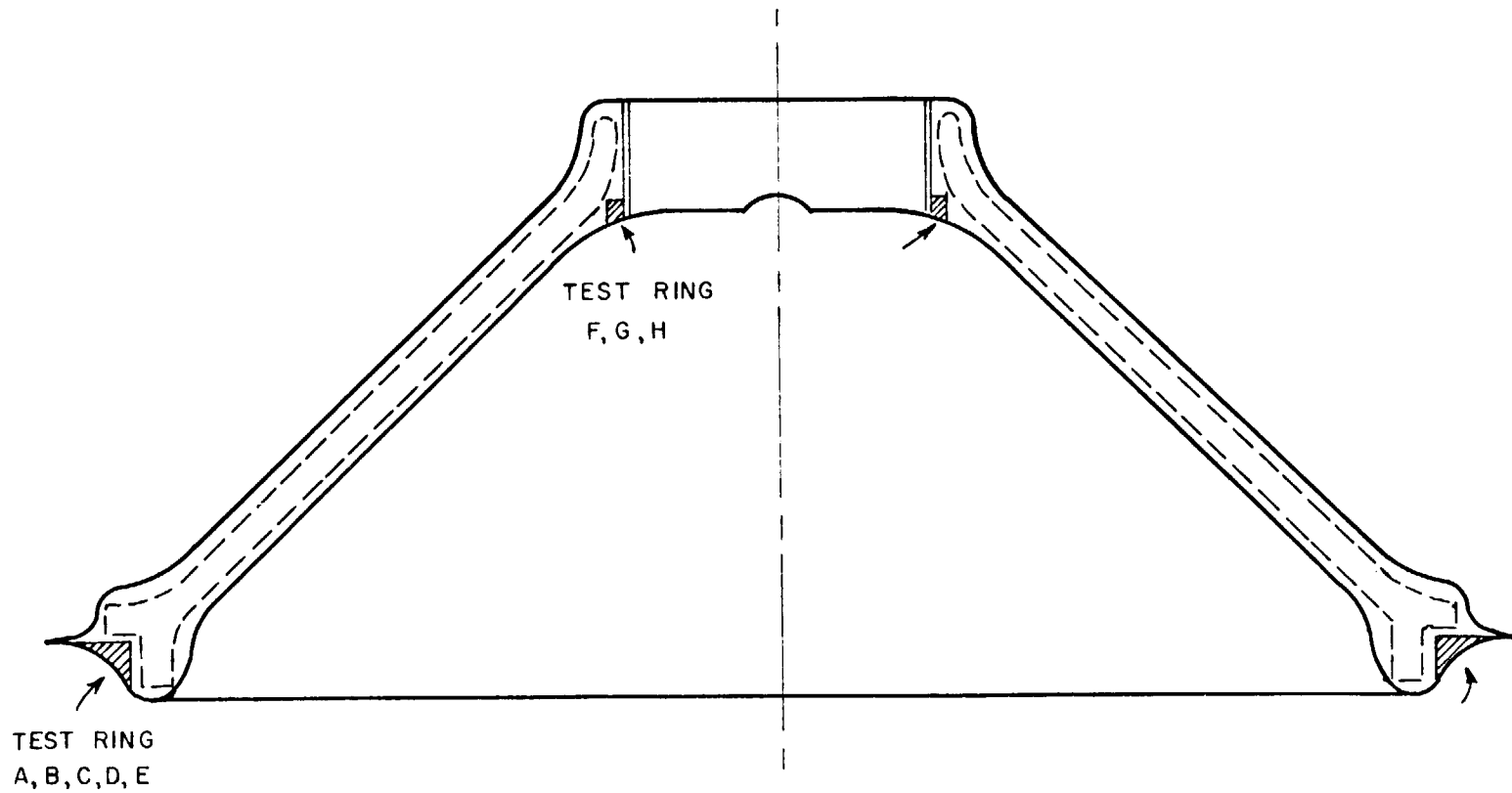


Figure 4.2 - Convergent Section Forging, P/N 1114856-7

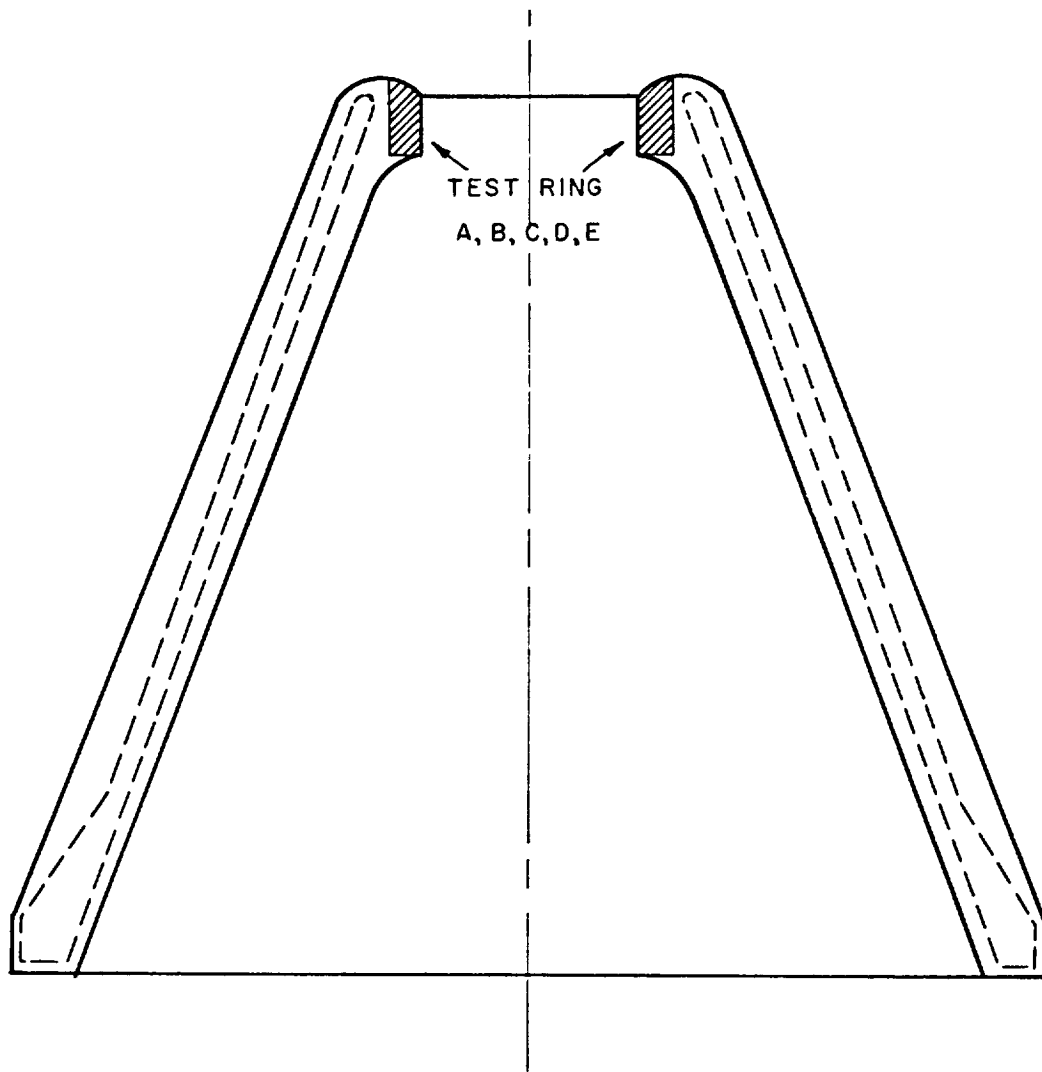


Figure 4.3 - Divergent Section Forging, P/N 1114856-11

TABLE 4.1

SUMMARY OF AVERAGE TENSILE PROPERTIES OF ANNEALED\* FORGINGS  
OF HASTELLOY X (AGC 90056)

(By Forging Number and Material Heat Number)

Forging Number

<u>No.</u>	<u>Name</u>	<u>Temp (°F)</u>	<u>UTS(ksi)</u>	<u>0.2% YS(ksi)</u>	<u>Elong. (%)***</u>	<u>No. of Forgings</u>	<u>No. of Heats</u>
1114856-13	Inlet	Room	104.3	44.3	42	7	3
1114856-7***	Converg.	↓	102.0	43.1	48	7	6
1114856-11	Diverg.		93.2	42.3	33	6	4
Average	All		100.8	43.3	42		
1114856-13	Inlet	1200	70.5	26.3	48	7	3
1114856-7***	Converg.	↓	72.2	27.5	46	7	6
1114856-11	Diverg.		69.2	26.7	36	6	4
Average	All		71.2	27.0	45		

Material Heat Number

<u>Heat No.</u>	<u>Temp (°F)</u>	<u>UTS(ksi)</u>	<u>YS(ksi)</u>	<u>Elong.(%)</u>	<u>No. of Forgings</u>	
260-5-2793	Room	95.8	41.5	49	4	
↓ -2820	↓	100.5	42.7	52	1	
↓ -2850		86.3	40.3	28	2	
↓ -2863		101.7	42.2	45	1	
260-6-2880		104.5	42.6	52	2	
↓ -2887		101.4	44.7	34	2	
↓ -2898		98.5	43.8	38	2	
↓ -2900		104.5	45.4	41	1	
↓ -2901		109.3	45.7	39	3	
↓ -2920		96.1	42.1	41	1	
↓ -2935		103.7	45.0	32	1	
Average			100.8	43.3	42	
Minimum			80.3	39.2	22	
Maximum			112.8	52.0	58	

Notes: \*One hour at 2150°F and fan cooled  
 \*\*All specimens R-3 with 1.0-inch gage length  
 \*\*\*Includes P/N 1114856-15

TABLE 4.1 (cont.)

<u>Heat No.</u>	<u>Temp(°F)</u>	<u>UTS(ksi)</u>	<u>YS(ksi)</u>	<u>Elong.(%)</u>	<u>No. of Forgings</u>	
260-5-2793	1200 ↓	66.0	26.5	53		
↓ -2820		75.4	26.2	51		
↓ -2850		63.8	24.9	28		
↓ -2863		73.5	27.8	45		
260-6-2880		76.3	26.0	50		
↓ -2887		75.9	28.5	42		
↓ -2898		71.3	27.9	38		
↓ -2900		75.3	29.4	37		
↓ -2901		78.5	28.8	40		
↓ -2920		72.3	26.4	47		
↓ -2935		-	-	-		
Average			71.2	27.0	45	
Minimum			61.5	24.2	24	
Maximum			82.9	33.8	56	

1. Strain rate 0.005-in./in./min to yield, then 0.05-in./in./min to failure.
2. Specimens oriented tangentially in rings sectioned from full-scale forgings.

TABLE 4.2

TENSILE PROPERTIES OF ANNEALED\* FORGINGS  
OF HASTELLOY X (AGC 90056)

Forging Material Forging No. S/N	Heat No.	Temp (°F)	UTS (ksi)	0.2% YS(ksi)	Elong. (%)**	Comments	
1114856-13	880600	260-5-2793	Room	98.0	41.4	54	} Room Temperature
	↓		99.4	42.0	52		
	↓		97.0	41.0	47		
	↓		97.6	41.0	55		
	880601		↓	96.4	42.0	49	
	↓		95.2	42.0	50		
	↓		92.2	41.5	44		
	880602		↓	95.0	41.5	48	
	↓		95.6	40.5	51		
	↓		93.4	41.5	45		
	↓		92.0	41.4	38		
	↓		95.7	41.2	49		
	880603		260-6-2901	111.6	46.1	40	
	↓		110.9	45.9	39		
	↓		110.9	45.9	39		
	↓		111.0	45.6	37		
	↓		111.0	44.6	38		
	↓		112.8	46.8	42		
	880604		↓	112.4	46.0	41	
	↓		108.0	46.2	31		
↓	110.0	46.8	41				
↓	106.0	47.0	29				
↓	110.0	43.8	38				
↓	109.8	46.0	42				
↓	109.8	46.4	38				
↓	109.2	47.0	43				
↓	110.4	45.8	42				
↓	111.0	46.4	43				
880605	↓	109.0	42.0	43			
↓	108.0	46.8	43				
↓	108.6	47.4	42				
↓	109.0	47.0	43				
880606	260-6-2935	104.6	44.2	44			
↓	105.0	46.0	28				
↓	105.2	44.2	33				
↓	104.2	45.4	37				
↓	100.4	44.2	32				
880600	260-5-2793	1200	68.2	24.7	56	} 1200°F	
↓	↓	↓	68.4	24.5	55		
↓	↓	↓	66.6	24.9	56		

TABLE 4.2 (cont.)

Forging Material		Heat No.	Temp (°F)	UTS (ksi)	0.2% YS(ksi)	Elong. (%)**	Comments		
Forging No.	S/N								
1114856-13	880601	260-5-2793	1200	63.5	25.7	50	} 1200°F		
	880602	260-5-2793		61.7	24.5	48			
	880603	260-6-2901		82.9	29.6	47			
	880604			74.5	27.3	27			
	880605			78.2	29.4	46			
	880606	260-6-2935		-	-	-			
1114856-7	880600	260-5-2793	Room	95.7	41.0	52	Center slug, 16-in. dia x 6-in. thick		
				93.7	40.6	48	Center slug, 16-in. dia x 6-in. thick		
				95.7	41.7	49	Radial, center slug, 16-in. dia x 6-in. thick		
				93.2	41.2	44	Radial, center slug, 16-in. dia x 6-in. thick		
				97.0	45.2	53***	Small diameter		
				100.0	40.9	55***	Large diameter		
	880601	260-5-2863		96.7	40.6	57***	Large diameter		
				99.0	40.0	47			
				104.5	44.0	43			
				100.7	40.4	47			
				102.6	44.3	42			
				880602	260-5-2820	97.1	40.9	50	Small diameter
						96.5	40.8	51	Small diameter
						100.6	40.0	57	Large diameter
103.0	52.0	49							
100.6	40.0	56							
101.0	41.5	54							
880603	260-5-2880	103.0	42.5	50					
		102.5	43.7	50					
		104.0	44.0	48	Small diameter				
		103.8	43.8	49	Small diameter				
		103.0	43.2	58	Large diameter				
		102.5	42.5	53					
		103.5	41.5	54					
		103.2	41.7	55					
		1114856-15	880602	260-5-2820	Room	97.1	40.9	50	Small diameter
1114856-7				96.5	40.8	51	Small diameter		
				100.6	40.0	57	Large diameter		
				103.0	52.0	49			
				100.6	40.0	56			
				101.0	41.5	54			
				103.0	42.5	50			
				102.5	43.7	50			
				104.0	44.0	48	Small diameter		
				103.8	43.8	49	Small diameter		
				103.0	43.2	58	Large diameter		
				102.5	42.5	53			
				103.5	41.5	54			
				103.2	41.7	55			



TABLE 4.2 (cont.)

Forging Material Forging No. S/N	Heat No.	Temp (°F)	UTS (ksi)	0.2% YS(ksi)	Elong. (%)**	Comments	
1114856-7	880604	260-6-2880	Room	106.8	43.4	48	Small diameter
				106.0	44.0	46	Small diameter
				107.5	43.5	52	Large diameter
				104.5	41.5	51	
				104.5	41.3	53	
	880605	260-6-2900		105.0	41.3	51	
				101.0	43.2	41	Small diameter
				101.4	42.6	42	Small diameter
				105.1	44.9	42	Large diameter
				104.3	46.8	37	
				106.0	46.8	36	
				107.0	46.4	39	
				105.7	46.0	45	
				105.2	46.5	45	
				101.8	40.0	45	Small diameter
	880606	260-6-2898		101.6	53.8	41	Small diameter
				105.0	46.0	44	Large diameter
				100.7	44.0	43	
				101.2	44.0	43	
				103.0	44.0	38.5	
			102.7	45.3	42		
			102.0	43.9	39.5		
880600	260-5-2793	1200	61.5	26.4	41***	Small diameter	
		1200	64.6	33.8	42***	Small diameter	
		1200	73.5	28.3	48***	Large diameter	
		1200	66.7	26.5	46***	Large diameter	
		1200	64.3	25.7	48	Center slug, 16-in. thick	
880601	260-5-2863	1200	73.5	27.8	45		
1114856-15	880602	260-5-2820	1200	77.2	27.0	47	Small diameter
1114856-15	880602	260-5-2820		73.5	25.4	55	Large diameter
1114856-7	880603	260-6-2880		73.5	26.4	48	Small diameter
				79.5	25.9	52	Large diameter
				77.2	26.1	53	Small diameter
				75.1	25.7	48	Large diameter
				72.5	26.6	41	Small diameter
	880605	260-6-2900		78.0	32.1	31	Large diameter
				76.0	27.7	43	Small diameter
				74.3	28.9	43	Large diameter
880600	260-5-2793	-320	135.0	78.5	27***	Large diameter	
880600	260-5-2793	-320	137.0	77.0	27***	Large diameter	

TABLE 4.2 (cont.)

<u>Forging Material</u> <u>Forging No. S/N</u>	<u>Heat No.</u>	<u>Temp</u> <u>(°F)</u>	<u>UTS</u> <u>(ksi)</u>	<u>0.2%</u> <u>YS(ksi)</u>	<u>Elong.</u> <u>(%)**</u>	<u>Comments</u>
1114856-11	880600	260-5-2850	Room	83.4	41.0	23
	↓	↓	↓	80.3	41.0	22
	↓	↓	↓	86.2	41.3	30
	880601	↓	↓	88.2	41.0	30
	↓	↓	↓	87.0	39.5	29
	↓	↓	↓	90.7	39.2	34
	↓	↓	↓	92.2	39.2	36
	880603	260-6-2887	↓	82.0	40.5	23
	↓	↓	↓	100.0	44.0	29
	↓	↓	↓	100.0	46.0	33
	↓	↓	↓	104.6	45.0	41
	↓	↓	↓	102.0	45.4	33
	880604	↓	↓	100.2	43.0	36
	↓	↓	↓	99.0	41.8	38
	↓	↓	↓	100.0	42.0	39
	↓	↓	↓	98.6	42.0	37
	880605	260-6-2898	↓	93.4	43.4	27
	↓	↓	↓	92.1	46.0	30
	↓	↓	↓	86.4	42.2	26
	880606	260-6-2920	↓	87.0	42.5	26
	↓	↓	↓	100.0	42.1	49
	↓	↓	↓	90.0	43.0	28
	↓	↓	↓	96.1	41.1	38.5
	↓	↓	↓	98.2	42.1	46
	880600	260-5-2850	1200	65.4	25.7	32
	880601	260-5-2850	↓	62.2	24.2	24
	880603	260-6-2887	↓	76.6	28.6	41
	880604	260-6-2887	↓	75.2	28.3	43
	880605	260-6-2898	↓	63.6	27.1	26.5
	880606	260-6-2920	↓	72.3	26.4	47

Notes:

\*One hour at 2150°F and fan-cooled

\*\*All specimens R-3 with 1.0-inch gage length

\*\*\*Tests conducted at Aerojet-General. All other tests conducted at Wyman-Gordon Company.

1. Strain rate 0.005-in./in./min to yield, then 0.05-in./in./min to failure.
2. Specimens oriented tangentially in rings sectioned from full-scale forgings.

<u>End Use</u>	<u>Size</u>
Mechanical & Physical Properties	17 inches ID x 23 inches OD x 6 inches long
Welding	17 inches ID x 20 inches OD x 6 inches long

The forgings were produced by upsetting an 8-inch round-cornered square into an 11- to 12-inch cube, then cross-forging to an 8- to 9-inch square bar. This was followed by upsetting to a pancake approximately 18 inches in diameter and 7 inches thick, piercing and then ring forging and ring rolling to the sizes specified. The rings were annealed one hour at 2150°F and air-blast cooled. The mechanical and physical properties of these forgings are presented in Section 8.0.

#### 4.3 FORGINGS OF IMPROVED STRENGTH

An investigation to provide better Hastelloy X forgings was undertaken and the improved strength and microstructural control attained are presented in Appendix A.

#### 4.4 STRIP

All strip stock was produced from 0.062-inch thick, hot-rolled and annealed sheet made by UCCSD. Conversion of the sheet was accomplished by Ulbrich, Incorporated, by cold-rolling, using Sendzimir mills, with intermediate and final annealing in a hydrogen atmosphere. A limited quantity of strip was produced by the W. B. Driver Co., Newark, N. J., as a second source of supply. AGC 90057 was the controlling specification.

#### 4.5 WIRE

All welding wire was produced by UCCSD from hot-rolled rod. The finished wire was dye-penetrant inspected for freedom from laps, seams, cracks, or pits. In addition, each wire lot had to meet a performance

requirement consisting of a bead-on-plate test to meet the following criteria of specification AGC 90058:

1. Smooth and even flow during welding.
2. Free of sparking or bubbling during welding.
3. Smooth appearance with visible weld-ripple.
4. Weld surface free of foreign matter.

## 5.0 SECONDARY FABRICATION

### 5.1 CONVENTIONAL MACHINING

Hastelloy X properties imply a material which is characteristically soft, galls in machining, and which tends to severely work-harden. Functionally, this means that sharp, positive-rake cutting tools must be used in conjunction with relatively low cutting speeds and moderate but positive power feeds.

#### 5.1.1 Recommended Cutting Conditions

##### 5.1.1.1 Turning

	<u>Roughing Cuts (0.125-inch depth and over)</u>	<u>Roughing Cuts (0.125-inch depth and under)</u>
Tool Material	Carbide Grade C-2*	Carbide Grade C-2*
Tool Geometry	Positive Rake**	Positive Rake**
Cutting Fluid	Heavy Duty Soluble Oil (1:20)	Heavy Duty Soluble Oil (1:20)
Speed-ft/min	70-90	90-120
Feed-in/rev.	0.010-0.015	0.007-0.010

\*Recommended brands of C-2 carbides are (in order of decreasing preference):  
Carboloy 895, Carboloy 883, Kennametal K-68, and Valenite VC-22

\*\*Geometry for standard positive-rake, indexable insert tools is:

Side Rake Angle (SR):	5°	Side Cutting-Edge Angle (SCEA):	0-30°
Back Rake Angle (BR):	0°	End Cutting-Edge Angle (ECEA):	15-60°

#### 5.1.1.2 Drilling

Drill Diameter (inch)	<u>1/8</u>	<u>1/4</u>	<u>3/8</u>	<u>1/2</u>	<u>3/4</u>
Type of Drill	Heavy Duty "Cobalt" HSS*				
Cutting Fluid	Thredkut 99 plus Pale Oil (2:1) or AGC Special Moly Oil				
Speed-ft/min	20-25				
Feed-in/rev	0.002	0.003	0.004	0.005	0.006

\*Recommended drills are (in order of decreasing preference): 1. Cleveland List #817, heavy-duty "Cobalt" HSS drill; 2. Cleveland "Cobalt" rail drill (special); and 3. National "Cobalt" rail drill Note: This drill must be re-ground to produce a 135° point angle.

#### 5.1.1.3 Milling 0.030-Inch Wide by 0.090-Inch Deep Slots

Machine Setup: A climb-milling setup must be used for this operation.

Cutter: Special HSS slitting cutter

Cutting Speed: 30-40 ft/min.

Feed: 0.001-0.002 in./tooth

#### 5.1.1.4 Cutter Recommendations

Cutters with the configuration of a standard metal-slitting saw could be used. However, the following recommendations will require that these cutters be specially ordered:

1. Cutter Material: Molybdenum-type high-speed steel, salt-bath nitrided.

2. Cutter Diameter: Smallest diameter consistent with the machine setup is recommended (2-1/2 to 4 inch diameter with 30 to 40 teeth).
3. Cutter Clearance Angles: 5-8° (Peripheral clearance).
4. Side Relief: Concave ground.
5. Tolerance: Cutters ground to maximum of 0.001 TIR, radial and axial.
6. Machine Setup: Machine setup must be as rigid as possible with backlash and free movement eliminated. Cutter "run-out" on the machine must be maintained at less than 0.001 inch.

#### 5.1.1.5 Grooving with Slitting Saw

The initial attempt to simulate conventional groove machining of a Phoebus nozzle was made on a Hastelloy X plate 1 inch thick, 4 inches wide, and 60.5 inches long. The desired dimensional groove size and tolerance requirements were 0.039 to 0.041 inch wide by  $0.100 \pm 0.010$  inch deep. The plate was mounted on a vertical-mill turntable at 45° to simulate grooving of the convergent section of a nozzle. An extension arm guided and extended the high-speed steel slitting-saws which were 3.991 inches in diameter with 36 teeth and ground to a thickness of  $0.039 \begin{matrix} +0.0005 \\ -0.0000 \end{matrix}$  inch. The coolant was a sulphur-base cutting oil applied by spray. A total of six grooves was machined under the following conditions: 15 to 28 saw rpm; 16 to 29 surface feet/minute.

The results were: 2 to 4 saws required per groove, with an average of 3; 5 to 50 inches cut per saw, with an average of 21 inches. In all cases, a new saw was used at the start of each groove. All grooves maintained required depth tolerances. Only two were held within the width tolerance with the oversize condition being attributed to saw damage. The straightness tolerance imposed ( $\pm 0.010$  inch between groove centerlines) was not maintained (deviations to 0.025-in. occurred).

The conclusions drawn from this specimen evaluation were that an improved extension saw control-arm would be required in addition to applying a higher viscosity sulphur-base coolant either by submersion or direct flow. These changes were incorporated successfully on a contoured braze sector prior to nozzle grooving.

## 5.2 ELECTRICAL DISCHARGE MACHINING (EDM)

Electrical discharge machining is a metal-removing technique that machines workpieces by the direct application of the energy contained in an electric arc discharge. By controlling voltage, amperage, capacitance, and frequency, the shape of an electrode tool can be imparted to the workpiece either as a hole or as a cavity impression. In relative terms, rough cuts are made with high amperage and capacitance while finishing cuts are made at high voltage and frequency with low amperage and capacitance. The process is unaffected by material hardness. Contour cuts can be made, using shaped electrodes, without sectioning the workpiece. Work can also be done in locations that are otherwise inaccessible for conventional machining operations.

The Phoebus-2 nozzle was contained in an indexing cage so machining of one full-length groove, a slot, and a related coolant hole could be conducted simultaneously by careful positioning and sequencing of the EDM heads. The grooving electrode was replaced by an electrode to perform a scalloping operation.



Equally significant with the development of multiple heads was the development of electrode fabrication techniques. It was necessary to fabricate the grooving electrode from several pieces of graphite bonded together and ground to critical tolerances to attain the close design dimensions. Flushing techniques to remove machining residue during grooving operations were also developed to clean and cool the multiple electrodes.

### 5.3 STRIP FORMING AND WELDING

Nozzle coolant-tubes were produced from 2-inch wide by 0.012-inch thick strip in the solution-annealed condition. Strip grain size was ASTM 6-8. Surface finish was better than 32 RMS. Initial forming was conducted in a brake press as shown in Figure 5.1. Thinning at the crown radius was negligible at this point. Final, or contour, forming was conducted in manually operated, bench-mounted, stretch-forming tooling. The straight U-tube was clamped securely, adjacent to forming dies, and contoured lengthwise as shown in Figure 5.2. A contoured male and female pressure-pad eliminated wrinkling during forming. A maximum crown thinning of 0.0005/0.0007 inch occurred at the smallest crown radius.

Metallurgical examination of a formed tube revealed little or no microstructural change at this point and no change in hardness of the leg compared to original stock (230 VHN). Maximum hardness change occurred at the tube crown (265 VHN). Exposure of the tube to the brazing operation increased leg hardness and decreased crown hardness to 250/240 VHN. Annealing 5 to 15 minutes at 1925°F changed leg and crown hardness to 265 VHN. Exposure to the 1925°F annealing temperatures followed by the braze cycle resulted in a uniform hardness of 270/275 VHN. Microexamination revealed that the 1925°F anneal and/or the brazing cycle produced an equivalent annealing/stress equalizing effect as evidenced by the decrease in the amount of grain twinning in the microstructure. Appendix B presents the detailed metallurgical analysis of the formed tube.



INITIAL FORM - FIRST PHASE



INITIAL FORM - FINAL PHASE

Figure 5.1 - Coolant Tube Forming

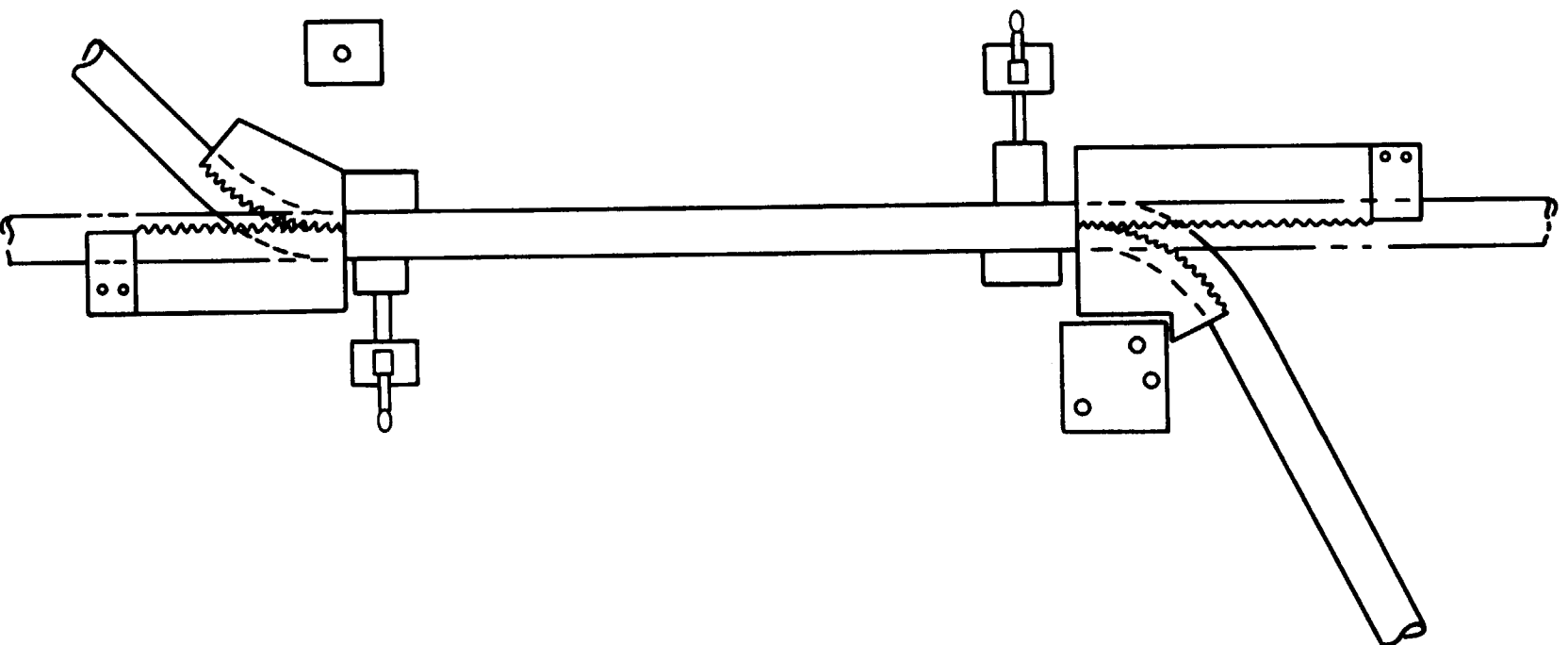


Figure 5.2 - Coolant Tube Contour Forming

The final tube fabrication operation entailed welding of end caps onto the ends of the tubes. Figure 5.3 illustrates the tooling configuration utilized in TIG welding end caps to the U-tubes.

#### 5.4 WELDING OF NOZZLE AND DEVELOPMENT FORGINGS

Welding of the nozzle jacket was based on the utilization of development welding information and the establishment of requirements for the selection of the welding process, joint design, filler wire, welding operator qualifications, inspection, cleaning, equipment, and tooling. With the establishment of the welding schedule (Specification AGC 90067), development forgings were welded concurrently with the first nozzle forgings.

##### 5.4.1 Process

The TIG process was selected because of its high reliability, minimal development cost, and its capability for good process-control.

##### 5.4.2 Joint Design

A double U-groove was selected because of the material thicknesses. The groove dimensions incorporated a root land 0.060-inch in thickness and a 30° groove-wall angle as shown in Figure 5.4

##### 5.4.3 Wire

Hastelloy X was selected as the weld wire because it presented the best potential for mechanical properties retention, compositional compatibility, and the fewest unknowns: thereby precluding special wire development or evaluation programs. A weld-wire specification (AGC-90058) was employed to control the quality of wire received. This specification incorporated a material weldability test and a bead-on-plate performance test on each lot of wire and each material heat. The bead-on-plate acceptance criteria included

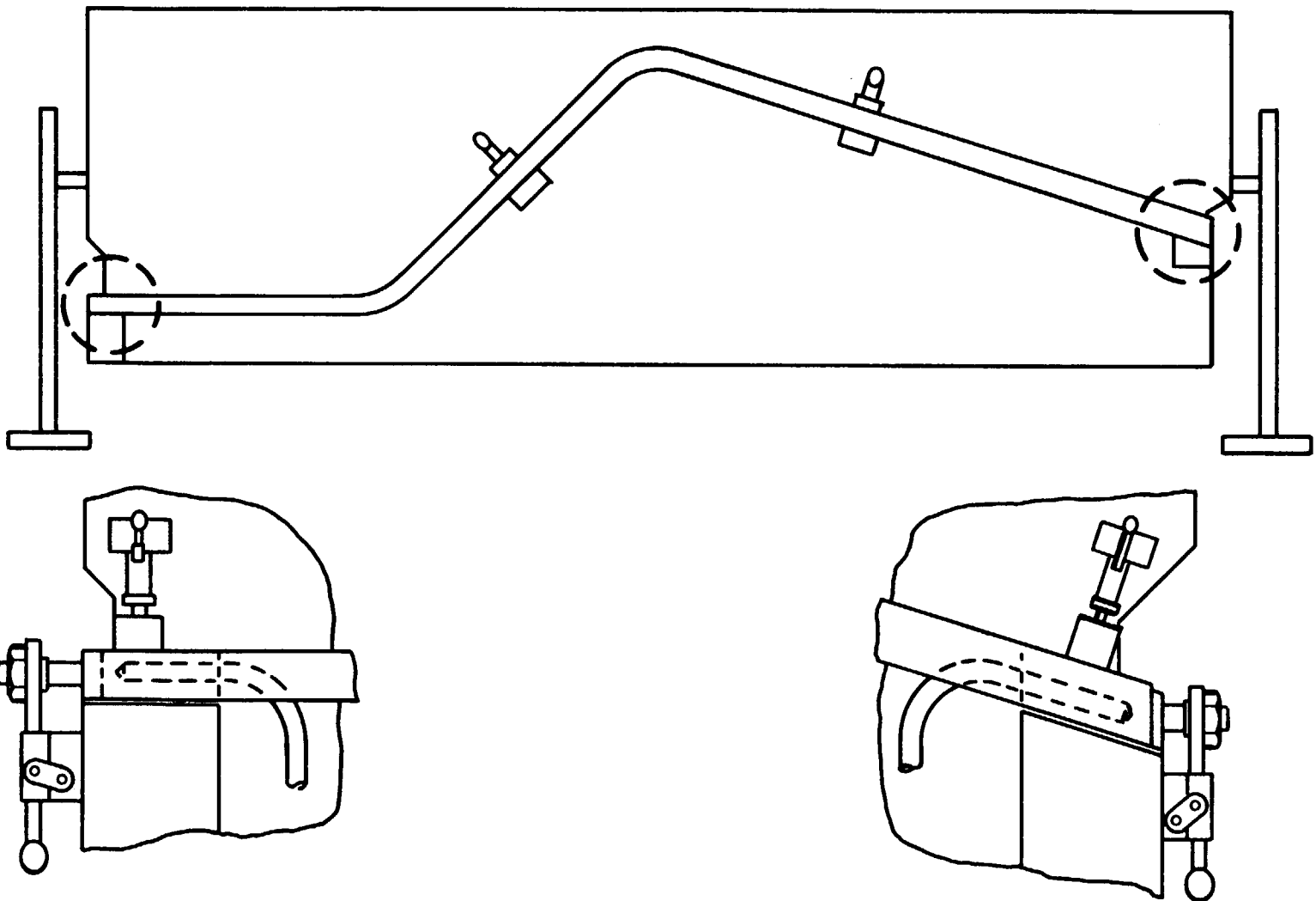


Figure 5.3 - Coolant Tube End-Cap Welding

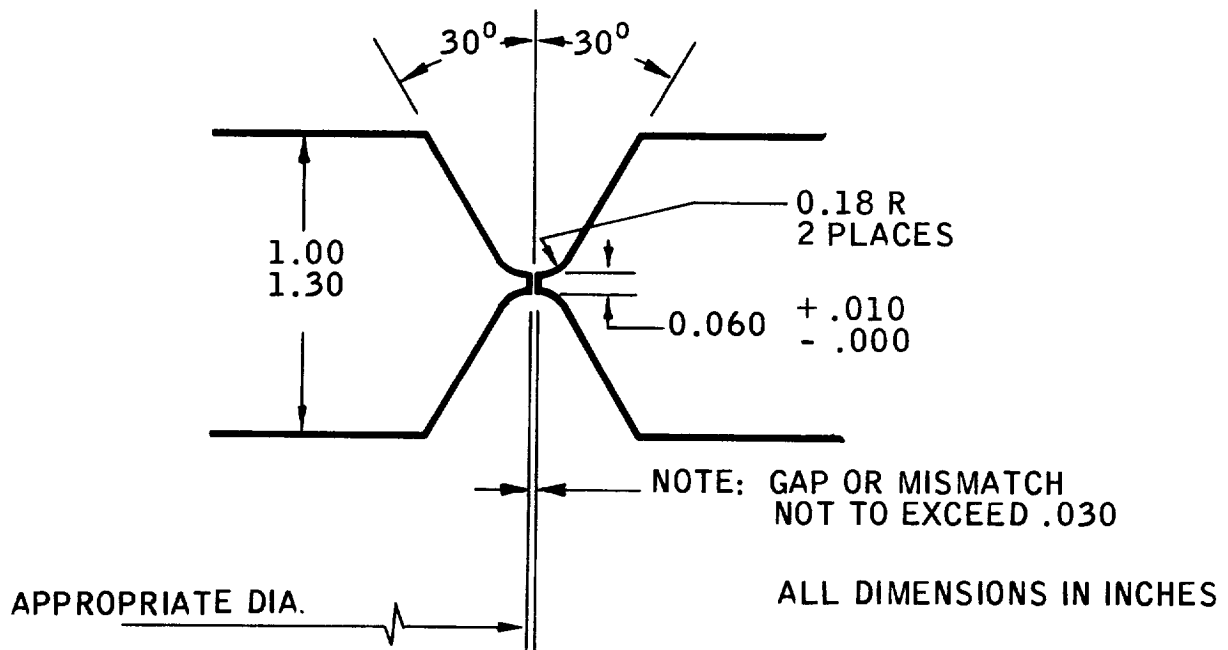


Figure 5.4 - Typical Double U-Groove Utilized in Nozzle Jacket Welds

visual appearance and arc characteristics, as well as radiographic and penetrant inspection of the weld beads. To further prevent the receipt of defective wire, the specification required a dye-penetrant inspection of specified lengths of wire from each spool. Wire which contained surface defects, (e.g., laps, cracks, and pits) was rejected.

#### 5.4.4 Operator Qualifications

The specific requirements for operator qualification are contained in the welding specification. Essentially, a group of welding operators was trained in all aspects of the welding operation, with special emphasis directed to the precise following of approved welding procedures. Insofar as possible, personnel employed on the development program were assigned to welding of the nozzle.

#### 5.4.5 Inspection Requirements

The following inspection methods and sequences were instituted at the beginning of the development welding program and were a requirement for all subsequent nozzle welding (Specification AGC 90058):

1. Visual inspection of doubtful areas required for each weld pass.
2. Penetrant inspection of doubtful areas, as required.
3. Penetrant inspection required following the root passes, mid-point (approximately 15th pass), and following the final weld pass.
4. Ultrasonic inspection of the completed weldment.

#### 5.4.6 Cleaning

Effective cleaning was recognized as a prerequisite to the production of high-quality welds. Cleaning requirements for each part and weld inter-pass cleanliness requirements were specified in AGC 90058.

#### 5.4.7 Weld Equipment

The equipment was a completely integrated system (with specifically designed controls for all variables) to assure accurate repeatability of the specified welding conditions. Welding controls consisted of a direct-current power supply, an automatic arc voltage-controlled head, and a welding sequence-timing control to sequentially initiate and terminate welding current, wire feed, positioner or roll rotation, and inert-gas pre-flow and post-flow. The equipment had suitable current-sloping controls and a means of accomplishing automatic arc-ignition. Figure 5.5 illustrates the control panel and welding boom in position for an outside diameter, aft-end weld.

#### 5.4.8 Tooling

A mobile welding cart with a load capacity of 20,000 pounds was designed to align, support, position, and rotate the nozzle sections as they were assembled, tack welded in place, and welded (see Figure 5.5). The roll support-platform was hinged between two "vee"-supported vertical columns providing capability to position the nozzle assembly at a maximum angle of 20° from the horizontal in either direction. Positive rotation of the nozzle was accomplished by a variable-speed Graham drive and a rack and pinion gear assembly attached to a center cage-turning roll-ring. All assembly, welding, and nondestructive testing inspection operations were performed with the nozzle on the weld cart.



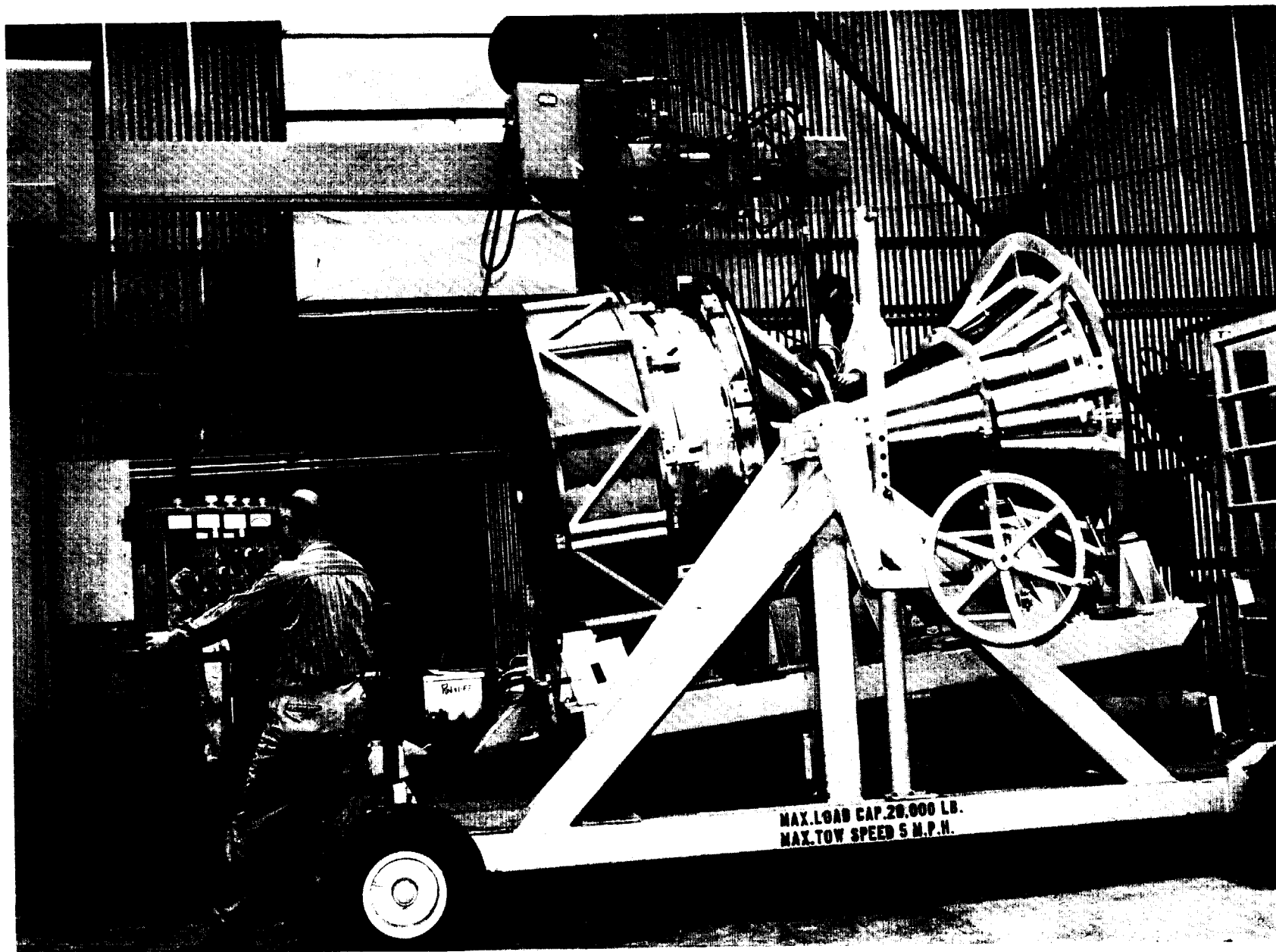


Figure 5.5 - Welding Control Panel and Boom in Position  
for Outside Diameter, Aft-End Weld

#### 5.4.9 Heat Treatment

Upon completion of welding and inspection, the nozzle was heated to 2080°F + 20°, held at temperature for 30 to 45 minutes in a hydrogen atmosphere, and then force-cooled (again in a hydrogen atmosphere) to 1200°F in not more than 60 minutes.

#### 5.4.10 Schedule

Typical welding parameters for the forward and aft nozzle joints were:

##### Forward Joint

<u>Pass</u>	<u>Amps</u>	<u>Volts</u>	<u>Weld Travel (IPM)</u>	<u>Wire</u>		<u>Shielding Gas</u>	
				<u>Size</u>	<u>Feed (IPM)</u>	<u>Torch</u>	<u>Back-up</u>
Root	220	9	5	0.045 inch	60	He @ 45 CFH A @ 15 CFH	A @ 30 CFH
Filler	210	9.5	5	0.062 inch	25	He @ 25 CFH A @ 25 CFH	

##### Aft Joint

Root	210	9	5	0.045 inch	60	He @ 45 CFH A @ 15 CFH	A @ 30 CFH
Filler	200	9.5	5	0.045 inch	60	He @ 25 CFH A @ 25 CFH	

## 5.5 WELDING-DISSIMILAR METALS

Six Hastelloy X and six AISI 347 longitudinally-welded cylinders, each 8 inches in diameter and 6 inches in length, were radiographed prior to their use on the dissimilar-metals welding program. Edges were prepared for welding and a Hastelloy X cylinder was welded circumferentially to each AISI 347 cylinder. The filler wires, quantities, and dispositions were:

<u>Cylinder No.</u>	<u>Weld Wire</u>	<u>Weld Method</u>	<u>Disposition</u>
1 and 2	Hastelloy W	Semi-automatic TIG	One for tensile and microexamination, one for hydrostatic proof test
4 and 6	Inconel A	Semi-automatic TIG	One for tensile and microexamination, both for hydrostatic proof test
5	Hastelloy W	Manual TIG	Procedure evaluation only
6	Inconel A	Manual TIG	Procedure evaluation only

The successful procedures utilized and the test results obtained are presented in Appendix C.

## 5.6 FURNACE BRAZING

Nozzle brazing is a classified process controlled by Specification AGC 90169. Briefly, the process entails cleaning of the jacket and tubes, the assembly of tubes and braze alloy into the jacket, and hydrogen-furnace brazing in multiple cycles in the 1725 to 1875°F range with controlled heat-up and cool-down.

## 6.0 SPECIFICATIONS

The following material and process specifications were published:

<u>AGC Spec. No.</u>	<u>Title</u>
90056	Nickel-Molybdenum-Chromium Wrought Alloy Forgings
90057	Nickel-Molybdenum-Chromium Alloy Plate, Sheet, and Strip
90058	Nickel-Molybdenum-Chromium Alloy Bare Welding Filler Wire
90059	Weldability of Nickel-Base Alloy Plate, Forgings, and Wire
90060	Nickel-Molybdenum-Chromium Alloy Bar
90067	Welding, Phoebus-2 Hastelloy X Nozzle Jacket
90109*	Radiographic Acceptance Criteria for Phoebus-2 Nozzle Jacket Welds
90112	Nickel Plating (Electrodeposited) Nickel-Base Alloys
90116	Repair of Leaks in Furnace-Brazed Phoebus Nozzles
90169 (Conf)**	Nozzle U-Tube, Tube Installation and Brazing Procedure for (U)
90180	Radiographic Acceptance of Phoebus Nozzle Coolant Channels and Torus Closure Welds
STD-9001	Nozzle, U-Tube, Cleaning and Protection of
STD-9007	Cleanliness Levels, Components and Assemblies
STD-3010	Inspection, Penetrant

\*Superseded STD-9005

\*\*Formerly identified as AGC 90006 (Confidential)

## 7.0 PHYSICAL PROPERTIES

The physical properties of Hastelloy X relative to thermal-stress calculations were determined because: (1) values available in the literature and supplier data did not cover the full temperature range; (2) the influence of heat treatment was not known; and (3) metallurgical experience was not available in great depth. The properties measured included moduli, thermal expansion, and thermal diffusivity (from which thermal conductivity was calculated). Specific heat, density, and Poisson's ratio also are included in this section.

### 7.1 MODULI:TENSION, SHEAR, AND TANGENT

The dynamic tensile and shear moduli of elasticity were determined by the Los Alamos Scientific Laboratory\*. Specimens, 0.25 inch in diameter and 4 inches in length, were provided by Aerojet-General. Specimens were oriented in the axial direction of the ring forging: i.e., parallel to the length of the forging. The data are tabulated in Table 7.1, with some computed values of Poisson's ratio provided. Because it was noted by Dickinson that the measured density was greater than that listed in vendor literature ( $8.23 \text{ g/cm}^2$ )\*\*, the actual value ( $8.296 \text{ g/cm}^2$ ) was used in the calculations. Samples from the same heat (261-5-4000) and forging used by LASL, as well as Heat 260-5-2813, were checked at Aerojet-General and the higher density confirmed.

Dynamic moduli data are plotted in Figure 7.1 and reveal a linear decline of values with increasing temperature. The moduli are somewhat higher than the older data in the supplier literature, which may be caused by the effects of vacuum melting and the braze heat-treatment.

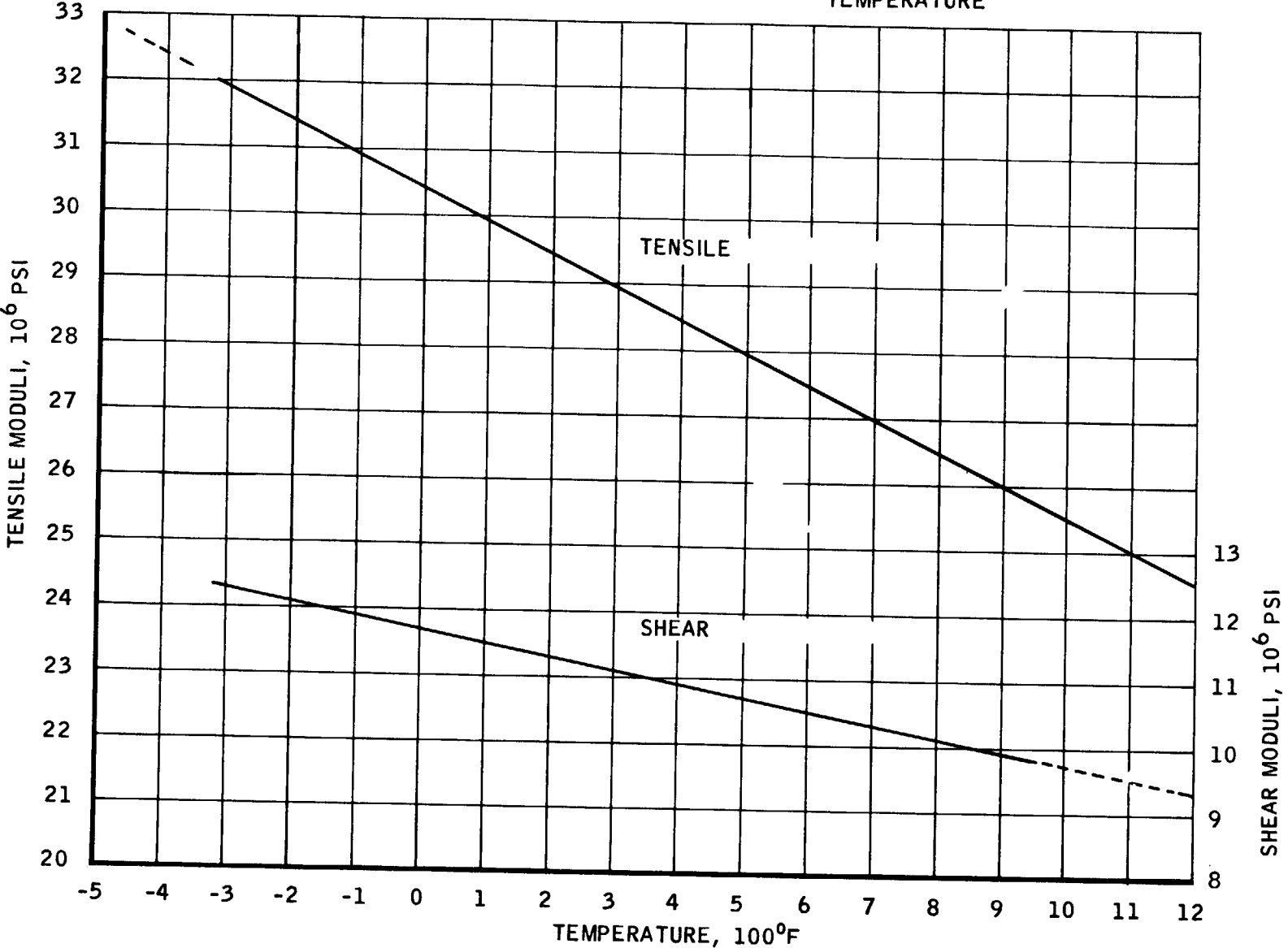
The static moduli of elasticity data, obtained from the tensile tests curves, are listed in Tables 7.2 and 7.3. The specimens evaluated were from

---

\*LASL Memorandum SN-A:HH (1196), J. J. Dickinson, 2 May 1966

\*\*ibid

HASTELLOY X BRAZED FORGINGS (AGC90056)  
 DESIGN TENSILE AND SHEAR MODULI VS  
 TEMPERATURE



42

Figure 7.1 - Hastelloy X Brazed Forgings (AGC 90056) Design  
 Tensile and Shear Moduli vs Temperature

TABLE 7.1

DYNAMIC MODULI OF HASTELLOY X RING FORGING  
HEAT 261-5-4000

Temperature		Modulus of Elasticity	Shear Modulus	Poisson's Ratio
(°C)	(°F)	(10 <sup>6</sup> psi)	(10 <sup>6</sup> psi)	
-193.5	-316	31.76	12.29	0.292
-193	-315	31.75	12.29	
-183	-301	31.72	12.28	
-136	-213	31.40	12.13	
- 91	-132	31.07	11.98	
- 90	-136	31.04	11.97	0.297
- 50	- 58	30.72	11.84	
- 16	+ 3	30.41	11.71	
- 2	28	30.27	11.65	0.299
+ 8	46	30.18	11.62	
10	50	30.17	11.61	
12	54	30.16	11.60	
21	70	30.03	11.54	
39	102	29.92	11.50	
56	133	29.80	11.43	
130	266	29.10	11.15	0.305
226	439	28.25	10.82	
228	442	28.34	10.83	0.308
320	608	27.47	10.49	0.309
324	615	27.48	10.49	
408	766	26.69	10.18	
420	788	26.61	10.12	0.315
470	878	26.09	9.92	
514	957	25.67	9.72	
516	979	25.64	9.70	0.322

- NOTES: 1. The density used in the calculation was 8.296 g/cm<sup>3</sup>: the average of four determinations from Heat 261-5-4000.  
 2. Measurements by J. M. Dickinson, LASL: LASL Memorandum SN-A:HH(1196), 2 May 1966.  
 3. Material processed through Phoebus braze-cycle prior to testing.  
 4. Poisson's ratio calculated.

TABLE 7.2

MODULUS OF ELASTICITY (STATIC) AND TANGENT MODULUS (0.2% OFFSET)  
HASTELLOY X HEAT 261-5-4000 (BRAZED FORGING)

Spec. No.	Specimen		Test Temp (°F)	Modulus of Elasticity		Tangent Modulus	
	Location (1)	Size (2)		(psi x 10 <sup>6</sup> )		(0.2% offset)	
						(psi x 10 <sup>6</sup> )	
W-50	AI	R3	-423	31.0		4.0	
W-60	AC	↓	↓	38.0		4.2	
W-61	AO	↓	↓	33.2		3.8	
W-47	TC	↓	↓	34.0		3.3	
				Average	<u>34.0</u>	Average	<u>3.8</u>
WA-112	AI	R1	-320	33.0		3.4	
WA-107	AC	↓	↓	32.2		3.0	
WA-102	AO	↓	↓	31.0		2.9	
WT-162	TI	↓	↓	31.4		3.1	
WT-157	TC	↓	↓	32.0		3.1	
WT-158	TO	↓	↓	31.5		3.2	
W-53	AO	R3		32.0		3.9	
W-59	AC	↓	↓	32.0		3.2	
W-58	AI	↓	↓	32.0		4.0	
W-48	TO	↓	↓	29.4		3.8	
W-15	TC	↓	↓	32.0		3.4	
W-83	ST-O	↓	↓	32.5		4.2	
W-80	ST-C	↓	↓	33.0		3.7	
				Average	<u>31.94</u>	Average	<u>3.5</u>

- NOTES: (1) Specimen sampling location is shown in Figure 8.1. The letter "A" = Axial, "I" = Inside Diameter, "C" = Center, "O" = Outside Diameter, "T" = Tangential, and "ST" = Short Transverse.
- (2) Size R3 refers to round R-3 tensile specimens. Size R1 refers to round R-1 tensile specimens.



TABLE 7.2 (cont.)

Spec. No.	Specimen		Test Temp (°F)	Modulus of Elasticity	Tangent Modulus		
	Location (1)	Size (2)		(psi x 10 <sup>6</sup> )	(0.2% offset) (psi x 10 <sup>6</sup> )		
W-2	TC	R3	Room	29.5	2.4		
W-8	TC	↓	↓	29.0	2.6		
W-81	STS			27.0	2.4		
W-82	STO			28.0	2.4		
W-52	AC			29.0	2.5		
WA-128	AC			R1	30.0	2.1	
WA-106	AC			↓	30.0	1.9	
WT-159	TC			↓	31.5	3.1	
WT-151	TC			↓	29.6	2.5	
					Average	<u>29.3</u>	Average <u>2.4</u>
WA-101	AC			R1	400	30.0	1.9
W-74	AC	R3	400	28.0	2.3		
			Average	<u>29.0</u>	Average <u>2.1</u>		
WT-152	TO	R1	800	30.0	1.9		
WT-156	TI	↓	↓	27.3	1.9		
WT-168	TI			26.5	1.9		
WT-169	TC			25.8	2.2		
WT-176	TO			27.5	1.9		
WA-100	AI			25.5	1.6		
WA-113	AC			27.5	1.8		
WA-114	AO			↓	27.0	1.8	

NOTES: (1) Specimen sampling location is shown in Figure 8.1. The letter "A" = Axial, "I" = Inside Diameter, "C" = Center "O" = Outside Diameter, "T" = Tangential, and "ST" = Short Transverse.

(2) Size R3 refers to round R-3 tensile specimens. Size R1 refers to round R-1 tensile specimens.

TABLE 7.2 (cont.)

Spec. No.	Specimen		Test Temp (°F)	Modulus of Elasticity (psi x 10 <sup>6</sup> )	Tangent Modulus (0.2% offset) (psi x 10 <sup>6</sup> )
	Location (1)	Size (2)			
W-5	TC	R3	800	26.0	1.8
W-29	TC	↓	↓	(30)	1.6
W-68	AC	↓	↓	26.8	1.8
W-69	AO	↓	↓	29.0	1.8
W-77	AI	↓	↓	26.0	1.8
			Average	<u>27.1</u>	Average <u>1.8</u>
WT-150	TI	R1	1200	24.5	1.5
WT-163	TC	↓	↓	24.0	1.6
WT-164	TO	↓	↓	23.5	1.7
WA-118	AI	↓	↓	23.0	1.0
WA-120	AO	↓	↓	21.5	1.5
WA-124	AC	↓	↓	21.6	1.4
			Average	<u>23.0</u>	Average <u>1.5</u>

- NOTES: (1) Specimen sampling location is shown in Figure 8.1.  
The letter "A" = Axial, "I" = Inside Diameter, "C" = Center  
"O" = Outside Diameter, "T" = Tangential, and "ST" = Short  
Transverse.
- (2) Size R3 refers to round R-3 tensile specimens.  
Size R1 refers to round R-1 tensile specimens.

TABLE 7.3

MODULUS OF ELASTICITY (STATIC) AND TANGENT MODULUS (0.2% OFFSET)  
HASTELLOY X HEAT 261-5-4001 (BRAZED FORGING)

Spec. No.	Specimen		Test Temp (°F)	Static	Tangent Modulus
	Location (1)	Size (2)		Modulus of Elasticity (psi x 10 <sup>6</sup> )	(0.2% offset) (psi x 10 <sup>6</sup> )
Z-3	TO	R3	-423	33.5	3.8
Z-23	TC	↓	↓	33.6	3.6
Z-29	TI			31.0	4.4
Z-48	TO			35.8	3.8
Z-53	AO			34.6	3.4
Z-66	AI			35.3	3.7
Z-68	AC			35.0	4.4
ZT-176	TI	R1		34.3	3.6
			Average	<u>34.1</u>	Average <u>3.8</u>
ZA-112	AI	R1	-320	31.6	4.4
ZA-117	AO	↓	↓	32.2	2.9
ZA-124	AC			28.8	3.5
ZA-125	AO			31.3	3.1
ZT-155	TO			31.8	3.4
ZT-156	TI			34.3	3.7
ZT-169	TC			29.4	4.4
ZT-174	TI	32.2	3.2		
Z-14	TC	R3		34.0	4.8
Z-40	TO	↓	↓	34.0	4.7
Z-45	TI	↓	↓	26.5	3.85

- NOTES: (1) Specimen sampling location is shown in Figure 8.1.  
The letter "A" = Axial, "I" = Inside Diameter, "C" = Center  
"O" = Outside Diameter, "T" = Tangential, and "ST" = Short  
Transverse.
- (2) Size R3 refers to round R-3 tensile specimens.  
Size R1 refers to round R-1 tensile specimens.

TABLE 7.3 (cont.)

Spec. No.	Specimen Location (1)	Size (2)	Test Temp (°F)	Static Modulus of Elasticity (psi x 10 <sup>6</sup> )	Tangent Modulus (0.2% offset) (psi x 10 <sup>6</sup> )
Z-52	AC	R3	-320	32.8	3.7
Z-58	AI	↓	↓	32.3	3.75
Z-76	AO	↓	↓	32.0	4.20
			Average	<u>31.7</u>	Average <u>3.8</u>
Z-80	STC	R3	Room	32.2	3.5
Z-81	STC	↓	↓	25.0	3.1
Z-82	STO	↓	↓	30.0	3.1
Z-83	STO	↓	↓	30.2	2.6
Z-11	TC	↓	↓	24.0	2.5
Z-39	TC	↓	↓	31.0	3.2
ZA-120	AO	R1		31.0	2.4
ZA-127	AC	↓	↓	30.4	2.15
ZT-160	TC	↓	↓	30.4	2.65
			Average*	<u>29.4</u>	Average <u>2.8</u>
ZA-128	AC	R1	400	29.6	2.2
ZT-157	TC	↓	↓	26.4	2.2
ZT-150	TI	↓	↓	29.0	2.6
Z-59	AC	R3		28.5	2.5
Z-30	TC	↓	↓	23.0	2.3
Z-51	AC	↓	↓	23.5	2.5
			Average	<u>26.8</u>	Average <u>2.4</u>

- NOTES: (1) Specimen sampling location is shown in Figure 8.1. The letter "A" = Axial, "I" = Inside Diameter, "C" = Center, "O" = Outside Diameter, "T" = Tangential, and "ST" = Short Transverse.
- (2) Size R3 refers to round R-3 tensile specimens. Size R1 refers to round R-1 tensile specimens.
- \*Omitting Specimens Z-11 and Z-39, which had poor stress strain curves, would result in an average modulus of 29.8 x 10<sup>6</sup> psi for room temperature.

TABLE 7.3 (cont.)

Spec. No.	Specimen		Test Temp (°F)	Static	Tangent Modulus			
	Location <sup>(1)</sup>	Size <sup>(2)</sup>		Modulus of Elasticity (psi x 10 <sup>6</sup> )	(0.2% offset) (psi x 10 <sup>6</sup> )			
ZA-100	AI	R1	800	26.0	1.8			
ZA-101	AC	↓		26.3	1.7			
ZA-102	AO			26.4	1.6			
ZT-152	TO			25.3	1.8			
ZT-158	TO			26.2	2.0			
ZT-159	TI			26.4	2.1			
ZA-106	AI			22.0	1.8			
ZA-107	AC			26.0	NA			
ZA-114	AO			25.3	1.6			
ZT-153	TI			30.5	1.9			
ZT-168	TI			25.2	1.9			
ZT-163	TC			27.8	1.8			
ZT-161	TO			27.0	1.9			
ZT-170	TO			26.6	1.8			
Z-2	TC			R3	22.0	2.1		
Z-8	TC			↓	22.0	2.1		
Z-37	TI				27.0	NA		
Z-31	TC				23.1	2.3		
Z-24	TO				23.5	2.1		
Z-50	AI				22.6	1.9		
Z-60	AC	23.0	1.9					
Z-69	AO	27.5	1.9					
					Average	25.3	Average	1.9

- NOTES: (1) Specimen sampling location is shown in Figure 8.1.  
The letter "A" = Axial, "I" = Inside Diameter, "C" = Center, "O" = Outside Diameter, "T" = Tangential, and "ST" = Short Transverse.
- (2) Size R3 refers to round R-3 tensile specimens.  
Size R1 refers to round R-1 tensile specimens.

TABLE 7.3 (cont.)

Spec. No.	Specimen		Test Temp (°F)	Static	Tangent Modulus
	Location <sup>(1)</sup>	Size <sup>(2)</sup>		Modulus of Elasticity (psi x 10 <sup>6</sup> )	(0.2% offset) (psi x 10 <sup>6</sup> )
ZA-118	AI	R1	1200	24.5	1.3
ZA-119	↓	↓	↓	23.5	1.4
ZT-162				23.0	1.4
ZT-151				23.3	1.5
ZT-164				23.2	1.7
ZA-108				AO	21.0
ZA-113	AC	23.0	1.6		
ZA-115	AI	21.0	1.7		
ZA-126	AO	↓	↓	25.0	1.4
			Average	<u>23.1</u>	Average <u>1.5</u>

- NOTES: (1) Specimen sampling location is shown in Figure 8.1.  
The letter "A" = Axial, "I" = Inside Diameter, "C" = Center,  
"O" = Outside Diameter, "T" = Tangential, and "ST" = Short  
Transverse.
- (2) Size R3 refers to round R-3 tensile specimens.  
Size R1 refers to round R-1 tensile specimens.

forgings from Heats 261-5-4000 and 261-5-4001, respectively. The static values of the tensile modulus of elasticity are generally lower than the dynamic modulus values and show a greater data spread. The static modulus values were taken from the tensile stress-strain curves and were affected by variations in the curves caused by strain rate, the extensometer response (lag), and the minor bending suffered at low stress-levels by nonperfect specimens.

The comparison of the static- and dynamic-modulus data from the same material is presented in Figure 7.2. The strain curves from tests at  $-423^{\circ}\text{F}$  tended to be more inaccurate because ice formed both on the specimens and the extensometer. At  $1200^{\circ}\text{F}$ , some evidence of creep is observed at the low strain-rates: thus, static values would be obtained better at higher strain rates. When a sizable number of tests were averaged, the results were not greatly influenced by omitting values from poor curves. All listed data, therefore, were used in the averages.

The tangent modulus data were also taken from the stress-strain curves and the values listed in Tables 7.1 and 7.2. The average tangent modulus data are plotted in Figure 7.3 to show temperature effects. It was noted that the two alloy heats (261-5-4000 and 261-5-4001) showed very good concurrence at both high and low temperatures.

## 7.2 THERMAL EXPANSION

The coefficient of thermal expansion values is shown in Figure 7.4. The elevated temperature (room to  $1800^{\circ}\text{F}$ ) portions of the curve were obtained from an average of four tests. Four additional tests were made to obtain the cryogenic contraction data from room temperature to  $-400^{\circ}\text{F}$ . The low-temperature values were lower than the literature data, but were verified by re-runs and by three separate specimens in the brazed condition. The original specimens in the "as-machined" condition tended to be erratic in the low and intermediate temperature regions which was corrected by stress

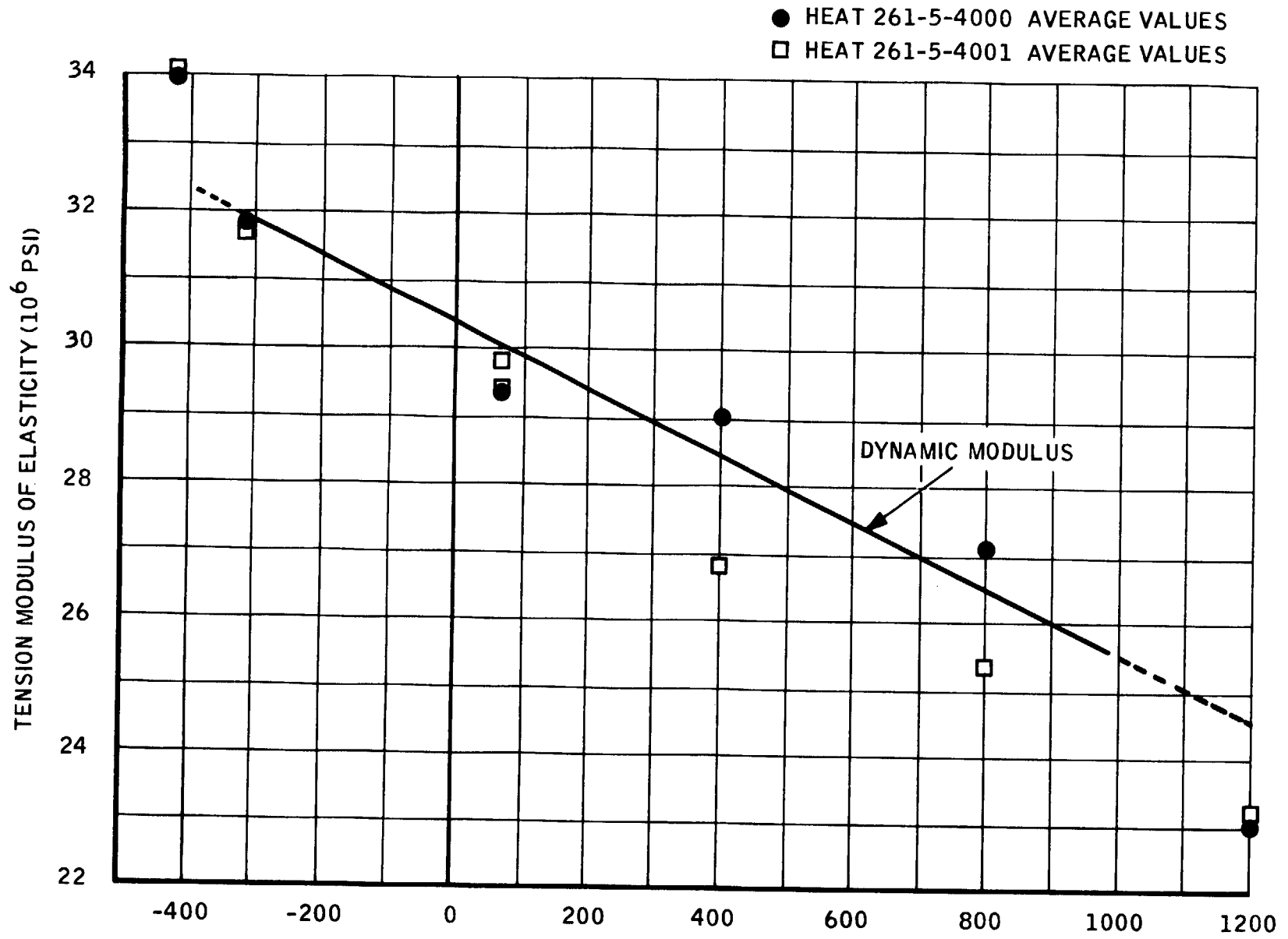


Figure 7.2 - Hastelloy X Braze Forgings (AGC 90056) Modulus of Elasticity in Tension, Dynamic Versus Static



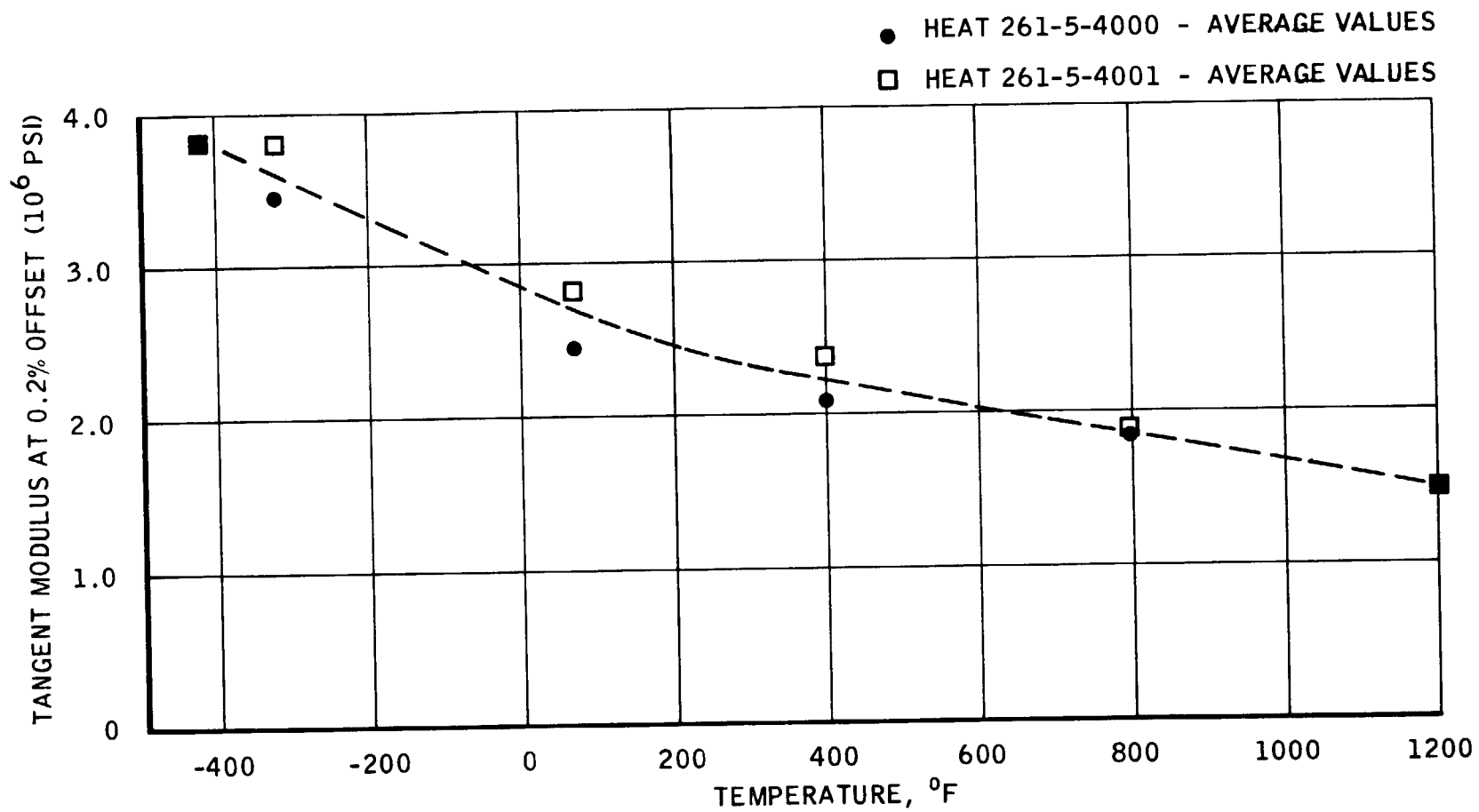


Figure 7.3 - Hastelloy X Brazed Forgings (AGC 90056) Tangent Modulus at 0.2% Offset Versus Temperature

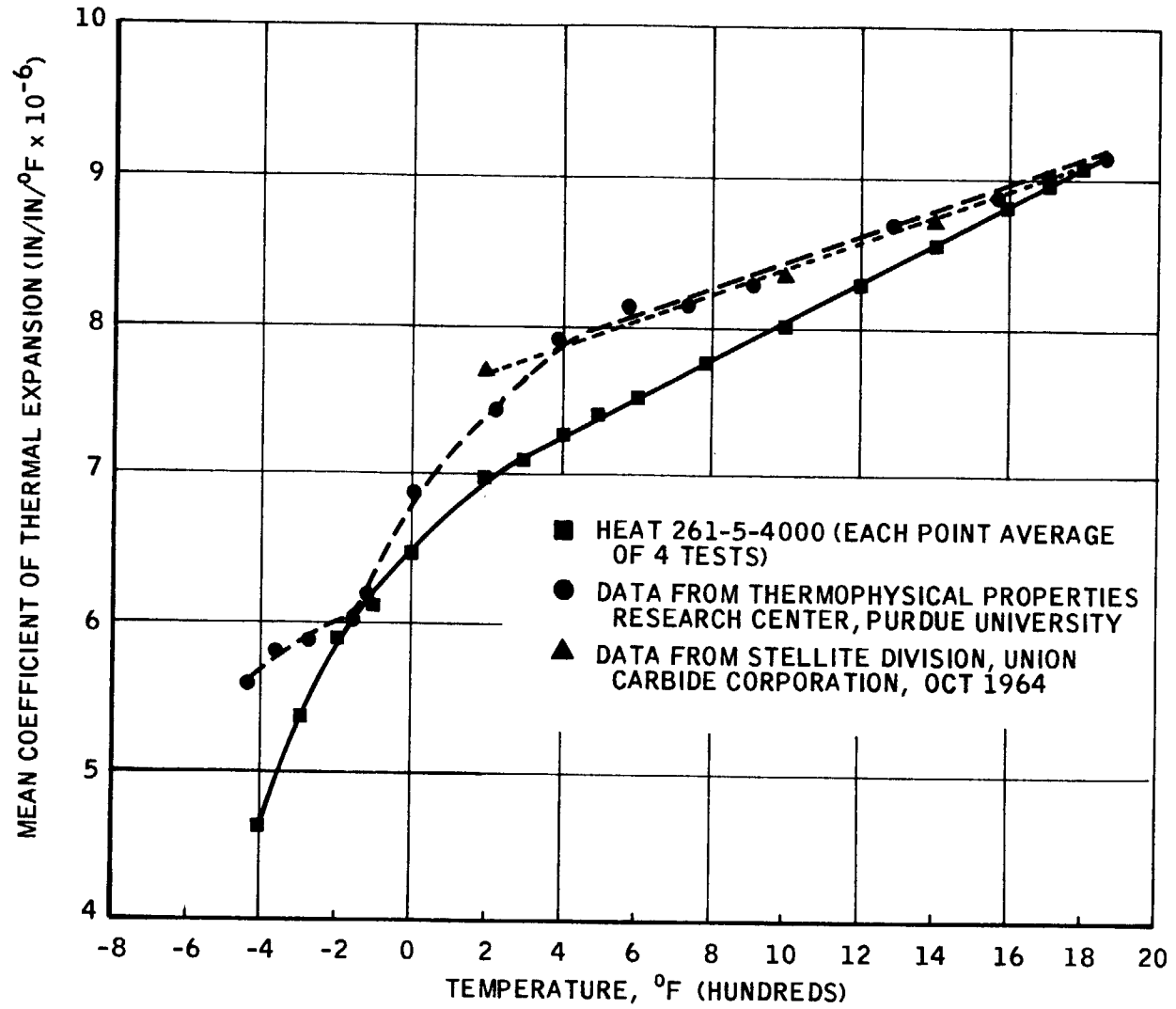


Figure 7.4 - Hastelloy X Brazed Forgings (AGC 90056) Mean Coefficient of Thermal Expansion

relieving at 1700°F prior to measurement. The elevated temperature measurements were made by means of a Leitz dilatometer, while the cryogenic runs employed a vertical, quartz-tube dilatometer adapted to a hydrogen cryostat. The specimens were oriented axially in the forging: i.e., parallel to the length of the forging.

Table 7.4 lists the actual results of elevated temperature and cryogenic measurements. The observed values of the mean coefficient are approximately 10% lower than the literature values for the temperature range from 200 to about 500°F (see Figure 7.4). At higher temperatures, the data converge with good agreement above 1500°F.

The possibility that the anisotropy observed in the elongation and the ultimate strength data from the ring forgings may have contributed to the apparent divergencies in available data was explored. The tangential and axial values of Table 7.4 indicate that there is no detectable directionality in the expansion data. Therefore, the variance is attributed, at least in part, to the effects of the brazing cycle.

### 7.3 THERMAL DIFFUSIVITY (CONDUCTIVITY)

The thermal conductivity data shown in Table 7.5 were computed from the thermal diffusivity data by means of the relationship: thermal diffusivity =  $\frac{K}{\rho C_p}$ . The specific heat ( $C_p$ ) and density ( $\rho$ ) were known (or could be computed at varying temperatures) so no disadvantage was evident from this indirect approach. One definite advantage cited was the need for accurate thermal-diffusivity data at low temperatures for the thermal-stress calculations.

Below -200°F, specific heat values decline rapidly with temperature. Thus, the errors in such data may be greater than those recorded for other properties. Therefore, the direct measurement of diffusivity was preferred where thermal data were needed at cryogenic temperatures. The thermal-diffusivity specimens (0.60 inch in diameter and 0.10 inch in length) were

TABLE 7.4

MEAN COEFFICIENT OF THERMAL EXPANSION  
HASTELLOY X BRAZED RING FORGING (AGC 90056)  
(HEAT 261-5-4000)

Temp. (°F)	$\Delta L/L$	Actual <sup>(1)</sup> CTE x 10 <sup>6</sup> (in./in./°F)	Average CTE x 10 <sup>6</sup> (in./in./°F)
<u>Orientation - Axial</u>			
-400	224.8	4.79	4.62 ↓
↓	208.3	4.43	
↓	215.9	4.59	
↓	220.0	4.68	
-300	195.2	5.28	5.37 ↓
↓	201.0	5.43	
↓	202.2	5.45	
↓	197.1	5.32	
-200	160.0	5.92	5.88 ↓
↓	155.5	5.75	
↓	158.1	5.85	
↓	161.8	6.03	
-100	99.64	5.85	6.11 ↓
↓	103.57	6.09	
↓	105.21	6.20	
↓	107.12	6.30	
0	44.82	6.40	6.49
0	45.80	6.58	

(1) Reference temperature was 70°F for all values of mean coefficient of thermal expansion

TABLE 7.4 (cont.)

<u>Orientation - Tangential</u>		<u>Orientation - Axial</u>		
<u>Temp (°F)</u>	<u>CTE x 10<sup>6</sup></u>	<u>Warming CTE x 10<sup>6</sup></u>	<u>Cooling CTE x 10<sup>6</sup></u>	<u>Average CTE x 10<sup>6</sup></u>
200	6.83	6.86	7.11	6.98
300	7.06	7.04	7.15	7.08
400	7.23	7.30	7.30	7.28
500	7.38	7.38	7.38	7.38
600	7.52	7.48	7.57	7.52
800	7.72	7.73	7.84	7.77
1000	7.89	7.96	8.04	8.00
1200	8.24	8.26	8.31	8.29
1400	8.57	8.59	8.52	8.56
1600	8.81	8.80	8.84	8.82
1700	8.92	8.90	8.98	8.93
1800	9.08	9.05	9.12	9.08

TABLE 7.5

THERMAL CONDUCTIVITY, DIFFUSIVITY, AND SPECIFIC HEAT  
HASTELLOY X BRAZED FORGING (HEAT 261-5-4000)

Temperature		Density (a)		Specific (c) Heat	Thermal Diffusivity (b)	Thermal Conductivity	
°C	°F	g/cc	lb/in <sup>3</sup>	cal/gm°C	cm <sup>2</sup> /sec	Cal/Sec°C	Btu/hr/ft°F
-180	-292	8.343	.3014	.045	.0341	.0128	3.09
-160	-256	8.340	.3013	.057	.0318	.0151	3.65
-123	-190	8.334	.3011	.076	.0300	.0190	4.60
-100	-148	8.328	.3009	.830	.0294	.0203	4.92
- 73	-100	8.323	.3007	.900	.0291	.0218	5.27
- 18	0	8.310	.3002	.100	.0290	.0241	5.83
21	70	8.296	.2995	.105	.0294	.0256	6.19
100	212	8.275	.2990	.110	.0309	.0281	6.80
204	400	8.243	.2975	.115	.0335	.0318	7.68
316	600	8.205	.2964	.119	.0369	.0360	8.71
427	800	8.163	.2949	.123	.0402	.0407	9.84
500	932	8.130	.2937	.127	.0424	.0438	10.59
538	1000	8.120	.2934	.129	.0434	.0455	11.01
649	1200	8.066	.2913	.139	.0467*	.0523	12.68

- (a) Densities listed are based on measured values at 70°F for Heat 261-5-4000. The vendor literature value of 8.23 g/cm<sup>3</sup> was found to be low as compared to the value of 8.296 g/cm<sup>3</sup> measured by Dickinson of LASL and by Aerojet. Densities at other temperatures were computed from expansion data.
- (b) Measured by Baker and Nightingale, Battelle Memorial Institute, Northwest, using the method of D. E. Baker, Journal of Nuclear Materials 12, 1(1964), pp 120-124.
- (c) Cp values from vendor literature from room temperature to 1200°F. The low temperature values were computed by the Debye Theory using atomic heats from R. Hultgren, R. L. Orr, P. D. Anderson and K. K. Kelley, Selected Values of Thermodynamic Properties of Metals and Alloys, John Wiley and Sons, 1963.

\*Extrapolated.

made at Aerojet-General and the tests performed by D. E. Baker and R. E. Nightingale at Battelle Memorial Institute, Northwest.

The thermal conductivity data are presented in Figure 7.5 together with data from UCCSD and the Thermo-Physical Properties Research Center, Purdue University. The concurrence from 200 to 1200°F is very good, but some discrepancy exists between +200 and -200°F. Since the three sources of data check well at elevated temperatures, the difference observed at room temperature and lower either may be due to experimental error or to inaccurate specific-heat values which had to be computed in the absence of measured values. The specific-heat and density values used are shown in Figure 7.6. Two specific-heat values at room temperature have been reported: 0.105 and 0.116 Cal/gm °C.\*

The lower  $C_p$  value was used since it was consistent with the curve (see Figure 7.6). The higher  $C_p$  value would yield a computed room temperature conductivity value of 6.8 Btu/hr ft °F which is 10% higher than the upper curve on Figure 7.5

The density data in Table 7.5 was computed to correct for the effect of thermal expansion. The density of Heat 261-5-4000 was higher (8.296 g/cm<sup>3</sup>) than that reported in vendor literature (8.23 g/cm<sup>3</sup>). The higher density observed by Dickinson at LASL was confirmed by Aerojet-General on two heats of material. The difference is probably the result of carbide precipitation caused by the brazing cycle. The thermal diffusivity values plotted in Figure 7.7 are those reported by Baker and Nightingale.

---

\*The lower value agrees with that computed by the Debye Theory, as shown in Table 7.5.

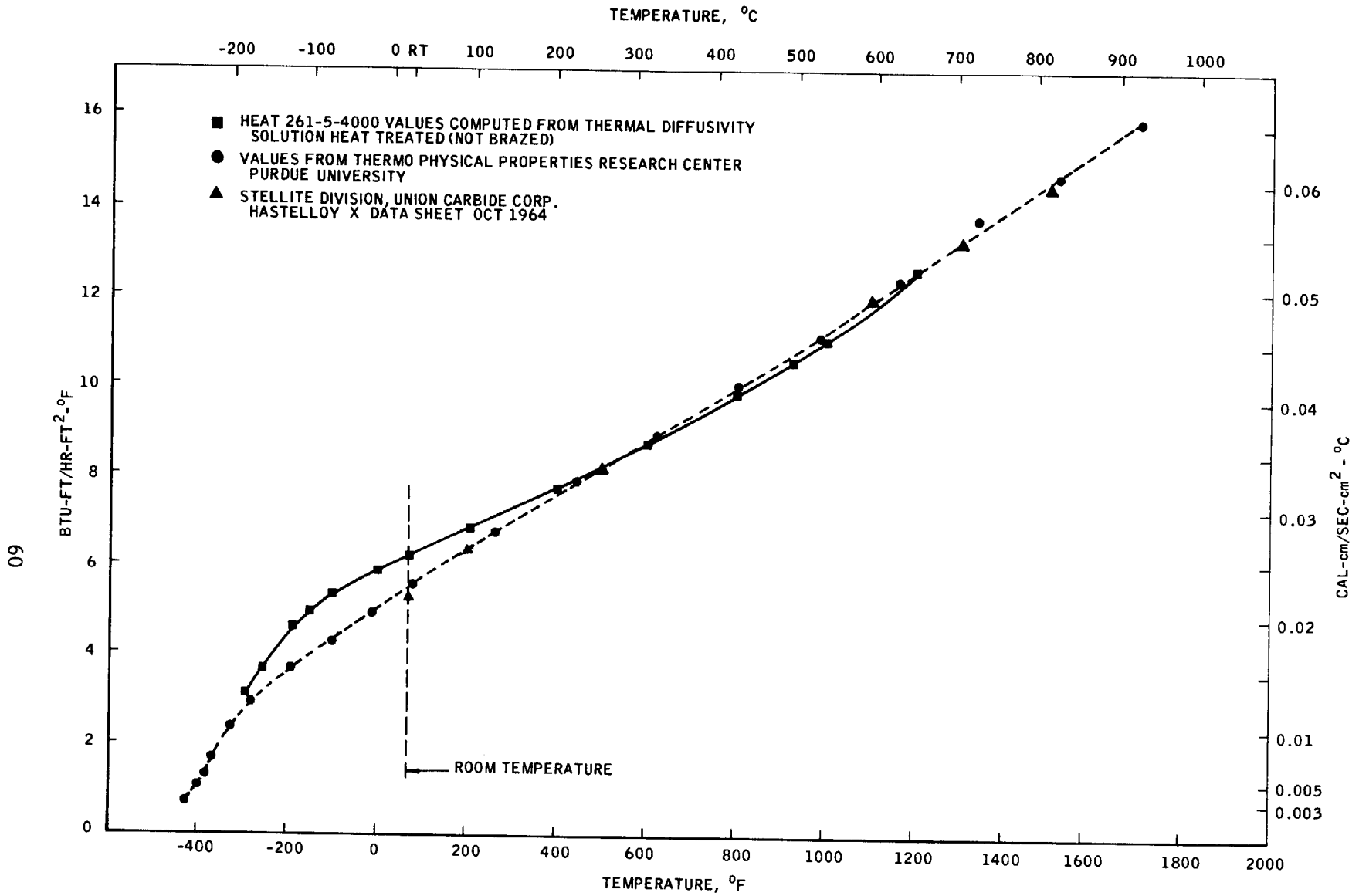
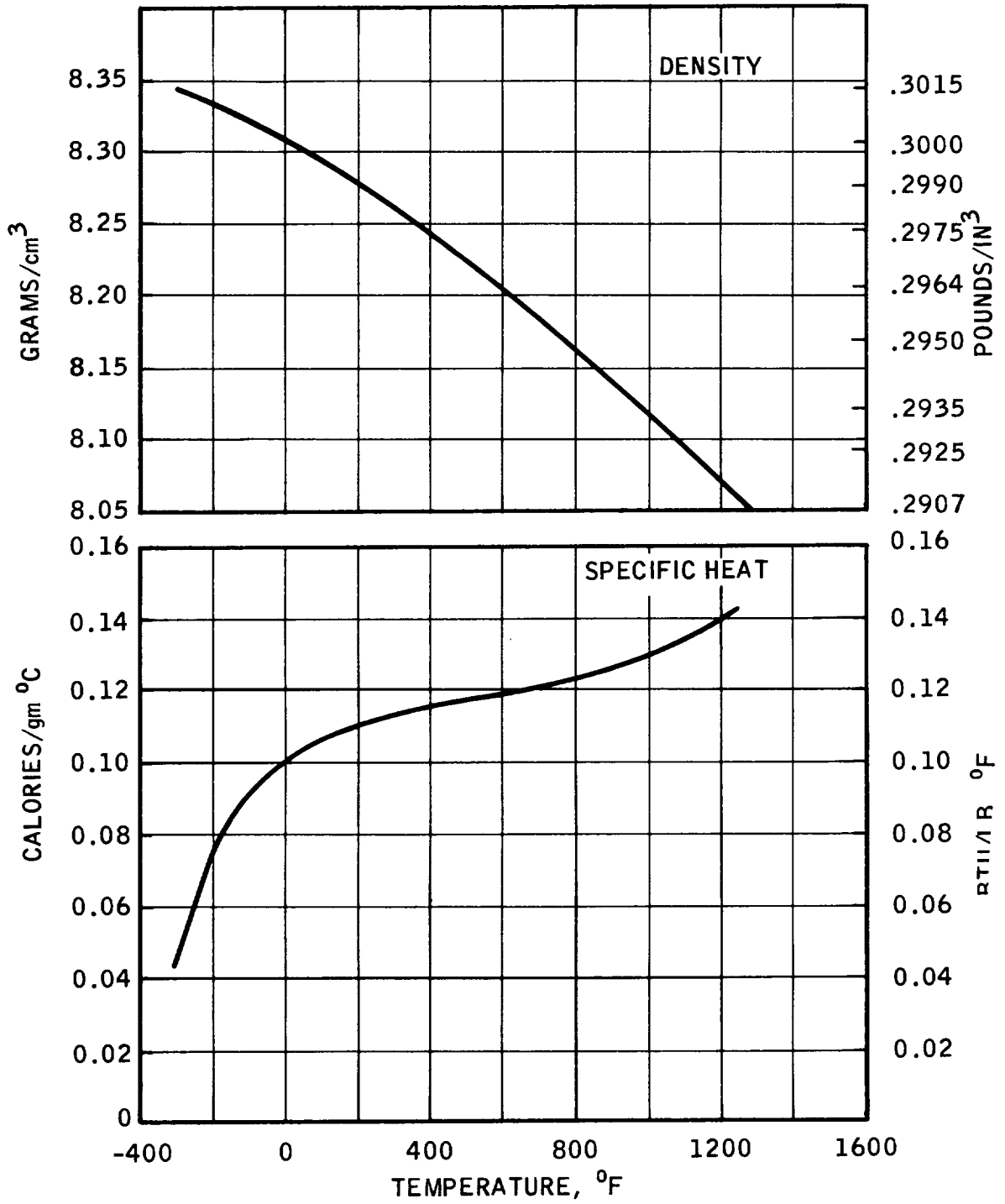


Figure 7.5 - Hastelloy X Brazed Forging Thermal Conductivity





NOTE: VALUES BELOW 70°F WERE COMPUTED

Figure 7.6 - Hastelloy X Brazed Forging Specific-Heat and Density Values

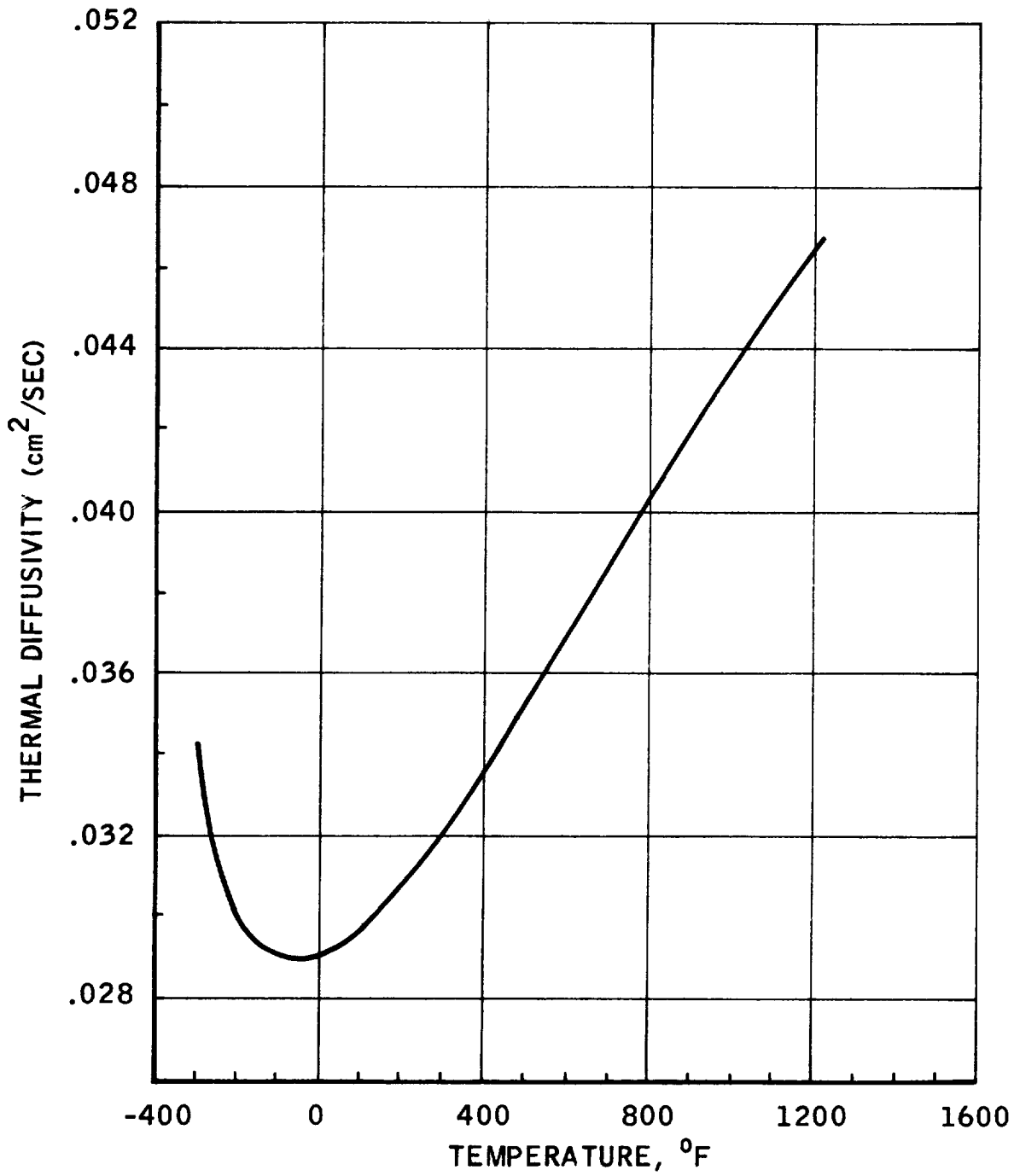


Figure 7.7 - Hastelloy X Brazed Forging Thermal Diffusivity Values,  
Heat 261-5-4000 (Source: D. E. Baker and R. E. Nightingale  
Battelle, Northwest)

## 8.0 MECHANICAL PROPERTIES

The objective of the design properties data program was to provide representative design (or minimum) data for Hastelloy X forgings and coolant tube strip over the full range of temperature to be experienced in nozzle operation. Despite many years of experience with this alloy, there was a significant lack of property data from which reliable design properties could be obtained for the heavy-wall forgings required. There was also little data regarding the effects of thermal treatments, such as the brazing operation employed in nozzle fabrication. All data presented in this section were developed from ring forgings and strip stock processed through a representative, simulated nozzle-brazing operation. Data obtained included:

<u>Forgings</u>	<u>Strip</u>
Tensile properties	Tensile properties
Compression properties	Bearing properties
Shear properties	

The temperature range was -423 to 1200°F for the forgings and -423 to 1800°F for the strip stock.

Physical properties were also obtained and are presented in Section 7.0. The fabrication and processing of the forgings and strip stock are discussed in Sections 2.0, 3.0, 4.0 and 5.0. Materials procured met all requirements of respective specifications. In addition, all machined specimens were dye-penetrant and ultrasonic or X-ray inspected prior to testing.

The 2150°F solution heat-treated tensile properties of materials utilized in the design properties program are listed in Tables 8.1 and 8.2. The tensile properties of the welded plates and rings in the solution heat-treated condition are shown in Tables 8.3 and 8.4.

TABLE 8.1

SUMMARY OF AVERAGE TENSILE PROPERTIES OF ANNEALED\* HASTELLOY X  
PLATE AND STRIP (AGC 90057) UTILIZED IN DEVELOPMENTAL PROGRAMS

<u>Material Heat No.</u>	<u>Form</u>	<u>Temp. (°F)</u>	<u>UTS (ksi)</u>	<u>0.2% YS (ksi)</u>	<u>Elong. (%)**</u>
260-5-2813	1-1/2-in. plate	Room	104.8	45.2	57
261-5-4000	↓	↓	100.0	42.1	48
261-5-4001	↓	↓	99.1	44.4	50
All	↓	↓	101.3	43.9	52
260-5-2813	1-1/2-in. plate	1200	75.2	26.8	59
261-5-4000	↓	↓	73.6	25.3	40
261-5-4001	↓	↓	76.4	27.9	68
All	↓	↓	75.0	26.7	56
261-5-4000	0.012-in. strip	Room	112.0	55.9	40
261-5-4001	↓	↓	113.7	56.2	39
261-5-4002	↓	↓	109.0	49.6	40
All	↓	↓	111.6	53.9	40
261-5-4000	0.012-in. strip	1200	80.0	31.4	43
261-5-4001	↓	↓	82.8	36.3	53
261-5-4002	↓	↓	81.0	32.9	49
All	↓	↓	81.1	33.5	48

Notes: \* One hour at 2150°F and water-quench for plate;  
5 to 10 minutes at 2150°F and jet-blast cool for strip.

\*\* R-1 specimens with 2.0-inch gage length for plate and  
flat 0.5-inch wide by 2.0-inch gage length for strip.

1. Strain rate 0.005-in./in./min to yield, then 0.05-in./in./min  
to failure.

2. Specimens oriented parallel to direction of rolling.

TABLE 8.2

TENSILE PROPERTIES OF ANNEALED\* HASTELLOY X  
PLATE, SHEET, AND STRIP (AGC 90057) AND BAR  
(AGC 90056) UTILIZED IN DEVELOPMENT PROGRAM

<u>Material Heat No.</u>	<u>Form</u>	<u>Temp. (°F)</u>	<u>UTS (ksi)</u>	<u>0.2% YS (ksi)</u>	<u>Elong. (ksi)**</u>
260-5-2813 ↓	1-1/2-in. plate ↓	Room	104.7	45.0	56 (S)
		Room	105.0	45.5	58 (V)
		1200	75.8	26.8	61 (S)
		↓	78.8	27.4	61 (S)
		↓	71.1	26.1	56 (V)
261-5-4000 261-5-4000	1-1/2-in. plate	Room	100.0	42.1	48 (V)
	1-1/2-in. plate	1200	73.6	25.3	40 (V)
261-5-4000 ↓	0.050-in. sheet ↓	Room	109.0	47.6	44 (S)
		1200	83.2	34.1	48 (S)
		1200	84.3	32.4	48 (S)
261-5-4000 ↓	0.012-in. strip ↓	Room	113.7	52.8	41 (S)
		↓	112.0	57.8	39
		↓	110.8	55.7	43
		↓	111.6	57.6	35
		1200	80.7	33.2	43 (S)
		1200	79.4	29.7	43 (S)
261-5-4001 261-5-4001	1-1/2-in. plate	Room	99.1	44.4	50 (V)
	1-1/2-in. plate	1200	76.4	27.9	68 (V)
261-5-4001 ↓	0.012-in. strip ↓	Room	113.7	56.2	39 (S)
		1200	84.1	33.2	46 (S)
		1200	81.5	39.4	61 (S)
261-5-4002 ↓	0.012-in. strip ↓	Room	109.0	49.6	40 (S)
		1200	81.9	30.1	49 (S)
		1200	80.1	35.7	49 (S)
261-5-4003 ↓	3/4-in. bar*** ↓	Room	102.0	40.5	53 (S)
		1200	76.1	25.3	62 (S)
		↓	75.5	26.0	60 (S)
		↓	75.9	25.9	61 (S)
260-5-2783 ↓	1-1/2-in. plate*** ↓	Room	111.5	55.0	46 (S)
		1200	101.5	32.4	62 (S)
		1200	75.6	29.8	63 (S)
260-5-2784 ↓	1-1/2-in. plate*** ↓	Room	111.7	49.9	44 (S)
		1200	84.7	34.3	42 (S)
		1200	81.1	29.1	56 (S)

TABLE 8.2 (cont.)

- NOTES:
- \* One hour at 2150°F and water quench for plate and bar;  
3 to 5 minutes at 2150°F and jet-blast cool for strip.
  - \*\* R-1 specimens with 2.0-inch gage length for plate and bar,  
0.5-inch wide by 2.0-inch long gage length for strip and  
sheet.
  - \*\*\* End product 0.045-inch and 0.062-inch weld wire to require-  
ments of AGC 90058.
1. Strain rate 0.005-in./in./min to yield, then 0.05-in./in./min  
to failure.
  2. Specimens oriented parallel to direction of rolling.
- (V) Tested by Viking Forge, Albany, California.
- (S) Tested by Stellite Division, Union Carbide Corporation

TABLE 8.3

SUMMARY OF AVERAGE TENSILE PROPERTIES OF ANNEALED\* WELDMENTS  
OF HASTELLOY X FORGINGS (AGC 90056) AND PLATE (AGC 90057)

<u>Material Heat No.</u>	<u>Orientation</u>	<u>Form</u>	<u>Temp (°F)</u>	<u>UTS (ksi)</u>	<u>0.2% YS (ksi)</u>	<u>Elong (%)**</u>
260-5-2813	Axial	Forged Ring***	Room	95.6	46.6	62/52
261-5-4000	↓	↓	↓	102.5	51.5	48/42
261-5-4001	↓	↓	↓	101.5	49.4	46/42
All Heats	↓	↓	↓	99.9	49.2	52/45
260-5-2813	Axial	Forged Ring	1200	64.6	29.1	70/56
261-5-4000	↓	↓	↓	68.3	28.5	39/38
261-5-4001	↓	↓	↓	67.2	25.5	31/36
All Heats	↓	↓	↓	66.7	27.7	47/43
261-5-4000	Transverse	Plate****	Room	94.7	50.8	23/25
261-5-4001	↓	↓	↓	100.5	49.8	41/36
All Heats	↓	↓	↓	97.6	50.3	34/30

NOTES:

- \* One hour at 2150°F, water quench.
- \*\* R-1 specimens with 2.0-inch gage length: first number 1.0-inch gage; second number 2.0-inch gage
- \*\*\* Forged and rolled ring made by Viking Forge, 20-inch OD, 17-inch ID, by 6 inches long.
- \*\*\*\* 1-1/2 inches thick plate, specimens transverse to rolling direction.

1. All specimens failed in parent metal and were semi-automatic welded.
2. Strain rate 0.005-in./in./min to yield, then 0.05-in./in./min to failure.

TABLE 8.4

TENSILE PROPERTIES AND HARDNESS OF ANNEALED\* WELDMENTS  
OF HASTELLOY X FORGINGS (AGC 90056) AND PLATE (AGC 90057)

<u>Material Heat No.</u>	<u>Orientation</u>	<u>Form</u>	<u>Temp (°F)</u>	<u>UTS (ksi)</u>	<u>0.2% YS(ksi)</u>	<u>Elong (%)**</u>	<u>Hardness, R<sub>b</sub></u>		<u>Weld Wire Heat No.</u>
							Base	Weld	
260-5-2813	Axial	Forged Ring***	Room	95.5	46.9	60/50	89	86	261-5-4003
			Room	95.7	46.2	64/54			
			1200	64.6	29.1	70/56			
260-5-2813 261-5-4000	Transverse	Plate****	Room	98.7	50.3	28/32	-	-	260-5-2784
				95.8	50.9	- /23			
				89.5	51.2	17/20			
	Axial	Forged Ring***	Room	102.0	50.2	48/43	93	92	260-5-2784
			Room	103.0	52.8	48/42			
			1200	65.6	31.0	24/30			
			1200	71.0	25.9	54/46			
261-5-4001	Transverse	Plate****	Room	97.6	49.5	33/32	-	-	260-5-2783
				100.0	48.3	47/37			
				104.0	51.6	43/40			
	Axial	Forged Ring***	Room	101.0	49.1	46/42	95	95	260-5-2783
			Room	102.0	49.7	47/43			
			1200	64.4	24.3	18/23			
			1200	70.0	26.6	44/49			

NOTES:

\* One hour at 2150°F, then water-quench.

\*\* R-1 specimens with 2.0-inch gage length: first number 1.0-inch gage; second number 2.0-inch gage.

\*\*\* Forged and rolled ring made by Viking Forge, 20-inch OD, 17-inch ID, by 6 inches long.

\*\*\*\* 1-1/2 inch thick plate, specimens transverse to rolling direction.

1. All specimens failed in parent metal and were semi-automatic welded.
2. Strain rate 0.005-in./in./min to yield, then 0.05-in./in./min to failure.



## 8.1 SPECIMEN LOCATIONS, ORIENTATION, AND CONFIGURATION

Specimen identification, location, and orientation for the 3-inch wall-thickness ring forgings are illustrated in Figure 8.1 for Heat 261-5-4000. The same layout was employed with Heat 261-5-4001 except the letter "Z" replaced the letter "W". The double-letter specimens were the ASTM R-1 type tensiles. The single-letter specimens were R-3 tensiles. Tensile specimen configurations are illustrated in Figure 8.2.

The typical specimen layout for the welded ring forgings is shown in Figure 8.3 for Heat 261-5-4000. Heats 261-5-4001 and 260-5-2813 were the same except the code letters were "H" and "G", respectively.

The strip tensile specimens were tested in the direction parallel to the rolling direction for Heats 261-5-4000, 261-5-4001, and 261-5-4002. Tensile specimen configurations are shown in Figure 8.4.

## 8.2 STATISTICAL TENSILE TEST PLANS

To improve the usefulness and reliability of tensile test data, the original ring forging (welded and unwelded) testing plans were altered for statistical analysis. Briefly, the plans involved testing at various temperatures to establish "property-vs-temperature" curves and then concentrating testing at specific temperatures to establish standard deviation limits. The test plans for ring-forging Heats 261-5-4000 and 261-5-4001 are shown in Table 8.5, while Table 8.6 illustrates the test plan employed for the welded forged rings. The plans provided for "pooling" test results for design use as well as analysis of the specimen size and orientation/location effects.

The tensile test results for the 0.012-inch thick strip material were analyzed statistically, but the plan was not altered from the conventional

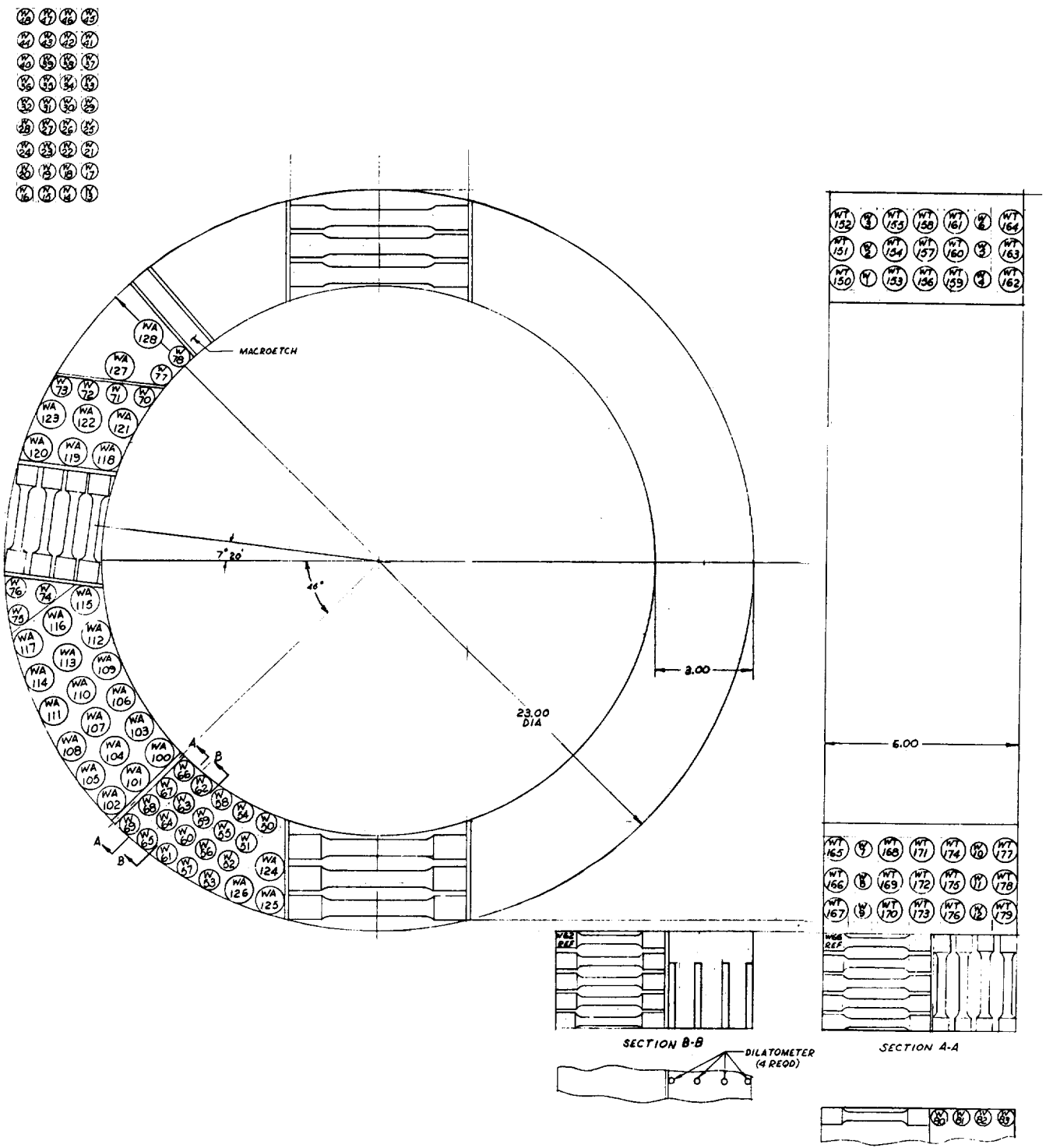


Figure 8.1 - Specimen Layout Plan, Forging Heat 261-5-4000

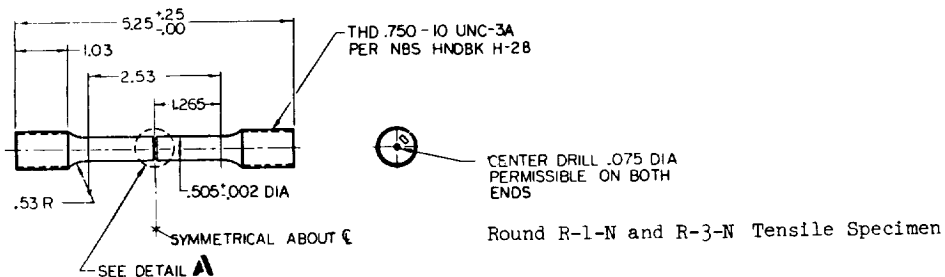
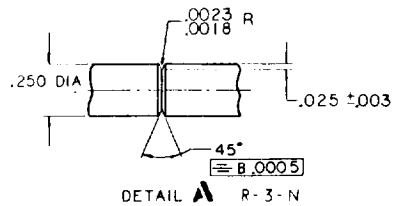
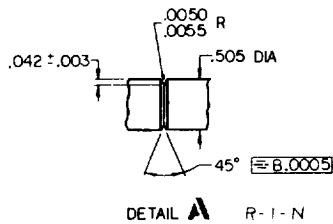
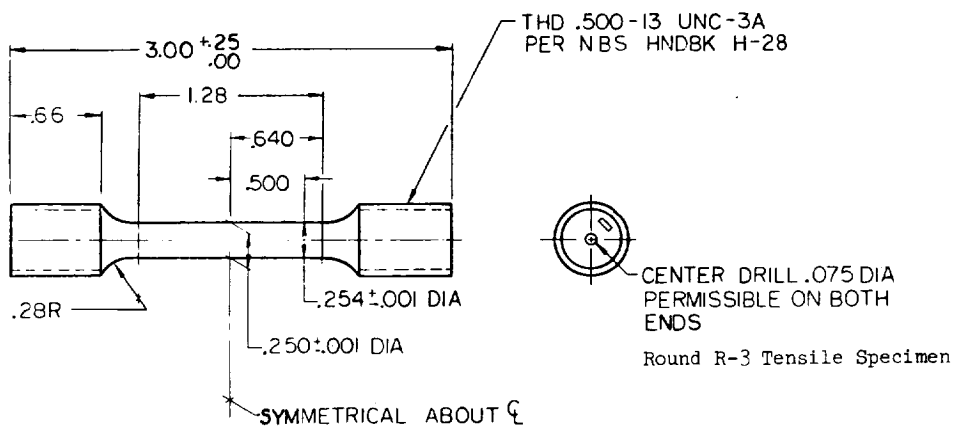
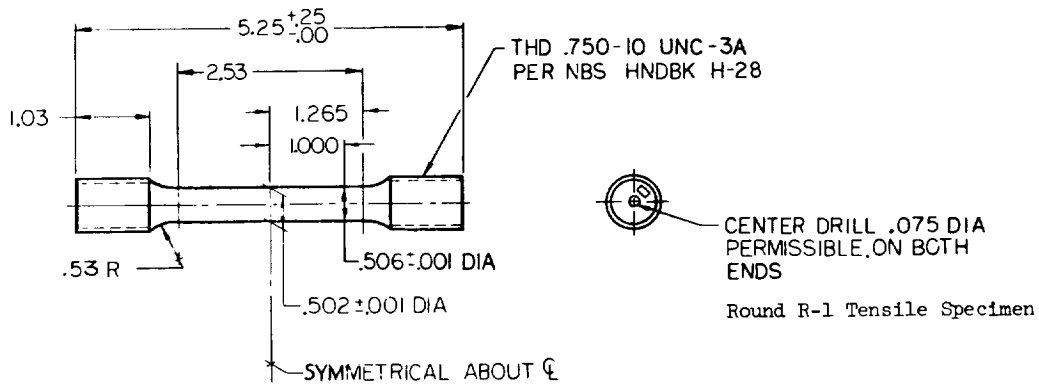


Figure 8.2 - Tensile Test Specimens Used for Forging and Welded Ring Evaluation

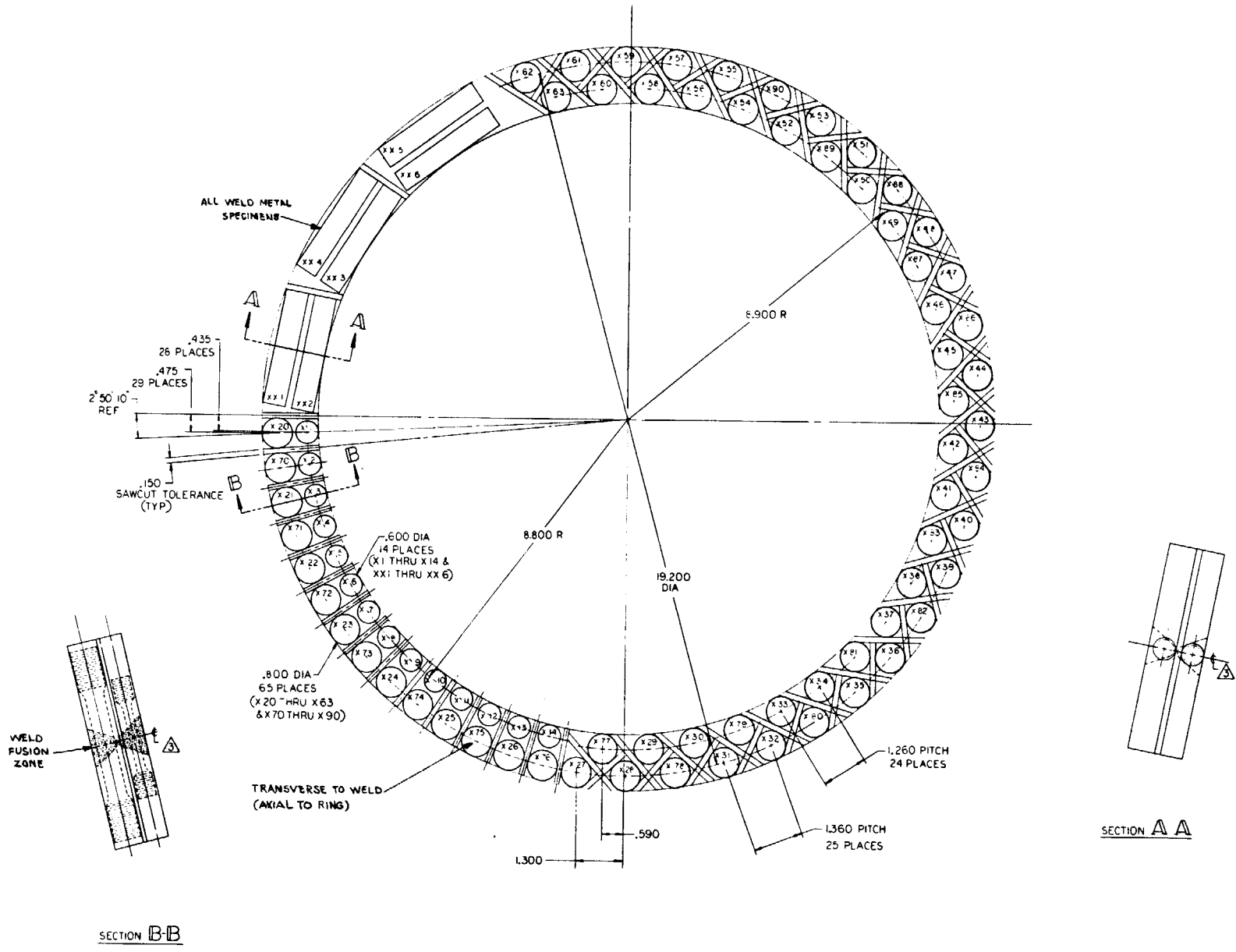
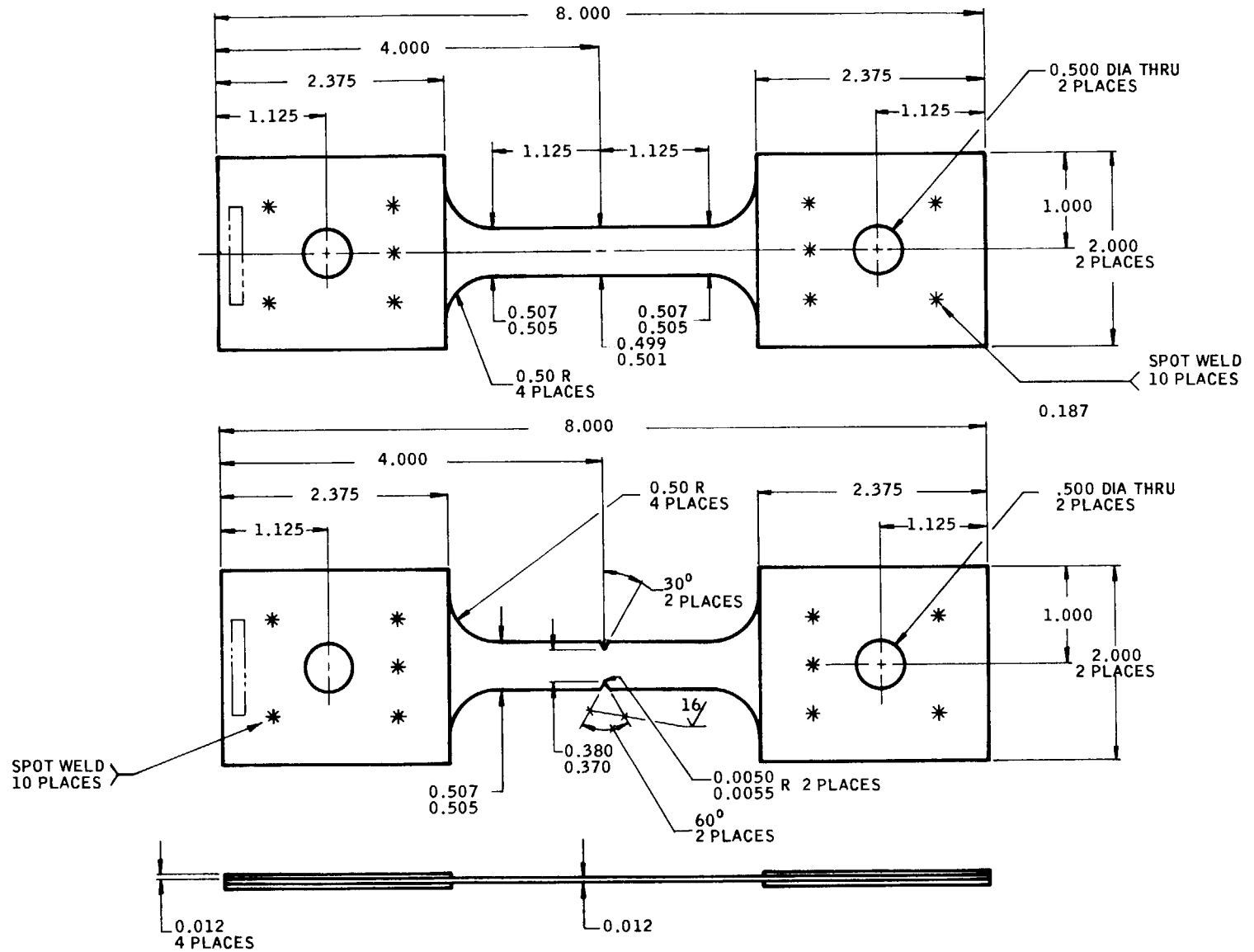


Figure 8.3 - Sample Plan Specimen Layout for Welded Ring Forging, Heat 261-5-4000



NOTE: DIMENSIONS IN INCHES

Figure 8.4 - Notched and Unnotched Coolant Tube Strip Tensile Specimens

TABLE 8.5

STATISTICAL TEST PLANS FOR RING FORGINGS

Heat 261-5-4000

Temp.	Orient.	Smooth Specimens						Notched Specimens												
		R <sub>1</sub>	R <sub>1</sub>	C	R <sub>1</sub>	R <sub>3</sub>	OD	R <sub>1</sub>	R <sub>3</sub>	C	R <sub>1</sub>	R <sub>3</sub>	OD							
-423	Ax.	W	W	W	W	W	W	W	W	W	W	W	W	W	W	W	W	W		
		50	50	60	60	61		54	55	57										
		W	W	W	W	W	W	W	W	W	W	W	W	W	W	W	W	W	W	
-320	Ax.	W	W	W	W	W	W	W	W	W	W	W	W	W	W	W	W	W	W	
		50	50	59	59	107		53	102	62	115	72	104	75	123					
		W	W	W	W	W	W	W	W	W	W	W	W	W	W	W	W	W	W	W
70	Ax.	W	W	W	W	W	W	W	W	W	W	W	W	W	W	W	W	W	W	W
		37	37	162	15	157		148	158	17	177	26	172	20	173					
		W	W	W	W	W	W	W	W	W	W	W	W	W	W	W	W	W	W	W
400	Ax.	W	W	W	W	W	W	W	W	W	W	W	W	W	W	W	W	W	W	W
		77	77	100	68	113		69	114	70	103	71	110	73	111					
		W	W	W	W	W	W	W	W	W	W	W	W	W	W	W	W	W	W	W
800	Ax.	W	W	W	W	W	W	W	W	W	W	W	W	W	W	W	W	W	W	W
		29	29	156/168	W/N/W	169		32	152/176	41	165	34	166	28	167					
		W	W	W	W	W	W	W	W	W	W	W	W	W	W	W	W	W	W	W
1200	Ax.	W	W	W	W	W	W	W	W	W	W	W	W	W	W	W	W	W	W	W
		118	118	124	124	124		120	120	109	127	105	105	119						
		W	W	W	W	W	W	W	W	W	W	W	W	W	W	W	W	W	W	W

NOTE: WA Specimens - Axial - R<sub>1</sub> (Round Tensiles) W-1 thru W49 Tangential - R<sub>3</sub> Specimens  
 WT Specimens - Tangential - R<sub>1</sub> W-50 thru W79 Axial - R<sub>3</sub> Specimens

Heat 261-5-4001

RAD. LOC. Temp.	Orient.	Smooth Specimens						Notched Specimens											
		R <sub>1</sub>	R <sub>1</sub>	C	R <sub>1</sub>	R <sub>3</sub>	OD	R <sub>1</sub>	R <sub>3</sub>	C	R <sub>1</sub>	R <sub>3</sub>	OD						
-423	Ax.	W	W	W	W	W	W	W	W	W	W	W	W	W	W	W	W	W	
		66	66	69	69	53		62	56	75									
		W	W	W	W	W	W	W	W	W	W	W	W	W	W	W	W	W	W
-320	Ax.	W	W	W	W	W	W	W	W	W	W	W	W	W	W	W	W	W	W
		94	94	112	52	124		76	125	70	121	63	122	65	105				
		W	W	W	W	W	W	W	W	W	W	W	W	W	W	W	W	W	W
70	Ax.	W	W	W	W	W	W	W	W	W	W	W	W	W	W	W	W	W	W
		45	45	156	2	14		40	155	25	165	19	154	36	167				
		W	W	W	W	W	W	W	W	W	W	W	W	W	W	W	W	W	W
400	Ax.	W	W	W	W	W	W	W	W	W	W	W	W	W	W	W	W	W	W
		51	51	2	2	128		128	128	34	178	34	178						
		W	W	W	W	W	W	W	W	W	W	W	W	W	W	W	W	W	W
800	Ax.	W	W	W	W	W	W	W	W	W	W	W	W	W	W	W	W	W	W
		50	50	106	2	60		107	107	54	103	55	110	57	123				
		W	W	W	W	W	W	W	W	W	W	W	W	W	W	W	W	W	W
1200	Ax.	W	W	W	W	W	W	W	W	W	W	W	W	W	W	W	W	W	W
		37	37	153/168	2/2/2	2/9/31		24	161/170	17	171	43	172	28	173				
		W	W	W	W	W	W	W	W	W	W	W	W	W	W	W	W	W	W

NOTE: All specimens "ZA" Axial R<sub>1</sub>, "ZT" Tangential R<sub>1</sub>, "Z" R<sub>3</sub>

triplicate specimens at each temperature for three heats, of material. Specimen size was constant and only one orientation (parallel to direction of rolling) was utilized.

TABLE 8.6

STATISTICAL TEST PLAN - WELDED RING FORGING  
HEAT 261-5-4000\*

	<u>Smooth Tensiles</u>		<u>All Weld Specimens</u>	<u>Notched</u>	
	<u>R1</u>	<u>R3</u>	<u>R3</u>	<u>R1</u>	<u>R3</u>
-423°F		X1 X3 X5			X2 X4 X6
-320°F	X20 X21 X22		XX1 XX2 XX3	X70 X71 X72	
70°F	X24 X25 X26			X73 X74 X75	
400°F	X28 X29 X30			X77 X78 X79	
800°F	X32 X33 X34	X9 X11 X13	XX4 XX5 XX6	X80 X81 X82	
1200°F	X36 X37 X38				

\* The same plan applied to Heats 261-5-4000 and 260-5-2813, except code letters were "H" and "G", respectively.

### 8.2.1 Ring Forgings

Statistical analysis of the tensile results for the combined heats of ring forgings are shown in Table 8.7, which also lists the mean value for each temperature and the sigma (standard deviation) values computed at  $-320^{\circ}$  and  $800^{\circ}\text{F}$ . The design tensile properties versus temperature are presented in Figure 8.5 for the ultimate tensile strength and the 0.2% offset yield strength. The minus 3 sigma curves, faired between data points, are also plotted. Included also are minus 3 sigma data for the 0.3% and 0.4% offset yield strengths.

The analysis of the same tensile data from the combined heats (two ring-forgings), also defined the effects of specimen orientation and specimen size. Table 8.8 shows the effect of specimen orientation on the tensile properties and the standard deviation from the mean values at  $-320^{\circ}$  and  $800^{\circ}\text{F}$ . The tangential properties were uniformly better with respect to the ultimate tensile strength and elongation when compared with the corresponding axial values.

The R3 specimens (0.250-inch diameter) exhibited higher ultimate strength as compared with the R1 specimen (0.500-inch diameter) at  $-320^{\circ}\text{F}$ , but not at room temperature. Specimen size was not a significant influence on yield strength data or elongation values. The specimen orientation within the forging also did not have a significant effect on yield strength. Ultimate strength values were affected by the location within the ring forgings: for example, the outside diameter values were higher when compared with the center and inside diameter tensile values. The yield strength values, on the other hand, were not significantly affected by the radial location of the specimens.

The notched ( $K_t = 6.3$ ) tensile strength properties of the two ring forgings were treated statistically in the same fashion as the unnotched properties. Table 8.9 presents the statistical values of both



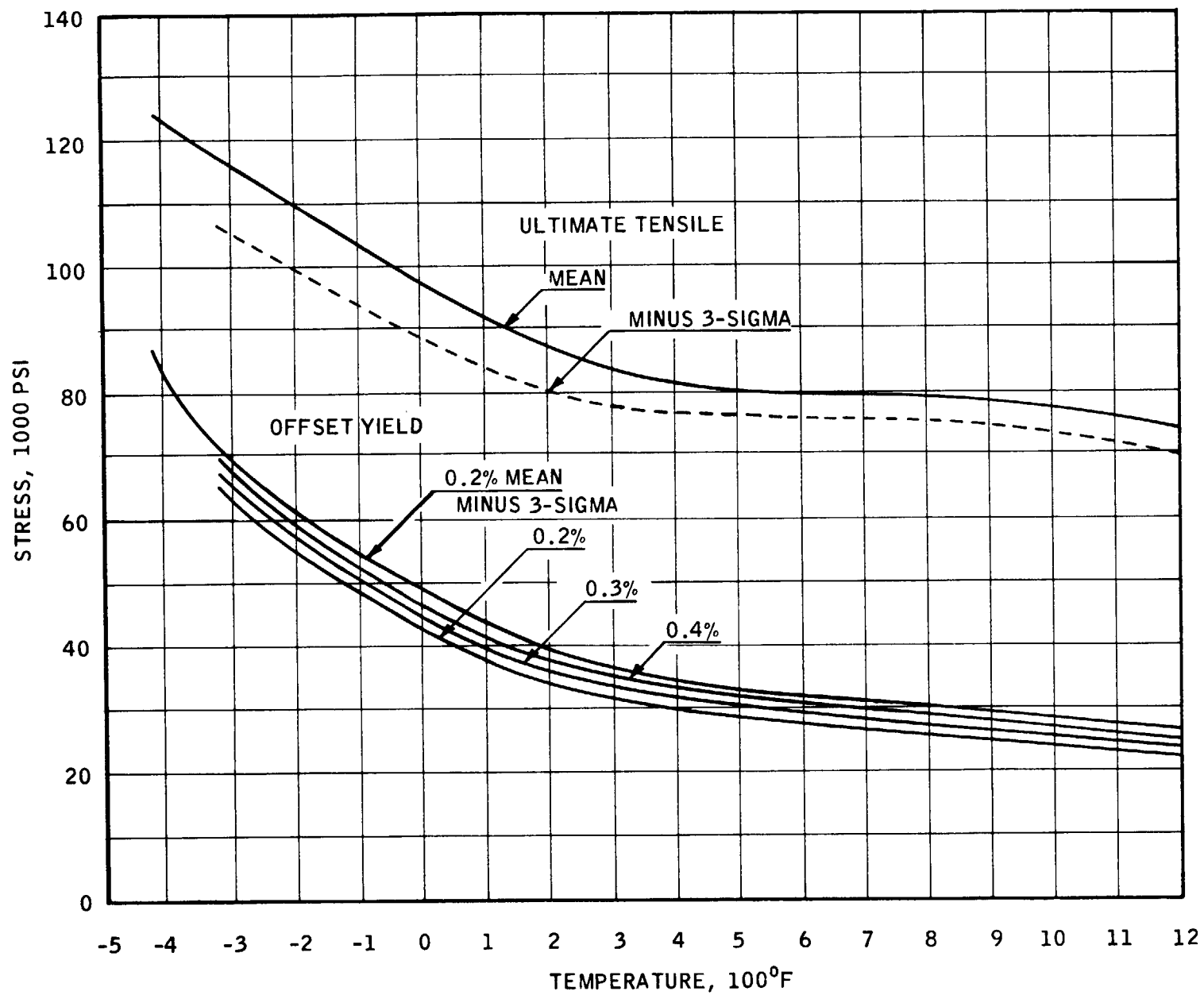


Figure 8.5 - Hastelloy X Forging Design Tensile Strengths vs Temperature

TABLE 8.7

HASTELLOY X FORGING (AGC 90056)

STATISTICAL TENSILE (UNNOTCHED) DATA VERSUS TEMPERATURE

Ultimate Tensile Strength (ksi)

<u>Temp (°F)</u>	<u>Average Value</u>	<u>Deviation, One Sigma</u>	<u>Sample Size</u>
-423	123.2	--	12
-320	117.4	3.7	30
70/80	93.3	--	11
400	81.7	--	9
800	79.8	1.3	37
1200	74.8	--	19

0.2 Offset Yield Strength (ksi)

-423	86.6	--	12
-320	71.7	2.2	30
70/80	45.0	--	11
400	34.7	--	9
800	30.8	1.6	37
1200	26.8	--	19

Elongation (%)

-423	8.1	--	12
-320	13.1	1.9	30
70/80	24.4	--	11
400	24.0	--	9
800	32.3	3.5	37
1200	31.4	--	19

NOTES:

1. Data obtained from two heats of material (261-5-4000 and 261-5-4001) as forged rings with 23-inch-OD, 17-inch ID, by 6 inches long.
2. All specimens heat-treated through three-cycle simulated braze treatment.
3. Analysis includes all specimen orientation and locations on forgings.

TABLE 8.8

STATISTICAL TENSILE (UNNOTCHED) PROPERTIES AND TEST VARIABILITY VERSUS  
TEMPERATURE FOR AXIAL AND TANGENTIAL PROPERTIES OF HASTELLOY X FORGINGS  
(HEATS 261-5-4000 AND 261-5-4001)

Axial Orientation

Temp (°F)	UTS (ksi)		YS (ksi) 0.2% Offset		Elong (%)	
	Mean	One Sigma	Mean	One Sigma	Mean	One Sigma
-423	115.8	-	-	-	-	-
-320	110.0	3.0	71.2	1.4	10.1	1.3
70/80	86.8	-	45.5	-	16.6	-
400	78.9	-	35.1	-	19.7	-
800	76.2	1.7	30.3	5.7	25.7	5.7
1200	73.0	-	26.8	-	27.2	-

Tangential Orientation

-423	130.6	-	-	-	-	-
-320	124.9	5.3	72.3	3.5	16.1	2.6
70/80	97.0	-	44.7	-	30.0	-
400	85.3	-	34.1	-	29.3	-
800	82.2	1.1	31.1	2.3	36.7	1.8
1200	77.2	-	26.7	-	37.2	-

Mean Values for Axial and Tangential R3 Specimens

-320	120.11	2.49	73.33	3.70	13.91	1.13
70/80	92.13	-	45.99	-	24.64	-
400	80.86	-	34.28	-	24.96	-
800	79.37	0.29	31.22	2.22	30.39	0.89
1200	74.04	-	28.91	-	29.96	-

R1 Specimens

-320	113.44	4.94	69.29	1.14	11.87	2.20
70/80	98.30	-	42.13	-	23.73	-
400	82.82	-	35.15	-	22.72	-
800	80.37	2.24	29.25	0.65	34.76	3.48
1200	75.16	-	25.52	-	32.26	-

The mean values for axial and tangential orientations represent summation over both sizes and three radial locations. The mean values for R3 and R1 sizes represent summation over both orientations and three radial locations.

TABLE 8.9

STATISTICAL UNNOTCHED AND NOTCHED TENSILE STRENGTH OF HASTELLOY X FORGINGS  
MEAN VALUES AND VARIABILITY VERSUS TEMPERATURE  
(HEATS 261-5-4000 AND 261-5-4001)

Axial and Tangential Combined

Test Temp (°F)	Ultimate Tensile Strength (ksi) Unnotched Specimens			Notched- Unnotched Ratio	Ultimate Tensile Strength (ksi) Notched Specimens	
	Mean	One Sigma	Mean		One Sigma	
	-423	123.2	-		1.06	130.3
-320	117.4	3.7	0.97	114.7	2.9	
70	93.3	-	0.97	90.5	-	
400	81.7	-	0.94	76.6	-	
800	79.8	1.3	0.96	76.9	1.5	
1200	74.8	-	0.93	69.4	-	

Test Temp (°F)	Ultimate Tensile Strength (ksi) Unnotched Specimens				Ultimate Tensile Strength (ksi) Notched Specimens			
	Axial		Tangential		Axial		Tangential	
	Mean	One Sigma	Mean	One Sigma	Mean	One Sigma	Mean	One Sigma
-423	115.8	-	130.6	-	124.5	-	132.2	-
-320	110.0	3.0	124.9	5.3	112.2	3.1	117.1	3.1
70	86.8	-	97.0	-	84.9	-	93.8	-
400	78.9	-	85.3	-	74.8	-	80.3	-
800	76.1	1.7	82.1	1.1	73.4	1.2	80.4	1.0
1200	73.0	-	77.2	-	65.8	-	73.1	-

NOTES:

1.  $K_t = 6.3$
2. Forging size, 23-inch OD, 17-inch ID, by 6 inches long.
3. All specimens heat treated through three-cycle simulated braze treatments.

unnotched tensile specimens to provide a notched-to-unnotched ratio based on the statistical mean value. Note that the sigma values for the notched specimens are comparable to those of the smooth specimens and that the influence of the forging direction is similar in both the notched and unnotched specimens.

The notched-to-unnotched ratios ranged between 0.9 and 1.1 for both orientations. The cryogenic values at -320 and -423°F clearly indicate that Hastelloy X retains its notched toughness at low temperatures.

### 8.2.2 Welded Ring Forgings

Data obtained from the tensile tests of the welded ring-forgings were statistically analyzed to develop the mean values and the sigma values for tensile strength, yield strength, and elongation in the same manner and over the same temperature range as for the parent-metal forgings. The tensile results for the combined heats are presented in Table 8.10 with the notched tensile strength.

It is interesting to note that tensile strength and yield strength of the welded rings were superior to the corresponding parent metal. For example, the yield strengths at 800 and 1200°F for the welded rings were 32.2 and 28.8 ksi respectively, which compared with the combined heat averages of unwelded parent-metal of 30.8 ksi at 800° and 26.8 ksi at 1200°F. Conversely, the elongations of the welded specimens were lower than the parent-metal specimens. While the higher weld strength may appear conflicting with the parent-metal results (since fractures took place in the parent metal) it should be pointed out that the rings used for the welded rings were forged to a 1.5-inch wall thickness, whereas the parent metal rings were three inches thick. An improvement in strength could be expected with the added forging reduction. In addition, the welding conditions, especially heat input, were tightly controlled and resulted in very-fine-grained weld deposits. The statistical values for the notched ( $K_t = 6.3$ ) tensile strength compared

TABLE 8.10

HASTELLOY X WELDED FORGING TENSILE PROPERTY STATISTICAL MEAN VALUES\* AND TEST  
VARIABILITY VERSUS TEMPERATURE (UNNOTCHED AND NOTCHED)

## Unnotched Specimens

Test Temp (°F)	Specimen Size R1						Specimen Size R3					
	UTS (ksi)		0.2% YS (ksi)		Elong. (%)		UTS (ksi)		YS (ksi)		Elong. (%)	
	Mean	One Sigma	Mean	One Sigma	Mean	One Sigma	Mean	One Sigma	Mean	One Sigma	Mean	One Sigma
-423	--		--		--		131.9	3.04	92.8	4.48	6.8	0.88
-320	117.3	1.64	72.8	1.43	9.67	0.54	124.3	1.92	74.7	1.79	10.4	1.09
Room	95.5	0.51	45.9	0.45	18.3	0.95	92.17	4.33	46.8	1.71	16.0	3.26
400	85.3	1.63	36.2	1.77	20.8	1.83						
800	82.0	1.11	32.2	1.04	26.6	2.85						
1200	76.6	1.74	28.2	1.49	26.1	2.83						

## Notched Specimens

-423	--					163.8	6.83
-320	136.5	2.91				146.5	3.03
Room	103.9	2.19				115.1	1.37
400	89.8	5.70				--	--
800	86.4	1.13				94.8	3.58
1200	82.1	0.86				--	--

\*Mean values represent summation of three welded forgings, each from a different heat and each welded with a different heat of weld wire.

with the unnotched specimens indicated that the welded rings had notched-to-unnotched ratios substantially above 1.0 at all temperatures. Tensile tests on all-weld-metal specimens were also conducted, but not analyzed statistically. The data are presented in Section 8.3.2.

### 8.2.3 Coolant Tube Strip

The statistical mean values and the one-sigma values for the 0.012-inch thick coolant-tube strip were obtained by "pooling" the test results of three heats. The data obtained are shown in Table 8.11. The data indicate that the tensile and yield strengths were higher than the corresponding values for the ring forgings as expected from the fine-grain character of the thin sheet (ASTM 6 to 8). The notched tensile strengths, however, were lower; therefore, the notched-to-unnotched ratios were lower than for the ring forgings or weld metals.

## 8.3 ACTUAL TENSILE PROPERTIES

The actual and individual test results from which the statistical tensile properties were obtained and were documented in Section 8.2, are presented in this section.

### 8.3.1 Ring Forgings

Tables 8.12 and 8.13 list the unnotched individual tensile data for ring forgings from Heats 261-5-4000 and 261-5-4001, respectively. Table 8.14 lists the individual notched tensile results for the same heats. Tables 8.12 and 8.13 also list uniform and total elongation values.

The uniform elongation values were essentially the same as the total elongation from -423 to 400°F, although some variation occurred in specimens at 800 and 1200°F. The tangential specimens (which generally had more than 32% total elongation) usually exhibited more strain beyond the uniform elongation value at 800 and 1200°F.

TABLE 8.11

HASTELLOY X STRIP TENSILE PROPERTY STATISTICAL MEAN VALUES AND  
TEST VARIABILITY VERSUS TEMPERATURE,  
(UNNOTCHED AND NOTCHED)

Test Temp, °F	Unnotched Strip					
	UTS (ksi)		0.2% YS (ksi)		E (%)	
	<u>Mean</u>	<u>Std. Dev.</u>	<u>Mean</u>	<u>Std. Dev.</u>	<u>Mean</u>	<u>Std. Dev.</u>
-423	135.2	10.25	93.8	2.91	6.98	3.01
-320	145.3	1.55	77.9	1.99	21.2	1.75
Room	110.7	2.07	49.4	1.71	26.5	3.82
800	92.4	1.11	38.0	1.58	31.9	3.92
1200	81.4	4.24	33.3	1.36	33.7	3.43
1600	34.8	1.95	26.4	1.78	39.5	3.30
1800	17.8	0.33	15.5	0.33	43.0	1.62

Test Temp. °F	Notched Strip	
	UTS (ksi)	
	<u>Mean</u>	<u>Std. Dev.</u>
-423	115.4	2.01
-320	103.6	2.21
Room	79.1	1.35
800	64.2	1.06
1200	59.0	0.94
1600	39.2	3.43
1800	20.6	1.21

Note: Mean values represent summation of three heats: 261-5-4000, 261-5-4001, and 261-5-4002



TABLE 8.12

TENSILE PROPERTIES (UNNOTCHED) FROM HASTELLOY X RING FORGING (AGC 90056)  
HEAT 261-5-4000

Specimen No.	Specimen		Test Temp (°F)	UTS (ksi)	0.2% Yield (ksi)	Elongation		Reduction In Area (%)
	Location	Size				Total (%)	Uniform (%)	
W - 50	AI <sup>(a)</sup>	R3 <sup>(b)</sup>	-423	115.0	85.0	3.5		3.9
W - 60	AC	↓	↓	114.0	87.2	5.0		5.1
W - 61	AO	↓	↓	125.8	85.2	8.0		9.1
W - 40	TO	↓	↓	132.0	87.8	12.0		11.2
W - 45	TI	↓	↓	130.8	91.4	9.0		10.3
W - 47	TC	↓	↓	136.0	87.6	12.0		10.4
WA-112	AI	R1	-320	97.7	69.6	5.5		5.1
WA-107	AC	↓	↓	108.1	69.5	9.0		7.8
WA-102	AO	↓	↓	110.3	69.3	9.5		8.9
WT-162	TI	↓	↓	118.5	69.6	14.0		11.9
WT-157	TC	↓	↓	119.3	69.1	14.0		12.3
WT-158	TO	↓	↓	120.5	68.7	14.0		11.6
W - 66	AI	R3	-320	102.2	75.4	6.5	6.5	5.5
W - 53	AO	↓	↓	118.2	68.0	13.0	-	13.9
W - 65	AO	↓	↓	122.4	76.2	15.0	15.0	14.5
W - 59	AC	↓	↓	111.7	71.0	11.0	-	8.5
W - 58	AI	↓	↓	104.5	69.3	-	-	-
W - 67	AC	↓	↓	107.5	76.0	9.5	9.5	7.1
W - 48	TO	↓	↓	133.0	71.2	18.0	-	15.4
W - 14	TC	↓	↓	122.8	76.0	17.0	17.0	13.1

(a) Specimen sampling location is defined in Table 8.5. The letter "A" = Axial, "I" = Inside Diameter, "C" = Center, "O" = Outside Diameter, "T" = Tangential, and "ST" = Short Transverse.

(b) Size R3 refers to round R-3 tensile specimens.  
Size R1 refers to round R-1 tensile specimens.

TABLE 8.12 (cont.)

<u>Specimen No.</u>	<u>Specimen</u>		<u>Test</u> <u>Temp (°F)</u>	<u>UTS</u> <u>(ksi)</u>	<u>0.2%</u> <u>Yield</u> <u>(ksi)</u>	<u>Elongation</u>		<u>Reduction In</u> <u>Area</u> <u>(%)</u>
	<u>Location</u>	<u>Size</u>				<u>Total</u> <u>(%)</u>	<u>Uniform</u> <u>(%)</u>	
W - 16	TO	R3	-320	131.3	78.4	17.0	16.9	15.4
W - 13	TI	↓	-320	123.0	76.4	15.0	15.0	14.7
W - 15	TC	↓	-320	132.0	78.0	16.0		12.4
W - 37	TI	↓	-320	131.3		10.5	10.0	9.4
W - 83	ST-O	↓	-320	117.6	69.9	11.5		10.9
W - 80	ST-C	↓	-320	106.7	67.2	7.0		7.9
W - 2	TC	R3	Room	98.8	50.9	30.5	(30) <sup>(c)</sup>	24.0
W - 8	↓	↓	↓	98.2	54.2	24.0	-	18.1
W - 18	↓	↓	↓	97.0	45.5	26.5	26.0	25.2
W - 38	↓	↓	↓	100.2	50.8	29.5	28.5	21.2
W - 81	ST-C	↓	↓	86.8	42.9	16.5	-	12.2
W - 82	ST-O	↓	↓	92.5	44.0	20.0	-	21.0
W - 52	AC	↓	↓	87.2	42.0	17.5	-	16.1
W - 51	AC	↓	↓	86.4	46.7	17.5	-	12.5
WA-128	AC	R1	Room	84.8	41.8	15.0		13.4
WA-106	AC	↓	↓	84.7	38.2	22.0		20.0
WT-159	TC	↓	↓	98.0	44.0	25.0		24.0
WT-151	TC	↓	↓	99.1	42.7	26.0		21.7
WA-101	AC	R1	400	77.0	33.8	17.5		14.6
W - 74	AC	R3	400	79.0	34.6	20.0		18.9

(c) The uniform elongation values in parenthesis were obtained by observation during testing, though not recorded on chart.

TABLE 8.12 (cont.)

Specimen No.	Specimen		Test Temp (°F)	UTS (ksi)	0.2% Yield (ksi)	Elongation		Reduction In Area (%)	
	Location	Size				Total (%)	Uniform (%)		
WT-152	TO	R1	800	86.8	30.0	35.0	-	30.4	
WT-156	TI	↓	↓	82.2	30.2	41.0	32.0	31.0	
WT-168	TI			82.4	29.4	40.5	31.5	30.7	
WT-169	TC			81.0	29.7	32.0	(30) <sup>(c)</sup>	29.2	
WT-176	TO			81.6	28.7	40.0	-	30.0	
WA-100	AI			70.6	29.4	16.0*	-	-	
WA-113	AC			75.9	29.4	28.5	-	22.1	
WA-114	AO			76.8	29.7	23.5	-	21.4	
W-5	TC			R3	800	83.1	31.0	29.0	-
W-29	↓	↓	↓	83.2	32.0	32.0	-	34.6	
W-22				84.7	-	31.5	31.0	33.4	
W-23				83.3	-	37.5	36.0	35.2	
W-11				86.8	-	27.0	26.0	25.7	
W-24				TO	84.9	-	33.5	33.0	30.7
W-68				AC	76.6	29.7	26.0	-	22.6
W-69				AO	78.4	30.1	26.0	(26) <sup>(c)</sup>	23.2
W-77				AI	74.1	29.1	21.0	-	19.0
W-32	TC	83.3	31.1	-	-	-			

(c) The uniform elongation values in parenthesis were obtained by observation though not recorded on chart.

\* Specimen fractured outside gage marks.

TABLE 8.12 (cont.)

Specimen No.	Specimen		Test Temp (°F)	UTS (ksi)	0.2% Yield (ksi)	Elongation		Reduction In Area (%)
	Location	Size				Total (%)	Uniform (%)	
W - 76	AO	R3	1200	77.8	27.7	32.0	31.5	26.7
W - 78	AI	R3	↓	69.5	29.4	20.0	20.0	20.4
WT-150	TI	R1		76.6	26.0	33.5	(31) <sup>(c)</sup>	27.9
WT-163	TC	↓		77.7	26.6	36.5	-	32.0
WT-164	TO			80.5	27.0	37.0	(33) <sup>(c)</sup>	34.6
WA-118	AI			71.9	24.2	22.5	22.0	20.0
WA-120	AO			75.7	25.8	25.0	-	21.7
WA-124	AC			74.8	25.9	29.5	-	24.9

(c) The uniform elongation values in parentheses were obtained by observation during testing.

- NOTES: 1. Strain rate 0.005 in./in./min to yield, then 0.05 in./in./min to failure.  
 2. All specimens heat-treated through simulated braze treatment.

TABLE 8.13

TENSILE PROPERTIES (UNNOTCHED) FROM HASTELLOY X FORGING (AGC 90056)  
HEAT 261-5-4001

<u>Specimen Number</u>	<u>Location</u> <sup>(a)</sup>	<u>Size</u> <sup>(b)</sup>	<u>Test Temp</u> (°F)	<u>UTS</u> (ksi)	<u>0.2% Yield</u> (ksi)	<u>Total Elongation</u> (%)	<u>Uniform Elongation</u> (%)	<u>Reduction In Area</u> (%)	
Z-3	TO	R3	-423	133.4	82.8	9.5	( 9.5) <sup>(c)</sup>	10.7	
Z-23	TC	↓	↓	125.1	88.6	10.5	(10.5) <sup>(c)</sup>	9.3	
Z-29	TI			129.6	84.9	8.5	( 8.5) <sup>(c)</sup>	9.7	
Z-48	TO			129.8	85.9	10.0	(10.0) <sup>(c)</sup>	7.6	
Z-53	AO			111.5	83.5	5.0	( 5.0) <sup>(c)</sup>	6.0	
Z-66	AI			111.4	88.4	5.0	( 5.0) <sup>(c)</sup>	8.0	
Z-68	AC			117.1	87.4	7.0	( 7.0) <sup>(c)</sup>	8.8	
ZT-176	TI			R1	128.5	96.5	16.0	(16.0) <sup>(c)</sup>	17.1
ZA-112	AI			R1	-320	106.4	70.0	8.0	
ZA-117	AO	↓	↓	116.0	68.5	13.5		10.4	
ZA-124	AC			110.2	69.5	10.5		8.6	
ZA-125	AO			106.8	68.7	8.0		8.9	
ZT-155	TO			124.8	67.0	19.0		16.0	
ZT-156	TI			117.0	69.0	13.0		12.3	
ZT-169	TC			121.8	71.8	16.5		12.7	
ZT-174	TI			118.2	69.0	14.5		12.0	
Z-14	TC			R3	-320	127.3	67.6	16.5	16.5
Z-40	TO	↓	↓	125.2	67.0	16.0	16.0	16.1	
Z-45	TI			131.4	71.3	18.5	18.5	14.7	
Z-52	AC			111.9	72.9	10.0	10.0	7.8	
Z-58	AI			110.0	69.6	9.5	9.5	8.6	

(a) Specimen sampling location is defined in Table 8.5. The letter "A" = Axial, "I" = Inside Diameter, "C" = Center, "O" = Outside Diameter, "T" = Tangential, and "ST" = Short Transverse.

(b) Size R3 refers to round R-3 tensile specimens.  
Size R1 refers to round R-1 tensile specimens.

(c) Uniform elongation values in parentheses were obtained by observation during testing.

TABLE 8.13 (cont.)

Specimen Number	Location	Size	Test Temp (°F)	UTS (ksi)	0.2% Yield (ksi)	Total Elongation (%)	Uniform Elongation (%)	Reduction In Area (%)
Z-76	AO	R3	-320	106.3	67.7	8.5	8.5	9.4
Z-46	TC	↓	↓	120.0	70.0	16.4	16.4	12.4
Z-13	TI	↓	↓	132.0	-	18.8	18.8	11.6
Z-78	AI	↓	↓	108.7	69.0	8.9	8.9	9.0
Z-33	TI	↓	↓	125.9	72.4	16.6	16.6	11.6
Z-67	AC	R3	Room	84.4	42.0	15.0	15.0	11.0
Z-64	AC	↓	↓	89.0	42.2	17.7	17.0	12.5
Z-32	TO	↓	↓	98.2	41.0	27.6	27.0	26.1
Z-38	TC	↓	↓	97.8	45.0	30.7	30.0	27.5
Z-80	STC	R3	Room	90.0	45.2	21.4	-	16.9
Z-81	STC	↓	↓	92.7	44.4	22.5	-	19.6
Z-82	STO	↓	↓	96.1	44.2	26.3	-	21.8
Z-83	STO	↓	↓	97.8	44.0	24.8	-	17.6
ZA-120	AO	R1	Room	92.3	41.6	17.8	-	23.5
ZA-127	AC	↓	↓	88.3	42.1	16.9	16.0	19.2
ZT-160	TC	↓	↓	97.5	41.9	30.2	-	25.3
Z-11	TC	R3	Room	95.7	43.0	38.4	-	26.7
Z-39	↓	↓	↓	94.7	45.4	29.3	-	25.2
Z-5	↓	↓	↓	96.6	45.6	31.8	-	27.3
Z-42	↓	↓	400	84.5	36.2	29.0	29.0	27.5
Z-7	TI	↓	↓	83.9	-	31.0	31.0	26.7
Z-59	AC	↓	↓	77.6	32.6	21.0	20.0	16.1
Z-30	TC	↓	↓	86.4	33.8	30.0	(30) <sup>(c)</sup>	31.0
Z-51	AC	↓	↓	76.8	36.2	25.0	(24) <sup>(c)</sup>	18.8

(c) Uniform elongation values in parentheses were obtained by observation during testing.

TABLE 8.13 (cont.)

Specimen Number	Location	Size	Test Temp (°F)	UTS (ksi)	0.2% Yield (ksi)	Elongation Total (%)	Elongation Uniform (%)	Reduction In Area (%)
ZA-128	AC	R1	400	76.2	32.3	18.0	(18) <sup>(c)</sup>	16.5
ZT-157	TC	↓	↓	87.3	33.6	32.5	(32) <sup>(c)</sup>	28.6
ZT-150	TI	↓	↓	83.0	33.9	25.5	(25) <sup>(c)</sup>	23.0
Z-7	TI	R3	400	83.9	-	31.0	31	26.7
Z-42	TC	↓	↓	84.5	-	29.0	29	27.5
Z-59	AC	↓	↓	77.6	32.6	21.0	-	16.1
ZA-100	AI	R1	800	71.2	29.3	21.0	-	20.7
ZA-101	AC	↓	↓	74.8	29.4	24.0	-	18.6
ZA-102	AO	↓	↓	76.6	29.4	26.5	-	21.1
ZT-152	TO	↓	↓	83.9	30.2	36.5	-	33.3
ZT-158	TO	↓	↓	81.6	28.3	41.5	-	34.6
ZT-159	TI	↓	↓	79.8	29.3	37.5	-	28.6
ZA-106	AI	↓	↓	72.8	28.8	21.0	(21) <sup>(c)</sup>	24.2
ZA-107	AC	↓	↓	79.1	-	32.0	(29) <sup>(c)</sup>	25.2
ZA-114	AO	↓	↓	79.9	28.4*	35.5	30	30.3
ZT-153	TI	↓	↓	82.1	29.0	41.5	32	37.9
ZT-168	TI	↓	↓	79.8	28.6	42.0	32	38.6
ZT-163	TC	↓	↓	83.0	29.2	37.0	31	34.8
ZT-161	TO	↓	↓	81.8	29.3	39.0	32	33.6
ZT-170	TO	↓	↓	79.8	28.5	41.5	32	35.8
Z-2	TC	R3	800	80.6	30.4	36.5	31	37.3
Z-8	TC	↓	↓	79.2	29.2	37.0	32	36.6
Z-37	TI	↓	↓	81.0	32.8	38.0	31	37.3
Z-31	TC	↓	↓	81.5	31.8	36.5	31	35.4
Z-24	TO	↓	↓	81.0	29.3	36.0	32	33.3

(c) Uniform elongation values in parentheses were obtained by observation during testing.

\* Specimen fractured outside gage marks.

TABLE 8.13 (cont.)

Specimen Number	Location	Size	Test Temp (°F)	UTS (°F)	0.2% Yield (ksi)	Elongation Total (ksi)	Elongation Uniform (%)	Reduction In Area (%)
Z-50	AI	R3	800	72.9	28.7	24.0	-	17.5
Z-60	AC	↓	↓	76.2	29.8	26.0	-	24.0
Z-69	AO	↓	↓	74.3	29.9	22.5	-	21.2
Z-16	TO	↓	↓	83.9	32.0	35.0	32.5	34.0
Z-15	TC	↓	↓	83.5	32.2	35.5	32.0	34.0
Z-10	TI	↓	↓	80.3	33.2	36.0	32.0	32.8
Z-74	AC	↓	↓	75.6	30.3	26.0	25.0	21.0
Z-73	AO	↓	↓	76.5	-	23.0	23.0	23.0
Z-77	AI	↓	↓	75.7	-	26.5	25.0	24.0
Z-44	TO	R3	1200	77.6	28.0	38.5	32.0	37.2
Z-47	TC	↓	↓	77.2	29.0	37.5	34.0	37.9
Z-71	AC	↓	↓	71.5	29.7	32.5	31.0	28.1
Z-61	AO	↓	↓	73.1	27.7	27.0	26.0	24.6
ZA-118	AI	R1	1200	67.3	24.2	21.0	21.0	21.4
ZA-119	AC	↓	↓	72.8	25.1	29.5	28.0	26.7
ZA-116	AO	↓	↓	75.0	24.9	37.0	31.0	27.0
ZT-162	TI	↓	↓	75.5	25.1	37.5	32.0	34.6
ZT-151	TC	↓	↓	76.6	25.0	39.5	34.0	35.0
ZT-164	TO	↓	↓	77.5	26.0	40.0	32.0	34.6
ZA-108	AO	↓	↓	76.2	24.7	32.0	(31) <sup>(c)</sup>	25.4
ZA-113	AC	↓	↓	73.6	25.3	29.0	(28) <sup>(c)</sup>	21.4
ZA-115	AI	↓	↓	69.5	25.0	21.5	(21) <sup>(c)</sup>	20.7
ZA-126	AO	↓	↓	75.0	24.9	37.0	(32) <sup>(c)</sup>	27.0

(c) Uniform elongation values in parentheses were obtained by observation during testing.

Notes: 1. Strain rate 0.005 in./in./min to yield, then 0.05 in./in./min to failure.  
2. All specimens heat-treated through simulated braze treatment.



TABLE 8.14

TENSILE PROPERTIES (NOTCHED) FROM HASTELLOY X RING FORGINGS (AGC 90056)  
HEATS 261-5-4000 AND 261-5-4001

Orientation	Size	Test Temp (°F)	ID of Ring		Center		OD of Ring	
			Heat 4000	Heat 4001	Heat 4000	Heat 4001	Heat 4000	Heat 4001
Axial	R3	-423	123.1	127.1	126.3	136.9	132.5	132.2
Tangential	R3	-423	131.2	135.9	131.2	131.8	124.3	136.9
Axial	R3	-320	115.5	121.9	116.4	115.9	122.4	118.3
Axial	R1	↓	108.0	106.2	106.3	109.3	106.4	108.6
Axial	R1		103.0	-	-	-	-	-
Tangential	R3		116.9	121.1	126.1	119.0	124.0	130.0
Tangential	R1		109.3	109.5	117.0	111.9	-	-
Tangential	R1		109.6	-	109.5	-	117.2	117.9
Axial	R3		70			88.2	-	
Axial	R1		↓			83.6	-	
						83.0	-	
Tangential	R3					99.5	90.1	
Tangential	R1					88.0	100.3	
Tangential					90.9	-		
Axial	R3	400			77.3	79.3		
Axial	R1	↓			71.3	71.4		
Tangential	R3				-	84.7		
Tangential	R1				-	75.8		
Axial	R3	800	76.5	75.2	76.4	78.0	79.5	76.2
Axial	R1	↓	68.9	67.3	71.3	69.8	71.6	70.0
Tangential	R3		87.2	82.3	86.2	81.7	85.9	81.2
Tangential	R1		74.5	76.0	76.4	76.4	79.8	77.4
Axial	R1	1200	62.6	64.4	68.1	63.1	67.9	68.8
Tangential	R1	1200	74.6	72.3	73.4	71.4	73.3	73.3

93

- Notes: 1. Strain rate 0.005 in./in./min to yield, then 0.05 in./in./min to failure.  
2. All specimens heat-treated through simulated braze treatment.

### 8.3.2 Welded Ring Forgings

Tables 8.15, 8.16 and 8.17 list the individual notched and unnotched tensile results from Heats 261-5-4000, 261-5-4001, and 260-5-2813, respectively.

The notched and unnotched tensile results of all weld-metal specimens are presented in Tables 8.18 and 8.19. For comparison, two all weld-metal R3 specimens were tested at room temperature in the as-welded condition (not exposed to post-weld annealing on the braze cycle). Test results were:

<u>UTS</u> <u>(ksi)</u>	<u>0.2%</u> <u>YS (ksi)</u>	<u>Elong.</u> <u>(%)</u>	<u>RA</u> <u>(%)</u>
116.0	77.2	25	32.2
115.8	79.3	31	35.5

The weld wire was from Heat 261-5-4003: specimens were oriented transverse to the weld-bead length.

### 8.3.3 Coolant Tube Strip

The individual unnotched tensile test results for 0.012-inch thick coolant-tube strip material are shown in Table 8.20. Individual notched tensile results are presented in Table 8.21.

## 8.4 0.3% AND 0.4% OFFSET YIELD STRENGTHS - RING FORGING

In the development of the nozzle design, there was a need for forging yield-stress values at strain levels higher than the customary 0.2% offset. The data were evolved from the available stress-strain curves obtained with each individual test. The 0.3% and 0.4% offset data available from ring

forging Heat 261-5-4000 are presented in Table 8.22 for the temperature range from -423 to 1200°F. The values shown include the 0.2% offset values for comparison, as well as the increased stress increment from 0.2 to 0.3% and from 0.2 to 0.4%. Averages for the yield increase also are tabulated and summarized for each temperature. A similar treatment for Heat 261-5-4001 is presented in Table 8.23.

TABLE 8.15

TENSILE PROPERTIES OF WELDED HASTELLOY X RING FORGING, HEAT 261-5-4000<sup>(a)</sup>  
(WELDED WITH HEAT 260-5-2784 WIRE)

Test Temperature (°F)	Specimen Size (b)	UTS (ksi)	0.2% YS (ksi)	EL (%)	RA (%)	Notched <sup>(d)</sup> Tensile (ksi)
-423 ↓	R3	133.7	97.2	7.5	10.5	175.0
	↓	141.8	95.3	8.7	8.5	175.0
	↓	134.3	95.9	8.0	9.2	176.0
-320 ↓	R1	126.6	76.4	12.0	9.0	137.8
	↓	126.3	77.8	11.5	11.0	139.0
	-	-	-	-	-	131.4
	R3	128.9	73.5	10.0	12.0	
	R3	125.9	77.4	11.0	12.0	
70 ↓	R1	99.0	48.0	21.0	20.0	
	↓	99.7	48.6	20.0	20.0	
	↓	99.4	48.4	20.0	19.0	
400 ↓	R1	85.9	39.4	18 <sup>(c)</sup>	18 <sup>(c)</sup>	
	↓	89.9	40.1	22.0	19.0	
	↓	88.7	36.9	25.0	25.0	
800 ↓	R1	84.9	34.6	32.0	29.0	82.6
	↓	83.0	36.8	24.0	22.0	85.0
	↓	84.3	36.4	26.0	26.0	82.9
	R3	86.4	36.9	23.0	32.0	
	R3	86.8	36.6	23.0	28.0	
	↓					
1200 ↓	R1	78.3	30.1	30.0	32.0	
	↓	79.8	31.7	30.0	32.0	
	↓	80.3	31.9	27.0	26.0	

(a) Specimens oriented axially in forging.

(b) R1 specimens contained weldments which amounted to 15 to 20% of the gage length.  
R3 specimens contained weldments which amounted to 35 to 45% of the gage length.

(c) Fracture occurred outside the gage length.

(d)  $K_t = 6.3$

Note: Strain rate 0.005 in./in./min to yield, then 0.05 in./in./min to failure.

TABLE 8.16

TENSILE PROPERTIES OF WELDED HASTELLOY X RING FORGING,  
HEAT 261-5-4001(a)  
(WELDED WITH HEAT 260-5-2783 WIRE)

Temp (°F)	Specimen <sup>(b)</sup> Size	UTS (ksi)	0.2% YS (ksi)	Elong (%)	RA (%)	Notched <sup>(d)</sup> Tensile
-423 ↓	R3 ↓	136.6	87.0	9.0	10.0	161.7
		136.0	86.9	7.0	11.0	164.0
		---	---	---	---	162.5
-320 ↓	R3 ↓	123.2	74.5	10.0 <sup>(c)</sup>	10.1 <sup>(c)</sup>	147.2
		124.0	71.5	11.8	11.7	144.0
		---	---	---	---	144.0
-320 ↓	R1 ↓	123.1	68.9	11.5	13.4	135.3
		118.8	70.9	11.0	12.6	137.8
		118.6	67.9	11.5	13.0	136.2
		118.3	71.1	10.0	11.9	---
Room ↓	R1 ↓	94.1	43.5	19.5	18.8	105.1
		94.6	42.7	22.0 <sup>(c)</sup>	18.0	100.4
		95.0	43.8	19.5 <sup>(c)</sup>	17.3	105.0
400 ↓	R1 ↓	83.9	36.5	21.0	20.7	92.8
		86.7	31.6	25.5	26.8	91.4
		85.1	33.2	24.0	23.3	82.0
800 ↓	R1 ↓	80.2	31.7	26.5	31.1	84.3
		79.9	30.4	31.0	25.8	85.8
		77.6	31.7	25.0	26.5	85.8
		81.1	30.6	26.5 <sup>(c)</sup>	27.7	---
1200 ↓	R1 ↓	74.9	28.5	21.5	21.4	77.4
		75.3	27.8	27.0	31.4	79.5
		76.2	27.7	28.0	33.3	78.6
		75.9	28.6	29.0	32.5	---

(a) Specimens oriented axially in forging

(b) R1 specimens contained weldments which amounted to 15 to 20% of gage length.

R3 specimens contained weldments which amounted to 35 to 45% of the gage length.

(c) Fracture occurred outside the gage length.

(d)  $K_t = 6.3$

Note: Strain rate 0.005 in./in./min to yield, then 0.05 in./in./min to failure.

TABLE 8.17  
TENSILE PROPERTIES OF WELDED HASTELLOY X RING FORGING  
HEAT 260-5-2813<sup>(a)</sup>  
(WELDED WITH HEAT 261-5-4003 WIRE)

Temp (°F)	Specimen <sup>(b)</sup> Size	UTS (ksi) <sup>(e)</sup>	0.2% YS (ksi)	Elong (%)	RA (%)	Notched <sup>(d)</sup> Tensile
-423 ↓	R3 ↓	126.1	85.5	5.5	9.4	139.9 <sup>(e)</sup>
		124.1	96.2	5.0	6.3	160.0
		122.9	98.7	4.0	4.8	160.5
-320 ↓	R3 ↓	120.3	75.0	8.5 <sup>(c)</sup>	9.3 <sup>(c)</sup>	149.7
		123.0	76.1	10.5	10.8	150.6
		124.7	75.2	11.0	8.9	143.5
Room ↓	R3 ↓	88.2	48.7	12.5	15.2	113.6
		96.8	46.3	18.5	15.0	116.3
		91.5	45.4	17.0	16.8	115.4
-320 ↓	R1 ↓	108.4	74.3	6.0	7.8	138.7
		108.4	75.3	6.0	5.9	138.5
		107.4	72.5	6.5	6.7	134.0
Room ↓	R1 ↓	92.2	45.8	14.0	13.4	103.7
		93.2	45.9	15.0	13.4	103.2
		91.9	46.6	14.0	14.4	106.1
400 ↓	R1 ↓	83.5	36.4	17.0	16.2	84.6
		80.9	35.4	16.0	16.2	95.1
		82.7	36.5	16.5	15.8	92.8
800 ↓	R1 ↓	82.7	28.9	24.5	22.5	89.1/95.7*
		82.9	30.8	24.5	26.3	91.4/90.9*
		83.1	31.4	26.0	25.6	90.7/97.9*
1200 ↓	R1 ↓	77.6	-	25.5	26.9	86.1
		71.8	23.6	20.0	21.5	85.1
		75.9	24.0	23.0	22.3	86.2

(a) Specimens oriented axially in forging

(b) R1 specimens contained weldments which amounted to 15 to 20% of the gage length.

R3 specimens contained weldments which amounted to 35 to 45% of the gage length.

(c) Fracture occurred outside the gage length.

(d)  $K_t = 6.3$

(e) Failed in heat-affected zone.

Note: Strain rate 0.005 in./in./min to yield, then 0.05 in./in./min to failure.

\*First number is R1 specimen, Second number is R3 specimen.

TABLE 8.18

ALL-WELD METAL-TENSILE PROPERTIES OF HASTELLOY X RING FORGING,  
HEAT 261-5-40001  
(WELDED WITH HEAT 260-5-2784 WIRE)

<u>Test Temp (°F)</u>	<u>UTS (ksi)</u>	<u>0.2% YS (ksi)</u>	<u>Elong (%)</u>	<u>RA (%)</u>
-320	154.0	77.6	18.0	18.0
-320	155.5	82.5	16.0	18.0
Room	115.5	48.6	25.0	30.0
Room	111.2	53.4	16.0*	24.0
800	98.5	40.6	25.0	29.0
800	97.1	42.8	21.0	28.0

\*Pin-point defect recorded by dye-penetrant inspection. Failure occurred at defect.

Notes: All specimens R3.  
Strain rate 0.005 in./in./min to yield, then 0.05 in./in./min to failure.

TABLE 8.19

ALL-WELD METAL TENSILE PROPERTIES OF HASTELLOY X RING FORGING  
HEAT 261-5-4001  
(WELDED WITH HEAT 260-5-2783 WIRE)

<u>Test Temp (°F)</u>	<u>UTS (ksi)</u>	<u>0.2% YS (ksi)</u>	<u>Elong (%)</u>	<u>RA (%)</u>	<u>Notch Tensile</u>
-423	-	-	-	-	161.7
↓	-	-	-	-	164.0
↓	-	-	-	-	162.5
-320	159.1	75.0	29.5	24.0	147.2
↓	144.0	73.0	22.0	21.0	144.0
↓	152.0	79.0	18.5	16.0	144.0
800	97.0	38.0	30.0	35.0	84.3
↓	99.0	38.0	32.0	37.0	85.8
↓	99.0	38.0	30.0	28.0	85.8

Notes: All specimens R3. Strain rate 0.005 in./in./min to yield, then 0.05 in./in./min to failure.  $K_t = 6.3$ .



TABLE 8.20

## TENSILE PROPERTIES (UNNOTCHED) FOR 0.012-INCH THICK COOLANT-TUBE STRIP

Test Temp (°F)	(Heat 261-5-4000)			(Heat 261-5-4001)			(Heat 261-5-4002)		
	UTS (ksi)	YS (ksi)	Elongation (%)	UTS (ksi)	YS (ksi)	Elongation (%)	UTS (ksi)	YS (ksi)	Elongation (%)
-423 ↓	127.9	98.2	6.0	152.0	-	13.5	131.4	93.6	(6.0)
	140.3	94.4	7.0	143.9	93.0	(6.0)	131.0	94.0	(5.5)
	131.7	90.0	7.0	123.1	93.3	(5.0)	162	-	-
-320 ↓	140	73	22.0	144	80	19.0	148	80	(21.0)
	139	72	(20.0)	145	83	19.0	148	80	(21.0)
	141	71	(21.0)	148	78	24.0	151	81	(22.0)
Room ↓	107	46	32	112	52	26.0	115	51	32.0
	103	47	(21.5)	109	47	26.0	115	49	30.0
	104	47	(20.5)	115	51	28.0	115	50	27.0
800 ↓	89	35	(32.0)	92	37	29.0	96.2	40	(30.0)
	88	35	37.0	95	38	33.0	95	38	34.0
	88	35	(32.0)	92	42	25.0	94	42	33.0
1200 ↓	80	31	37.0	83	36	31.0	87	35	38.0
	71	28	37.0	86	-	24.0	89	36	36.0
	77	31	35.0	79	-	34.0	79	33	34.0
1300 ↓	-	-	-	75	33	34.0	-	-	-
	32	26	51.0	37.0	28	39.0	34	23	40.0
	34	28	53.0	40.0	27	40.0	35	27	37.0
1600 ↓	32	28	47.0	-	-	-	36	26	32.0
	-	-	-	-	-	-	34	27	35.0
	-	-	-	-	-	-	-	-	-
1800 ↓	18	16	41.0	-	-	-	-	-	-
	18	16	44.0	-	-	-	-	-	-
	17	15	45.0	-	-	-	-	-	-
	18	15	32.0	-	-	-	-	-	-

- Notes: 1. Strain rate 0.005 in./in./min to yield, then 0.05 in./in./min to failure.  
2. Elongation values in parentheses indicate failure outside gage marks.

TABLE 8.21

TENSILE PROPERTIES (NOTCHED) FOR 0.012-INCH THICK COOLANT-TUBE STRIP

<u>Test Temp.</u> (°F)	<u>Heat No.</u> 261-5-4000	<u>Heat No.</u> 261-5-4001	<u>Heat No.</u> 261-5-4002
-423	115.3		117.1
↓	114.4		114.0
↓	112.7		119.0
-320	106.9		103.4
↓	104.4		104.0
↓	101.1		101.8
Room	79.6		78.4
↓	78.1		78.6
↓	78.5		81.5
800	62.3		67.1
↓	63.6		64.5
↓	62.6		65.3
1200	57.3		59.4
↓	56.7		61.2
↓	57.3		61.9
1600	42.0	41.6	34.3
↓	36.8	40.6	33.9
↓	40.4	40.2	43.2
1800	19.7		
↓	20.2		
↓	22.0		

Notes: Strain rate 0.005 in./in./min to yield, then 0.05 in./in./min to failure.  $K_t = 6.3$ .

TABLE 8.22

0.3% and 0.4% OFFSET YIELD STRENGTH OF  
HASTELLOY X RING FORGING, HEAT 261-5-4000

Test Temperature: -423°F

Specimen No.	0.2% Offset (psi)	0.3% Offset (psi)	0.4% Offset (psi)	Increase From 0.2% Offset to	
				0.3% Offset (psi)	0.4% Offset (psi)
W - 40	87,800	89,800	91,800	2,000	4,000
W - 45	92,100	94,100	96,200	2,000	4,100
W - 47	87,600	90,100	92,200	2,500	4,600
W - 50	84,700	87,800	89,600	3,100	4,900
W - 60	89,000	94,800	97,400	5,800	8,400
W - 61	94,600	98,200	101,400	<u>3,600</u>	<u>6,800</u>
			Average	3,200	5,500

Test Temperature: -320°F

WT - 158	68,200	71,100	73,200	2,900	5,000
WT - 157	69,200	72,000	74,100	2,800	4,900
WA - 112	69,600	71,700	73,500	2,100	3,900
WA - 102	69,100	71,500	73,500	2,400	4,400
WA - 107	69,900	72,600	74,800	2,700	4,900
WT - 162	69,600	72,100	74,100	<u>2,500</u>	<u>4,500</u>
			Average	2,600	4,600
W - 59	72,200	74,300	76,400	2,100	4,200
W - 58	69,300	72,400	74,700	3,100	5,400
W - 53	68,100	71,900	73,900	3,800	5,800
W - 80	68,000	71,800	74,300	3,800	6,300
W - 83	69,800	73,900	76,500	4,100	6,700
W - 48	71,500	75,200	77,600	3,700	6,100
W - 15	86,600	89,200	91,600	<u>2,600</u>	<u>5,000</u>
			Average	3,300	5,600

TABLE 8.22 (cont.)

Test Temperature: Room

Specimen No.	0.2% Offset (psi)	0.3% Offset (psi)	0.4% Offset (psi)	Increase From 0.2% Offset to	
				0.3% Offset (psi)	0.4% Offset (psi)
W - 2	50,900	53,400	54,900	2,500	4,000
W - 8	54,200	56,400	57,900	2,200	3,700
W - 81	42,700	45,000	46,600	2,300	3,900
W - 82	43,200	45,500	47,500	2,300	4,300
W - 52	42,200	44,600	46,500	2,400	4,300
WT - 151	42,700	44,800	46,500	2,100	3,800
WA - 128	42,300	44,300	45,800	<u>2,000</u>	<u>3,500</u>
			Average	2,300	3,900

Test Temperature: +400°F

WA - 101	34,100	35,500	36,900	1,400	2,800
W - 74	34,600	36,700	38,300	<u>2,100</u>	<u>3,700</u>
			Average	1,700	3,200

Test Temperature: +800°F

WT - 152	30,600	32,500	33,400	1,900	2,800
WT - 156	30,300	32,100	33,500	1,800	3,200
WT - 168	29,400	31,200	33,100	1,800	3,700
WT - 169	29,800	32,100	34,000	2,300	4,200
WT - 176	28,800	30,700	32,100	1,900	3,300
WA - 100	29,400	30,900	32,300	<u>1,500</u>	<u>2,900</u>
			Average	1,900	3,400
W - 5	31,300	33,100	34,700	1,800	3,400
W - 29	32,300	33,700	34,800	1,400	2,500
W - 32	31,200	33,300	34,600	2,100	3,400
W - 68	29,500	31,100	32,500	1,600	3,000
W - 69	30,100	31,800	33,100	1,700	3,000
W - 77	29,100	30,800	32,300	<u>1,700</u>	<u>3,200</u>
			Average	1,700	3,100

TABLE 8.22 (cont.)

Test Temperature: +1200°F

Specimen No.	0.2% Offset (psi)	0.3% Offset (psi)	0.4% Offset (psi)	Increase From 0.2% Offset to	
				0.3% Offset (psi)	0.4% Offset (psi)
WA - 118	24,300	25,300	26,400	1,000	2,100
WA - 120	25,800	27,300	28,400	1,434	2,617
WA - 124	25,800	27,300	28,400	1,434	2,617
WA - 150	25,900	27,300	28,600	1,384	2,668
WA - 163	26,700	28,100	29,300	1,365	2,578
WT - 164	27,000	28,700	29,900	1,649	2,917
			Average	1,400	2,600

Notes: W specimen size: R-3. WA and WT specimen size: R-1.

TABLE 8.23

0.3% AND 0.4% OFFSET YIELD STRENGTH OF  
HASTELLOY X RING FORGING, HEAT 261-5-4001

Test Temperature: -423°F

Specimen No.	0.2% Offset (psi)	0.3% Offset (psi)	0.4% Offset (psi)	Increase From 0.2% Offset to	
				0.3% Offset (psi)	0.4% Offset (psi)
Z - 3	85,000	89,100	91,100	4,100	6,100
Z - 23	88,600	91,100	93,400	2,500	4,800
Z - 48	85,900	89,900	93,600	4,000	7,700
Z - 53	83,500	86,500	89,500	3,000	6,000
Z - 66	86,900	90,400	93,600	3,500	6,700
Z - 68	87,300	91,900	94,400	4,600	7,100
			Average	3,600	6,400

Test Temperature: -320°F

ZA - 112	70,000	75,800	79,300	5,800	9,300
ZA - 117	68,200	70,700	72,800	2,500	4,600
ZA - 124	68,900	74,500	78,000	5,600	9,100
ZA - 125	68,700	74,300	78,400	5,600	9,700
ZT - 155	67,000	70,600	73,300	3,600	6,300
ZT - 156	68,700	72,400	75,700	3,700	7,000
ZT - 169	71,000	75,800	79,300	4,800	8,300
ZT - 174	68,700	71,900	74,000	3,200	5,300
			Average	4,300	7,400
Z - 14	68,700	73,100	76,200	4,400	7,500
Z - 40	66,700	71,300	74,800	4,600	8,100
Z - 45	69,900	74,300	77,400	4,400	7,500
Z - 52	71,900	75,500	78,000	3,600	6,100
Z - 58	69,200	72,800	75,900	3,600	6,700
Z - 76	67,700	71,800	74,500	4,100	6,800
			Average	4,100	7,100

TABLE 8.23 (cont.)

Test Temperature: Room

Specimen No.	0.2% Offset (psi)	0.3% Offset (psi)	0.4% Offset (psi)	Increase From 0.2% Offset to	
				0.3% Offset (psi)	0.4% Offset (psi)
ZA - 120	41,400	43,700	45,700	2,300	4,300
ZA - 127	41,900	43,600	45,300	1,700	3,400
ZT - 160	41,900	44,600	46,000	<u>2,700</u>	<u>4,100</u>
			Average	2,200	4,000
Z - 11	44,800	47,400	49,100	2,600	4,300
Z - 80	47,000	50,400	52,400	3,400	5,400
Z - 81	43,300	46,100	48,000	2,800	4,700
Z - 82	43,000	45,600	47,500	2,600	4,500
Z - 83	44,000	46,100	48,000	<u>2,100</u>	<u>4,000</u>
			Average	2,700	4,600

Test Temperature: 400°F

ZA - 128	31,800	33,600	35,400	1,800	3,600
ZT - 150	33,300	36,100	38,500	2,800	5,200
ZT - 157	32,200	34,400	36,100	2,200	3,900
Z - 30	33,100	35,400	37,200	2,300	4,100
Z - 51	36,100	38,400	39,900	2,300	3,800
Z - 59	32,000	34,400	36,700	<u>2,400</u>	<u>4,700</u>
			Average	2,300	4,200

TABLE 8.23 (cont.)

Test Temperature: 800°F

Specimen No.	0.2% Offset (psi)	0.3% Offset (psi)	0.4% Offset (psi)	Increase From 0.2% Offset to	
				0.3% Offset (psi)	0.4% Offset (psi)
ZA - 101	29,400	30,900	32,600	1,500	3,200
ZA - 102	29,300	30,900	32,100	1,600	2,800
ZT - 152	30,300	31,800	33,300	1,500	3,000
ZT - 153	29,100	31,100	32,200	2,000	3,100
ZT - 159	29,300	31,100	32,800	1,800	3,500
ZT - 161	29,100	30,800	32,400	1,700	3,300
ZT - 163	29,300	31,100	32,600	1,800	3,300
ZT - 168	28,600	30,200	31,800	1,600	3,200
ZT - 170	28,400	29,900	31,700	1,500	3,300
			Average	1,600	3,200
Z - 2	30,000	32,400	33,900	2,400	3,900
Z - 8	28,900	31,100	32,600	2,200	3,700
Z - 24	29,300	31,300	32,700	2,000	3,400
Z - 31	31,100	33,200	34,800	2,100	3,700
Z - 50	28,500	30,300	31,900	1,800	3,400
Z - 60	29,800	31,900	33,100	2,100	3,300
Z - 69	29,900	31,800	33,600	1,900	3,700
			Average	2,100	3,600

Test Temperature: +1200°F

ZA - 108	24,600	25,900	26,900	1,300	2,300
ZA - 113	25,100	26,800	28,100	1,700	3,000
ZA - 115	25,000	26,700	28,200	1,700	3,200
ZA - 118	24,300	25,600	26,700	1,300	2,400
ZA - 119	25,000	26,300	27,400	1,300	2,400
ZA - 126	24,900	26,200	27,400	1,300	2,500
ZA - 151	25,000	26,400	27,800	1,400	2,800
ZA - 162	25,100	26,500	27,700	1,400	2,600
ZA - 164	26,000	27,700	28,900	1,700	2,900
			Average	1,400	2,700

Notes: Z specimen size: R-3. ZA and ZI specimen size: R-1.



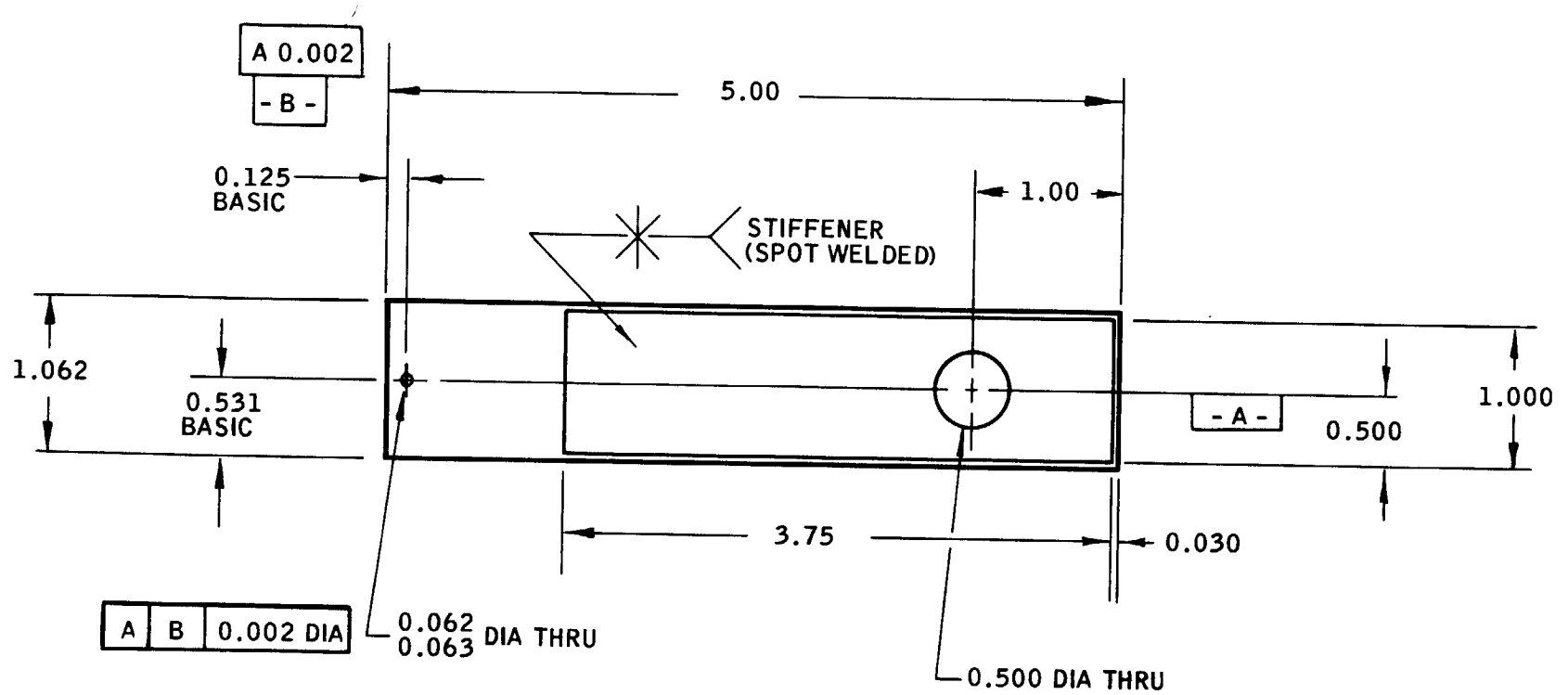
## 8.5 SHEAR STRENGTH

The design properties program included ultimate-shear-strength data, but since there was no requirement for statistical confidence, testing was confined to one heat of material (261-5-4000). The test temperature range was -320 to 400°F. The individual test data obtained are shown in Table 8.24. The values listed were obtained by use of a double-shear technique with a fixture that had been developed previously for NERVA testing. Specimen configuration is shown in Figure 8.6.

The results show that the ratio of shear strength to tensile strength is very high for Hastelloy X in comparison with other structural alloys. At -320°F, for example, the shear-to-tensile strength ratio is 0.92, while at 400°F the ratio is 0.81, which compares with a ratio of about 0.65 for the AISI 300 series stainless steels. A comparison of tangential with axial values (see Table 8.24) shows that the differences are insignificant at -320°F and at room temperature, but that at 400°F the tangential strength is somewhat higher. The relationship of the shear ultimate and tensile ultimate, as a function of temperature, are illustrated in Figure 8.7 with bearing strength.

## 8.6 BEARING STRENGTH

The interest in Hastelloy X bearing-strength data was for the coolant-tube strip material for which there was no published data and no established testing history in gages as thin as 0.012 inch. It was decided to evaluate two thicknesses (0.012 and 0.050-in.) for comparison. The tests were made over the temperature range of -320° to 800°F using the specimen configuration shown in Figure 8.6. The results are presented in Table 8.25 for the longitudinal and transverse properties of strip and sheet. The data for bearing-load ultimate strength ( $F_{bru}$ ) are normally listed for specific values of the ratio of the edge distance ( $e$ ) to the diameter ( $D$ ) of the pin



NOTE: DIMENSIONS IN INCHES

Figure 8.6 - Ultimate Bearing Strength Specimen

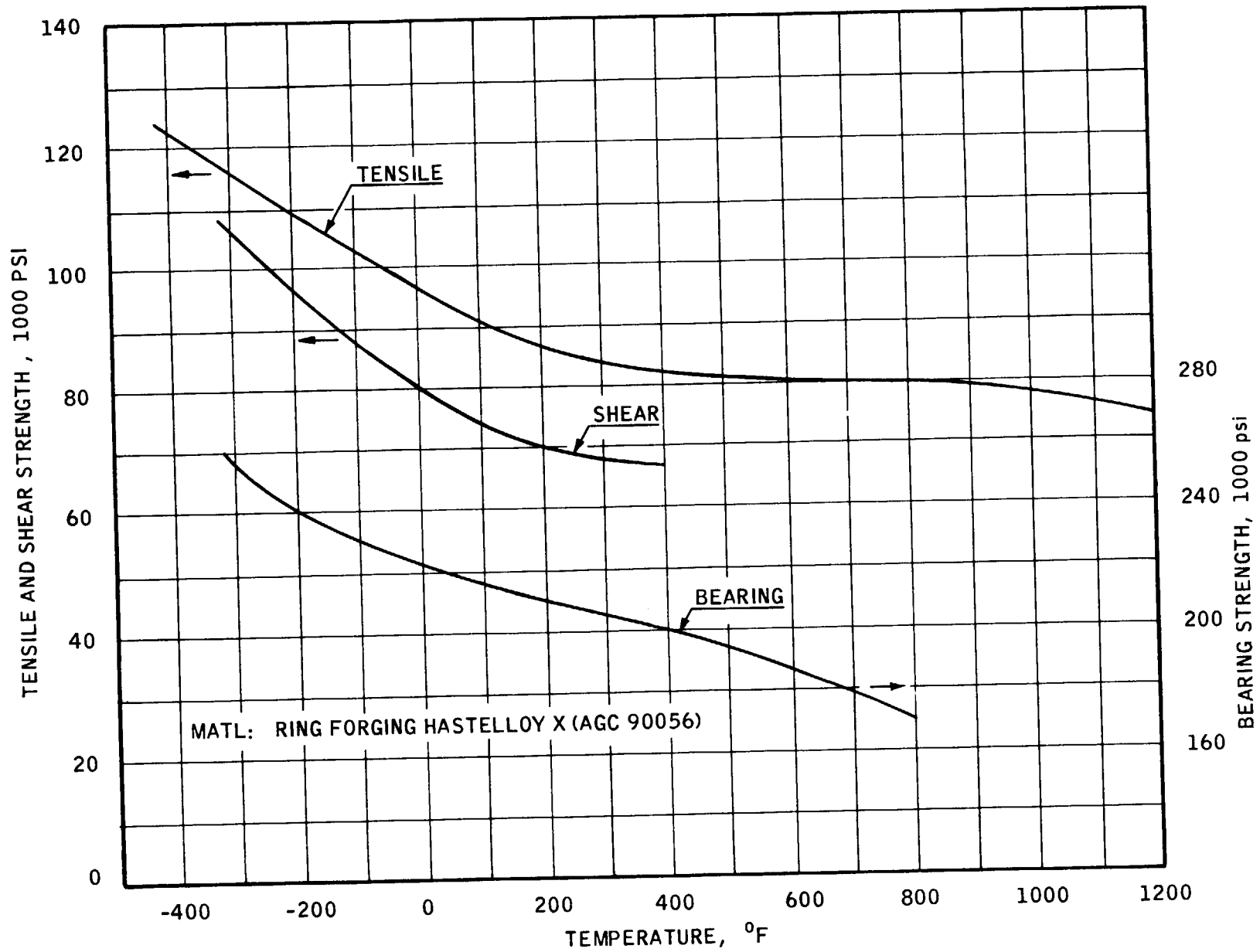


Figure 8.7 - Tensile, Shear, and Bearing Strength of Hastelloy X

TABLE 8.24

ULTIMATE SHEAR STRENGTH OF HASTELLOY X RING FORGING (AGC 90056)  
(HEAT 261-5-4000)

<u>Test Temp (°F)</u>	<u>Orientation</u>	<u>Ultimate Shear (ksi)</u>
-320 ↓	Axial	111.8
		104.0
		106.3
	Tangential	109.2
		108.8
		106.3
		Average <u>107.7</u>
Room ↓	Axial	75.4
		75.4
		73.5
	Tangential	74.9
		73.7
		71.4
		Average <u>74.0</u>
400 ↓	Axial	65.6
		64.0
		64.0
	Tangential	68.0
		68.9
		68.8
		Average <u>66.5</u>

NOTES: Material procured as rings 23-inch OD, 17-inch ID, by 6 inches long rings. Specimens tested using double-shear technique.

TABLE 8.25

BEARING STRENGTH OF HASTELLOY X SHEET AND STRIP  
(HEAT NO. 261-5-4000)

Sheet Thickness, in.	Test Temperature, °F	Ratio: Edge Dist, Dia	Specimen Direction	Bearing Ultimate, Fbru, ksi	Nature of Fracture
.012	-320	1.90	Longitudinal	252	Bearing
.012	-320	2.11	Longitudinal	265	Bearing
.052	-320	2.04	Longitudinal	(>323)	Tensile
↓	↓	2.01	↓	(>310)	↓
↓	↓	2.07	↓	(>303)	↓
.012	70	2.00	Longitudinal	205	Bearing
↓	↓	2.06	↓	229	↓
↓	↓	2.08	↓	238	↓
.012	70	2.03	Transverse	245	Bearing
↓	↓	1.81	↓	202	↓
↓	↓	2.11	↓	244	↓
.052	70	2.03	Longitudinal	233	Bearing First
.052	70	2.03	Longitudinal	241	Bearing First
.012	400	2.08	Longitudinal	197	Bearing
↓	↓	1.70	↓	184	↓
↓	↓	2.06	↓	201	↓
.012	400	2.02	Transverse	207	Bearing
.012	400	1.72	Transverse	171	Bearing
.053	400	2.00	Longitudinal	207	Bearing
.053	400	2.00	Longitudinal	203	Bearing
.012	800	2.06	Longitudinal	181	Bearing
.012	800	2.07	Longitudinal	172	Bearing
.052	800	2.03	Longitudinal	173	Bearing
↓	↓	2.05	↓	167	↓
↓	↓	2.05	↓	173	↓

loading. The most common tabulated values are for an e/D ratio of 2.0. It was observed for the specimens with an e/D ratio below 2.0 that the Fbru value was affected.

Values of the bearing ultimate-strength (Fbru) were computed from the load divided by the pin diameter times the sheet thickness. The ratio of edge distance divided by the pin diameter was controlled at 2.0 in most cases to correlate with other data.

The Fbru values for Hastelloy X are substantially higher than corresponding values for the austenitic stainless steels (e.g., AISI 304 has a value of 100 to 140 ksi at room temperature which compares with Fbru values ranging from 200 to 244 ksi for the same e/D ratio for Hastelloy X). The high bearing ultimate-strength correlates with the high shear strength. The 0.052-inch thick sheet specimens, illustrated in Figure 8.8, show the unusual fracture patterns for the low temperature specimens (-320°F) which withstood loads without bearing failure at values above 300 ksi when tearing at the pin was observed. The values used to plot the bearing ultimate-strength curve in Figure 8.7 were limited to  $e/D = 2.00 \pm 0.06$ .

## 8.7 COMPRESSIVE YIELD STRENGTH

Compression tests were performed on Heats 260-5-2813 and 261-5-4000 (ring forgings) in two directions (axial and short transverse) using square-end columns to determine if plastic deformation in compression was isotropic. Individual test results are shown in Table 8.26. Values were obtained for 0.2% and 0.4% offset yield. In addition, stress-strain diagrams were obtained for a number of the specimens. The mode of deformation in going to higher compression reductions was also determined. It was found that after exceeding 10% compression, specimens developed a decided "orange-peel" surface and a non-uniform bulging became apparent in the center of the specimens (see Figure 8.9). Values obtained from the two heats of material were generally in the same relationship as their tensile properties.

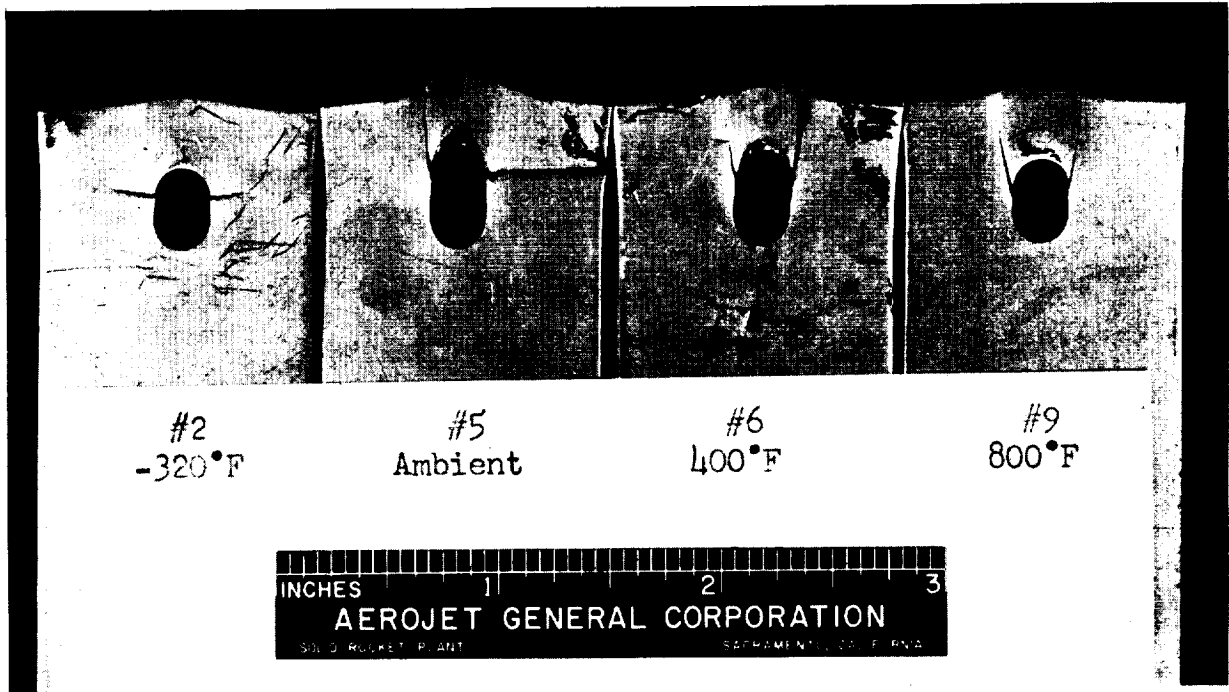


Figure 8.8 - Bearing-Load Test Specimens from 0.052-Inch Thick Hastelloy X Sheet (Heat 261-5-4000) After Testing

TABLE 8.26

COMPRESSION TESTS OF HASTELLOY X RING FORGINGS  
(HEATS 261-5-4000 AND 260-5-2813)

Heat 261-5-4000

Axial Specimens

Compressive Yield (ksi)		Final Stress (ksi)	Area (Max) Increase (%)	Compression in Length (%)
0.2%	0.4%			
44.8	48.3	114.6	12.8	11.0
45.3	49.4	132.0	16.4	12.0
45.2	48.8	135.9	17.5	15.0

Short Transverse Specimens (Heat 261-5-4000)

44.3	48.1	142.5	22.9	16.0
45.2	49.2	140.0	22.0	15.2
45.0	48.7	140.0	22.9	15.4
46.0	49.6	140.6	22.4	15.2
45.9	49.4	139.6	22.2	15.0
45.1	48.5	139.4	22.1	15.2

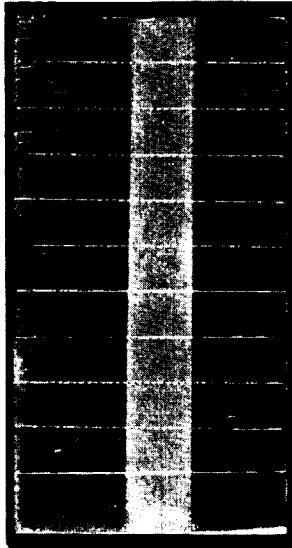
Heat 260-5-2813

Axial Specimens

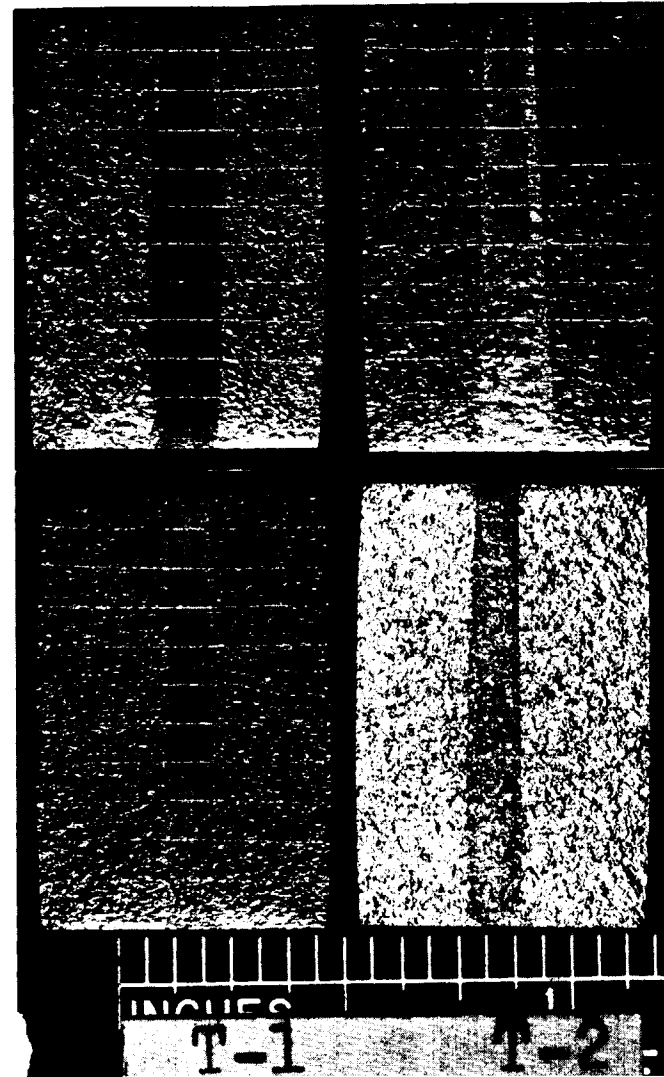
43.8	46.6	203.4	39.1	23.8
44.7	47.8	226.9	47.3	27.1
43.3	46.6	218.2	41.9	25.5
45.4	48.2	219.1	42.2	25.7
43.1	46.4	213.3	41.5	25.4
44.9	48.6	217.6	45.2	26.4

- Notes:
1. Strain rate 0.005-in./in./min to yield, then 0.05 in./in./min to final load.
  2. The maximum area represents area of the specimen at the maximum bulge after testing, transverse to the axis of compression.
  3. All tests at room temperature.





Front view of short transverse compression block after 16% reduction in height. Note surface "orange peel" appearance.

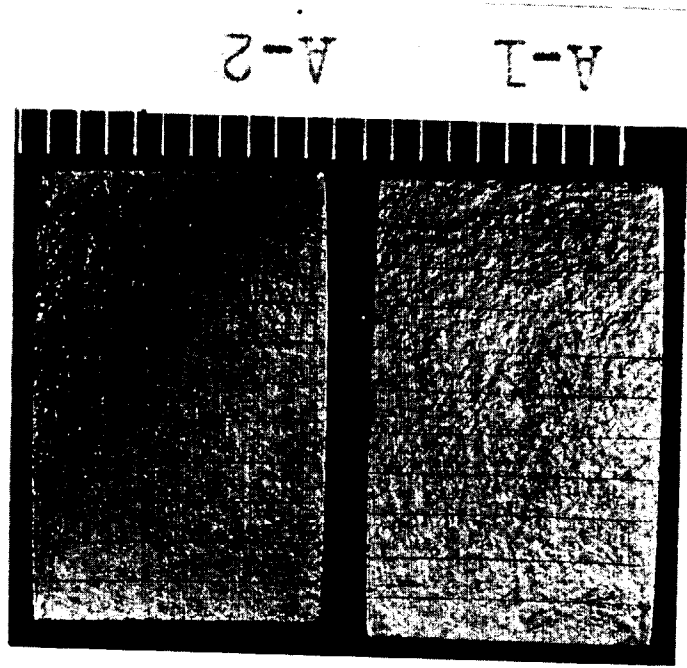


Side view of compression block above.

Short Transverse (vertical) compression block before testing showing scribed gage lines and gold plated stripe for incremental compressive strain measurement.

Figure 8.9 - Compression Test Specimens

Front view of axial compression blocks  
after 11% (A-1) and 12% (A-2) reduction  
in height.



Side view of same block on left.

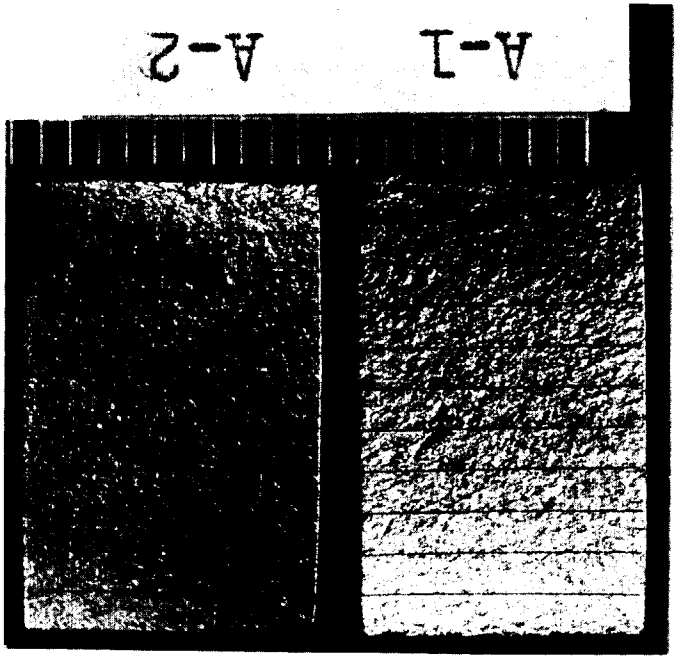


Figure 8.9 - Compression Test Specimens

The stress-strain diagrams in compression were similar to the corresponding curves for the tensile tests up to 1 or 2% strain: however, at higher strains the compression curves tend to increase upward as a result of the increase in area due to bulging. Despite the substantial deformation, there were no fractures or cracks observed in the compressive specimens, even for those which had been reduced as much as 25% in length.

The compression tests on Heat 261-5-4000 were planned in such a way as to obtain isotropy data by means of the directional behavior of the square-ended columns. It was observed, however, that for the first 10 or 11% of compression strain, expansion (diametral increase) was uniform in the two directions. With greater compression, a small amount of anisotropy was apparent. The "orange-peel" surface made accurate measurements difficult.

## 8.8 STRESS-STRAIN CURVES

Stress-strain curves for Hastelloy X were required for design use. Strain curves normally obtained during tensile testing record the elastic and plastic deformation at high magnification to 1/2 to 1% total strain. When the full curves are recorded, a lower magnification is used because of instrumentation limits and to prevent the curve from becoming excessively long. The full-length curves do not offer good resolution of offset yield strengths. Full-length curves were obtained on a limited number of specimens at each temperature because of the greater interest in the offset yield statistics. A representative group of the full stress-strain curves is shown in Figure 8.10 covering temperatures from -423 to 1600°F. The specimens employed were round R3 specimens from the ring forgings, except for the data shown at 1600°F which were from 0.012-inch thick sheet specimens. Low ductility at -320 and -423°F was due to the influence of the brazing cycle on the microstructure. For example, at -320°F solution heat-treated specimens had 40% elongation, while the highest value at -320°F after brazing was 19%. The influence of the lower ductility on the stress-strain curve was to terminate the curve before reaching

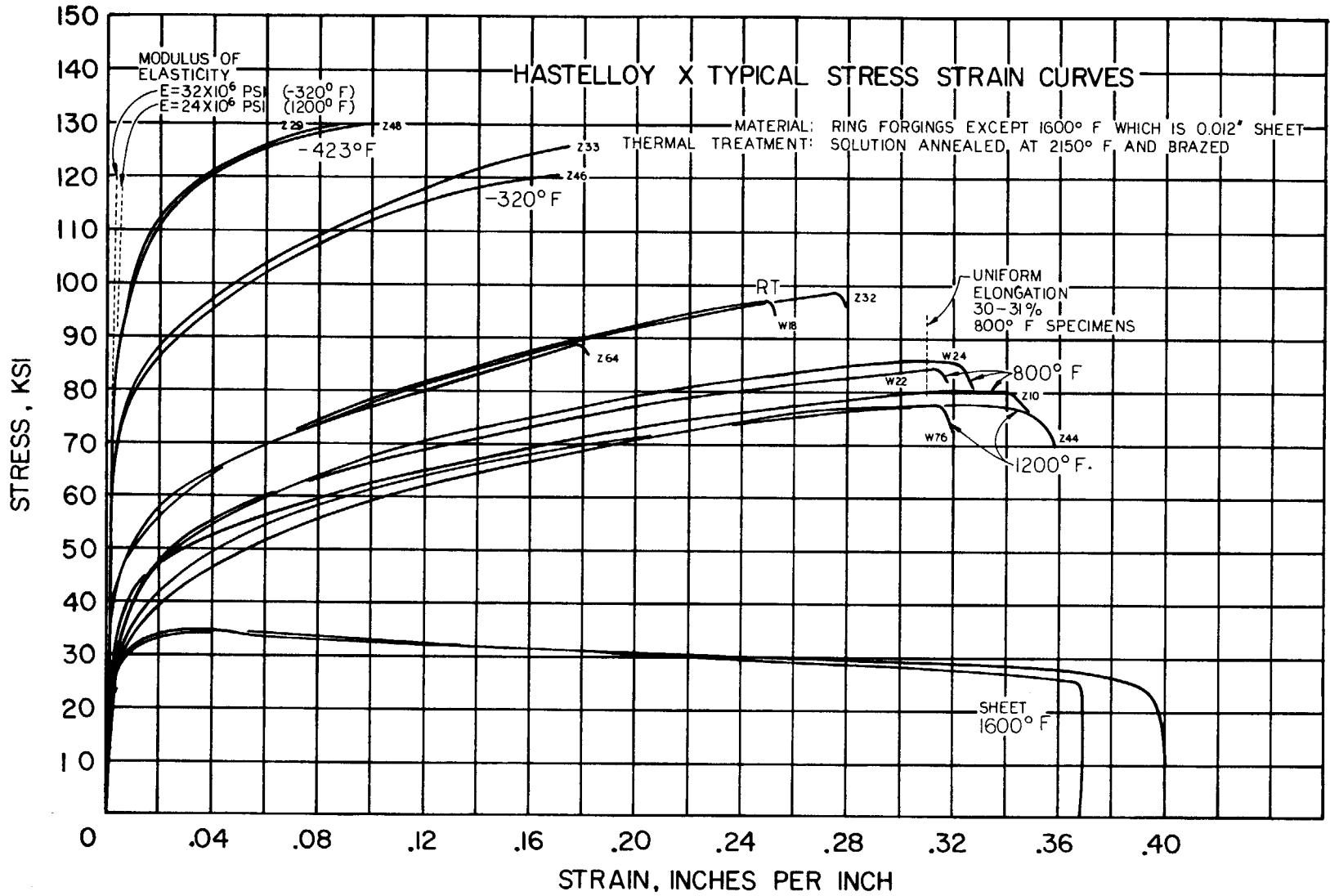


Figure 8.10 - Hastelloy X Typical Stress Strain Curves

the expected maximum load. At increasing temperatures, the effect of the brazing became less and less significant.

The influence of temperature is very pronounced at 1600°F, as compared with 1200°F. The stress-strain curves indicate a maximum stress after 3 to 3-1/2% strain, followed by a long plastic deformation with declining loads. This means that the uniform elongation values fall sharply from more than 30 to 3-1/2% at the higher temperature, although total elongation was not reduced. This effect has been observed at ORNL and elsewhere.

Higher magnification stress-strain curves are presented in Figure 8.11 which portrays the elastic-plastic region to 1.0% strain. The moduli and offset yield-strengths are illustrated by broken lines. Also shown are the tangent modulus ( $E_t$ ) values at the 0.2% offset strain. The tangent modulus values are lower than reported for solution heat-treated sheet material.

Test results at -320 and -423°F demonstrated a linear elastic behavior to 60 or 70% of the 0.2% offset yield value. At higher temperatures, the proportional limits were between 45 and 60% of the 0.2% yield.

One observation that could not be presented properly on the curves (Figures 8.10 and 8.11) was the discontinuous yielding that occurred at 800°F. No other temperature produced this effect, but it was shown to occur with different tensile machines and instrumentation. The effect was evidenced by numerous small "pips" in the stress-strain curves beyond the yield stress. Some specimens exhibited fewer, larger jumps which continued nearly to the maximum load. Two possible explanations are suggested: (1) formation of mechanical twins in the large-grain forging material; or (2) manifestation of strain-aging during deformation. Since only the 800°F specimens indicated discontinuous yielding, the latter seems more likely. Twinning has been observed in Hastelloy X after substantial reduction at high temperature

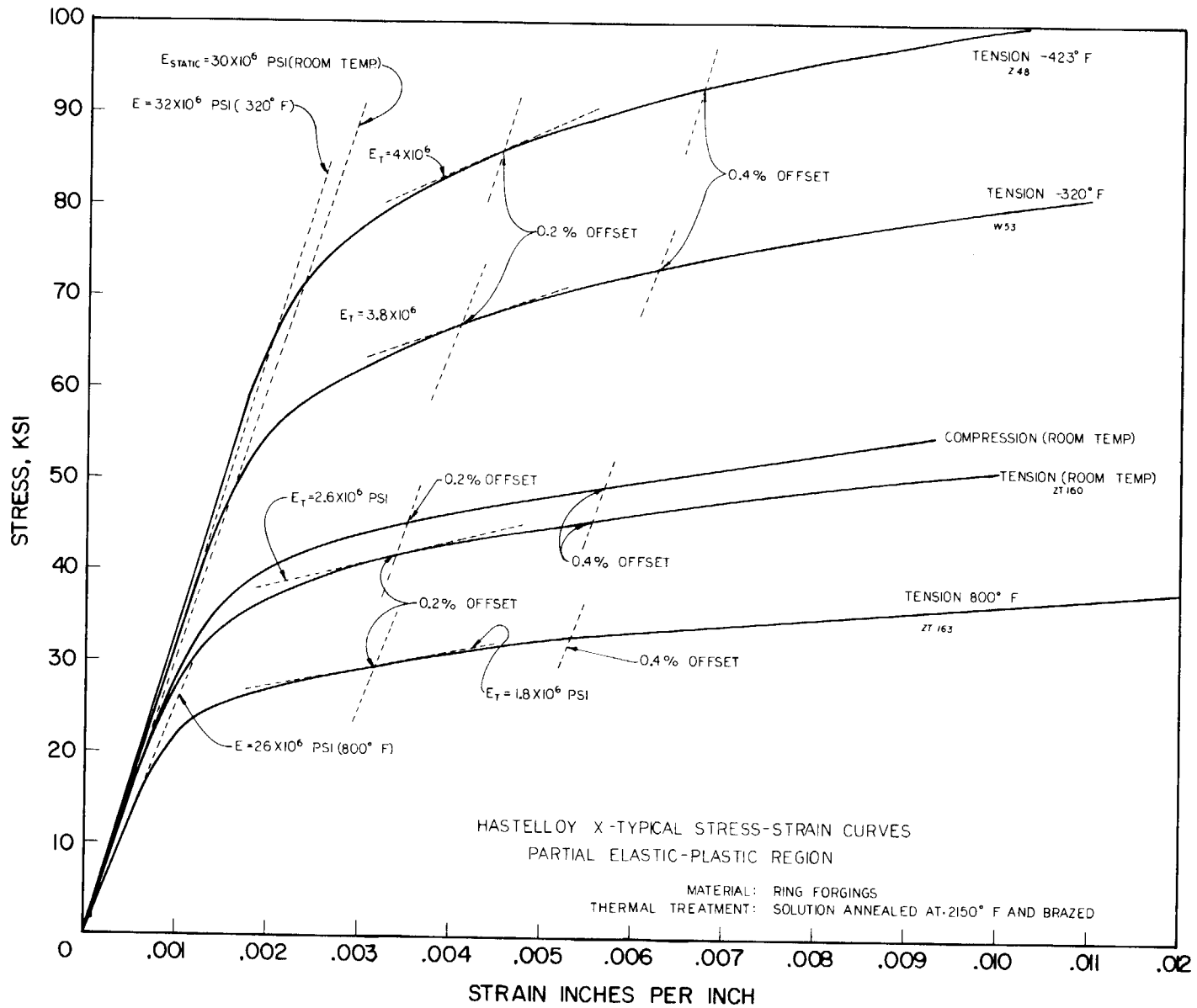


Figure 8.11 - Hastelloy X Typical Stress Strain Curves, Partial Elastic Plastic Region

(e.g., forging), but with deformations as small as 0.2% strain, twinning is doubtful.

One representative compression-test curve is plotted in Figure 8.10 to show the great similarity at low deformations. The curves were parallel but slightly above the corresponding tensile curve in all cases. At greater strain levels, the compression values curve upward as a result of the area increase. A plot of the true stress-true strain may show compression and tension to be the same.

## 8.9 LOW-CYCLE FATIGUE TESTING

The initial low-cycle fatigue (thermal-stress simulation) testing was unsatisfactory because of excessive yielding (elongation and area reduction) of the test specimen when loaded under a constant axial tensile load and simultaneously subjected to reversed bending stresses imposed by a constant lateral deflection (see Figure 8.12). The specimens work-hardened rapidly within the first few cycles so lateral deflection was reduced to a minor level to maintain surface-strain requirements. This low-level deflection was indicative of low dynamic-stress in the specimen.

A review of the results and the plastic-strain mechanisms involved was made and the testing method revised. The revised test eliminated the axial tensile-loading to minimize elongation, area reduction, and work-hardening of the specimen. The specimen was tested as a simple free-ended beam in reversed two point bending (see Figure 8.13) without tensile loading and instrumented with post-yield strain gages. The strain level was established at 8000 microinches (240 ksi equivalent elastic stress), or a 16,000 microinches range.

The first specimen (Heat 261-5-4001) was bent with controlled deflections in tension and compression, in the test fixture shown in Figure 8.13 to provide the required surface strain of 8000 microinches at

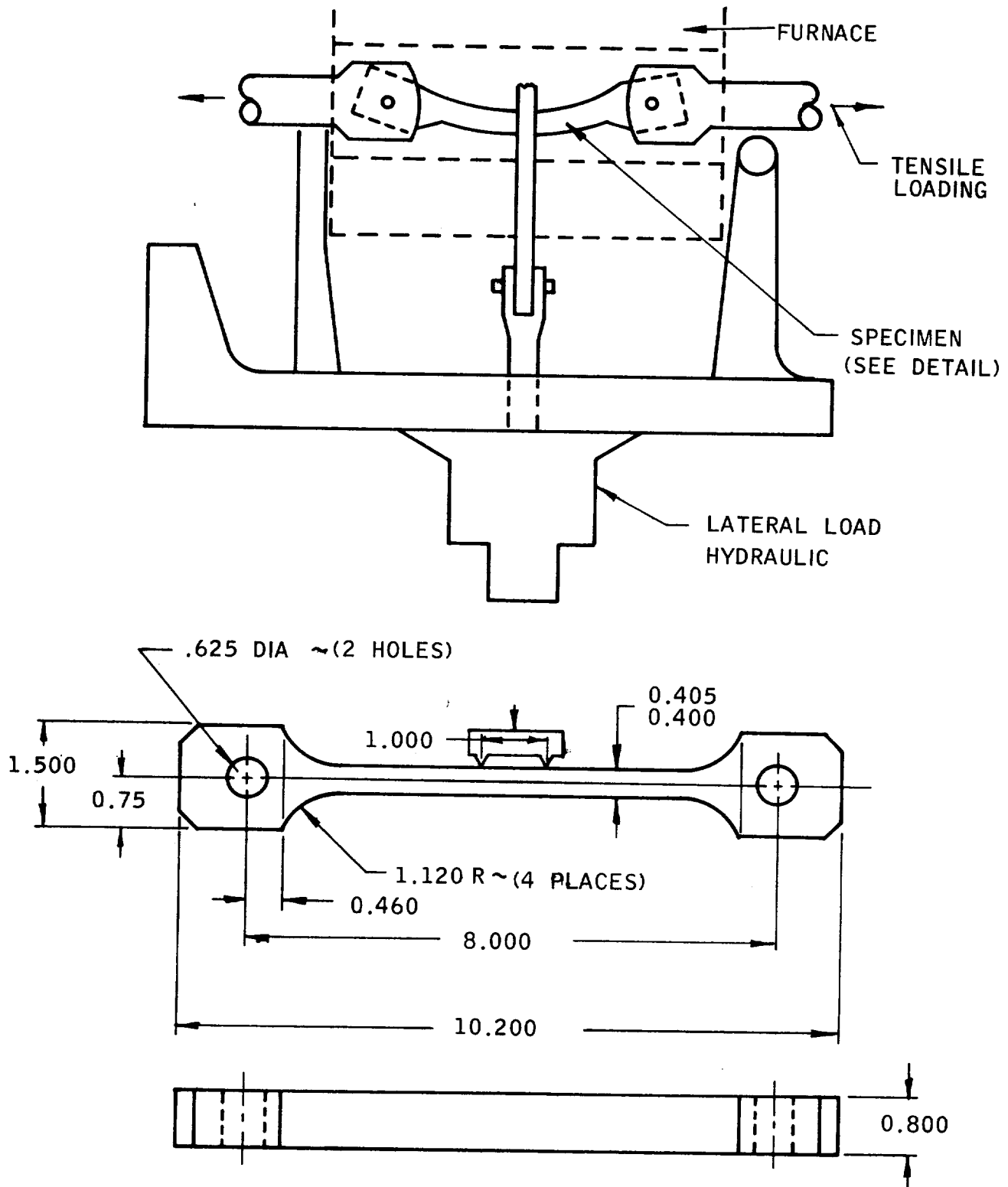


Figure 8.12 - Low-Cycle Fatigue Specimen (Lower) and Original Test Method (Upper)



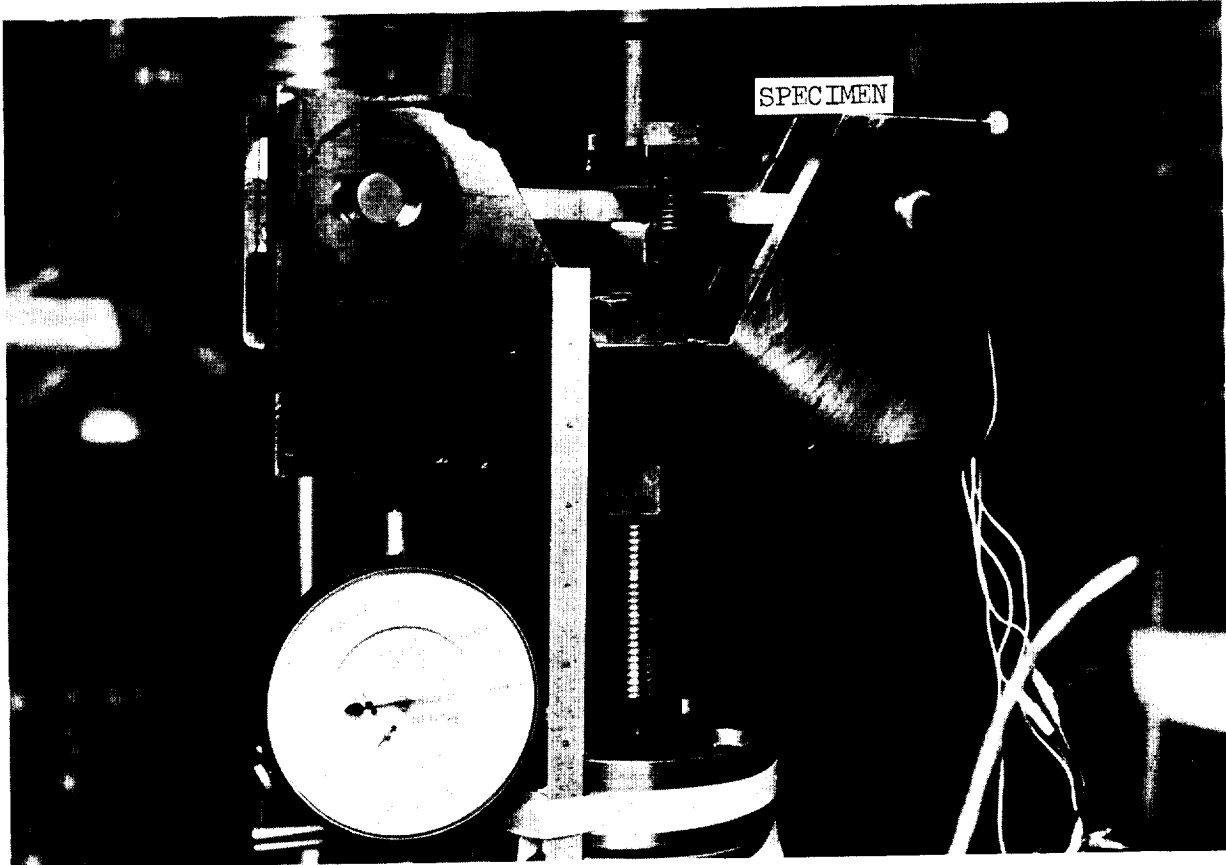


Figure 8.13 - Low-Cycle Fatigue Test Assembly (Specimen is supported between pins eight inches apart and stressed in bending at the center in both tension and compression)

room temperature. The specimen failed in 950 cycles: however, the surface-strain range varied from 16,000 to 11,000 microinches as a result of work hardening and test method inexperience. Work hardening caused the bend radius to change (see Figure 8.14): thus, while the specimen was under constant deflection (constant load), the surface strain varied. In the latter 400 cycles of the test, lateral deflection was increased to maintain the 16,000 microinches of surface strain range. The second specimen (Heat 260-5-4000) failed after 545 cycles at room temperature. All but a few of the initial cycles were at the specified total strain level. The second specimen, therefore, represented a more accurate life at the required strain level when compared to the first specimen.

The third low-cycle fatigue specimen was placed in the testing fixture with post-yield strain gages on both sides. The specimen was tested and strained identically to the room-temperature tests except that the temperature was  $-320^{\circ}\text{F}$ . The full-cycle strain range was 16,000 microinches in reversed bending and the specimen was from Heat 261-5-4001. Failure occurred in 934 cycles. Figure 8.15 depicts the typical load-deflection curve instrumentally plotted during testing and illustrates the load changes during the last four cycles as the specimen failed.

The increased number of cycles to failure (at  $-320^{\circ}\text{F}$  compared to room temperature) is as anticipated since fatigue strength increases as the tensile strength increases with decreasing temperature. This is illustrated by the average tensile properties of brazed Hastelloy-X at room temperature and  $-320^{\circ}\text{F}$ :

Average Tensile Properties of Brazed Hastelloy X

<u>Temp (<math>^{\circ}\text{F}</math>)</u>	<u>UTS (ksi)</u>	<u>YS (ksi)</u>	<u>Elastic Modulus (<math>10^6</math> psi)</u>
Room	93.3	45.0	30.0
-320	117.0	71.6	32.0

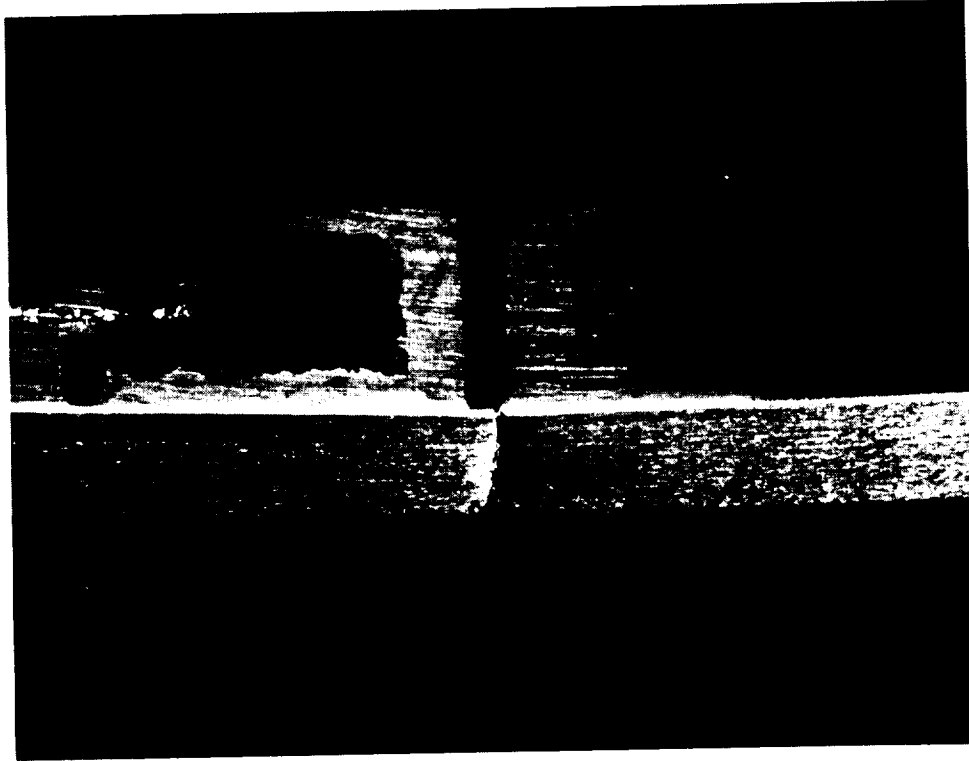


Figure 8.14 - Unetched, Slightly Enlarged Specimen, Tested at Room Temperature, From Heat 260-5-4001 Showing Location of Fracture (The initial fracture was from the bottom surface. Note localized reduction of area which was present on four surfaces but greatest on edges.)

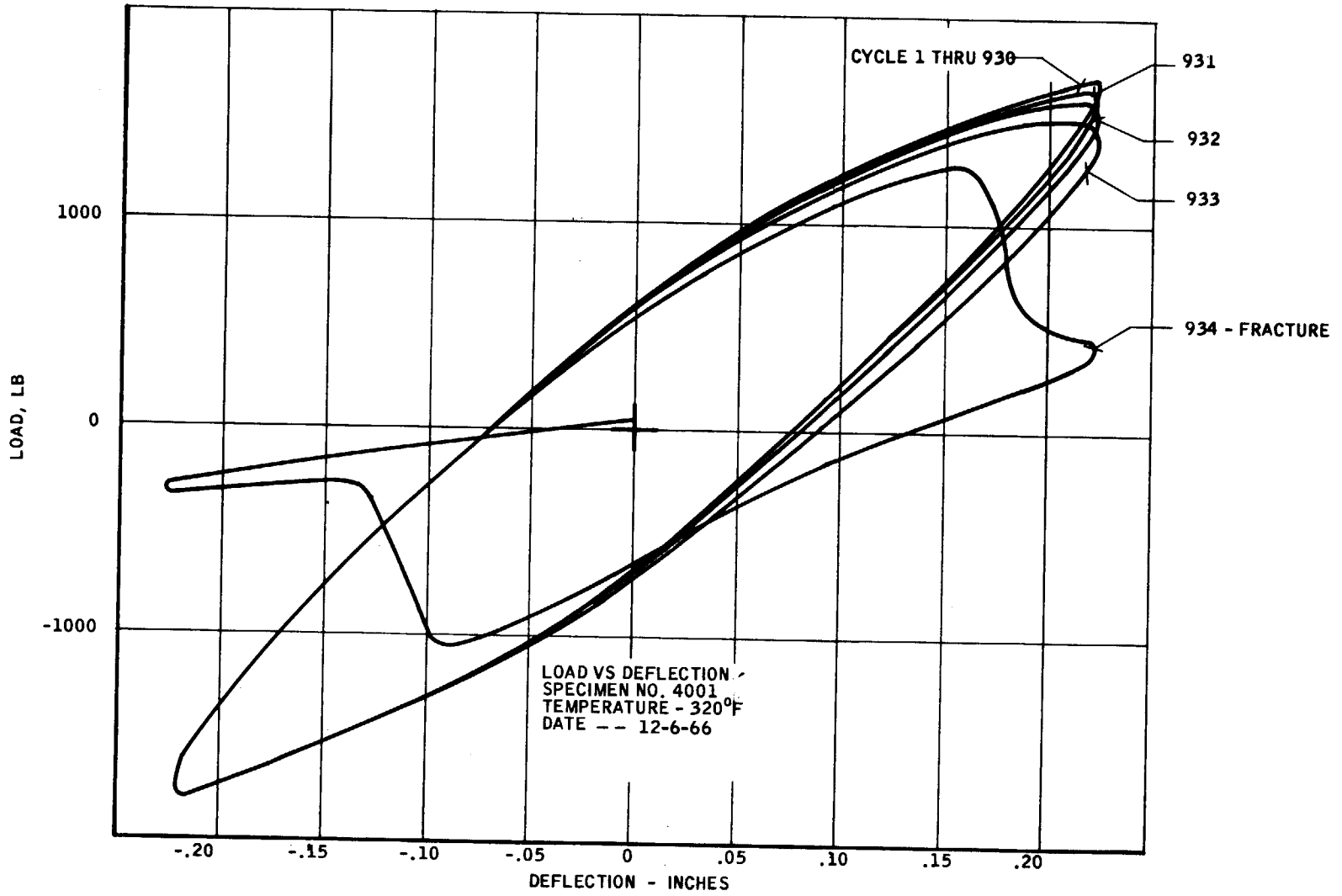


Figure 8.15 - Typical Load-Deflection Curve, Low-Cycle Fatigue Testing

Utilizing the stress-strain curves at the respective test temperatures (see Figure 8.16), the 240-ksi equivalent thermal stress based upon 8000 microinches of strain (0.8%) produces the following actual stresses based on first cycle loading):

Total and Plastic Strain for Hastelloy X

<u>Temp (°F)</u>	<u>Total Strain (%)</u>	<u>Plastic Strain (%)</u>	<u>Actual Stress (ksi) at 0.8% Strain</u>
Room	0.8	0.63	52.0
-320	0.8	0.55	80.5

Plotting the actual stress at each temperature versus the cycles-to-failure with the ultimate tensile stress (at one cycle for failure) provides a preliminary S-N curve, on log-log coordinate paper, as shown in Figure 8.17. The curve utilizes one cycle as the ultimate tensile-stress failure point; however, in a reversed bending analogy a tensile test technically represents failure in 1/4 cycle. This produces a small variance in the slope of each curve.

Although admittedly incomplete, the data indicate a life margin of greater than 10 cycles at an equivalent thermal stress of 240 ksi.

The increase in hardness (strength) of the test specimens was consistent with the progressive change in the load-versus-deflection curves: i.e., hardness increased in proportion to the bending strain but the neutral axis, which was subjected to the least strain, showed little or no change in hardness. The microhardness surveys are shown in Figures 8.18 and 8.19. The scatter of hardness values was partly attributable to the hard primary-phase concentrations in the microstructure and the grain orientation of the large-grain forgings. There appear to be bands of hardness (as illustrated by the dotted lines in Figure 8.19) for the specimen from Heat 260-5-4000.

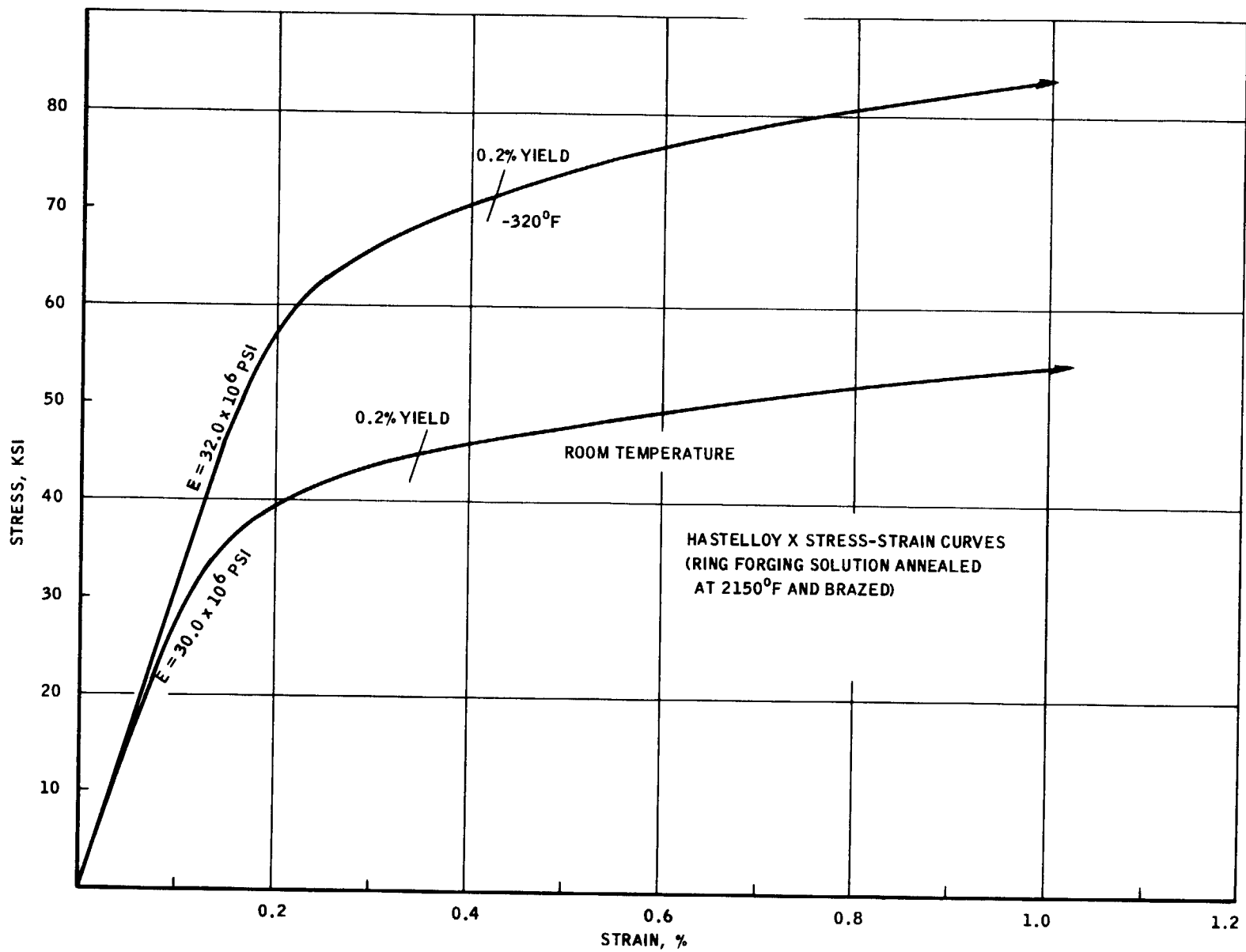


Figure 8.16 - Hastelloy X Stress Strain Curves

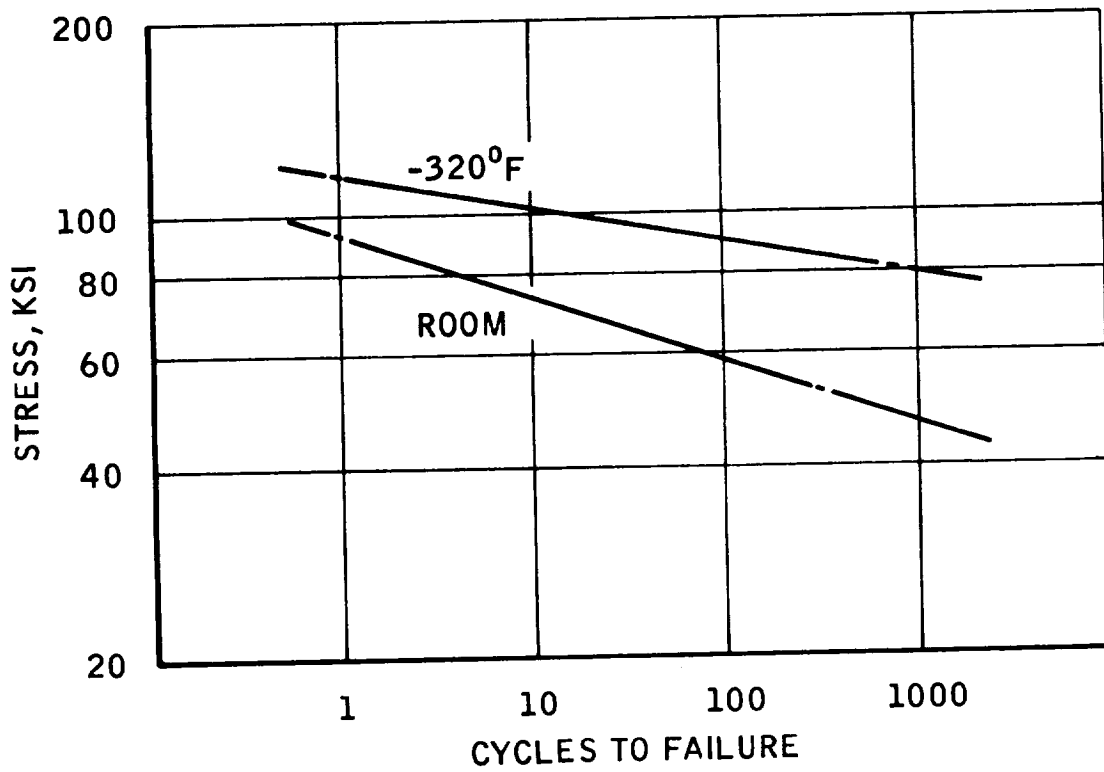


Figure 8.17 - Stress Cycles to Failure of Hastelloy X

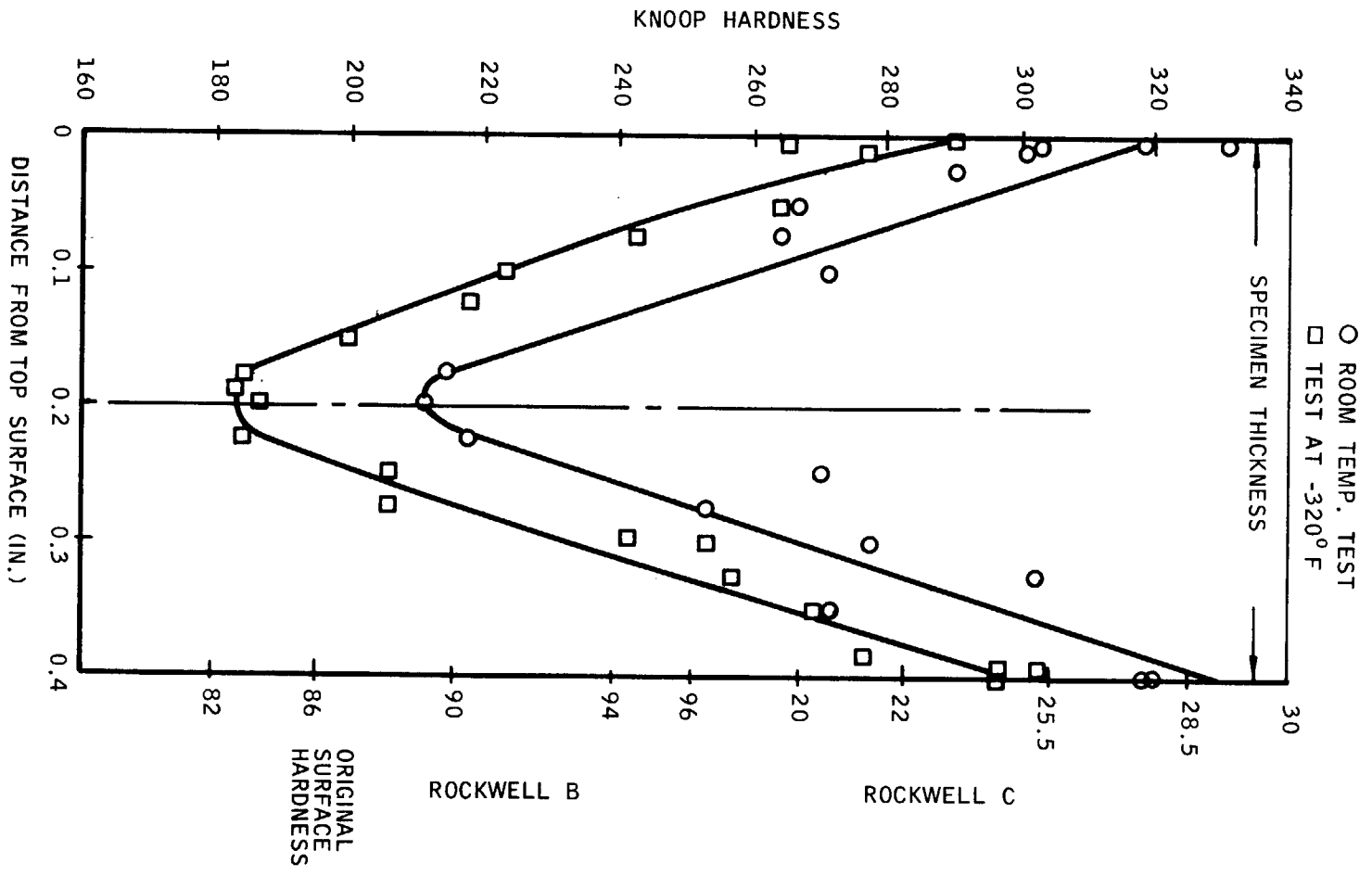


Figure 8.18 - Microhardness Profile, Room Temperature and Liquid Nitrogen Tests, Heat 260-5-4001



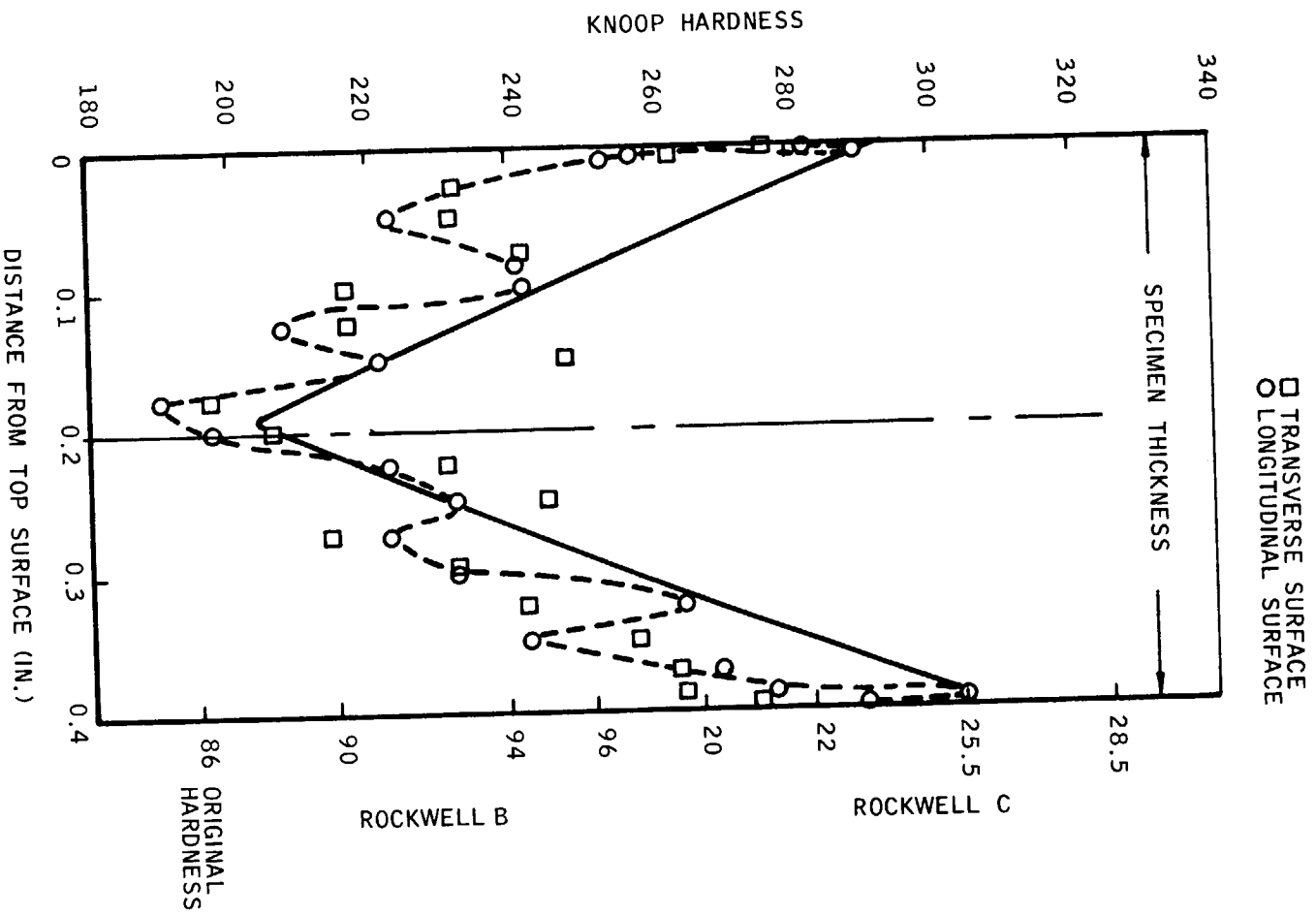


Figure 8.19 - Microhardness Profile, Room Temperature Test, Heat 260-5-4000

It should be noted that the specimens showed an increase in hardness at 0.004 to 0.010 inch below the surface when compared to that 0.002 inch below the surface. This effect may be due to: (1) the free surface on the strain distribution, so maximum plastic deformation was affected at 0.008 to 0.010 inch below the surface; or (2) the induced surface compression strain, on the reverse cycle, which produced a counteracting effect and caused maximum tensile strain below the surface of the specimen.

The difference in maximum microhardness between the room-temperature and the  $-320^{\circ}\text{F}$  specimen of Heat 260-5-4001 (see Figure 8.18) may have been expected from the greater plastic deformation exhibited by the room temperature specimen, as shown in Figures 8.14 and 8.20. There was some difference in the history of testing for these two specimens. The room-temperature specimen was originally tested at constant deflection which resulted in lower, true surface-strain at the center as the material strain hardened. After about 280 cycles, the amplitude was increased to provide the originally desired surface-strain level of 8000 microinches in both directions (16,000 microinch total range). The specimen tested at  $-320^{\circ}\text{F}$  was maintained at a constant deflection throughout the test, hence less strain-hardening occurred. It is also significant that the yield strength at  $-320^{\circ}\text{F}$  is considerably higher than at room temperature; thus, for a given plastic deflection, a larger component is contributed by the elastic portion of the stress-strain curve than occurs at room temperature.

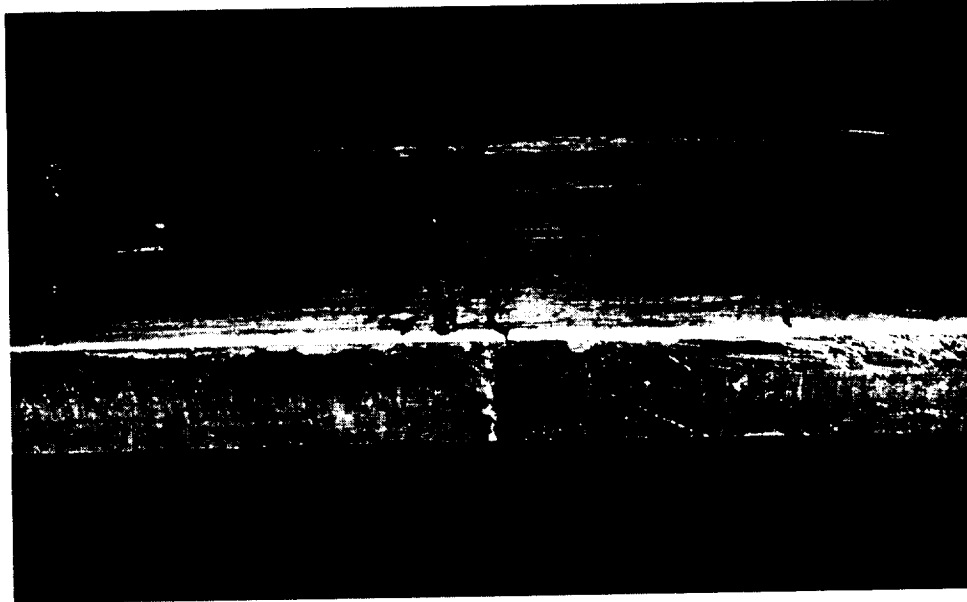


Figure 8.20 - Unetched, Slightly Enlarged Specimen Tested at 320°F, from Heat 260-5-4001 Showing Location of Fracture (Oblique view shows fracture location about 0.2 inch away from loading contact area. Strain gage shows as dark area on left. No significant reduction of area was observed. Initial fracture area was on top surface.)

## 9.0 BRAZE-JOINT MECHANICAL PROPERTIES

### 9.1 TENSILE TESTS

The tensile test results are presented in Table 9.1 for the parent metal (exposed to Nicro braze cycle), Nicro brazed, copper brazed, Palniro-7 brazed and Nicoro-80 brazed specimens (see Figure 9.1). Nickel-plated joint surface data are shown in Table 9.2. All failures occurred in the braze joint, indicating the braze alloy is lower in strength than Hastelloy X. With the exception of the copper braze, tensile strengths approximated those of the parent metal at room temperature. At 1200°F, the braze-joint strengths ranged from 34 to 70% of the parent metal, reflecting the more pronounced effect of temperature on the braze alloys than on the Hastelloy X parent metal. Test data at -320°F were restricted to the Nicro alloy, because of its contact with the low-temperature environment of the nozzle: nevertheless, they reveal a strength equivalent to the parent metal. Data at -320°F were not available on the actual parent metal bar-stock utilized in this investigation but parent-metal data from full braze-cycle exposure (Specification AGC 90169) were employed: based upon the 106.0 ksi room-temperature tensile strength, the 140 ksi strength at -320°F is as anticipated.

Flat tensile specimen (see Figure 9.2) data (0.012-in. thick strip) are presented in Table 9.3, which compares parent-metal strength and ductility with the effects of surface diffusion by each braze alloy. The results revealed that the brazed specimens possessed: (1) tensile strength equivalent to the parent metal at room temperature and at 1200°F; (2) slightly higher yield strengths than the parent metal at room temperature and at 1200°F; and (3) lower elongation than the parent metal (except for Nicoro 80 at room temperature) at room temperature and at 1200°F.

TABLE 9.1

TENSILE TEST RESULTS FOR 0.250-INCH ROUND HASTELLOY X BAR STOCK

Parent Metal (Heat 260-5-2783); Held three hours at 1850°F, then cooled at rate equivalent to slow air-cool.

<u>Test Temp (°F)</u>	<u>UTS (psi)</u>	<u>0.2% YS (psi)</u>	<u>1-in. Elong. (%)</u>
-320	139,000	71.6	18.5
↓	140,000	75.4	19.5
	141,000	72.1	19
	140,000	73.0	19
	Room	104,000	44,900
↓	106,000	47,000	38
	106,000	45,300	39
	105,000	44,200	38
	104,000	44,400	38
	Average	105,000	45,200
1200	74,500	29,200	64.5
↓	75,900	29,900	64
	77,100	30,000	59
	75,400	28,700	63
	77,100	28,400	60
	76,000	29,200	62.1

TABLE 9.1 (cont.)

Nicro Braze: Held three hours at 1850°F, then cooled at rate equivalent to slow air-cool.

<u>Test Temp (°F)</u>		<u>UTS (psi)</u>
-320		131,000
		121,000
		141,000
		116,000
		128,000
		131,000
	Average	128,000
Room		94,600
		100,000
		101,000
		82,100
		96,700
	Average	94,900
1200		50,900
		35,900
		48,100
		42,700
		46,600
	Average	44,800

TABLE 9.1 (cont.)

Copper Braze: Held three hours at 2025°F, then cooled at rate equivalent to slow air-cool.

<u>Test Test (°F)</u>	<u>UTS (psi)</u>
Room	63,500
↓	68,600
	56,500
	66,300
	65,900
	Average
1200	32,200
↓	32,100
	31,600
	33,400
	30,300
	31,900

Palniro-7 Braze: Held three hours at 1975°F, then cooled at rate equivalent to slow air-cool.

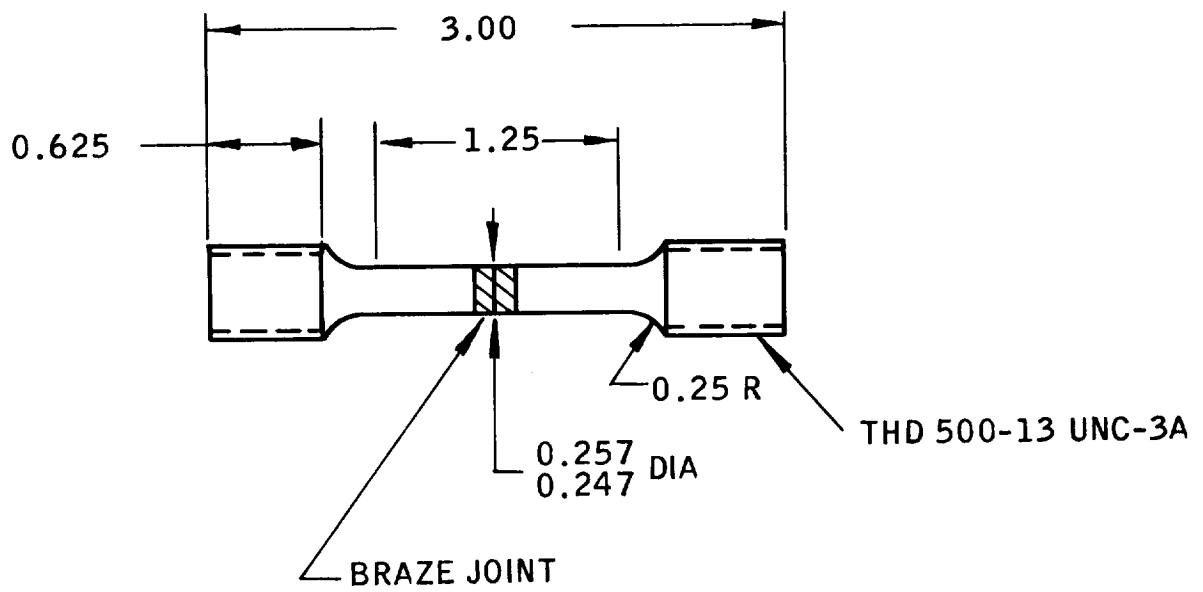
<u>Test Temp (°F)</u>	<u>UTS (psi)</u>	
Room	100,000	
↓	49,900	
	101,000	
	98,900	
	Average	88,300
	1200	53,000
↓	51,800	
	37,600	
	52,700	
	50,300	
	Average	49,100

TABLE 9.1 (cont.)

Nicoro-80 Braze: Held three hours at 1750°F, then cooled at rate equivalent to slow air-cool.

<u>Test Temp (°F)</u>	<u>UTS (psi)</u>
Room	108,000
↓	107,000
↓	107,000
Average	107,300
1200	26,000
↓	30,500
↓	27,000
↓	27,600
↓	28,800
Average	28,000





NOTE: ALL DIMENSIONS IN INCHES

Figure 9.1 - Standard Round Tensile Specimen

TABLE 9.2

TENSILE TEST RESULTS FOR 0.250-INCH ROUND HASTELLOY X BAR  
 STOCK EXPOSED TO BRAZE-CYCLE (FAYING SURFACES NICKEL PLATED)  
 PER AGC-90169

Nioro Braze Joint

<u>Test Temp (°F)</u>	<u>Nickel Plating Thickness (in.)</u>	<u>UTS (psi)</u>
Room	0.0002	104,000
↓	0.0002	65,100
	0.0002	88,000
	0.0002	106,000
	0.0002	83,800
	Average	0.0002
-320	0.0002	131,000
↓	0.0002	99,400
	0.0002	133,000
	0.0002	135,000
	0.0002	132,000
	Average	0.0002
Room	0.0005	101,000
↓	0.0005	83,200
	0.0005	99,700
	0.0005	102,000
	0.0005	102,000
	Average	0.0005

TABLE 9.2 (cont.)

<u>Test Temp (°F)</u>	<u>Nickel Plating Thickness (in.)</u>	<u>UTS (psi)</u>
-320	0.0005	130,000
↓	0.0005	136,000
	0.0005	100,000
	0.0005	134,000
	0.0005	137,000
	Average	0.0005
Room	0.0008	86,200
↓	0.0008	73,600
	0.0008	68,600
	0.0008	93,700
	0.0008	65,700
	Average	0.0008
-320	0.0008	124,000
↓	0.0008	117,000
	0.0008	116,000
	0.0008	110,000
	0.0008	135,000
	Average	0.0008

TABLE 9.2 (cont.)

Parent Metal

<u>Test</u> <u>Test (°F)</u>	<u>UTS (psi)</u>	<u>0.2% YS (psi)</u>	<u>1-in. Elong. (%)</u>
Room	106,000	44,100	30.5
↓	106,000	44,100	32
↓	106,000	44,400	31.5
Average	106,000	44,200	31.5
-320	139,000	71,600	18.5
↓	140,000	75,400	19.5
↓	141,000	72,100	19
Average	140,000	73,000	19

TABLE 9.3

TENSILE TEST RESULTS FOR 0.012-INCH THICK  
HASTELLOY X STRIP\* BRAZE-ALLOY DIFFUSION SPECIMENS

Braze Cycle: Three hours at 1850°F, then cooled at rate equivalent to slow air cool

Braze Alloy: Nioro

Parent Metal

<u>Test Temp (°F)</u>	<u>UTS (psi)</u>	<u>0.2% YS (psi)</u>	<u>2-in. Elong. (%)</u>
Room	111,000	58,100	14.0
↓	116,000	58,500	15.5
↓	117,000	57,400	17.5
Average	114,500	58,000	15.5
1200	83,700	40,400	17.5
↓	93,500	40,100	32.0
↓	90,700	41,500	28.0
Average	89,300	40,700	26.0

Nioro Surface-Brazed

Room	113,000	63,900	13.5
↓	109,000	64,800	10.5
↓	113,000	68,400	10.5
↓	112,000	64,400	11.5
↓	114,000	64,200	11.5
Average	112,200	65,100	11.5
1200	88,600	45,100	18.0
↓	76,300	45,100	8.5
↓	86,300	45,700	17.5
↓	89,900	45,300	18.5
↓	88,500	43,800	18.5
↓	90,000	46,200	20.0
Average	86,600	45,200	17.0

\*Heat 261-5-4002

TABLE 9.3 (cont.)

Braze Cycle: Three hours at 2025°F, then cooled at rate equivalent to slow air-cool.

Braze Alloy: Copper

Test Temp (°F)	<u>Parent Metal</u>		
	UTS (psi)	0.2% YS (psi)	2-in. Elong. (%)
Room	116,000	52,500	32.0
↓	112,000	53,300	31.5
↓	114,000	53,200	23.5
Average	114,000	53,000	29.0
1200	80,100	35,100	29.5
↓	84,500	34,900	43.0
↓	84,700	35,500	42.5
Average	83,100	35,200	38.5

Test Temp (°F)	<u>Copper Surface-Brazed</u>		
	UTS (psi)	0.2% YS (psi)	2-in. Elong. (%)
Room	108,000	62,700	19.5
↓	103,000	57,600	18.5
↓	117,000	67,600	26.5
↓	112,000	59,500	26.0
↓	113,000	65,600	26.0
Average	110,600	62,600	23.5
1200	80,100	44,500	21.0
↓	83,400	43,100	26.0
↓	82,600	44,500	27.0
↓	79,600	44,500	25.5
↓	74,500	41,700	17.5
Average	80,000	43,700	23.5

TABLE 9.3 (cont.)

Braze Cycle: Three hours at 1975°F, then cooled at rate equivalent to slow air-cool.

Braze Alloy: Palniro-7

Test Temp (°F)	<u>Parent Metal</u>		
	<u>UTS (psi)</u>	<u>0.2% YS (psi)</u>	<u>2-in. Elong. (%)</u>
Room	110,000	52,200	19.5
↓	116,000	52,400	27.5
↓	115,000	52,400	26.5
Average	110,300	52,300	24.5
1200	86,300	36,600	37.0
↓	89,600	37,000	34.5
↓	87,000	37,900	32.0
Average	87,600	37,200	34.5

<u>Palaniro-7 Surface Brazed</u>			
Room	110,000	65,300	13.5
↓	95,300	69,600	5.0
↓	103,000	60,500	11.5
↓	112,000	60,300	21.0
↓	97,700	61,200	9.0
Average	103,600	63,400	12.0
1200	78,600	43,700	16.5
↓	80,300	42,800	16.0
↓	77,200	41,600	13.5
↓	88,900	43,200	28.5
↓	87,600	41,000	29.5
Average	82,500	42,300	21.0

TABLE 9.3 (cont.)

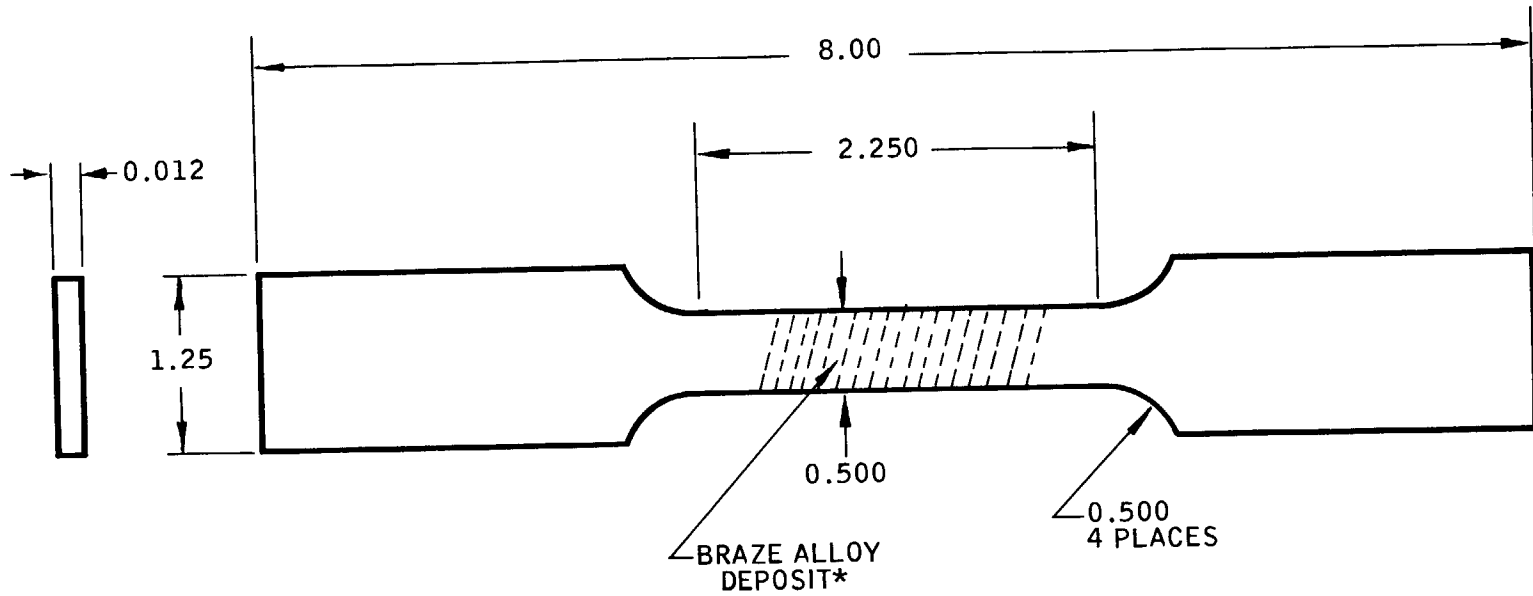
Braze Cycle: Three hours at 1750°F, then cooled at rate equivalent to slow air cool.

Braze Alloy: Nicoro-80

<u>Test Temp (°F)</u>	<u>Parent Metal</u>		
	<u>UTS (psi)</u>	<u>0.2% YS (psi)</u>	<u>2-in. Elong. (%)</u>
Room	113,000	51,900	23.0
↓	113,000	51,700	27.0
↓	115,000	53,000	23.0
Average	113,700	52,200	24.5
1200	89,600	38,300	36.5
↓	88,000	40,900	36.5
↓	85,000	39,400	37.5
Average	87,500	39,500	37.0

<u>Nicoro-80 Surface Brazed</u>			
Room	116,000	63,200	27.5
↓	117,000	62,400	28.0
↓	116,000	61,100	27.0
↓	116,000	61,700	28.0
↓	117,000	62,600	29.0
Average	116,500	62,200	28.0
1200	86,700	41,100	28.5
↓	85,600	42,400	30.0
↓	83,900	40,700	30.5
↓	87,200	41,700	30.5
↓	86,300	41,900	29.5
Average	85,900	41,600	30.0





\*SURFACE GRIND AFTER BRAZING TO  
0.011-INCH THICK FOR 2.250 GAGE  
LENGTH

NOTE: ALL DIMENSIONS IN INCHES

Figure 9.2 - Flat Tensile Specimen

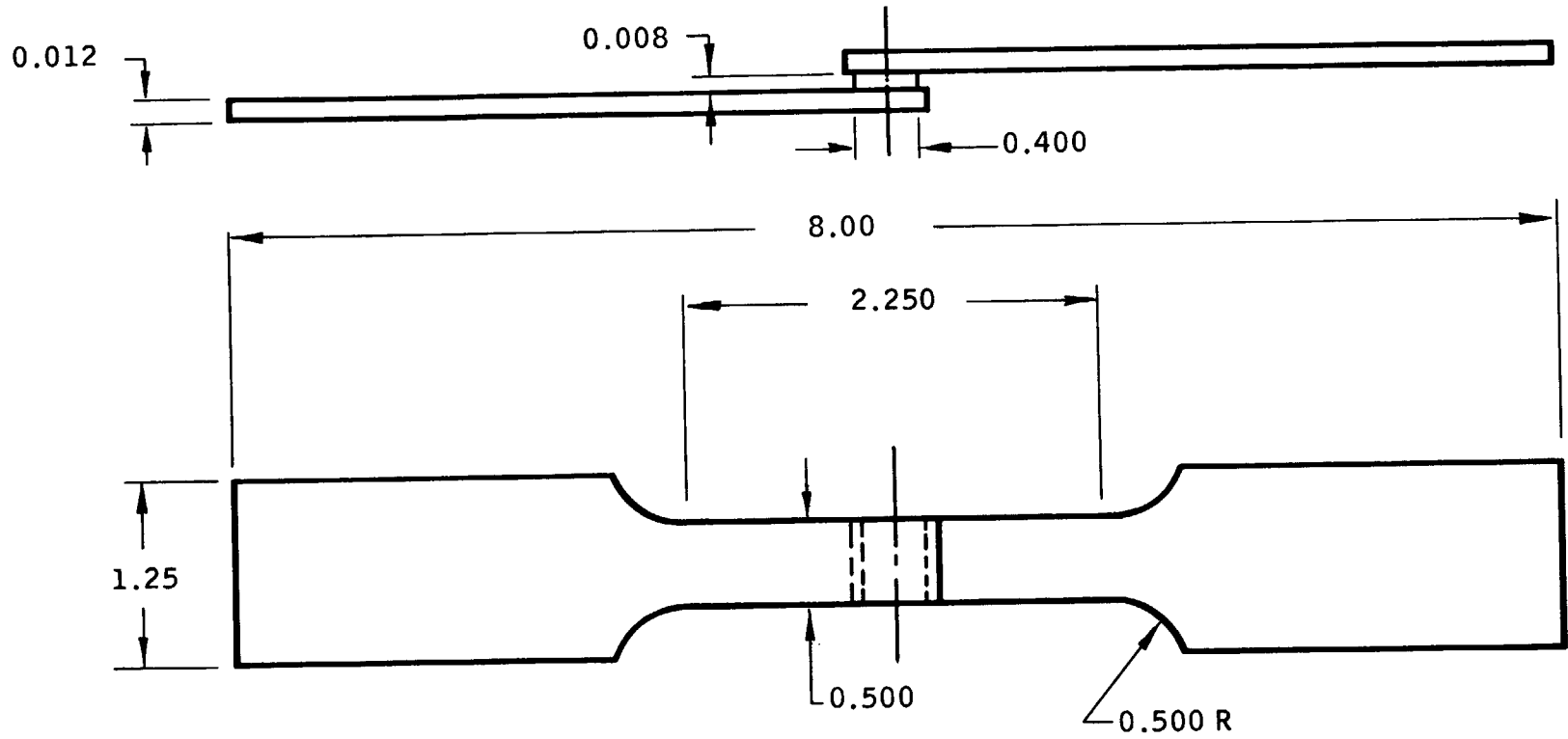
Results of the simulated seal-joint tests (see Figure 9.3 for the specimen used) are presented in Table 9.4 for two different multiple-cycle braze treatments. All failures occurred in the parent metal.

A slight loss in tensile strength occurred at room temperature for the parent metal and brazed specimens during the 1975/1950/1825 temperature cycle. At 1200°F, the parent metal was unaffected but the brazed specimens increased in strength. Since all specimens failed in the parent metal, it can be assumed that both sets of data represent normal spread in the parent-metal samples, in which case the room-temperature strength is lowered by the high-temperature braze cycle and an apparent slight increase occurs at 1200°F. The significant feature of these data is the effect on parent-metal ductility, which is lowered a pronounced amount at room temperature by the high-temperature braze cycle. Although considerable recovery occurs at 1200°F, the value has not returned to the level of the low-temperature braze cycle.

The effects of the individual braze alloys, using simulated seal-joint specimens, are shown in Table 9.5. The tensile strengths of the brazed specimens are comparable to the parent metal at room temperature and 1200°F, except for copper at 1200°F which averages about 10 ksi lower than the Nicro, Palniro-7 and Nicoro-80 specimens.

## 9.2 SHEAR TESTS

Miller-Peaslee shear-test specimens (see Figure 9.4 for the specimen used), brazed with Nicro, Palniro-7 and Nicoro-80, were shipped to ORNL for testing. The test results are shown in Table 9.6. Figures 9.5 through 9.7 present the shear stress-strain diagrams comparing the irradiated and unirradiated specimens. The curves representing a complex strain from parent metal and braze joint, reveal little or no change in strength at -320°F and room temperature but a definite decrease in available ductility. At 750°F, a pronounced decrease in strength occurs, presumably a manifestation of the braze alloy in the joint because of the greater strength of the parent-metal Hastelloy X at this temperature.



NOTE: ALL DIMENSIONS IN INCHES

Figure 9.3 - Flat, Simulated Seal-Joint Specimen

TABLE 9.4

TENSILE TEST RESULTS FOR SIMULATED SEAL-JOINT SPECIMENS\*  
EXPOSED TO MULTIPLE BRAZE CYCLES

Cycles: Three hours at 1850°F (Nioro) + three hours at 1825°F (Nioro + Palniro-7) + three hours at 1750°F (Nicoro-80): cooled at rate equivalent to slow air-cooled after each cycle.

Parent Metal

<u>Test Temp (°F)</u>	<u>UTS (psi)</u>	<u>0.2% YS (psi)</u>	<u>2-in. Elong. (%)</u>
Room	114,000	55,500	24.5
↓	114,000	52,700	30.0
↓	116,000	52,600	30.0
Average	114,700	53,600	28.0
1200	86,500	37,600	38.0
↓	87,800	37,600	39.0
↓	86,900	36,700	41.0
Average	87,100	37,300	39.5

Brazed

<u>Test Temp (°F)</u>	<u>UTS (psi)</u>
Room	110,000
↓	79,700
↓	97,900
↓	96,600
↓	99,200
Average	96,700
1200	83,600
↓	78,200
↓	75,700
↓	73,300
↓	82,100
Average	78,600

\*0.012-inch thick Hastelloy X strip, Heat 261-5-4002

TABLE 9.4 (cont.)

Cycles: Three hours at 1975°F (Palniro-7) + three hours at 1950°F (Palniro-1 and Palniro-7) + three hours at 1825°F (Niro): cooled at equivalent rate to slow air-cool after each cycle.

Parent Metal

<u>Test Temp (°F)</u>	<u>UTS (psi)</u>	<u>0.2% YS (psi)</u>	<u>2-in. Elong. (%)</u>
Room	107,000	50,500	12.5
↓	105,000	51,900	14.0
↓	100,000	51,700	10.5
Average	104,000	51,400	12.5
1200	85,800	37,400	25.5
↓	90,000	30,700	33.5
↓	89,400	36,000	37.0
Average	88,400	34,700	33.0

Brazed

<u>Test Temp (°F)</u>	<u>UTS (psi)</u>
Room	89,300
↓	91,400
↓	91,300
↓	97,300
↓	93,500
Average	92,600
1200	88,900
↓	73,800
↓	85,500
↓	93,100
↓	79,800
Average	84,200

TABLE 9.5

TENSILE TEST RESULTS FOR SIMULATED SEAL-JOINT SPECIMENS\*  
EXPOSED TO SINGLE BRAZE CYCLE

Cycle: Three hours at 1850°F (Nioro), then cooled at rate equivalent to slow air-cool.

Parent Metal

<u>Test Temp (°F)</u>	<u>UTS (psi)</u>	<u>0.2% YS (psi)</u>	<u>2-in. Elong. (%)</u>
Room	112,000	55,600	18.0
↓	99,400	53,600	13.0
↓	107,000	54,500	20.0
Average	109,100	54,600	17.0
1200	84,200	35,500	40.0
↓	82,700	36,500	33.0
↓	84,700	36,300	38.5
Average	83,700	56,100	37.0

Brazed

<u>Test Temp (°F)</u>	<u>UTS (psi)</u>
Room	111,000
↓	107,000
↓	105,000
↓	102,000
↓	109,000
Average	106,800
1200	83,300
↓	69,800
↓	76,800
↓	82,700
↓	79,500
Average	80,400

\*0.012-inch thick Hastelloy X strip, Heat 261-5-4002

TABLE 9.5 (cont.)

Cycle: Three hours at 2025°F (copper), then cooled at rate equivalent to slow air-cool.

Parent Metal

<u>Test Temp (°F)</u>	<u>UTS (psi)</u>	<u>0.2% YS (psi)</u>	<u>2-in. Elong. (%)</u>
Room	101,000	52,400	10.5
↓	108,000	55,500	18.0
↓	109,000	53,900	11.0
Average	106,000	53,900	13.0
1200	86,800	36,100	34.0
↓	88,100	36,200	36.0
↓	80,600	35,400	22.5
Average	85,200	35,900	31.0

Brazed

<u>Test Temp (°F)</u>	<u>UTS (psi)</u>
Room	96,800
↓	95,900
↓	93,600
↓	110,000
↓	106,000
Average	100,400
1200	69,000
↓	72,500
↓	72,700
↓	69,000
↓	73,000
Average	71,200

TABLE 9.5 (cont.)

Cycle: Three hours at 1975°F (Palniro-7), then cooled at rate equivalent to slow air-cool.

Parent Metal

<u>Test Temp (°F)</u>	<u>UTS (psi)</u>	<u>0.2% YS (psi)</u>	<u>2-in. Elong. (%)</u>
Room	112,000	52,500	26.0
↓	113,000	54,200	25.0
↓	116,000	55,300	30.0
Average	113,700	54,000	27.0
1200	84,200	36,200	42.0
↓	85,400	37,300	41.5
↓	87,800	37,700	43.0
Average	85,800	37,100	42.0

Brazed

<u>Test Temp (°F)</u>	<u>UTS (psi)</u>
Room	106,000
↓	104,000
↓	101,000
↓	94,200
↓	108,000
Average	102,600
1200	85,500
↓	80,900
↓	81,600
↓	80,800
↓	81,400
Average	82,000



TABLE 9.5 (cont.)

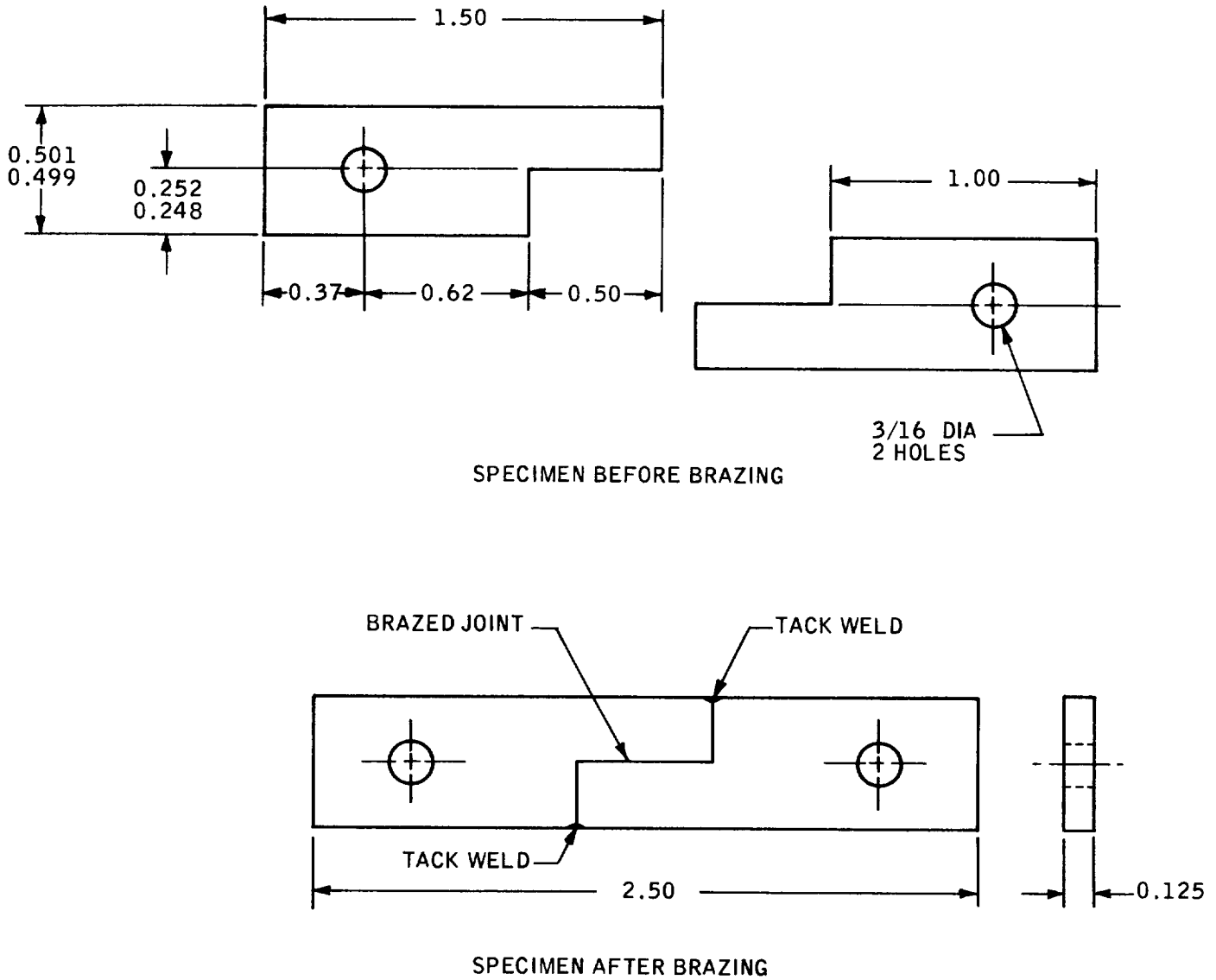
Cycle: Three hours at 1750°F (Nicoro-80), then cooled at rate equivalent to slow air-cool.

Parent Metal

<u>Test Temp (°F)</u>	<u>UTS (psi)</u>	<u>0.2% YS (psi)</u>	<u>2-in. Elong. (%)</u>
Room	115,000	52,900	27.0
↓	113,000	53,100	24.0
↓	109,000	52,700	18.5
Average	112,300	52,900	23.0
1200	80,500	38,300	23.0
↓	90,000	38,400	37.5
↓	86,800	37,200	37.5
Average	85,800	38,000	32.5

Brazed

<u>Test Temp (°F)</u>	<u>UTS (psi)</u>
Room	115,000
↓	117,000
↓	117,000
↓	111,000
↓	115,000
Average	115,000
1200	85,400
↓	85,200
↓	81,100
↓	85,200
↓	84,100
Average	84,200



NOTE: DIMENSIONS IN INCHES

Figure 9.4 - Miller-Peaslee Shear Test Specimen

TABLE 9.6

SHEAR-TEST RESULTS FOR HASTELLOY-X BRAZED  
WITH NIORO, PALNIRO-7, AND NICORO-80

<u>Braze Alloy</u>	<u>Test Temp (°F)</u>	<u>Shear Ultimate (ksi)</u>	<u>Test Condition</u>	<u>Nickel Plating (in.)</u>	<u>Comment</u>
Nioro	-320	82.8	Unirradiated	None	
		78.9		0.0002	
		82.7		0.0005	Broke in base metal
		82.1		0.0008/0.0009	
		79.9		Irradiated*	None
Nioro	Room	68.0	Unirradiated	None	
		60.2		0.0002	Broke in base metal
		60.1			
		57.4			
		59.5			
		62.6			
		52.3		0.0005	
		62.9			
		62.7			
		62.0			
		63.8			
		63.0		0.0008/0.0009	
		66.1			Broke in base metal
		59.5			Broke in base metal
		57.9			
		59.1			
65.4					
Nioro	750	53.4	Unirradiated	None	
Nioro	750	37.5	Irradiated	None	

\*@50°C,  $9 \times 10^{19}$  nvt (thermal) and  $5 \times 10^{18}$  nvt (fast)

TABLE 9.6 (cont.)

<u>Braze Alloy</u>	<u>Test Temp (°F)</u>	<u>Shear Ultimate (ksi)</u>	<u>Test Condition</u>	<u>Nickel Plating (in.)</u>	<u>Comment</u>
Palniro-7	-320	74.8	Unirradiated	None	
Palniro-7	-320	81.2	Irradiated	↓	
Palniro-7	Room	62.8	Unirradiated		
Palniro-7	Room	62.4	Irradiated		
Palniro-7	750	53.8	Unirradiated		
Palniro-7	750	39.9	Irradiated		
Nicoro-80	-320	56.4	Unirradiated		None
Nicoro-80	-320	63.2	Irradiated	↓	
Nicoro-80	Room	56.5	Unirradiated		
Nicoro-80	Room	54.9	Irradiated		
Nicoro-80	750	34.9	Unirradiated		
Nicoro-80	750	12.6	Irradiated		

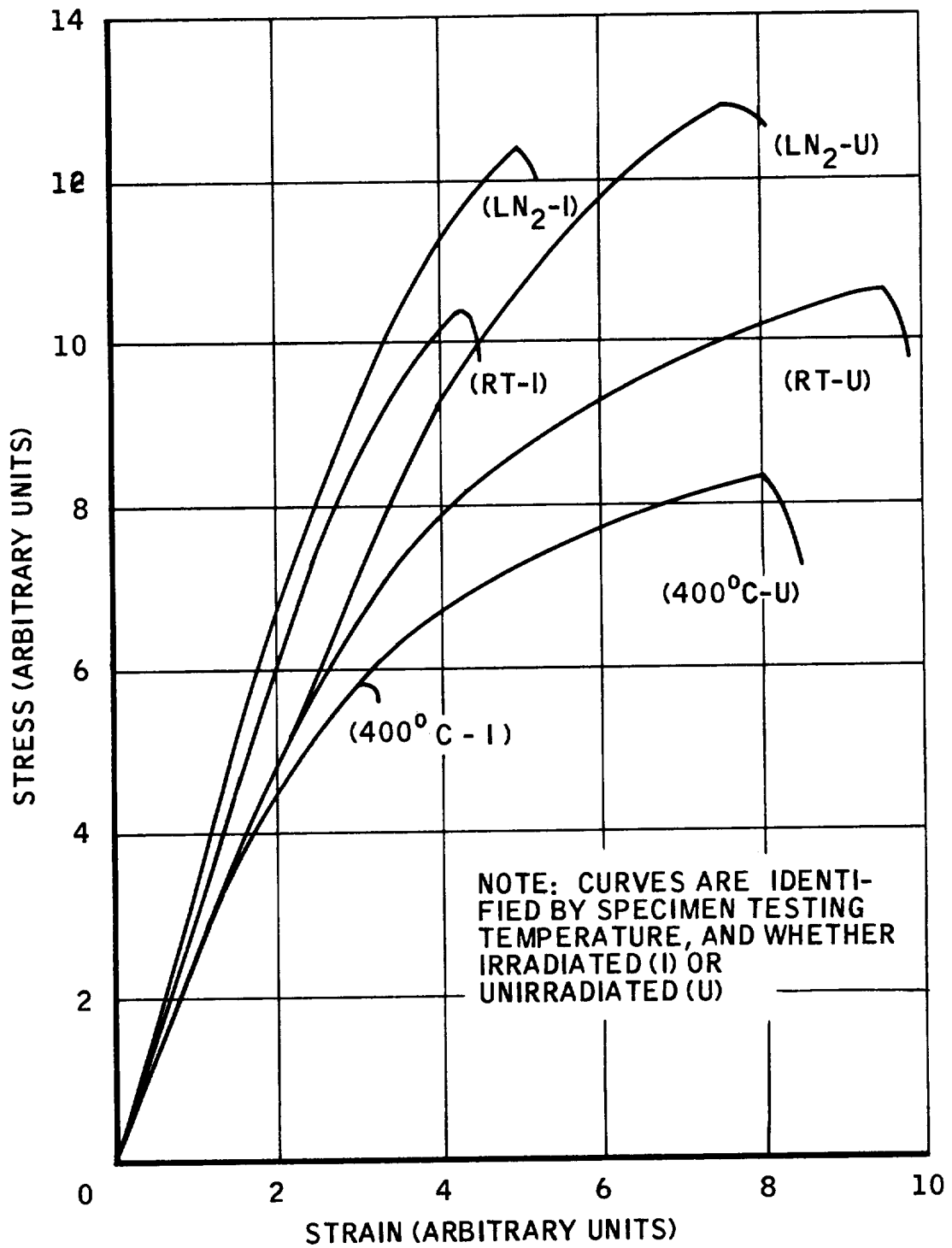


Figure 9.5 - Miller-Peaslee Shear Stress-Strain for Hastelloy X Brazed with Nioro

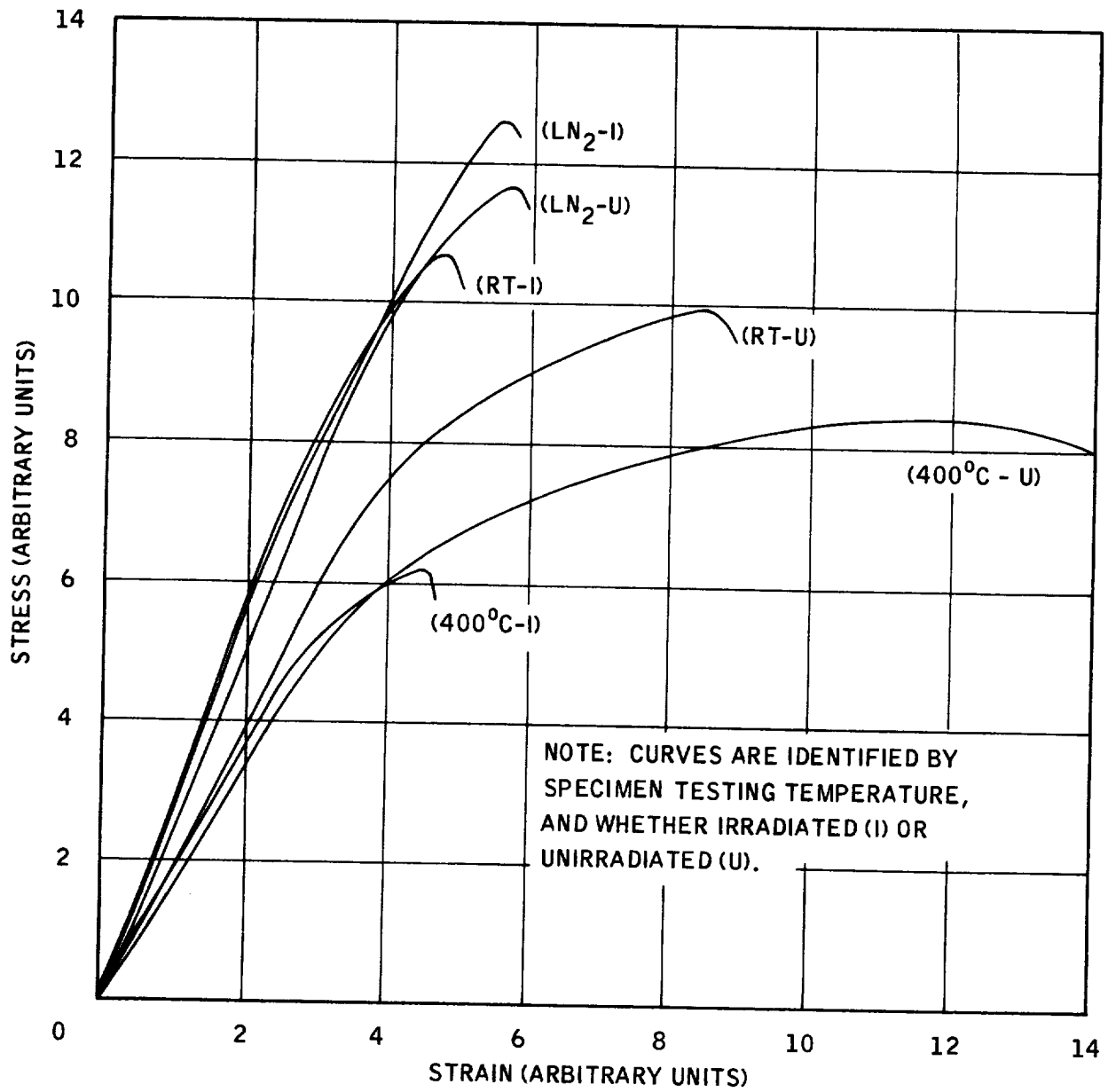
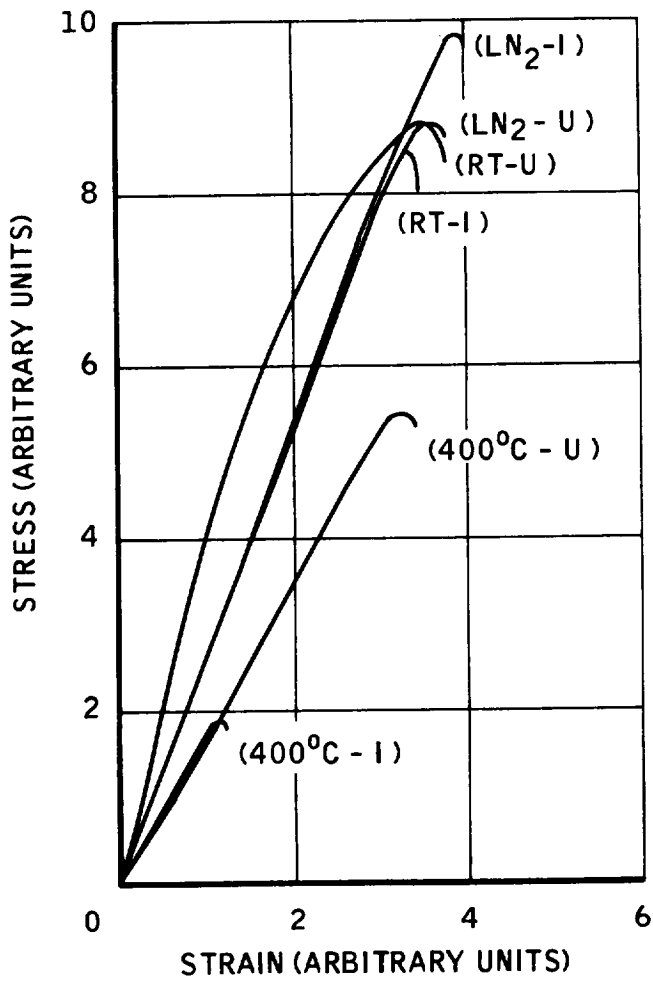


Figure 9.6 - Miller-Peaslee Shear Stress-Strain for Hastelloy X Brazed with Palniro-7



NOTE: CURVES ARE IDENTIFIED BY SPECIMEN, TESTING TEMPERATURE, AND WHETHER IRRADIATED (I) OR UNIRRADIATED (U).

Figure 9.7 - Miller-Peaslee Shear Stress-Strain for Hastelloy X Brazed with Nicoro-80

### 9.3 BRAZE-ALLOY TENSILE TESTS

The strength of the braze alloys Nioro, Palniro-7 and Nicoro-80 were also determined by ORNL. The room temperature at 750°F tensile data are presented in Table 9.7.

TABLE 9.7

TENSILE STRENGTH OF BRAZE ALLOYS  
NIORO, PALNIRO-7 AND NICORO 80

(Tests Conducted at ORNL)

<u>Alloy</u>	<u>Test Temp (°F)</u>	<u>UTS (ksi)</u>	<u>0.2% YS (ksi)</u>
Nioro	68	68.0	38.4
Nioro	750	53.4	31.5
Palniro-7	68	62.8	39.7
Palniro-7	750	53.8	31.4
Nicoro-80	68	56.5	44.8
Nicoro-80	750	34.9	32.5



#### 9.4 BRAZE ALLOY DIFFUSION

A study was performed to evaluate the extent of diffusion of braze alloys into Hastelloy X as a result of the brazing cycle. The specimen employed is shown in Figure 9.8. The test plan is illustrated in Table 9.8.

All specimens were furnace-brazed for three hours at the temperatures shown in Table 9.8, using a protective hydrogen atmosphere. After brazing, the specimens were sectioned normal to the hole axis and the amount of gross volume diffusion measured with an optical micrometer. The effect of the brazing temperature on the amount of penetration is summarized in Figure 9.9. The following observations were made:

1. The rate of penetration increased exponentially with increased braze temperature for all alloys except Palniro-1.
2. Maximum penetration at 2150°F was observed for those braze alloys with the minimum melting points.
3. All braze alloys penetrated less than 0.007 inch at their maximum recommended brazing temperatures\*.
4. The Nicoro braze alloy contained an excessive amount of porosity and accurate measurements were not obtainable. Data for this alloy are not included in Figure 9.9.

\*Recommended Brazing Temperatures:

Palniro-1	2050°F	60Cu-40Au	1950°F
Copper	2050°F	Nicoro	1800°F
Palniro-7	1950°F	Nicoro 80	1750°F
Nicoro	2050°F		

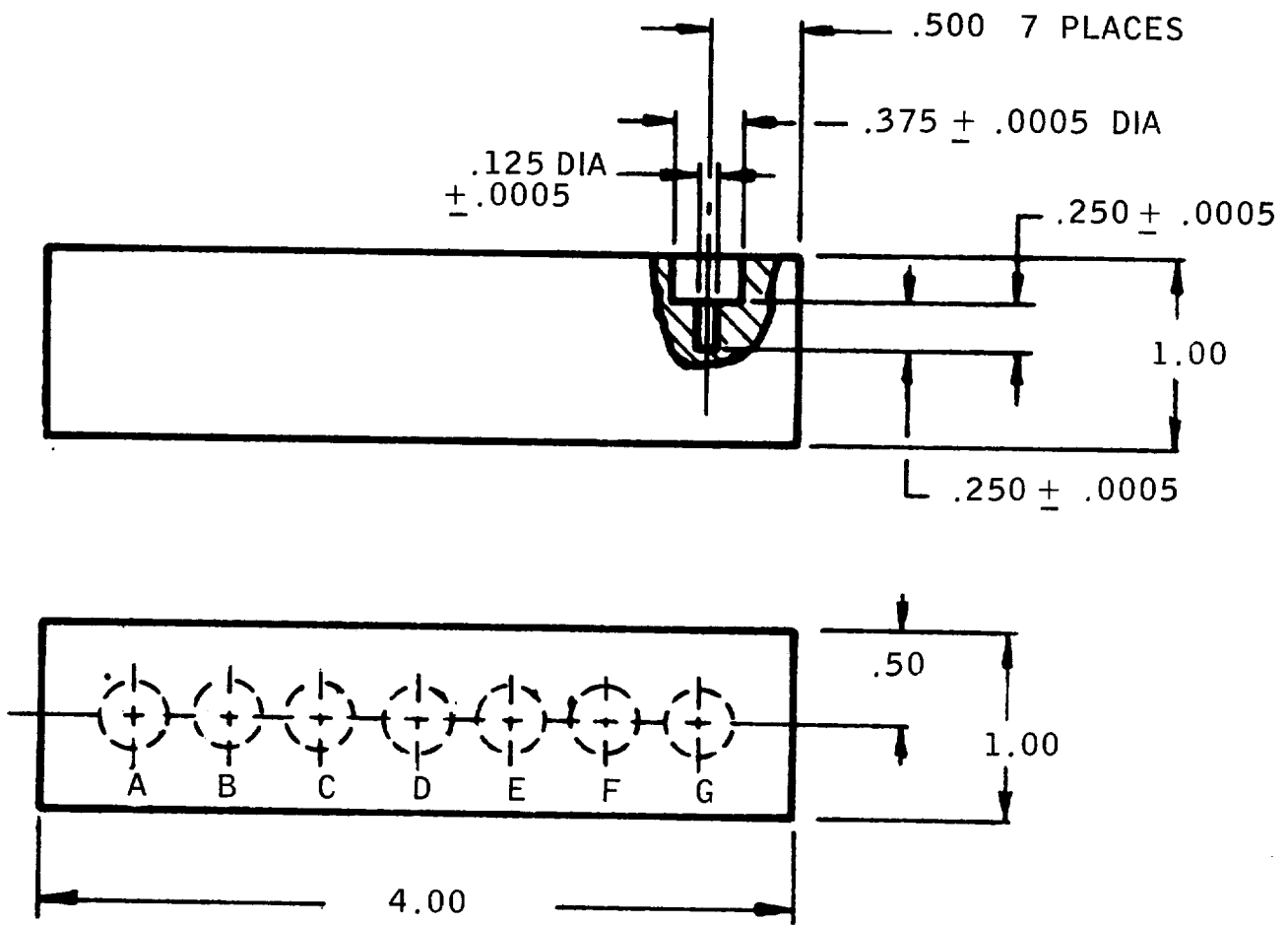


Figure 9.8 Braze-Alloy Diffusion Specimen

TABLE 9.8

BRAZE ALLOY DIFFUSION STUDY TEST PLAN FOR HASTELLOY X

<u>Braze Alloy</u>	<u>Trade Name</u>	Chemistry %				<u>Liquidus</u>	<u>Solidus</u>
		Au	Ni	Pd	Cu		
A	Palniro-1	50	25	25		2050	2016
B	Copper				100	1981	1981
C	Palniro-7	70	22	8		1899	1841
D	Nicoro	35	3		62	1886	1832
E	40Au-60Cu	40			60	1832	1796
F	Nioro	82	18			1742	1742
G	Nicoro 80	81.5	2		16.5	1697	1670

Brazing Temperatures °F  
(All Times at Temp = 3 hrs.)

Alloys

1700	G						
1750	G	F					
1800	G	F					
1850	G	F	E				
1900	G	F	E	D	C		
1950	G	F	E	D	C		
2000	G	F	E	D	C	B	
2050	G	F	E	D	C	B	A
2100	G	F	E	D	C	B	A
2150	G	F	E	D	C	B	A

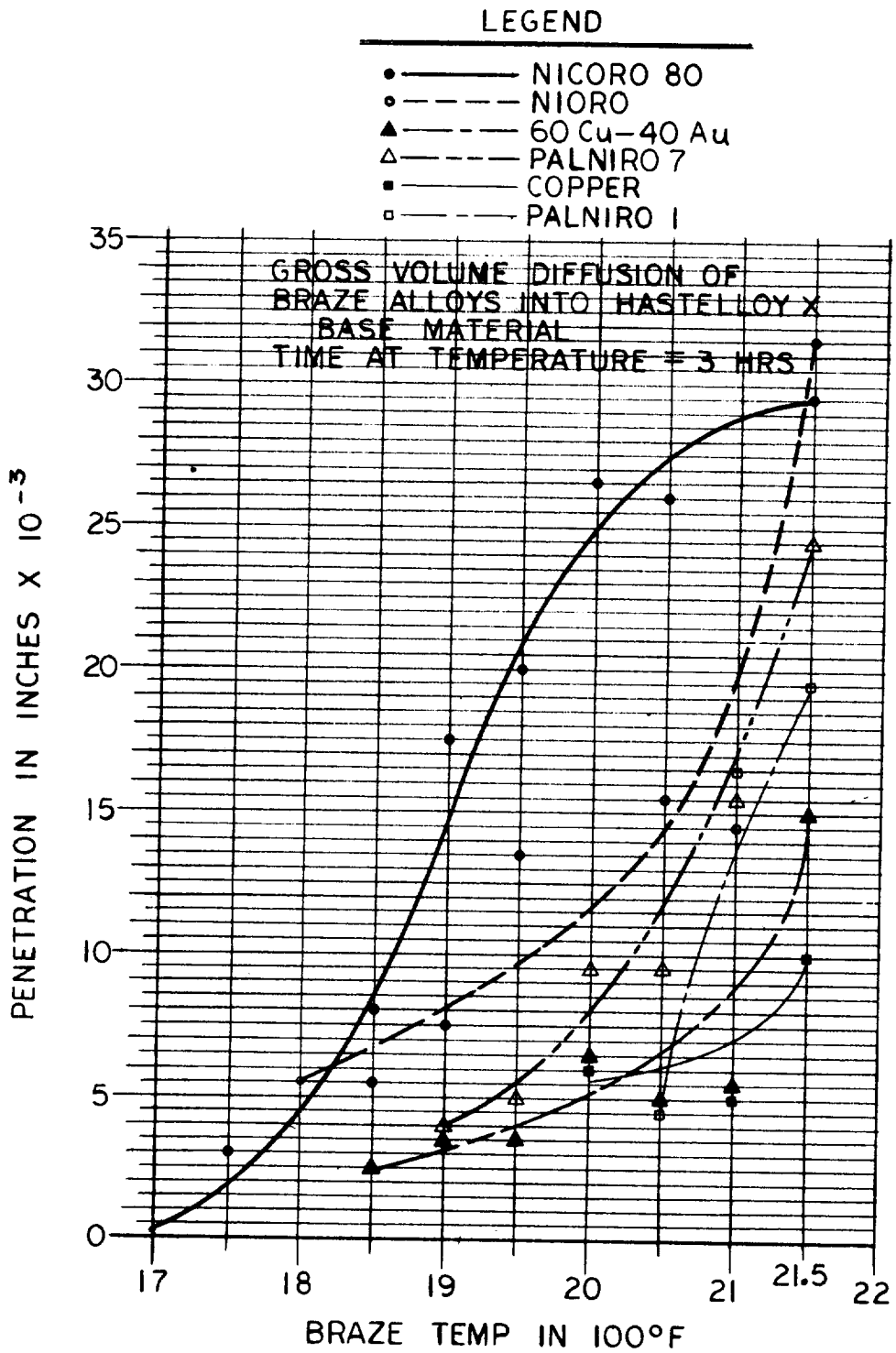


Figure 9.9 - Gross-Volume Diffusion of Braze Alloys into Hastelloy X Base

Specimens for each alloy investigated, using the recommended brazing temperatures\*, were etched with a KI solution, a Knoop hardness traverse obtained, and a microscopic structural examination made. The results are shown in Figures 9.10 through 9.16 based upon the recommended braze temperature. The effect of exposure to temperatures at 200 to 350°F above their recommended brazing temperatures are shown for Nicoro 80, Palniro-7 and Nioro in Figures 9.17, 9.18, and 9.19. The following observations were made with respect to microstructures and hardness:

1. Maximum intergranular penetration occurred with the 60Cu-40Au alloy.
2. Increased intergranular penetration occurred for the alloys exposed to higher-than-recommended brazing temperatures.
3. A major trend in the effect of braze-alloy elements on the base-metal hardness could not be established.
4. The palladium content of Palniro-1 and Palniro-7 appeared to increase the base metal hardness slightly.

In conclusion, no adverse metallurgical conditions were observed if the braze alloys were not utilized above their recommended temperatures where excessive gross volume diffusion and intergranular penetration proceeded rapidly.

\*Recommended Brazing Temperatures:

Palniro-1	2050°F	60Cu-40Au	1950°F
Copper	2050°F	Nioro	1800°F
Palniro-7	1950°F	Nicoro 80	1750°F
Nicoro	2050°F		

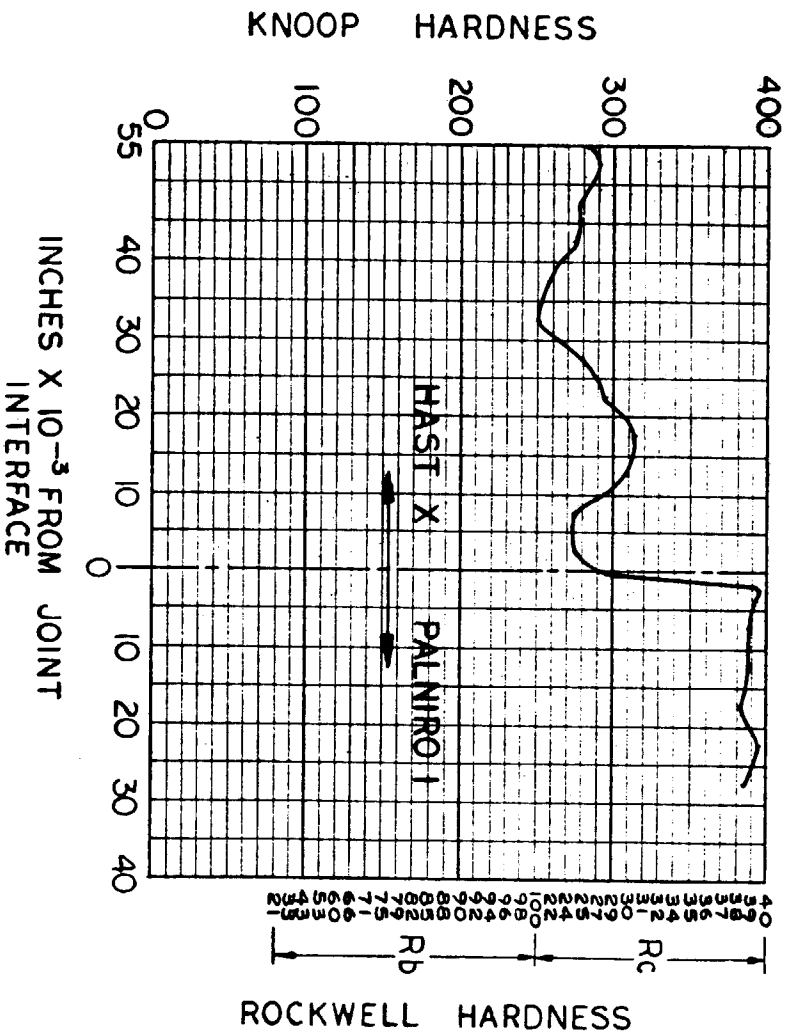
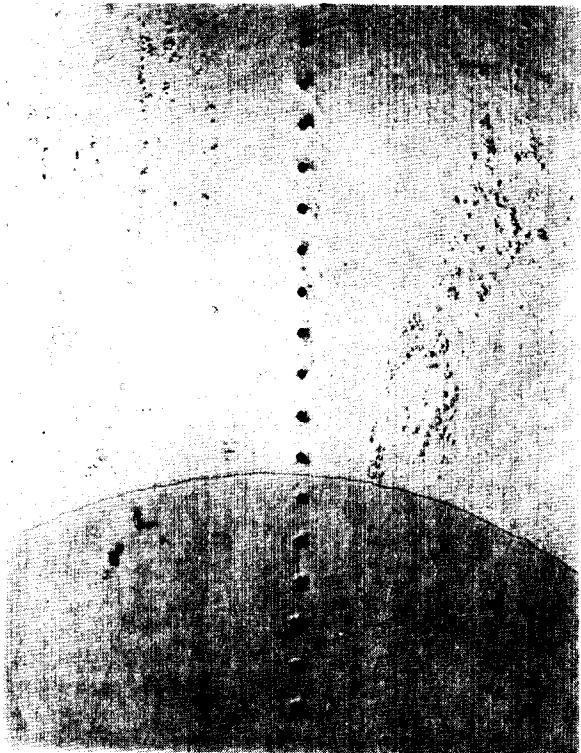
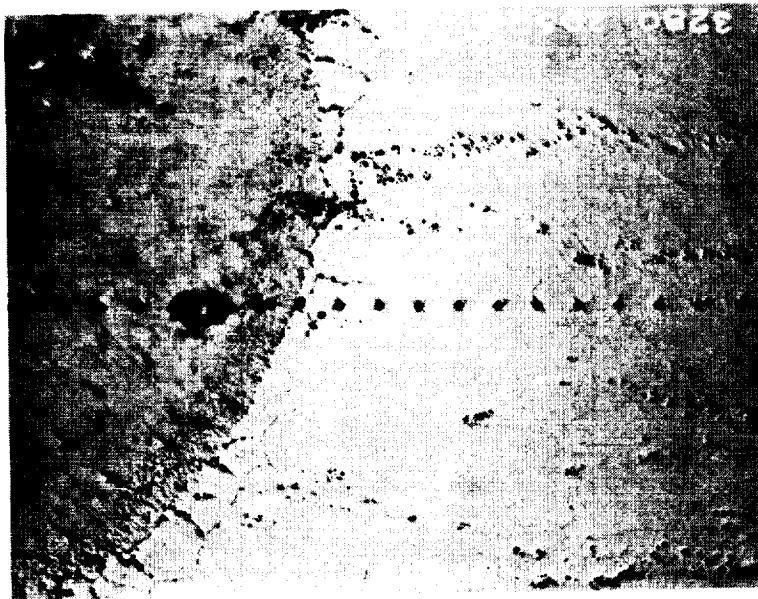
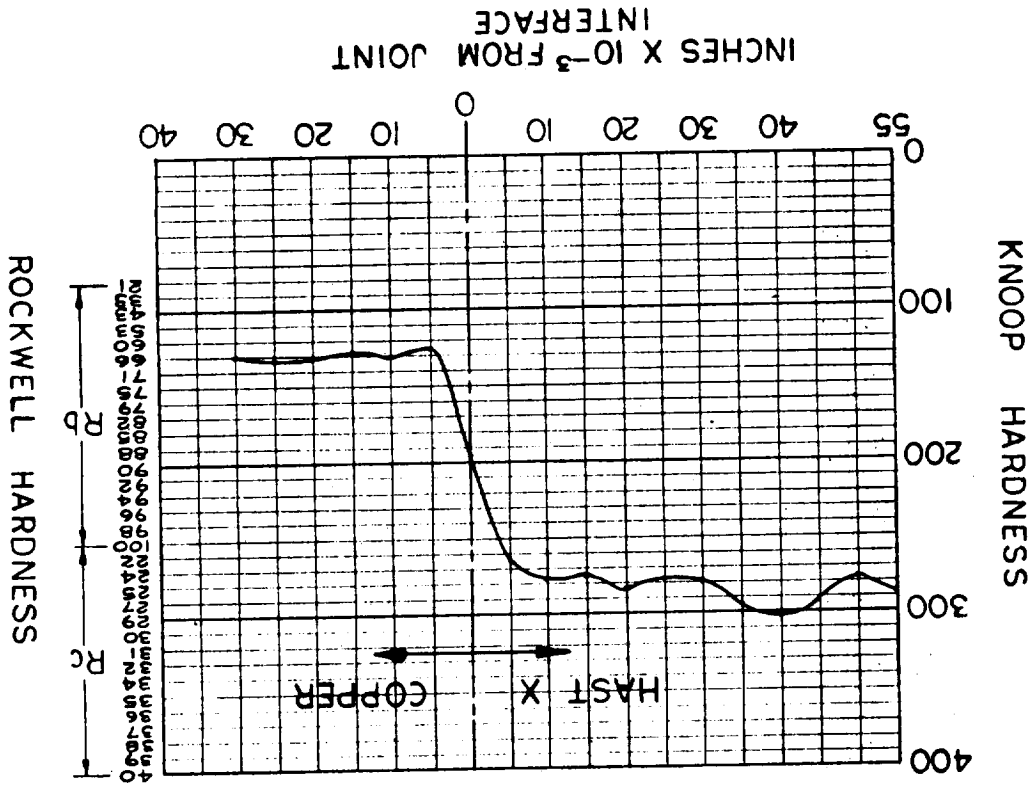


Figure 9.10 - Braze-Alloy Diffusion, Palnipro-1 Brazed at 2050°F

Figure 9.11 - Braze-Alloy Diffusion, Copper Brazed at 2050°F



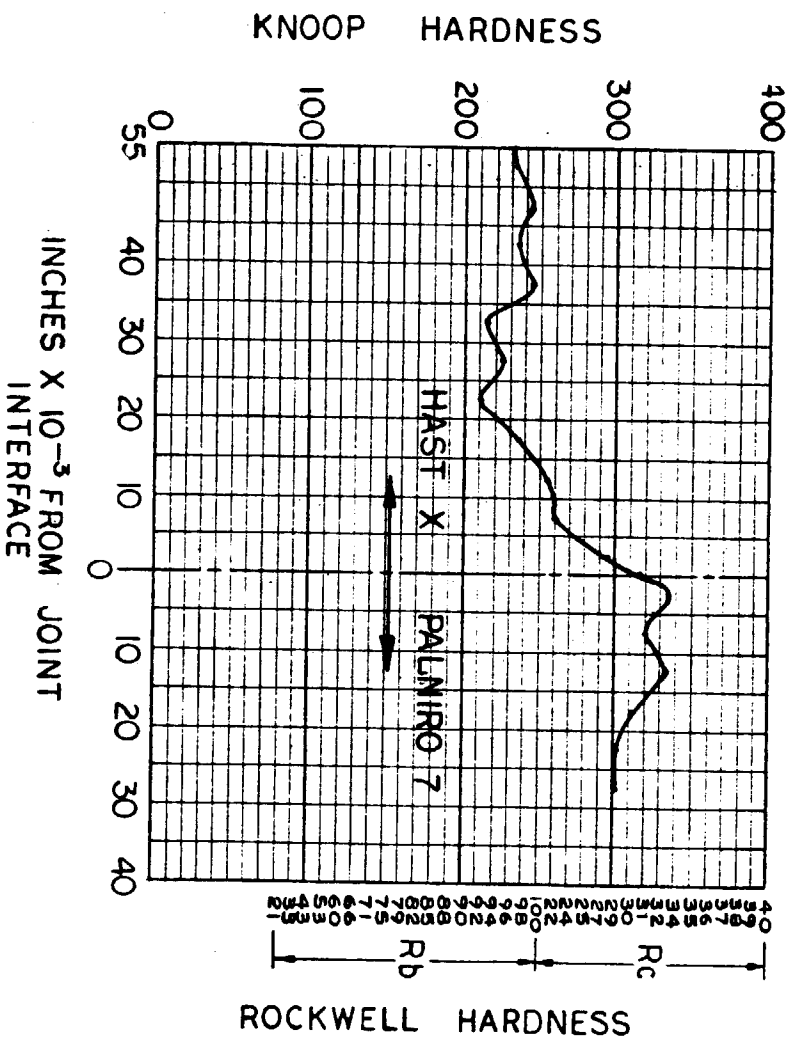
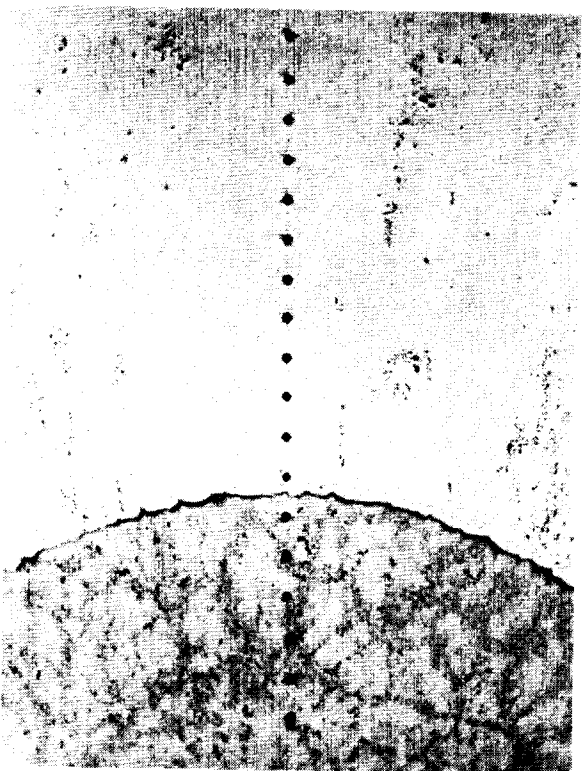


Figure 9.12 - Braze-Alloy Diffusion, Palniro-7 Brazed at 1950°F



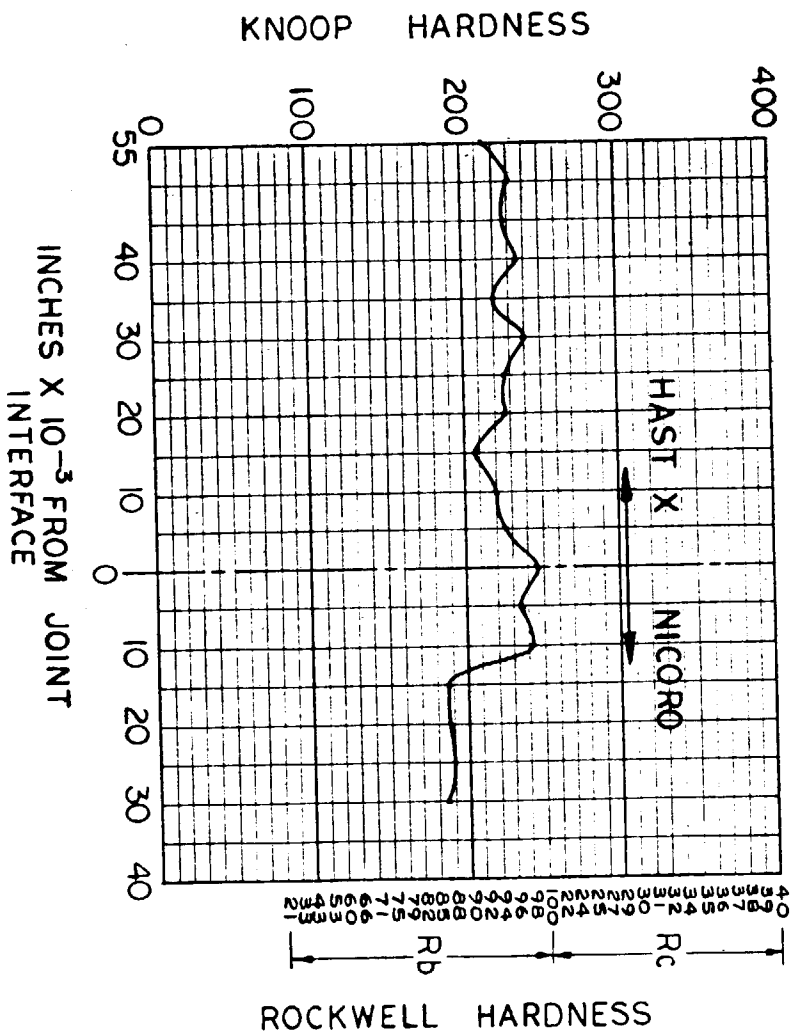
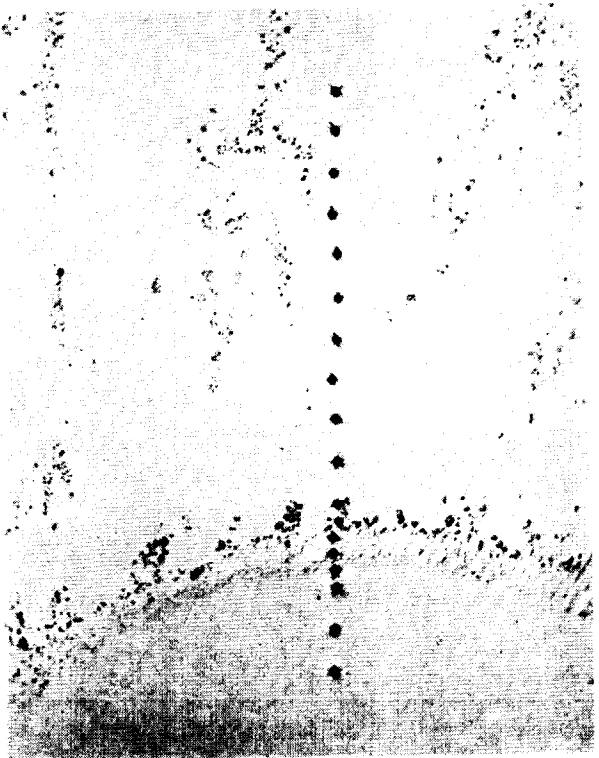


Figure 9.13 - Braze-Alloy Diffusion, Nicoro Brazed at 2050°F

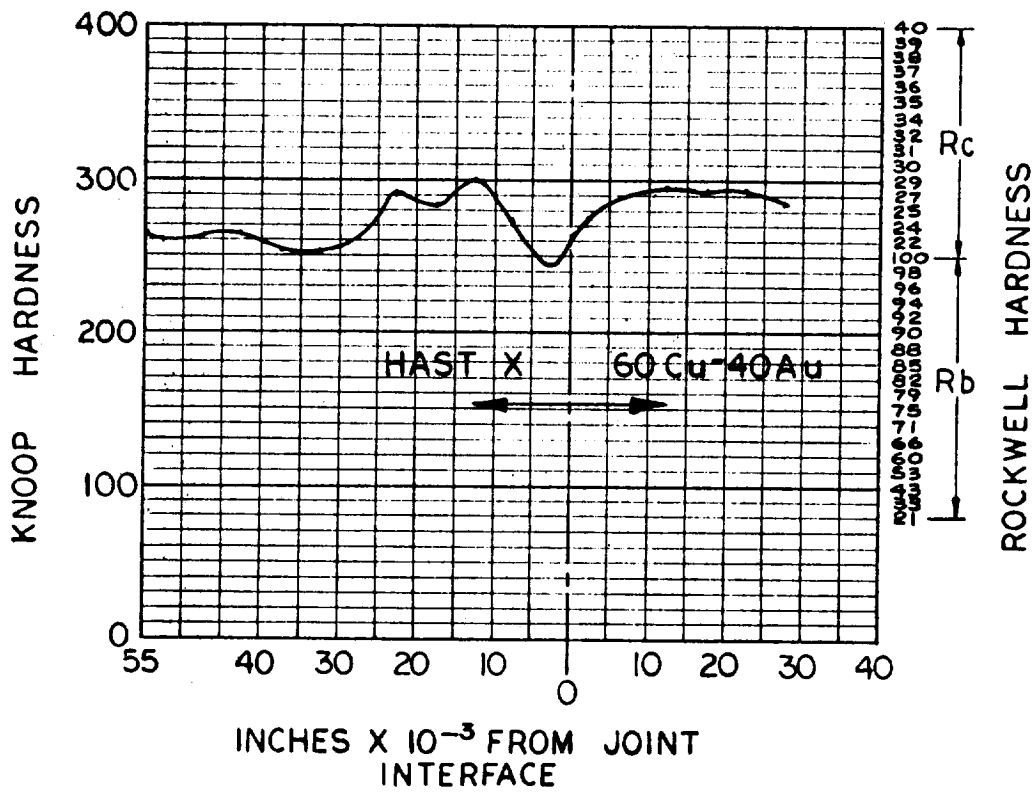


Figure 9.14 - Braze-Alloy Diffusion, 60 Cu-40 Au Brazed at 1950°F

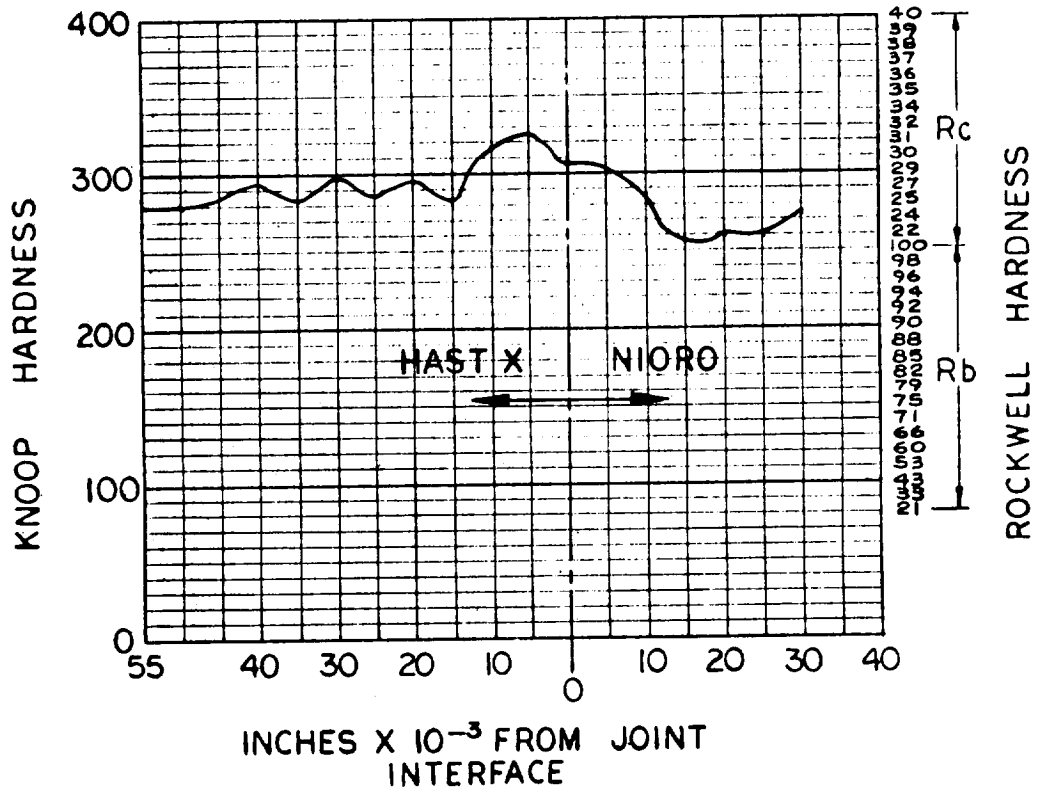
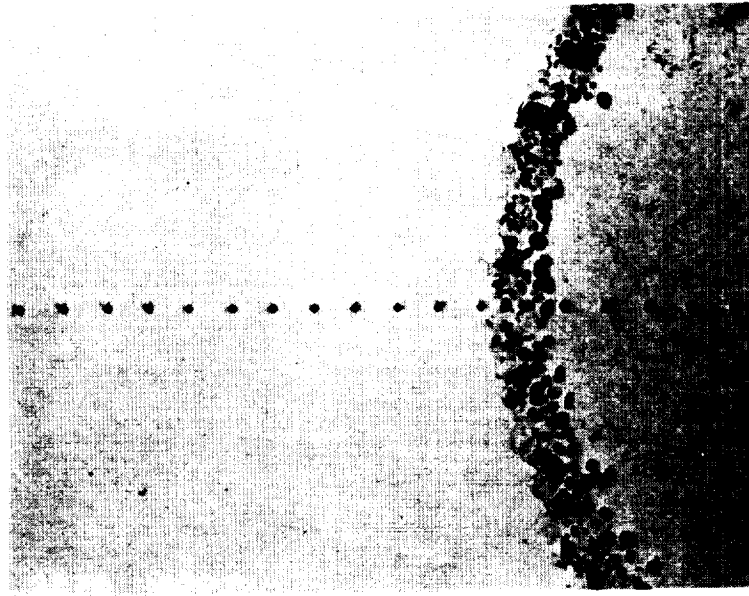


Figure 9.15 - Braze-Alloy Diffusion, Nicro Brazed at 1800°F

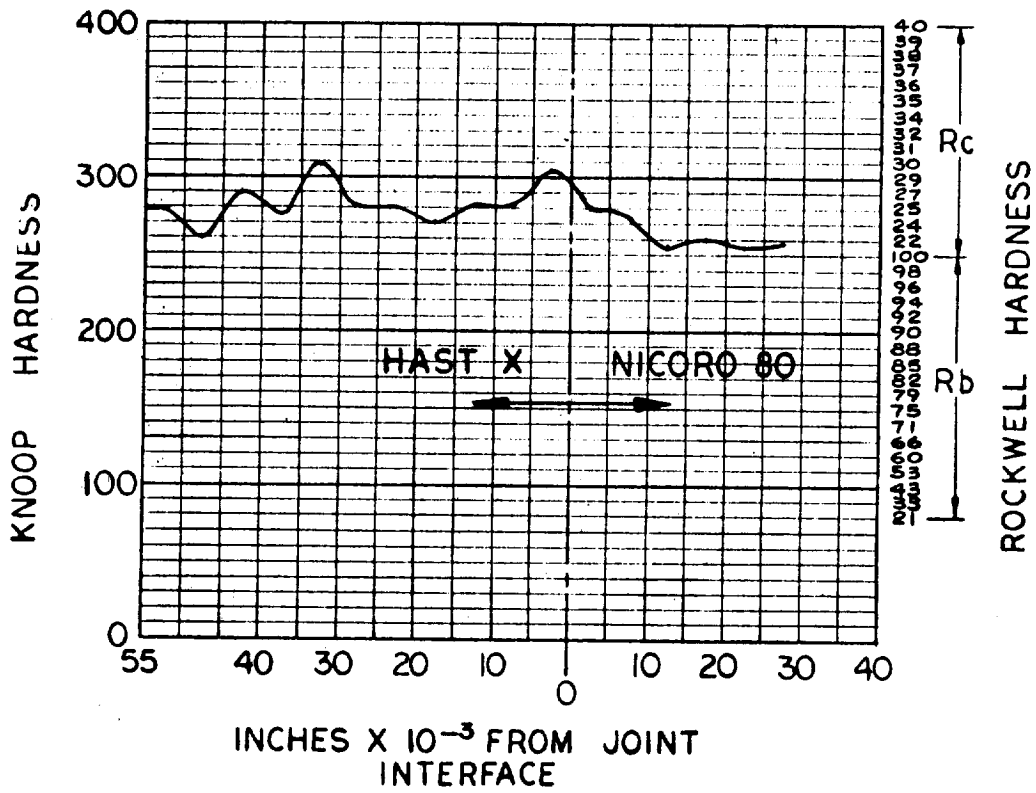
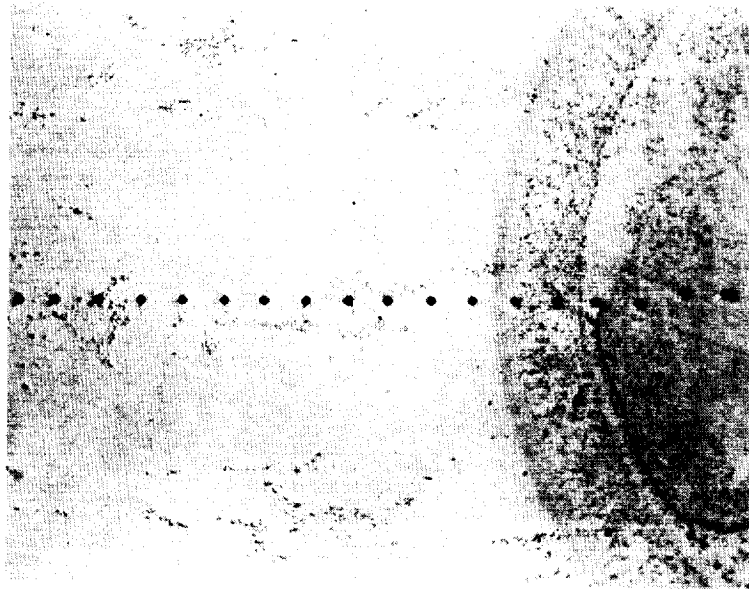


Figure 9.16 - Braze-Alloy Diffusion, Nicoro-80 Brazed at 1750°F

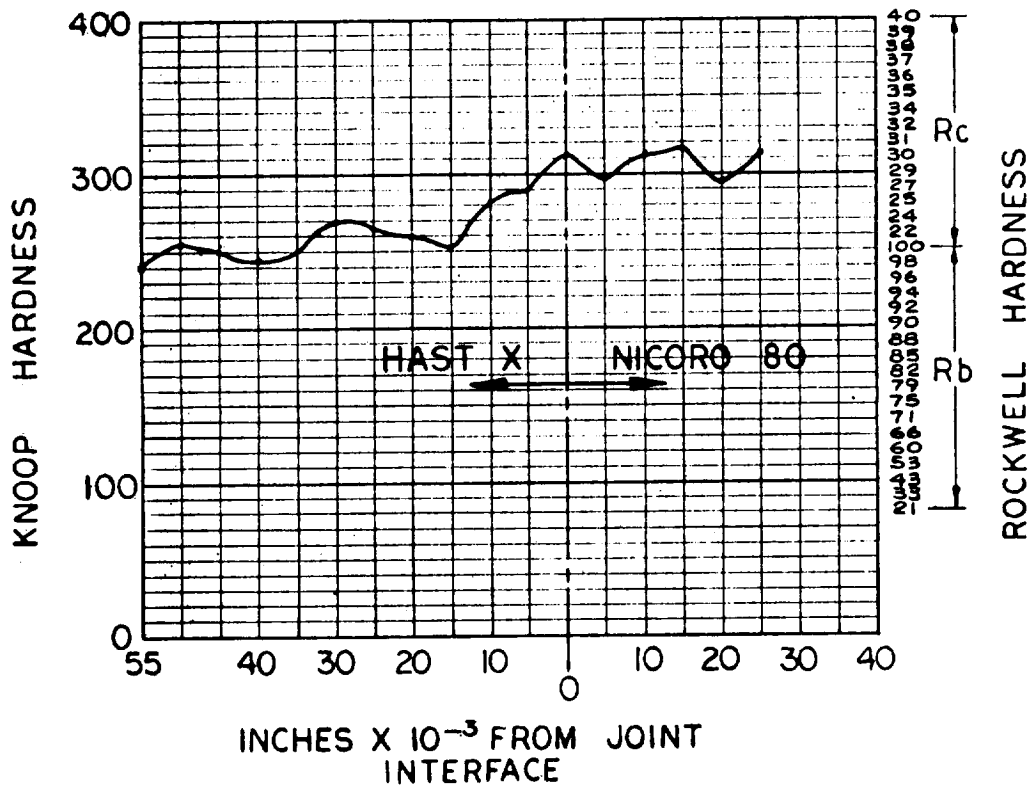
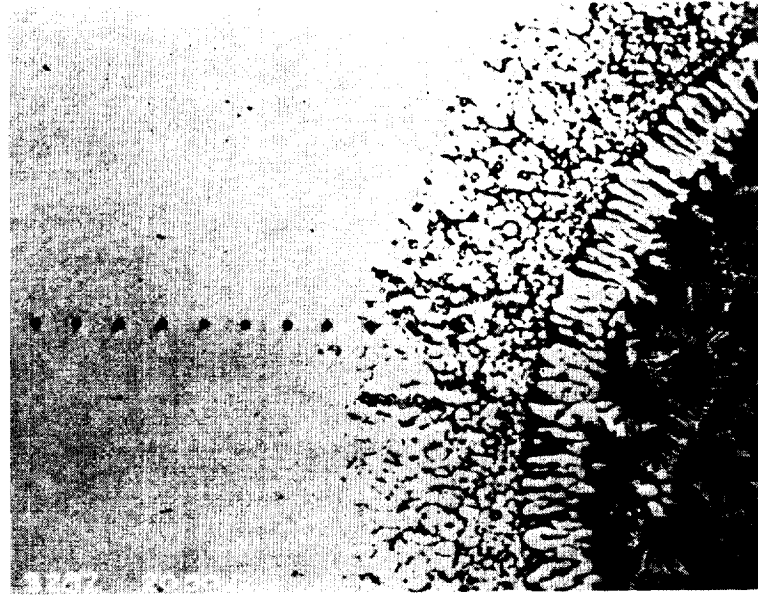


Figure 9.17 - Braze-Alloy Diffusion, Nicoro-80 Brazed at 2050°F

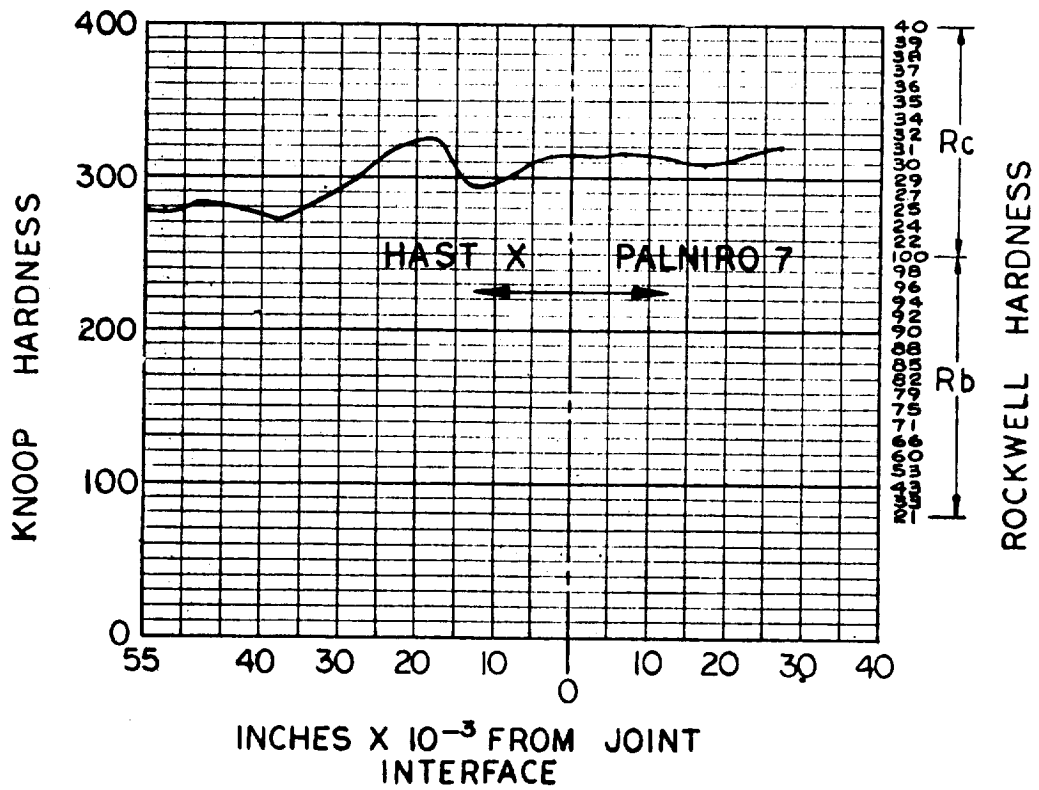
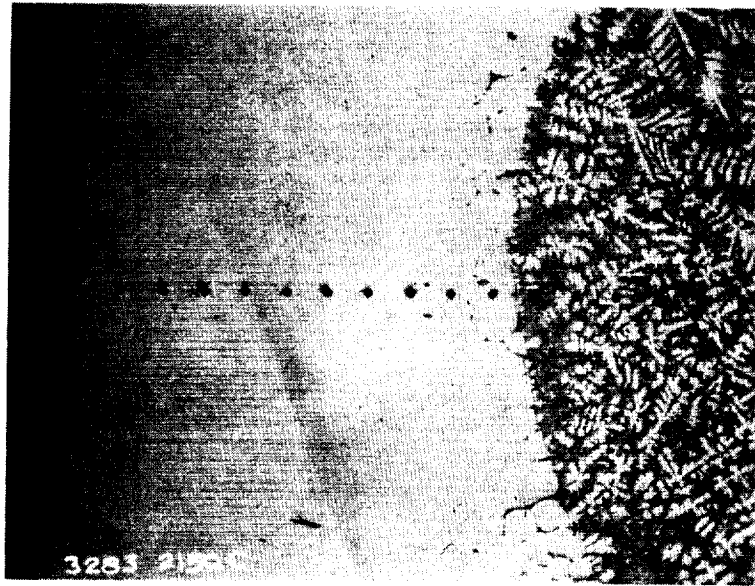


Figure 9.18 - Braze-Alloy Diffusion, Palniro-7 Brazed at 2150°F

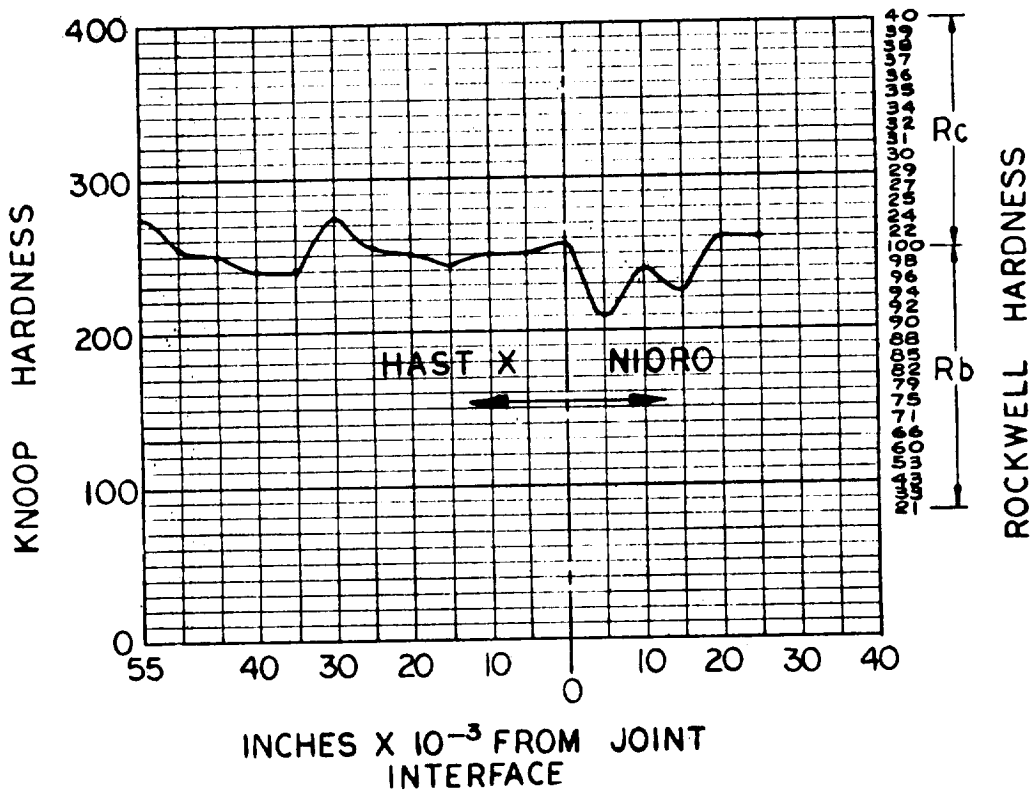
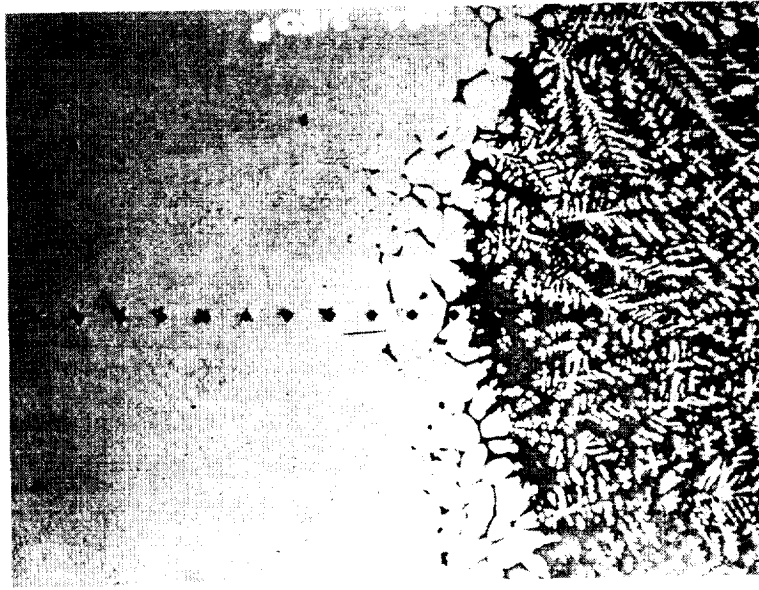


Figure 9.19 - Braze-Alloy Diffusion, Nioro Brazed at 2150°F

## 9.5 GROOVED-SPECIMEN TENSILE TESTING

Special testing was performed to evaluate the stress concentration and thermal-stress conditions expected in the nozzle jacket. The tests included grooved-tensile and low-cycle fatigue specimens. The low-cycle fatigue results are reported in Section 8.9.

The tensile tests were conducted on grooved specimens, (see Figure 9.20), which employed a 0.9-inch thick by 1.0-inch wide by 2.0-inch long gage length. The groove was filled with metal strips to simulate the jacket joint, and the specimen furnace-brazed prior to testing. The initial test results were not fully conclusive because of failures in the specimen loading pin-hole or grip areas. The results of testing with the groove and parent metal (ungrooved) specimens (Heat 260-5-2813) exposed to the braze cycle were as follows:

Room Temperature Tensile Tests of Grooved  
and Ungrooved Hastelloy X Jacket Material

<u>Specimen Type</u>	<u>UTS* (ksi)</u>	<u>Stress* at Grip Failure (ksi)</u>	<u>0.2% YS* (ksi)</u>	<u>Elongation (%)</u>
Parent Metal (ungrooved)	114.8		50.3	31.0
Grooved		97.6		13.0
		101.0		11.5
		100.1		10.5
		97.0	56.2	10.0

\*Computed on basis of load and total, or gross, area of gage (0.9 by 1.0-inch).



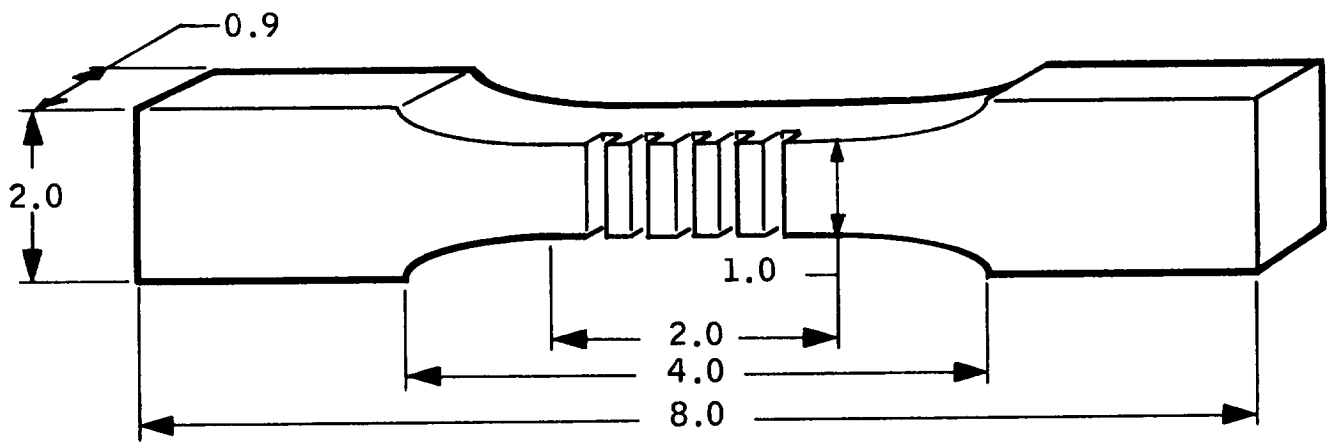


Figure 9.20 - Grooved Tensile Specimen

All grooved specimens exhibited some small tear-type cracks emanating from the bottom of the grooves. The stress at the grip failure load, based upon the area under the groove (0.8 by 1.0-inch), varied from 110.1 to 113.9 ksi, or extremely close to the parent-metal tensile strength. The results of notched tensile testing (see Section 8.2) would have indicated failure at approximately 111.0 ksi based upon an overall notched-to-unnotched tensile ratio of 0.97. In an effort to verify the grooved specimen strength, two specimens were re-machined to a narrower gage width (0.75-inch compared to 0.9-inch) to prevent failure in the grip ends. The specimens were tested at -320°F to accentuate notch sensitivity because of reduced ductility of the material. The test results were as follows:

-320°F Tensile Tests of Grooved Hastelloy X Jacket Material

<u>UTS*</u> <u>(ksi)</u>	<u>0.2% YS*</u> <u>(ksi)</u>	<u>Elong.</u> <u>(%)</u>	<u>Failure Location</u>
139.6	80.9	12	Parent metal between grooves
125.0	81.0	9	Through groove

\*Based upon load and total, or gross, area of gage (0.75 by 0.9-inch)

The tensile strengths based upon the area under the groove (0.75 by 0.8-inch) rather than the gross cross-sectional area, are 160.0 and 145.0 ksi, respectively. The foregoing data correspond to the following parent metal (ungrooved properties) at -320°F:

-320°F Tensile Tests of Ungrooved Hastelloy X Jacket Material

<u>UTS</u> <u>(ksi)</u>	<u>0.2% YS</u> <u>(ksi)</u>	<u>Elong.</u> <u>(%)</u>	<u>Comments</u>
139.0	80.9	17	Standard braze cycle
138.0	84.2	13	Standard braze cycle
130.0	81.7	11	Standard plus extra braze cycle
131.0	81.9	11	Standard plus extra braze cycle

The data reveal that the braze joint carries a satisfactory share of the loads involved.

## 10.0 EFFECTS OF VARIOUS THERMAL TREATMENTS

Several variations in the thermal history of Hastelloy X were evaluated during the course of the materials development program:

- (1) The effect of post-weld annealing at 2080°F.
- (2) The effect of the rate of cooling from the solution heat-treat temperature (2150°F) and the effect of time at various temperatures.
- (3) The effect of intermediate low-temperature annealing (1750° to 2050°F) for carbide stabilization.
- (4) The effect of exposure to an extra braze-cycle.

### 10.1 POST-WELD ANNEALING

The effects of post-weld annealing at 2080°F as the tensile properties of forgings are presented in Section 2.3.2.

### 10.2 COOLING RATE AND TIME AT TEMPERATURE

Testing on the effects of cooling rate and time at temperature was conducted on two heats of material:

1. Heat 261-5-4000 (to AGC Specification 90056).
2. Heat X5-2718EE (to AMS Specification 5754) but meeting the requirements of the AGC specification. The X5-2718EE heat, however, was inadequately hot-worked and contained massive stringers of carbides (as well as some ingotism) and was rejected. Nevertheless, data in Table 10.1 reveal variations in ultimate tensile and yield strength (with cooling rate and time

at solution heat-treat temperature) that are of negligible significance. The elongation data cannot be adequately evaluated because of the preponderance of data from the inadequately forged material.

TABLE 10.1

EFFECT OF COOLING RATE ON ROOM TEMPERATURE  
TENSILE PROPERTIES OF HASTELLOY X RING FORGINGS

Heat Treat: 2150°F

<u>Cooling Method</u>	<u>Time at Temp (hrs)</u>	<u>Orientation</u>	<u>UTS (ksi)</u>	<u>0.2% Offset YS (ksi)</u>	<u>Elong. %</u>	<u>Material Heat No./Spec</u>
Water Quench	1	Tangential	100.0	42.1	48	261-5-4000/ AGC 90056
Water Quench	1	↓	100.0	42.0	55	X5-2718EE/AMS
Air Cool	8	↓	108.0	45.0	26*	↓
↓	8	Axial	103.0	44.0	28*	
↓	6	Axial	100.0	49.0	28*	

\*Heavy carbide stringers present in structure.

Heat Treat: One hour at 2150°F, then cool + braze cycle

<u>Cooling Method</u>	<u>Orientation</u>	<u>UTS (ksi)</u>	<u>0.2% Offset YS (ksi)</u>	<u>Elongation %</u>	<u>Material Heat No./Spec</u>
Water Quench	Tangential	97.0	45.5	27	261-5-4000/AGC 90056
Air Cool	↓	98.1	45.1	26	261-5-4000/AGC 90056
Water Quench	↓	109.0	45.0	26	X5-2718EE/AMS
Air Cool	↓	112.0	46.0	27	X5-2718EE/AMS

### 10.3 INTERMEDIATE LOW-TEMPERATURE ANNEALING

The primary mechanical effect of intermediate annealing appears to be that of improving the basic ductility level after the brazing cycle, although intermediate anneals decrease the original solution-annealed ductility. This effect was also supported in the improved forging investigation (see Appendix A). Microexamination revealed coalescing of the grain-boundary carbides, disrupting the brittle crack path. The decreased yield strength, as shown in Table 10.2 for Heat 261-5-4000, was not observed in Heat X5-2718EE, or in subsequent work on the improved forging material.

### 10.4 EFFECT OF EXTRA BRAZING CYCLE

The effect of the extra braze cycle on the tensile properties of Hastelloy X first was analyzed empirically, with the result that a very small effect was anticipated. However, it was believed that elongation would probably present the most notable change (decrease). To quantitatively evaluate the effect on the jacket material, samples of 1-inch thick plate from Heat 260-5-2813 were exposed to the standard braze cycle and to the standard cycle plus an extra braze cycle. The tensile test results, at room temperature and  $-320^{\circ}\text{F}$ , are presented in Table 10.3, which also includes the solution-annealed properties (not brazed) of this heat of material.

Specifically, the results revealed a slight to negligible reduction in UTS and elongation and no change in YS at room temperature, while a greater change was evident in UTS and elongation at  $-320^{\circ}\text{F}$ , but very slight difference in YS. The previously determined three-sigma variation in elongation at  $-320^{\circ}\text{F}$  was found to be minus 5.6%. Application of the minus-three-sigma value to the average of 11% elongation obtained at  $-320^{\circ}\text{F}$  results in a design minimum of 5.4%, an acceptable value.

TABLE 10.2

EFFECT OF INTERMEDIATE ANNEALING ON HASTELLOY X RING FORGING -  
ROOM TEMPERATURE TENSILE PROPERTIES

Solution Heat Treat: 1 Hour at 2150°F, then water-quench  
Heat No.: 261-5-4000

<u>Intermediate Anneal Treatment</u>	<u>Orient</u>	<u>UTS (ksi)</u>	<u>0.2% Offset YS (ksi)</u>	<u>Elong. (%)</u>
None	Axial	102.5	51.5	42
None + Braze	Tangential	86.8	44.2	17
1 hr/2050°F, cool to 1900°F, hold 8 hrs, air cool to room temperature.	Axial	93.0	37.6	39
1 hr/2050°F, cool to 1900°F, hold 4 hrs, cool to 1825°F, hold 8 hrs, air cool to room temperature.		94.4	38.8	29
1 hr/1950°F, cool to 1900°F, hold 4 hrs, cool to 1820°F, hold 8 hrs, air cool to room temperature		84.7	38.2	22
Solution Heat Treat: 1 hour at 2150°F, then air-cool Heat No.: X5-2718EE				
None + Braze	Tangential	112.0	46.0	27
3 hrs/1910°F, cool to room temperature (17°F/sec) + braze		107.0	45.5	40
3 hrs/1910°F, cool to room temperature (2°F/sec) + braze		108.0 109.0	44.5 43.5	40 32
3 hrs/1750°F, cool to room temperature (15°F/sec) + braze		109.0	46.2	37

TABLE 10.3

EFFECT OF BRAZING CYCLES ON HASTELLOY X  
TENSILE PROPERTIES  
(Heat 260-5-2813)

Annealed: AGC 90056

<u>Temp (°F)</u>	<u>UTS (ksi)</u>	<u>YS (ksi)</u>	<u>Elong (%)</u>	
Room	104.7	45.0	56	
Room	105.0	45.5	58	
Average	99.9	43.2	41	(Annealed Forgings)
-320	-	-	-	
Average	136.0	77.8	27	(Annealed Forgings)

Standard Braze Cycle

<u>Temp (°F)</u>	<u>UTS (ksi)</u>	<u>YS (ksi)</u>	<u>Elong (%)</u>	
Room	108.0	48.5	22	
Room	108.0	48.7	23	
Design Average	93.3 <sup>+ 11*</sup>	45.0 <sup>+ 6.6*</sup>	24 <sup>+ 9*</sup>	
-320	139.0	80.9	17	
-320	138.0	84.2	13	
Design Average	117.4 <sup>+ 11*</sup>	71.7 <sup>+ 6.6*</sup>	13 <sup>+ 5.6</sup>	

Standard Braze +  
Extra Braze Cycle

<u>Temp (°F)</u>	<u>UTS (ksi)</u>	<u>YS (ksi)</u>	<u>Elong (%)</u>	
Room	106.0	47.6	21	
Room	107.0	47.2	21	
-320	130.0	81.7	11	
-320	131.0	81.9	11	

\*3-sigma

## 11.0 THERMAL FATIGUE TESTING

Two tests were conducted to evaluate the thermal cyclic-life of Hastelloy coolant tubes. The first method is presented in Appendix D and was conducted with pressurized liquid hydrogen-cooled tubing heated by electrical resistance. The tests demonstrated satisfactory life for 20 cycles from -423 to 1600°F.

Additional testing was conducted at ORNL on multitube samples, representative of the forward section of the nozzle. Although this test was more quantitative than that conducted with previous tubular samples, it simulated only axial thermal-restraint; the liquid nitrogen coolant was not circulated under pressure. The description of this test and the results obtained are presented in Appendix E. The results indicated satisfactory (greater than 10 cycles) life at nominal tube crown temperatures of 1600, 1800 and 1900°F.

Subsequent to this testing, an additional test was conducted at ORNL on a specimen that contained numerous simulated hand braze-joint repairs. The test results were to be compared with previous specimens tested at a maximum tube-crown temperature of 1800°F. The specimen was tested by heating to 1800°F, then holding for five minutes with liquid nitrogen flowing through the tube. One cycle consisted of a 5-second heat-up, a 5-minute hold at 1800°F and a 5-second cool-down. From the limited test results, it appears that a weld repair has an effect no worse than a tube dent and that braze repairs, per se, have no effect on cyclic life. The results are shown in Table 11.1 (with the summarized results from Appendix E) for both smooth and dented tubes.



TABLE 11.1

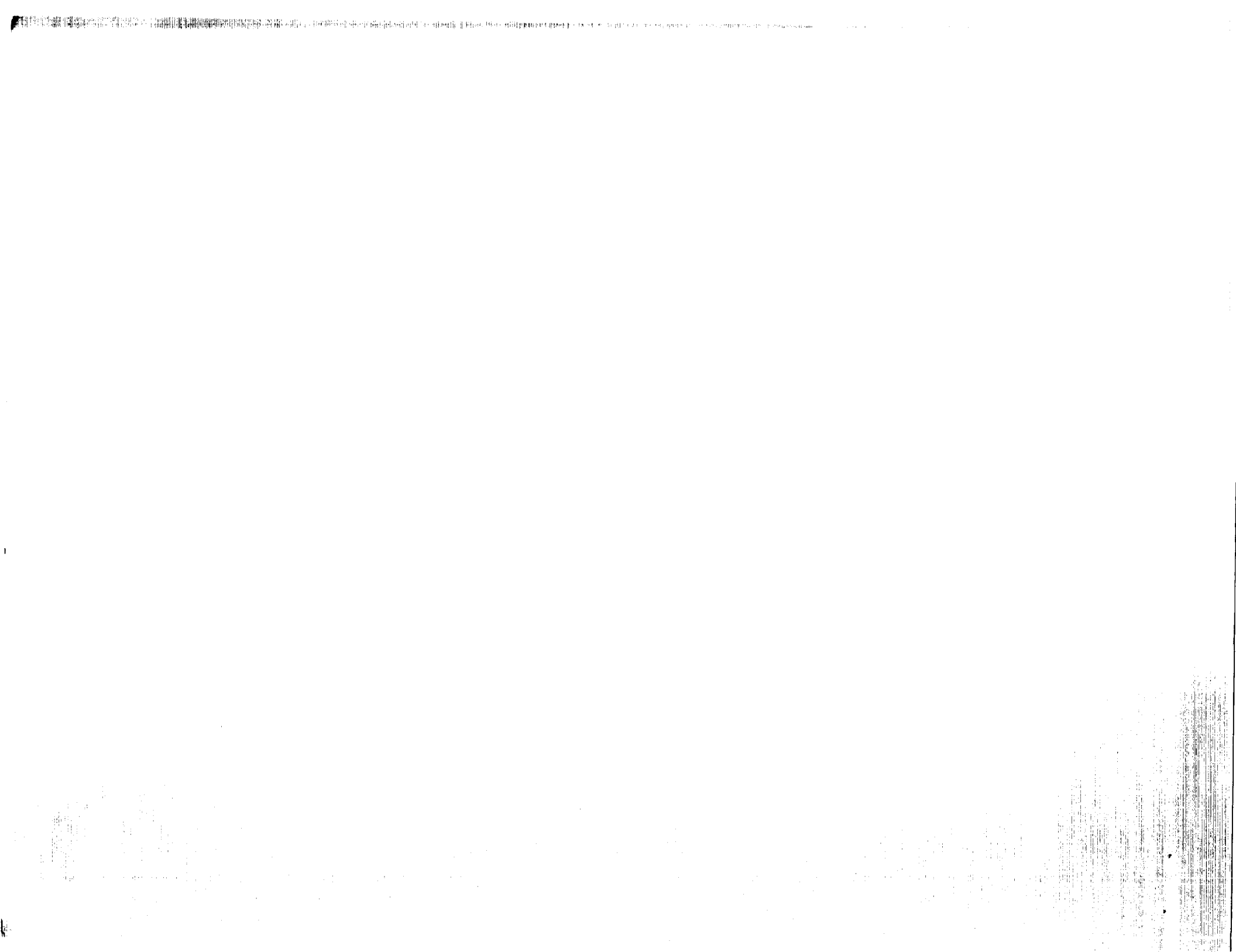
THERMAL FATIGUE TESTS OF FLAT TUBULAR HASTELLOY X SPECIMENS  
(HEAT 260-6-4002)

<u>Tube Condition</u>	<u>Cycles to Failure</u>	<u>Comments</u>
Braze repair	12	Failed at pin hole in tube wall between tubes, adjacent to braze.
↓	25	Failed at weld repair of a pin hole similar to first specimen.
↓	47	Smooth tube failure.
No repair	50 to 57	Smooth tube failure.
No repair but dented	28 to 49	Failure in dents.



APPENDIX A

DEVELOPMENT OF IMPROVED STRENGTH  
LARGE HASTELLOY X FORGINGS



## Appendix A

### I. SUMMARY

The 7000- to 8000-lb Hastelloy X, Phoebus-2 nozzles made from closed die forgings exceeded the state-of-the-art with respect to stock size and part size at the start of the program. The ingot to billet conversion cycle was bypassed and the ingot stock (approximately 22-in.-diameter) was forged directly. The ingot was vacuum melted by the consumable electrode process. The forgings were produced to meet the minimum room temperature tensile requirements of 85.0 ksi tensile strength, 40.0 ksi (0.2% offset) yield strength, and 40% elongation.

With product improvement as a goal, a development program was undertaken to demonstrate the practicability of improving the strength of these large forgings and to assess the effects on low temperature (-320°F) ductility. The program demonstrated that, remaining within the practical shop limitations for forgings of this size, the grain size could be controlled and enhanced strength attained. Some decrease in the room temperature minimum tensile ductility occurred in the annealed condition and exposure to the Phoebus-2 thermal treatment produced only a minor change. Testing at -320°F revealed a considerable improvement in tensile ductility after the thermal treatment.

The recommended revised minimum room temperature properties are 90.0 ksi ultimate tensile strength, 45.0 ksi yield (0.2% offset) strength, and 28% elongation.

### II. INTRODUCTION

The ingot and forging size requirements for the Phoebus-2 nozzle jacket exceeded the state-of-the-art for wrought Hastelloy X at the inception of the program. Specifically, the need was for large diameter forgings of heavy wall construction. The components indicated a starting multiple (billet or ingot) size of 22-in.-diameter and 7000- to 8000-lb with the requirement for very

Appendix A

large capacity forging equipment. The forging supplier was Wyman-Gordon Company, and the components were forged on their 50,000 ton press.

The three components employed to produce the nozzle jacket consisted of the following:

<u>Component</u>	<u>Approximate Size of Forging</u>
Inlet Ring	Right cylinder with 65-in.-diameter x 14-in. long x 3-in.-thick
Convergent Section	Cone with 72-in. maximum diameter x 33-in. long x 2-1/2-in. minimum thickness
Divergent Section	Cone with 53-in. maximum diameter x 46-in. long x 3-in. minimum thickness.

The inlet rings were produced from 14-in. billet stock by ring rolling. The convergent and divergent sections were the largest and heaviest closed die forgings of Hastelloy X made to date. They were produced direct from 24-in. diameter, consumable-electrode, vacuum-melted cast ingot, made by the Union Carbide Corporation, Stellite Division. The ingots were melted to provide the controlled chemistry listed in Table I. The following minimum tensile properties were required for the finished forgings in the 2150°F solution annealed and fan cooled\* condition:

	<u>Room Temp.</u>	<u>1200°F</u>
Ultimate Tensile Strength (ksi)	85.0	60.0
0.2% Yield Strength (ksi)	40.0	25.0
Elongation (%)	40	20

\*Size of components precluded adequate handling and facilities for water quenching.

Appendix A

TABLE I

SPECIFIED CHEMICAL ANALYSIS OF HASTELLOY X FORGINGS  
PRODUCED FOR PHOEBUS-2 PROGRAM

Carbon	0.05 to 0.15% by weight
Manganese	1.00 max
Silicon	1.00 max
Phosphorus	0.020 max
Sulfur	0.015 max
Boron	0.001 max
Vanadium	0.50 max
Copper	0.35 max
Aluminum + Titanium	0.50 max
Cobalt	0.50 to 2.50
Tungsten	0.20 to 1.00
Molybdenum	8.00 to 10.00
Iron	17.00 to 20.00
Chromium	20.50 to 23.00
Nickel	Remainder

Appendix A

In actuality, the following average tangential properties were obtained for the 13 annealed, closed-die forgings from nine different heats of material:

	<u>Nozzle Section</u>			
	<u>Convergent</u>		<u>Divergent</u>	
	<u>Room</u>	<u>1200°F</u>	<u>Room</u>	<u>1200°F</u>
Ultimate Tensile Strength (ksi)	102.0	72.8	93.2	69.2
0.2% Yield Strength (ksi)	43.2	26.9	42.3	26.7
Elongation (%)	48	47	33	36

The following tangential values were obtained for the 14 rolled inlet rings from three different heats of material:

	<u>Room</u> <u>Temp.</u>	<u>1200°F</u>
Ultimate Tensile Strength (ksi)	104.4	70.5
0.2% Yield Strength (ksi)	44.2	26.3
Elongation (%)	43	48

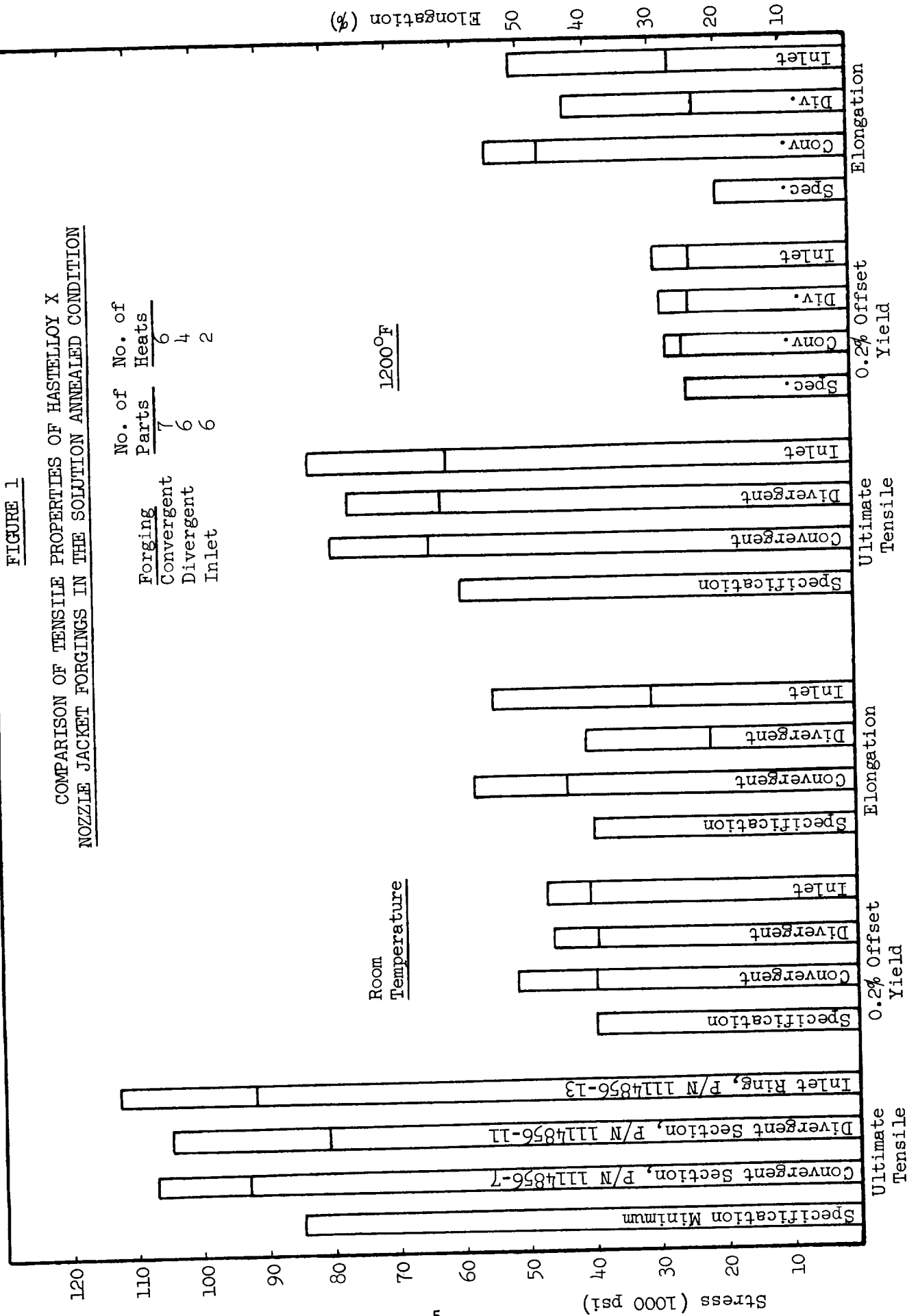
The tensile values are more conveniently compared in bar chart form in Figure 1. With the exception of a few room temperature results from the divergent section, the forgings readily met the tensile strength specification requirements at room temperature and 1200°F. The yield strength values, for practical purposes, all met the specification requirements at room temperature (40.0 ksi) and 1200°F (25.0 ksi), although the average values for the die forgings were a mere 5% above the minimums. The elongation values reflect greater variance and, although the 20% minimum was readily attained at 1200°F, there were several test results below the 40% minimum at room temperature. The spread (below minimum) for the inlet rings was the result of a few low test results because the over-all average is a ductile 48%. The low room temperature tensile strengths and elongations for the divergent sections were the result of localized concentrations of carbides in the area from which the test



FIGURE 1

COMPARISON OF TENSILE PROPERTIES OF HASTELLOY X  
NOZZLE JACKET FORGINGS IN THE SOLUTION ANNEALED CONDITION

Forging	No. of Parts	No. of Heats
Convergent	7	6
Divergent	6	4
Inlet	6	2



## Appendix A

material was obtained. The divergent section was forged by upsetting, pancaking, piercing, and closed die extrusion, with the major metal movement toward the large diameter. The test material for specimen fabrication was removed from the small diameter area of the conical forging such that the specimens were machined transverse to the carbide stringers. By comparison, the convergent section was forged by upsetting, pancaking, and then rough-and-finish-form closed die forging, with test material obtained from both ends of the conical forging.

The results obtained were acceptable from both the engineering design and functional basis, but improvement and assurance that all forgings would exceed the minimum strength criteria was a product improvement goal. Analysis of the forging practice, the experience accumulated, and the observed large grain size (ASTM 1 to 4) resulted in an optimistic plan to improve the forging strength by revision to the forging schedule and procedures. The program was undertaken by Wyman-Gordon utilizing a 4-in. thick slice of a 22-in. diameter production ingot (Heat 260-5-2863) and a piece of a large ring of excess material machined from a partially processed divergent section forging (Heat 260-5-2850).

### III. TEST RESULTS AND DISCUSSION

#### A. PROPERTIES

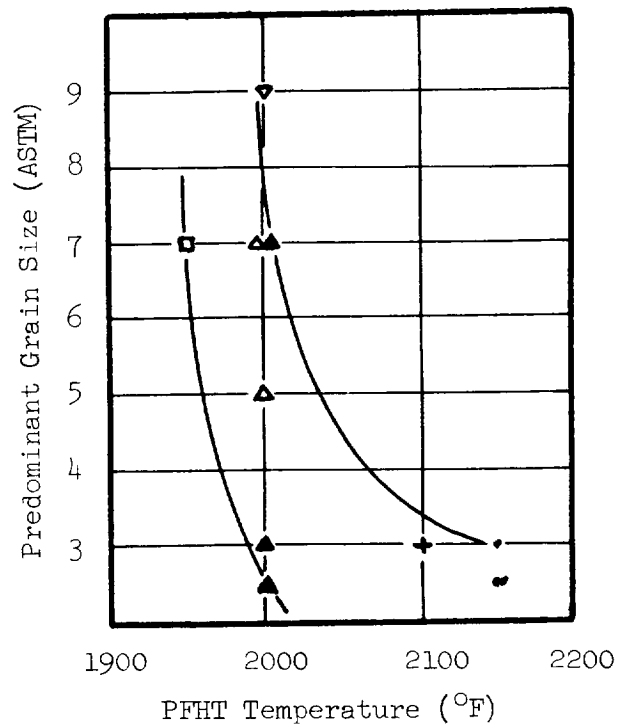
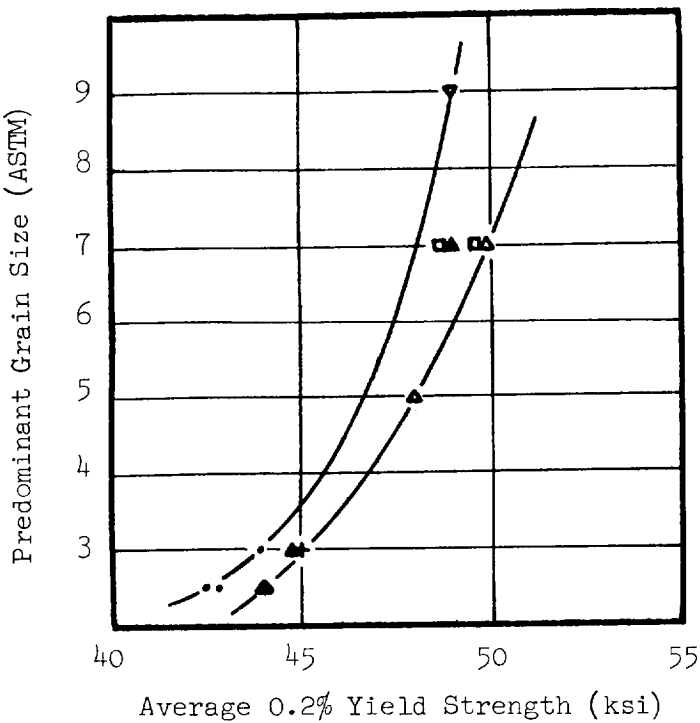
The Forging Improvement Program was directed toward providing a finer grain size, with the concomitant increased strength, through the control of final forging or restrike reductions, forging temperatures, and post-forge heat treatment (PFHT). Forging temperatures and reductions were selected based on actual forge practice capabilities evolved for the Phoebus-2 nozzles and consistent with acceptable metallurgical practice for Hastelloy X. The condensed and simplified results (yield strength and elongation only) are presented in Figures 2 and 3 for the ingot specimens and the forged ring section specimens, respectively, for all conditions evaluated.

FIGURE 2

INGOT UPSET SPECIMENS - FORGE CYCLE ANALYSIS \*

(Heat 260-5-2863)

PREDOMINANT GRAIN SIZE	FINAL FORGE (°F)	PFHT (°F)	FINAL REDUCTION	ROOM TEMPERATURE**	
				YS (ksi)	EL (%)
• 2½	2150	2150	50%	42.5	39½
• 3	2150	2150	10%	44.0	43
• 2½	2150	2150	5%	42.9	43
+ 3	2100	2100	10%	44.9	37½
▲ 5	2000	2000	5%	47.9	32½
▲ 7	2000	2000	10%	49.9	29
▲ 7	2150	2000	50%	49.0	30½
▲ 3	2150	2000	10%	44.8	35
▲ 2½	2150	2000	5%	44.0	36
▼ 9	2100	2000	10%	49.0	31½
□ 7	2000	1950	5%	48.8	33
□ 7	2000	1950	10%	49.6	29½



\*Wyman-Gordon Company Report No. RD 66-125, MD&E No. 204, May 1966

\*\*Average of four specimens for each condition.

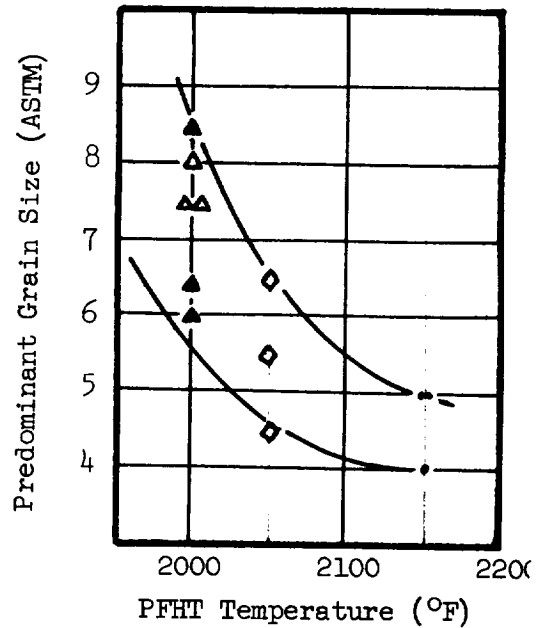
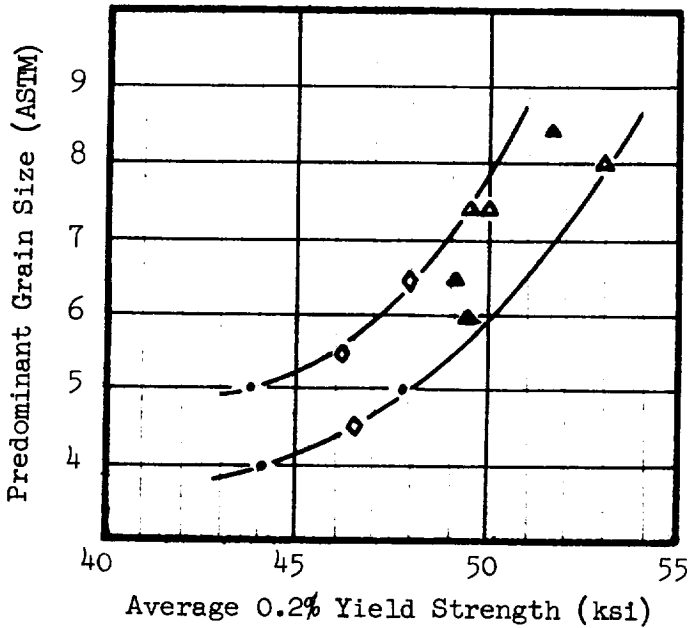
Appendix A

FIGURE 3

FORGED RING SECTION - FORGE CYCLE ANALYSIS \*

(Heat 260-5-2850 P/N 11148 56-11)

PREDOMINANT GRAIN SIZE	FINAL FORGE (°F)	PFHT (°F)	FINAL REDUCTION	ROOM TEMPERATURE **	
				YS (ksi)	EL (%)
• 5	2150	2150	5%	47.8	39½
5	2150	2150	10%	43.8	44
4	2150	2150	40%	44.1	44½
◊ 5½	2000	2050	5%	46.1	37
6½	2000	2050	10%	47.9	35
4½	2000	2050	25%	46.5	38
▲ 6½	2150	2000	5%	49.1	36
6	2150	2000	10%	49.4	36½
8½	2150	2000	40%	51.6	35
▲ 7½	2000	2000	5%	49.5	36
7½	2000	2000	10%	50.0	35
8	2000	2000	25%	53.0	34½



\* Wyman-Gordon Company Report No. RD 66-125, MD&E No. 204, May 1966

\*\* Average of two specimens for each condition.

## Appendix A

Using the recommended initial forging temperature of 2150°F and a heavy finish forging reduction (50%) with a reduced PFHT (2000°F) a room temperature yield strength of 49.0 ksi was attained; likewise, decreasing the finish forging temperature to 2000 or 2100°F and limiting the final forge reduction to a restrike level of 5 to 10% with a reduced PFHT (2000°F), room temperature yield strengths of 48.0 ksi to 50.0 ksi consistently were attained.

Limiting the PFHT to 2000°F and the forging grain sizes to a range from ASTM 6 to 9 resulted in (1) the tensile elongation at room temperature ranging from a low of 23% to a high of 35% (average 31%) on the ingot starting material and a range of 34 to 42% (average 36%) for the forged ring starting material; (2) the room temperature yield strength averaged 49.2 ksi; and (3) the yield strength and elongation at 1200°F averaged 32.1 ksi and 38%, respectively.

Figure 4 presents all the test data for the yield strengths and the tensile elongations plotted against grain size. The trends are obvious and the advantages and disadvantages of the finer grain sizes are noted respectively by the increasing yield strength and decreasing elongation. An ASTM grain size of 6 appears as a desirable and practicable value indicating a probably minimum yield strength of 45 ksi combined with a useful 28% minimum elongation.

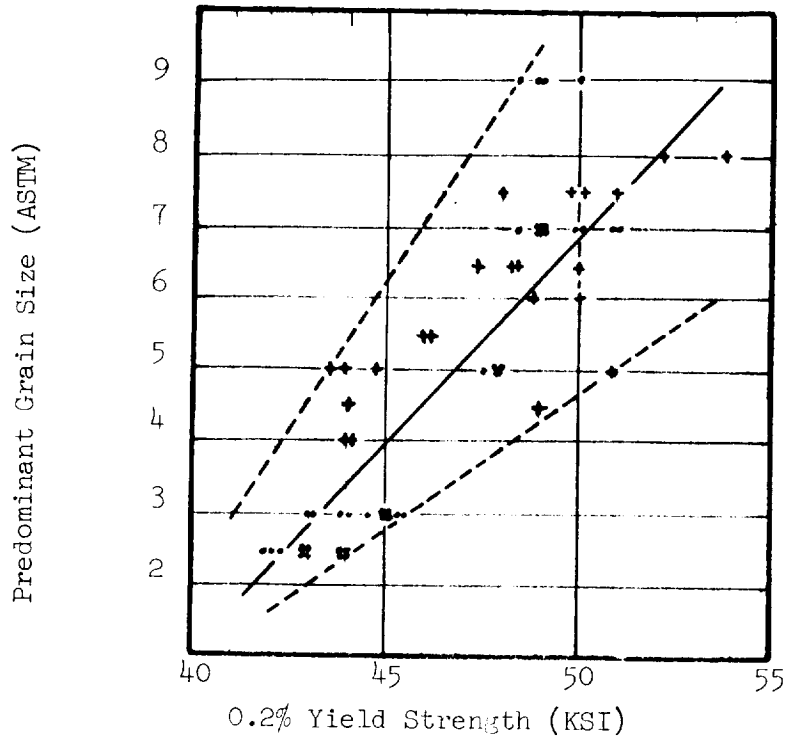
The significance and the inter-relationship of the finish forging temperatures, reductions, and PFHT are more graphically illustrated in Figure 5.

The yield strength of the forgings was improved by:

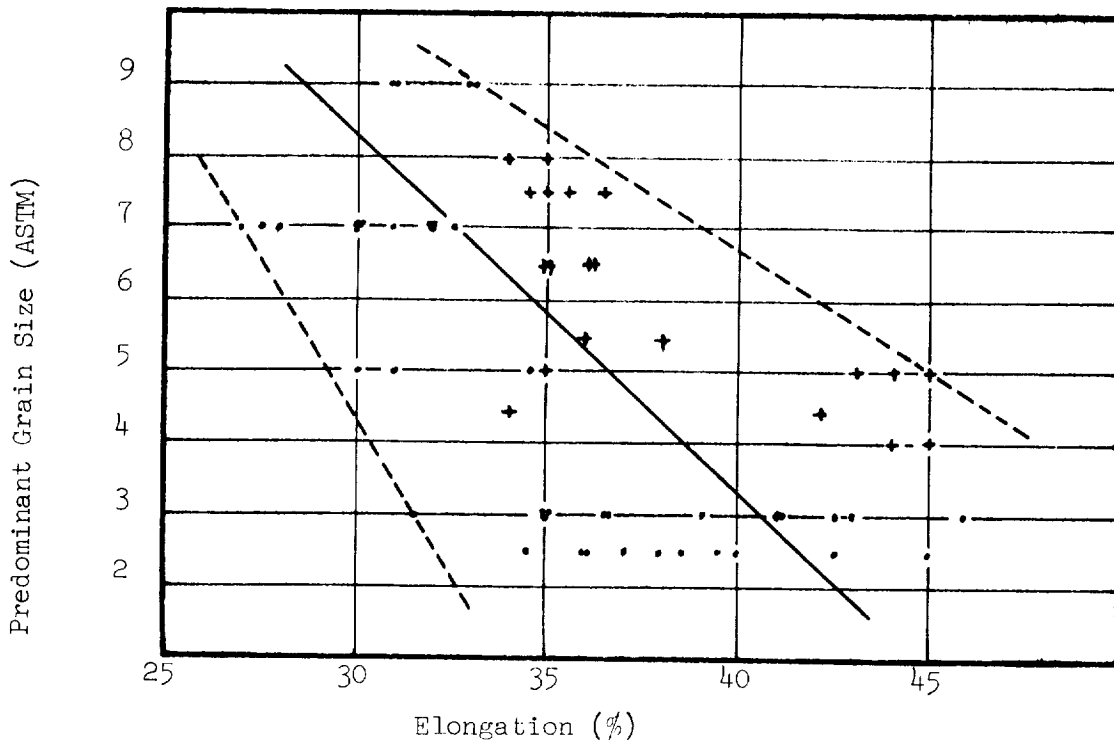
1. Decreasing the final forging temperature in order to reduce grain growth and retain some hot strain by minimizing annealing,
2. Decreasing PFHT in order to maintain the finer grain size and to minimize the removal of the benefits of hot strain, and

Appendix A

FIGURE 4



Upset Ingot Specimens + Forged Ring Specimens



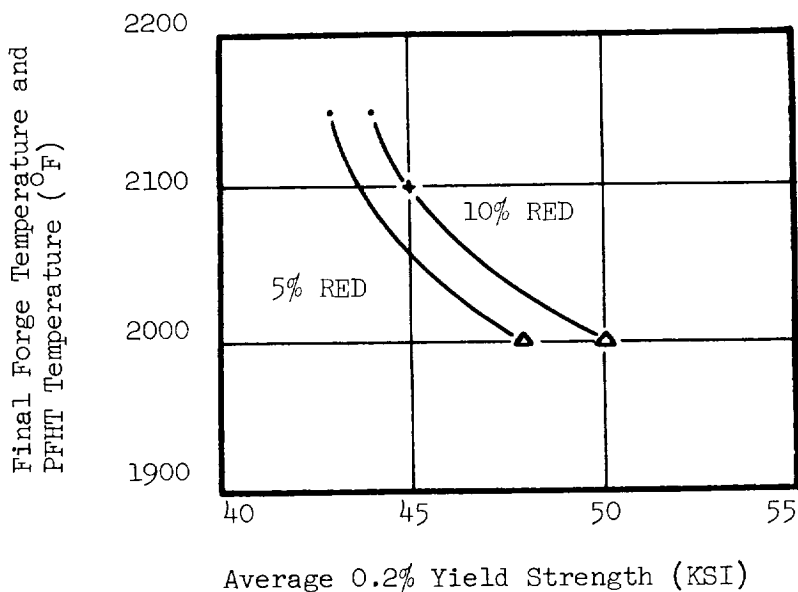
Relationship of 0.2% Yield Strength and Elongation to ASTM Grain Size

Appendix A

FIGURE 5

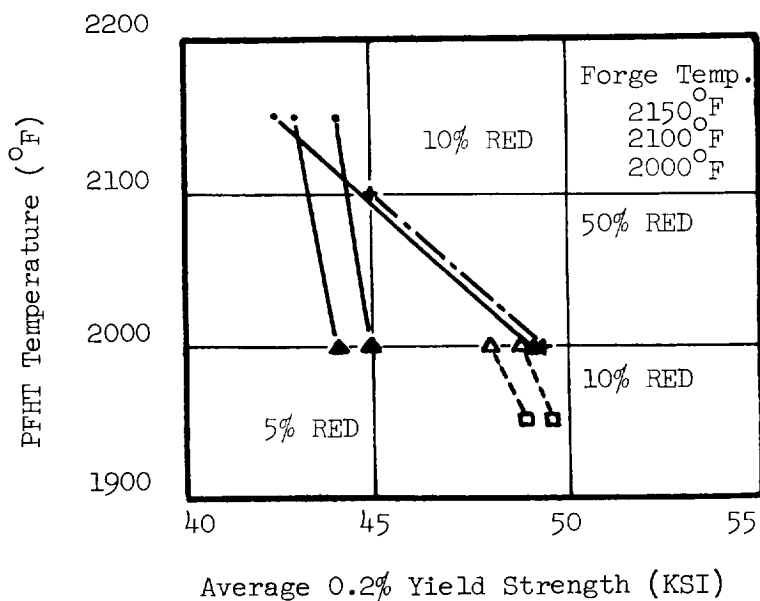
INTER-RELATIONSHIP OF FINISH FORGING TEMPERATURE, REDUCTION AND PFHT

(Ingot Upset Specimens, Heat 260-5-2863)



Effect of decreasing final forging temperature and PFHT with increasing restrike reduction on 0.2% Yield Strength.

Refer to Figures 2 and 3 for symbol identification



Effect of constant final forging temperature and decreasing PFHT with increasing reduction on 0.2% Yield Strength

Appendix A

3. Increasing the final reduction to introduce more hot strain for recrystallization and grain refinement.

From a thorough review of the data and results, the following conditions were selected for further testing following exposure to the braze cycle treatment required on the Phoebus-2 nozzle:

<u>Initial Forge Temp. (°F)</u>	<u>Finish Forge Temp. (°F)</u>	<u>Final Reduction (%)</u>	<u>PFHT (°F)</u>	<u>Serial No. of Ingot/Pancake</u>	<u>Comments</u>
2150	2150	50	2000	26/10	This was a minimum deviation from the Phoebus-2 practice, but because of heavy final reduction presupposed no restriking.
2150	2100	10	2000	25/11	Restrike condition of high probability.
2150	2100	5	2000	--/14	This condition originally was not tested, but it represented a real restrike reduction condition.
2150	2000	10	2000	27/13	Same as above; however, restrike temperature represented probable lower limit with existing part sizes and press capacity.
2150	2000	5	2000	20/12	

Sample pancake forgings (approximately 1-in. thick by 10-in. diameter, identified by Serial No. 10 through 14) produced from sections of an ingot were exposed to the Phoebus-2 braze cycle and tensile tested (in duplicate) at room temperature and -320°F. The brazing cycle employed was known to reduce the tensile elongation of Hastelloy X. The effect was considered especially significant at -320°F because of the noted reduction in elongation as the grain size decreased as a result of the new forging practices. For comparison, the tensile properties of Hastelloy X obtained from cross-forged



Appendix A

rolled rings\* (20-in. OD x 17-in. ID x 16-in. long) were as follows after being processed through the brazing cycle:

Temp (°F)	<u>Ultimate Tensile Strength (ksi)</u>		<u>Yield Strength (ksi)</u>		<u>Elongation (%)</u>	
	<u>Mean</u>	<u>Minus 3-Sigma</u>	<u>Mean</u>	<u>Minus 3-Sigma</u>	<u>Mean</u>	<u>Minus 3-Sigma</u>
-320	117.4	106.4	71.7	65.1	13.1	7.5
Room	93.3	85.0	45.0	38.4	24.4	18.8
1200	74.8	70.2	26.8	22.6	31.4	18.0

The average and minimum tensile properties of all the sample pancake forgings produced by Wyman-Gordon under the improvement program were as follows after being processed through the brazing cycle:

Temp (°F)	<u>Ultimate Tensile Strength (ksi)</u>		<u>Yield Strength (ksi)</u>		<u>Elongation (%)</u>	
	<u>Average</u>	<u>Minimum</u>	<u>Average</u>	<u>Minimum</u>	<u>Average</u>	<u>Minimum</u>
-320	152.5	142.9	79.7	77.0	26	16
Room	111.9	108.8	49.4	46.7	29	26

The detailed test results are itemized in Tables II and III; the significant differences between the improved forgings and previous forging are obvious. The yield strength and tensile strength are distinctly improved, but an outstanding feature is the tensile elongation. The tensile ductility for the improved forgings in the annealed condition averaged 31% at room temperature for the ingot specimens and decreased to 29% at room temperature in the braze cycle heat treated condition. A further decrease to only 26% occurred at -320°F in the brazed condition. The original Hastelloy X forgings

\*Total reduction from ingot to forging was approximately the same as the convergent and divergent nozzle section reductions. ASTM Grain Size was 1 to 4.

## Appendix A

TABLE II

TENSILE PROPERTIES OF HASTELLOY X  
 PANCAKE FORGINGS MADE  
 FROM CAST INGOT (HEAT 260-5-2863)

(All specimens exposed to Phoebus-2 Braze Cycle)

<u>Serial No. and Specimen Identification</u>	<u>Temp (°F)</u>	<u>Ultimate Tensile Strength (ksi)</u>	<u>Yield Strength (ksi)</u>	<u>Elongation (% in 1-in.)</u>	<u>Reduction In Area (%)</u>
10C	-320	142.9	80.0	16	15
10D	-320	146.7	77.0	21	19
11C	-320	155.2	80.9	25	22
11D	-320	157.5	80.6	29	27
12C	-320	153.8	-	29	23
12D	-320	147.6	84.3	19	15
13C	-320	156.0	77.3	30	25
13D	-320	154.4	80.1	28	23
14C	-320	156.6	77.5	28	20
14D	-320	154.1	-	31	25
Average	-320	152.5	79.7	26	21
10E	Room	112.0	50.9	31	29
10F	Room	108.8	46.8	26	25
11E	Room	112.8	48.9	29	28
11F	Room	113.3	46.7	32	34
12E	Room	109.3	49.3	32	29
12F	Room	111.9	54.1	26	25
13E	Room	113.1	49.7	29	28
14E	Room	111.5	50.3	31	30
14F	Room	112.4	48.1	31	30
Average	Room	111.9	49.5	29	27

## Appendix A

TABLE III

TENSILE PROPERTIES OF HASTELLOY X PANCAKE FORGINGS  
 MADE FROM CAST INGOT (HEAT 260-5-2863)  
 (All Specimens Annealed at 2000°F)

<u>Serial No. and Specimen Identification</u>	<u>Final Forging Temp (°F)/ Reduction (%)</u>	<u>Test Temp (°F)</u>	<u>Ultimate Tensile Strength (ksi)</u>	<u>Yield Strength (ksi)</u>	<u>Elongation (% in 1-in.)</u>	<u>Reduction In Area (%)</u>
10A (26)	2150/50	Room	106.9	55.5	31	27
10B (26)	2150/50	Room	105.9	49.4	25	24
11A (25)	2100/10	Room	110.0	45.8	32	33
11B (25)	2100/10	Room	111.0	49.4	32	34
12A (20)	2000/5	Room	109.2	--	30	26
12B (20)	2000/5	Room	108.7	56.9	25	25
13A (27)	2000/10	Room	111.4	50.4	35	35
13B (27)	2000/10	Room	113.0	52.7	34	32
14A	2100/5	Room	115.0	52.2	27	22
14B	2100/5	Room	115.1	53.5	35	35
Average	-	Room	110.6	51.8	31	29
26 (10)	2150/50	Room	106.4	49.0	32	31
26 (10)	2150/50	Room	107.6	49.0	32	32
26 (10)	2150/50	Room	104.2	48.8	28	28
26 (10)	2150/50	Room	107.0	49.0	30	30
25 (11)	2100/10	Room	108.0	49.0	33	31
25 (11)	2100/10	Room	108.0	48.4	33	33
25 (11)	2100/10	Room	108.0	49.0	30	29
25 (11)	2100/10	Room	107.4	50.0	30	23
20 (12)	2000/5	Room	108.0	48.0	30	30
20 (12)	2000/5	Room	109.0	48.0	34	36
20 (12)	2000/5	Room	108.0	47.6	35	38
20 (12)	2000/5	Room	109.0	48.0	31	29
27 (13)	2000/10	Room	111.0	50.0	32	30
27 (13)	2000/10	Room	111.0	49.0	31	31
27 (13)	2000/10	Room	109.6	49.4	30	27
27 (13)	2000/10	Room	108.4	51.0	23	25
-	2100/10	Room	NO TESTS CONDUCTED			
Average	-	Room	108.2	49.0	31	31

NOTE: Number in ( ) indicates related forging identification.

## Appendix A

decreased from an average annealed ductility of 41% at room temperature to 24% after brazing, which further decreased to 13% at  $-320^{\circ}\text{F}$ . The significance of the improved yield strength is obviously important to the design, while the improved ductility is less obvious but nevertheless highly important in the cyclic thermal performance of a nozzle. Improved ductility provides an increased margin in the nozzle cyclic thermal exposure life.

### B. MICROSTRUCTURE

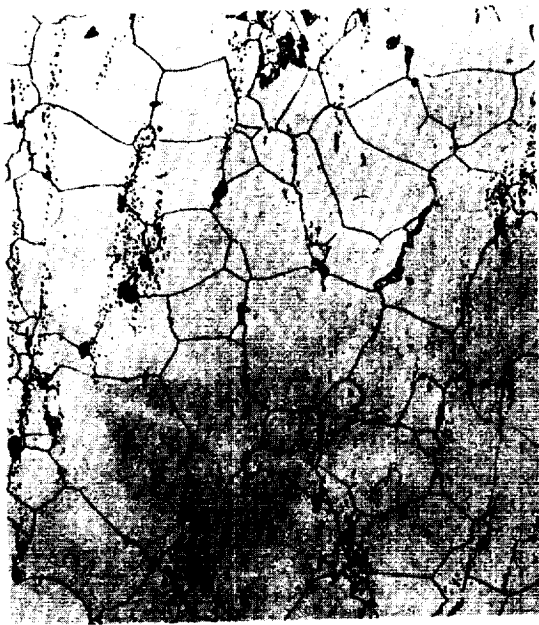
Micro-examination revealed significant differences in the distribution of the aging precipitates (carbides) in the microstructures of the forgings as a result of the post-forge annealing temperatures (PFHT) and exposure to a simulated brazing cycle.

The complete solution anneal treatment at  $2150^{\circ}\text{F}$  produced a large grain structure with heavy, continuous grain boundaries and no precipitate within the grains (matrix), except for some primary carbide more-or-less evident in all the microstructures (see Figure 6). After exposure to the brazing cycle treatment the grain boundaries contained more precipitate and carbides were evident in the matrix (Figure 7).

When solution annealed at lower temperatures ( $1950^{\circ}$  to  $2100^{\circ}\text{F}$ ), the microstructures revealed smaller worked grains, less grain boundary precipitate, discontinuous grain boundaries, and no precipitates in the matrix, as shown in Figures 8, 9, and 10. After the brazing cycle considerable precipitation was noted in the matrix with slight-to-no change in the grain boundary precipitates (Figures 11, 12, and 13). The discontinuity or agglomeration of the grain boundary precipitation appeared to increase with decreasing annealing temperature.

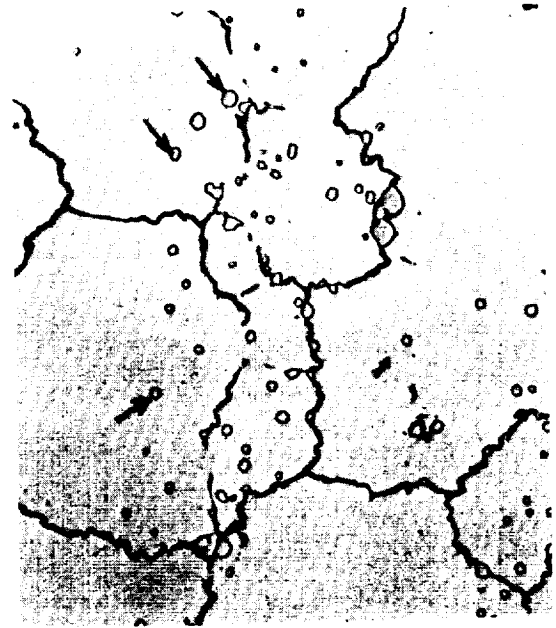
The observed phenomena supported the mechanical properties manifestation of the microstructures. The greater dispersion of the precipitates in a finer grained structure increased strength with some loss in

Appendix A



a.

100X



b.

1000X

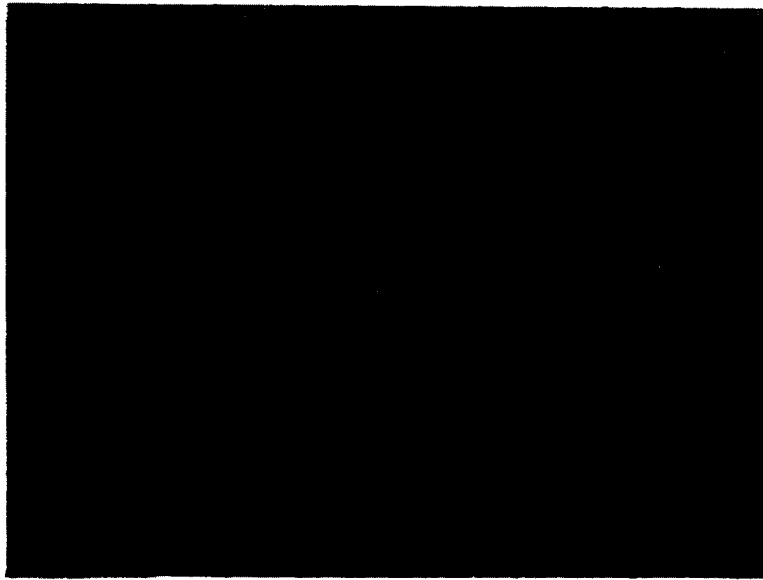
Figure 6. Microstructure of forging Serial No. 26 after 2150°F solution heat treatment. Scattered primary phase (arrows) and heavy, continuous grain boundary precipitate.

Appendix A



a.

100X

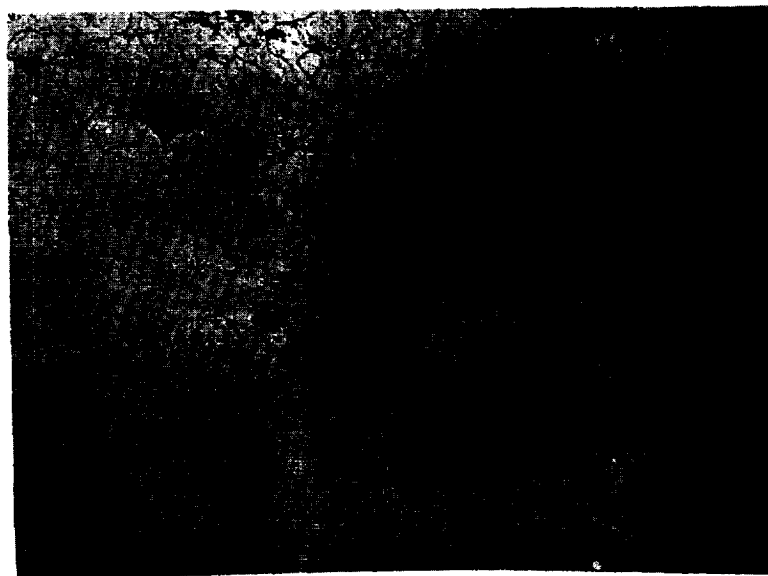


b.

1000X

Figure 9. Microstructure of Hastelloy X Forging  
Serial No. 20 After 2000 F Solution  
Heat Treatment.

Appendix A



a.

100X

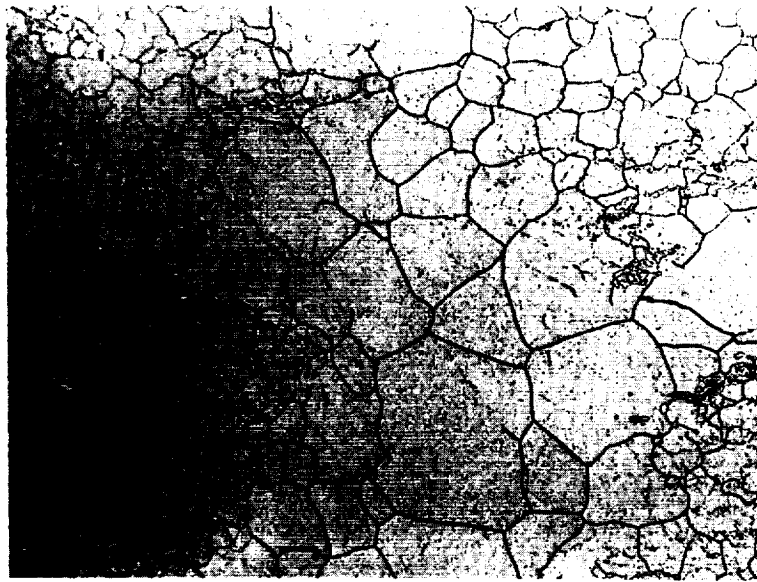


b.

1000X

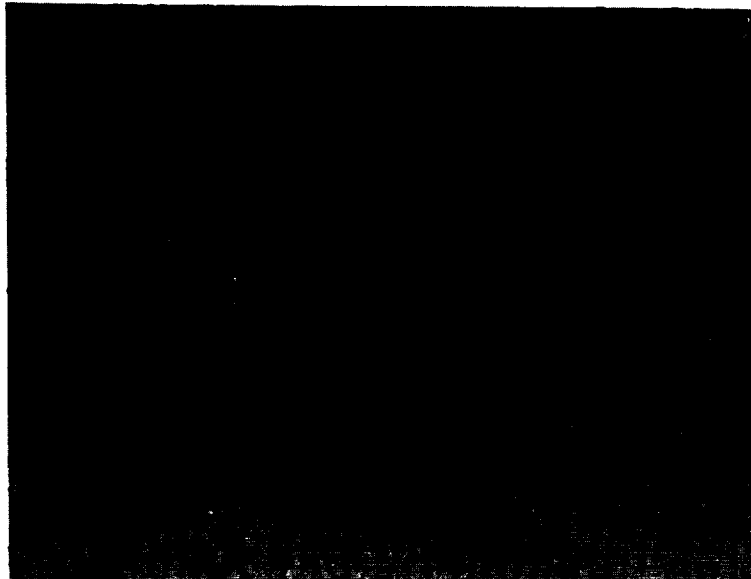
Figure 10. Microstructure of Hastelloy X Forging  
Serial No. 25 After 2100°F Solution  
Heat Treatment.

Appendix A



a.

100X



b.

1000X

Figure 13. Microstructure of Hastelloy X Forging Serial No. 25 After 2100° F Solution Heat Treatment and a simulated Phoebus braze cycle.



ductility. The finer grain size increased the amount of grain boundary interface, distributing the grain boundary precipitates over greater length, thereby producing a discontinuous network of the low ductility constituent. This, in turn, permitted the ductile matrix to exert a greater influence on the macro-tensile ductility.

IV. CONCLUSIONS

Remaining within the practical shop limitations for producing the large Phoebus-2 nozzle forgings of Hastelloy X, it was demonstrated that improved tensile strength properties were attained. It is estimated that the 0.2% offset yield strength can be increased from a minimum of 40.0 to 45.0 ksi and the minimum tensile elongation can be changed from 40 to 28%.

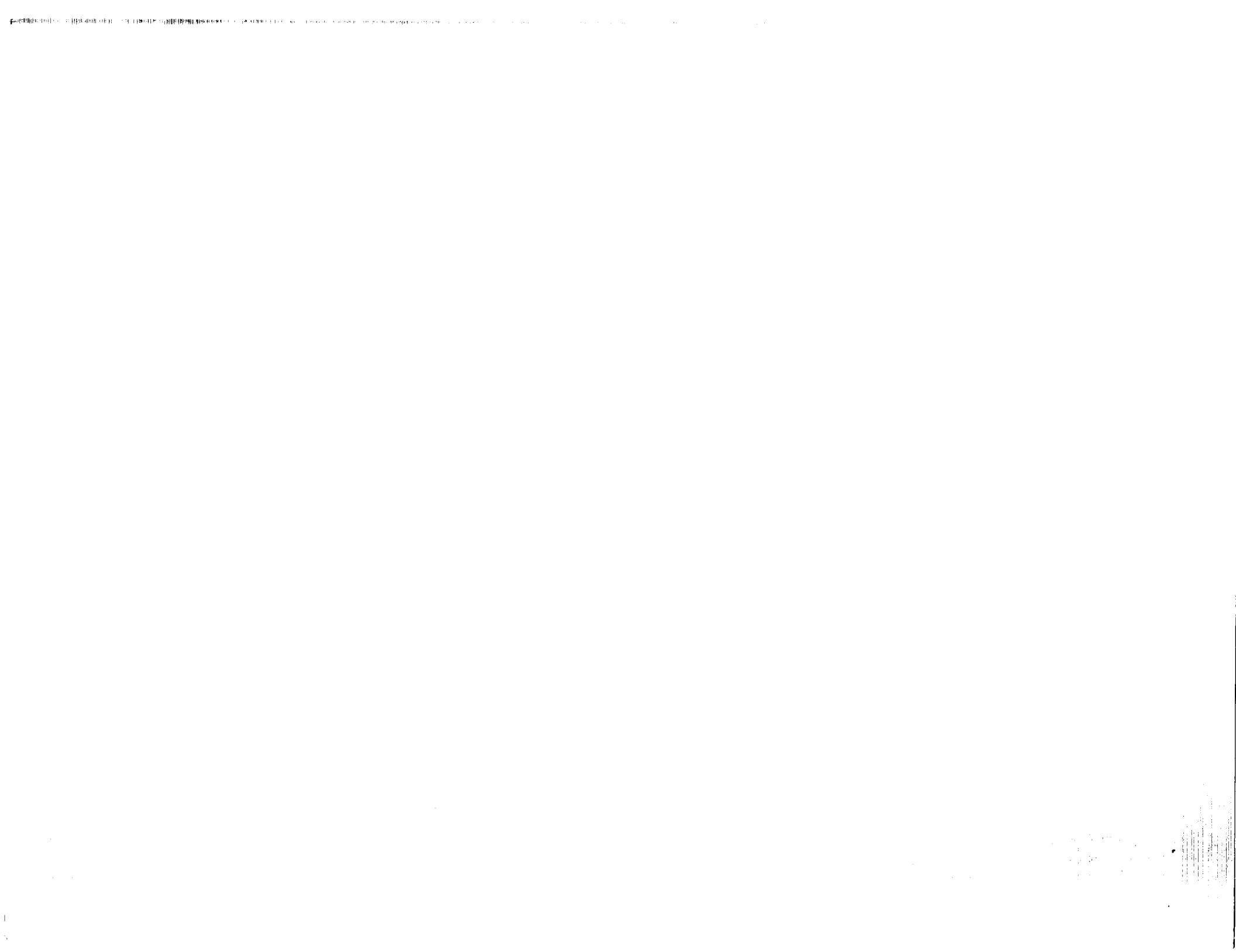
V. ACKNOWLEDGEMENT

The program was conducted under SNPO-C Contract SNPC-35, Task K.



APPENDIX B

HASTELLOY X COOLANT TUBE INVESTIGATION



## Appendix B

### I. SUMMARY

A metallurgical investigation was performed on a Hastelloy X coolant tube produced by Straza Industries. The investigation consisted of microstructural, dimensional, and hardness studies on samples from eight areas of the tube and a study of the effects of thermal treatment (simulated braze and annealing cycles per AGC-90071) on the test samples. Microstructural study and hardness determinations were also performed on a Hastelloy X strip (AGC-90057) sample representing the coolant tube raw stock. In this study, it was found that:

A. Both the as-formed coolant tube and the Hastelloy X strip sample were fine grained with the predominant grain size being ASTM 7. Grain size range was generally ASTM 6 to 8.

B. The simulated brazing, annealing, and annealing plus brazing cycles did not promote grain growth in the as-formed coolant tube.

C. The simulated brazing and annealing plus brazing cycles promoted carbide precipitation and produced a hardness increase in the coolant tubes.

D. The simulated annealing plus brazing cycle conferred slightly higher hardnesses than either annealing or brazing alone.

E. The annealing treatment conferred higher hardnesses than the simulated brazing cycle. The annealing treatment prior to the braze cycle reduced the amount of carbides precipitated at the grain boundaries.

F. A partial stress relief or stress equalizing of the cold worked Hastelloy X was achieved by the annealing and annealing plus simulated brazing cycles.

## Appendix B

G. As-formed tube samples from the throat radii region exhibited a hardness gradient due to stretch forming; viz., cold-working. Maximum hardness was observed at the crown of the tubes.

H. Annealing cycles caused no significant changes in the "H" (height) and "ID" (inside diameter) dimensions of the as-formed tubes.

I. Forward end-cap welds were sound. An aft end-cap sample, however, had a condition of oxide entrapment at the inner weld. This prevented complete weld fusion and formation of a sound weld.

J. Slight primary phase segregation exists in the coolant tube.

## II. INVESTIGATION AND RESULTS

### A. PROCEDURE

The Hastelloy X coolant tube was metallurgically examined in accordance with the testing plan outlined below. The testing plan was submitted by Phoebus-2 Materials.

#### 1. Phase A - Metallurgical Analysis of As-Formed Tube

a. Microstructure examination of six tube sections (see Figure 1) at 100 and 250 X in the transverse orientation.

b. Microhardness survey of the tube sections.

c. Thickness measurement of the tube sections.

d. Microstructure examination of two welded end-cap sections (see Figure 1) at 100 and 250 X in the longitudinal orientation.

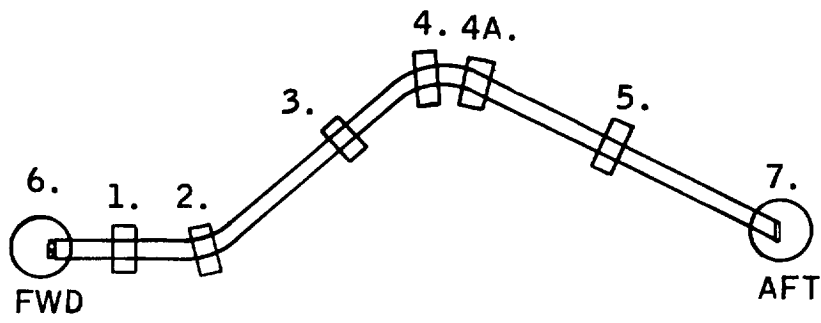


FIGURE 1  
SPECIMEN TEST LOCATION,  
HASTELLOY X COOLANT TUBE

Appendix B

2. Phase B - Study of the Effect of a Simulated Braze Cycle on the As-Formed Tube

a. Microstructure examination of six tube section samples (see Figure 1) at 100 and 250 X in the transverse orientation.

b. Microhardness survey on above tube section samples.

c. Microstructure examination of two welded end-cap tube section samples (see Figure 1) at 100 and 250 X in the longitudinal orientation.

3. Phase C - Study of the Effect of an Annealing Cycle and Annealing Plus Simulated Braze Cycle on the following Changes in the As-Formed Tube

a. Dimensional change.

b. Microstructural change.

c. Hardness change.

d. Annealing per AGC-90071.

Cycle A 1925°F/5 minutes in H<sub>2</sub>, fast cool

Cycle B 1925°F/15 minutes in H<sub>2</sub>, fast cool

The simulated braze cycle employed consisted of the following:

Cycle 1 Heat-up to 1830°F ± 20°F in 3 to 4 hours  
Hold at 1830°F ± 20°F for one hour  
Cool 100°F/hour to 975°F

Cycle 2 Heat-up to 1800°F ± 20°F  
Hold one hour at 1800°F ± 20°F  
Cool 100°F/hour to 975°F



## Appendix B

Cycle 3 Heat-up to 1775°F + 20°F  
Hold one hour at 1775°F  
Cool 100°F/hour to room temperature

Additionally, a strip of Hastelloy X (Heat 260-5-2813) representing the raw stock used in the coolant tubes was micro-examined for structure and was also microhardness tested. These results are included under Phase A finding in the report.

### B. TEST RESULTS

#### 1. Phase A - Metallurgical Analysis of As-Formed Tube and Raw Stock Strip Samples

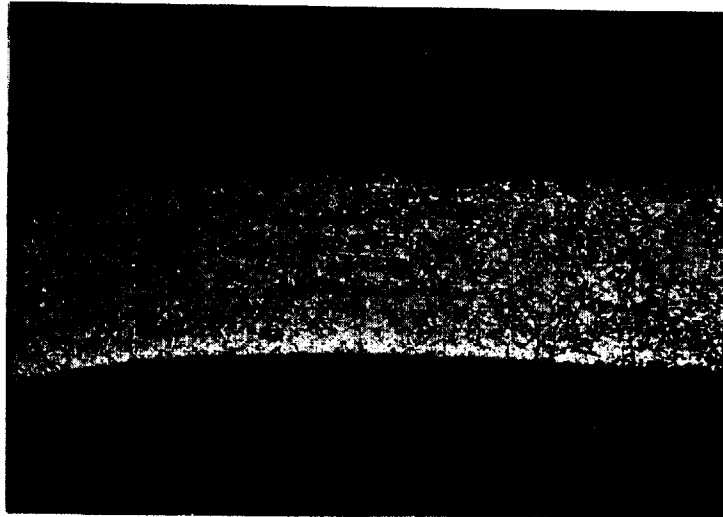
##### a. Microstructure Examination

Microstructure of the coolant tube sections and the raw stock strip samples are shown in Figures 2 and 3, respectively. The significant findings are listed below:

Coolant tube samples (Figure 2): The predominant grain size was ASTM No. 7. The grain size ranged from ASTM No. 6 to 8. There were no significant differences in grain size among samples taken from the six locations. There was evidence of considerable grain twinning (in all samples) due to cold work from tube forming and carry-over from the raw stock strip.

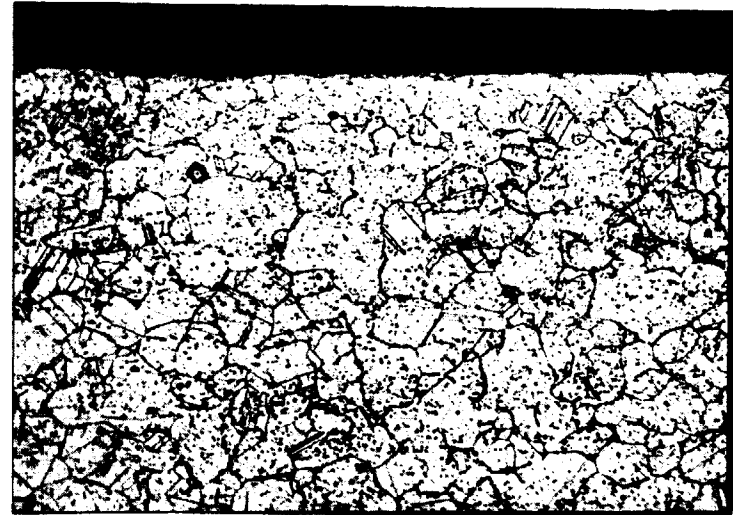
Raw stock strip samples (Figure 3): Like the coolant tube samples described above, the predominant grain size was ASTM No. 7, while the grain size range was ASTM No. 6 to 8. The longitudinal sample showed evidence of primary phase segregation in the matrix. This condition was not evident in the transverse sample nor in the transversely mounted coolant tube samples. Considerable grain twinning was also evident.

Comparative microstructures (Figures 2 and 3): Grain sizes of the tube and strip samples were essentially equivalent. Also, the



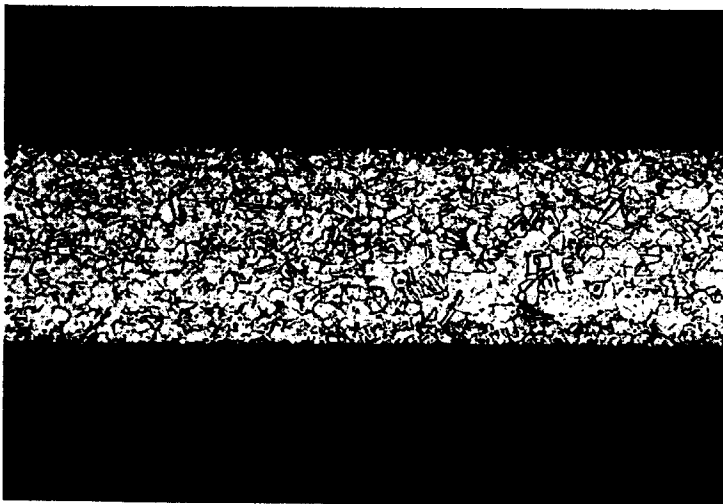
Tube Section 1-1

100X



Tube Section 1-1

250X



Tube Section 2-1

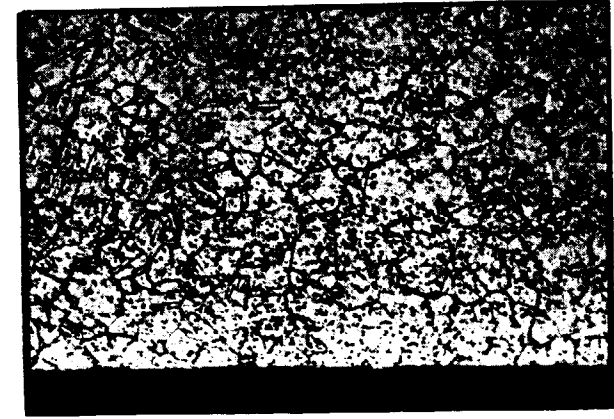
100X



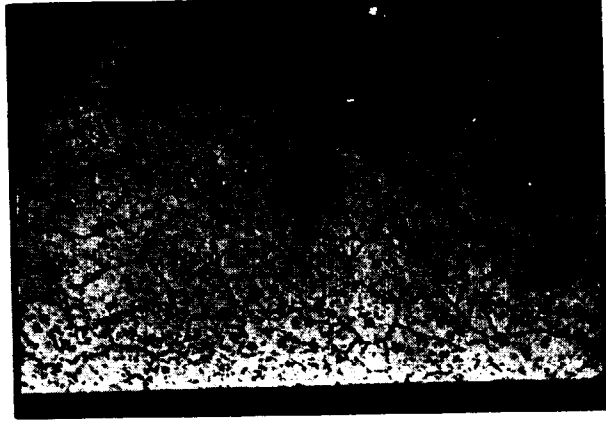
Tube Section 2-1

250X

FIGURE 2A - Microstructure of tube sections in as-formed condition.  
Etchant: 10% Oxalic, Electrolytic



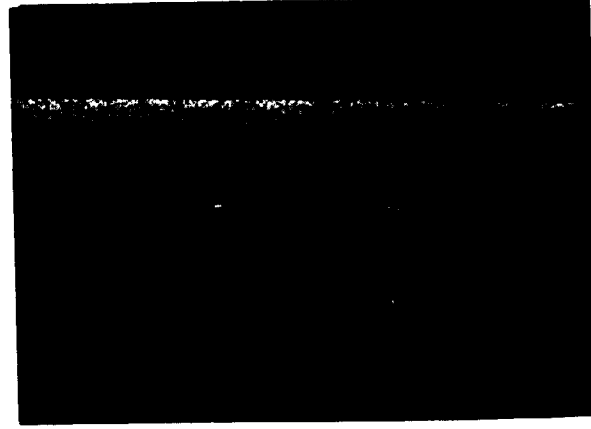
Tube Section 3-1  
250X



Tube Section 4-7  
250X

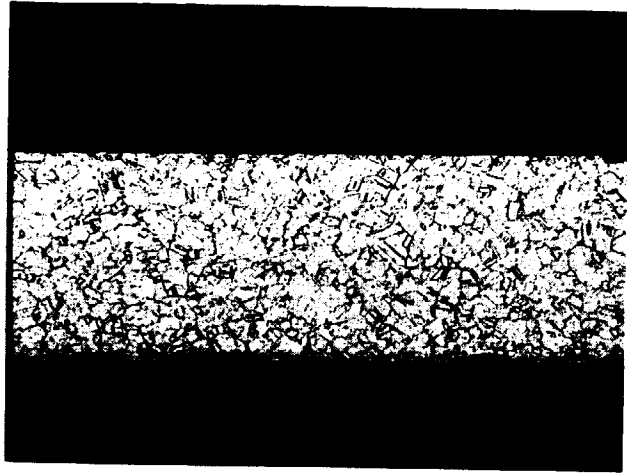


Tube Section 3-1  
100X



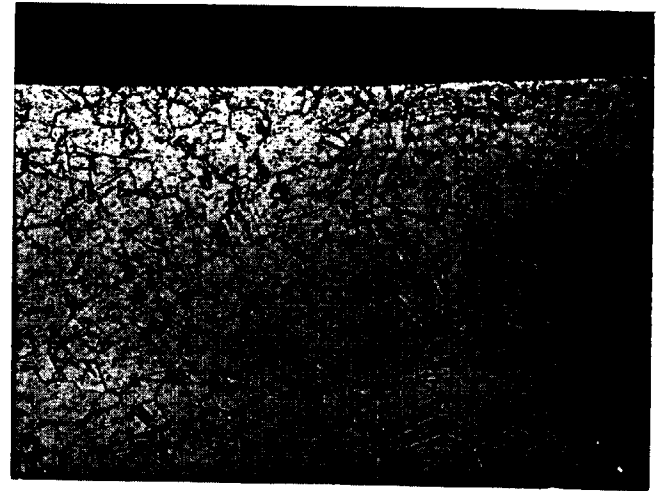
Tube Section 4-7  
100X

Figure 2B - Microstructure of tube sections in as-formed condition.  
Etchant: 10% Oxalic, Electrolytic.



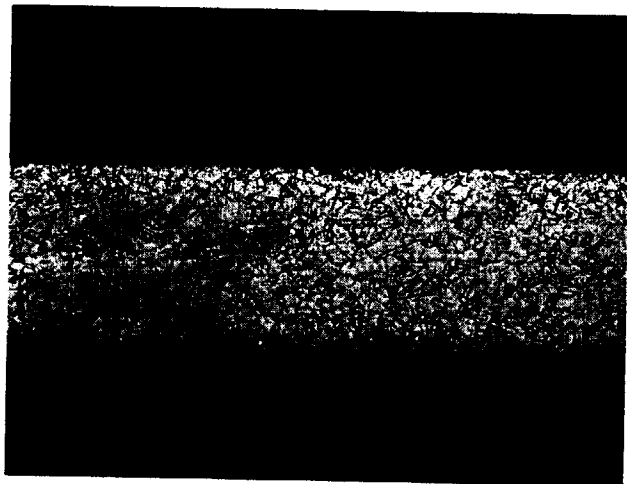
Tube Section 4A-7

100X



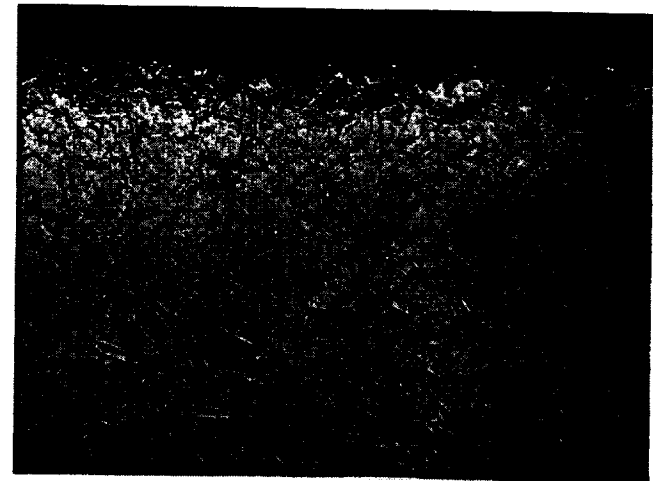
Tube Section 4A-7

250X



Tube Section 5A-0

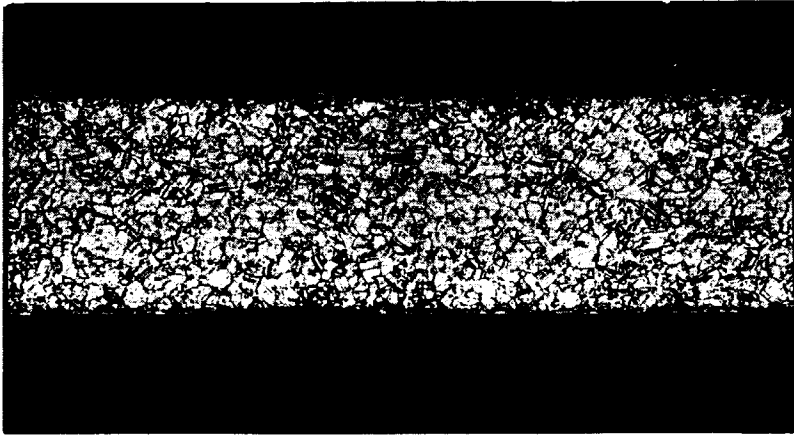
100X



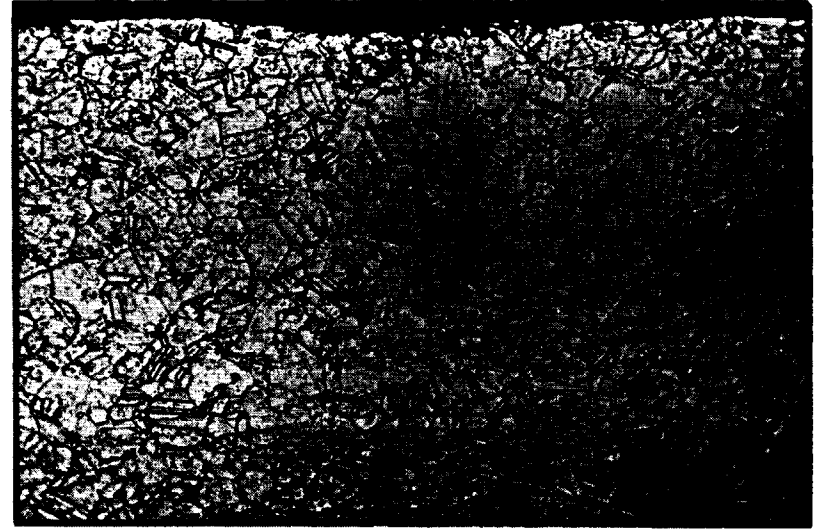
Tube Section 5A-0

250X

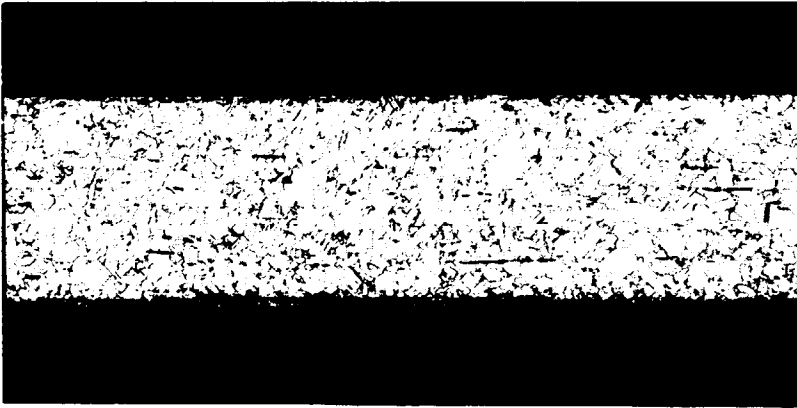
Figure 2C - Microstructure of tube sections in as-formed condition.  
Etchant: 10% Oxalic, Electrolytic



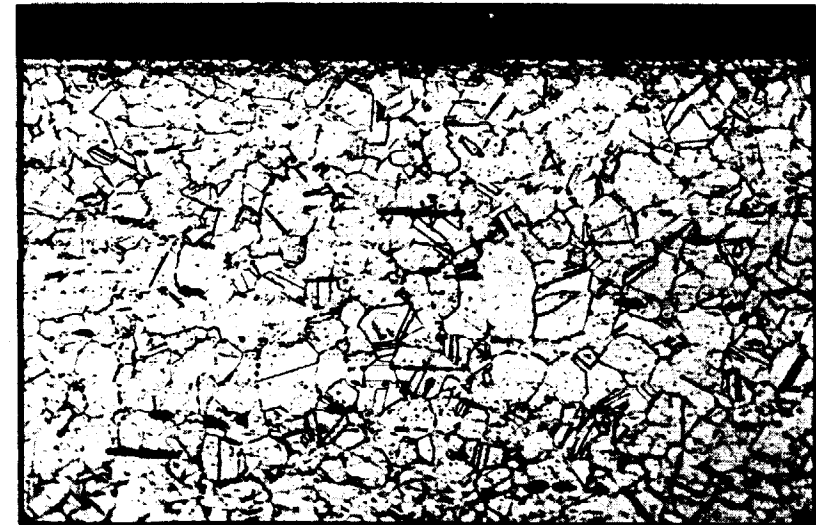
TRANSVERSE ORIENTATION  
MAGNIFICATION: 100X



TRANSVERSE ORIENTATION  
MAGNIFICATION: 250X



LONGITUDINAL ORIENTATION  
MAGNIFICATION: 100X



LONGITUDINAL ORIENTATION  
MAGNIFICATION: 250X

FIGURE 3  
MICROSTRUCTURE OF HASTELLOY X RAWSTOCK STRIP, HEAT 260-5-2813

## Appendix B

general morphology was similar; however, in several cases, the tube samples appeared to have areas of denser carbide precipitation than in the strip samples. Compare Figures 2 and 3. The grain boundaries of the tube samples, in several instances, are exaggerated due to over-etching with oxalic acid.

### b. Hardness Survey

Hardness survey results are listed in Tables I and II. The findings are as follows:

Coolant tube samples (Table I): Hardnesses ranged from KHN 204 to 325 (Rockwell B 90.5 to Rockwell C 32). Hardnesses were generally higher at the tube "crown" areas than at the "leg" areas. Also, samples from the throat radius region had highest hardness due to stretch forming. Hardnesses of the legs were generally consistent in all samples.

Raw stock strip sample (Table II): Hardnesses ranged from KHN 230 to 241 (Rockwell B 96 to 98).

Comparative hardnesses (Tables I and II): Hardness of the strip and the tube samples was essentially equivalent, except that the crown areas of the tube had higher hardnesses. The latter condition is due to cold working in forming of the tubes as noted previously.

### c. Wall Thickness Survey on Coolant Tube

Thickness results are listed in Table III. Thicknesses of the tube specimens were 0.0116 to 0.0124-inch.

### d. Microstructure Examination of Two Welded End-Caps

Microstructures are shown in Figures 4 and 5. Section 6-1 (forward end) had a sound weld joint. Section 7-1 (aft end) had a condition

## Appendix B

TABLE I

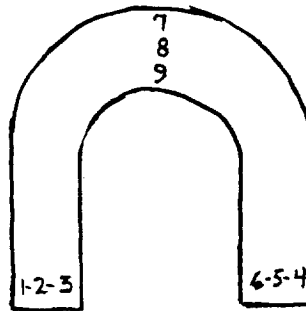
MICRO - HARDNESS SURVEY: AS - FORMED CONDITION ON TUBE SPECIMENS

<u>TUBE SPECIMEN</u>	<u>KNOOP HARDNESS</u>	<u>ROCKWELL HARDNESS (CONVERTED)</u>
1-1	$\frac{1}{229}, \frac{2}{229}, \frac{3}{233}$ (leg)	$R_B \frac{1}{95.5}, \frac{2}{95.5}, \frac{3}{96.5}$
	$\frac{4}{247}, \frac{5}{226}, \frac{6}{217}$ (leg)	$R_B \frac{4}{99}, \frac{5}{95}, \frac{6}{93}$
	$\frac{7}{284}, \frac{8}{224}, \frac{9}{245}$ (crown)	$R_C \frac{7}{26}, \frac{8}{94.5}, \frac{9}{99}$
2-1	$\frac{1}{227}, \frac{2}{230}, \frac{3}{236}$ (leg)	$R_B \frac{1}{95}, \frac{2}{96}, \frac{3}{97}$
	$\frac{4}{229}, \frac{5}{241}, \frac{6}{224}$ (leg)	$R_B \frac{4}{95.5}, \frac{5}{98}, \frac{6}{94.5}$
	$\frac{7}{274}, \frac{8}{271}, \frac{9}{270}$ (crown)	$R_C \frac{7}{24}, R_C \frac{8}{24}, R_C \frac{9}{24}$
3-1	$\frac{1}{245}, \frac{2}{239}, \frac{3}{226}$ (leg)	$R_B \frac{1}{99}, \frac{2}{98}, \frac{3}{95}$
	$\frac{4}{209}, \frac{5}{219}, \frac{6}{235}$ (leg)	$R_B \frac{4}{92}, \frac{5}{93.5}, \frac{6}{97}$
	$\frac{7}{204}, \frac{8}{204}, \frac{9}{204}$ (crown)	$R_B \frac{7}{90.5}, \frac{8}{90.5}, \frac{9}{90.5}$
4-1	$\frac{1}{248}, \frac{2}{239}, \frac{3}{240}$ (leg)	$R_B \frac{1}{99}, \frac{2}{98}, \frac{3}{98}$
	$\frac{4}{237}, \frac{5}{207}, \frac{6}{225}$ (leg)	$R_B \frac{4}{97}, \frac{5}{91}, \frac{6}{95}$
	$\frac{7}{270}, \frac{8}{271}, \frac{9}{282}$ (crown)	$R_C \frac{7}{24}, R_C \frac{8}{24}, R_C \frac{9}{26}$
4A-7	$\frac{1}{238}, \frac{2}{222}, \frac{3}{246}$ (leg)	$R_B \frac{1}{97.5}, \frac{2}{94}, \frac{3}{99}$
	$\frac{4}{216}, \frac{5}{212}, \frac{6}{204}$ (leg)	$R_B \frac{4}{93}, \frac{5}{92}, \frac{6}{90.5}$
	$\frac{7}{321}, \frac{8}{277}, \frac{9}{325}$ (crown)	$R_C \frac{7}{31}, R_C \frac{8}{25}, R_C \frac{9}{32}$

Appendix B

TABLE I (cont.)

<u>TUBE SPECIMEN</u>	<u>KNOOP HARDNESS</u>	<u>ROCKWELL HARDNESS (CONVERTED)</u>
5A-0	$\frac{1}{194}, \frac{2}{204}, \frac{3}{214}$ (leg)	$R_B \frac{1}{88.5}, \frac{2}{90.5}, \frac{3}{92.5}$
	$\frac{4}{218}, \frac{5}{235}, \frac{6}{259}$ (leg)	$R_B \frac{4}{93}, \frac{5}{97}, R_C \frac{6}{22}$
	$\frac{7}{300}, \frac{8}{263}, \frac{9}{290}$ (crown)	$R_C \frac{7}{28}, R_C \frac{8}{22.5}, R_C \frac{9}{27}$





Appendix B

TABLE II

MICRO - HARDNESS SURVEY: AS ANNEALED RAW STOCK STRIP SAMPLE

<u>KNOOP HARDNESS</u>	<u>ROCKWELL B HARDNESS (CONVERTED)</u>
241	98
230	96
230	96
238	97.5
238	97.5
238	97.5

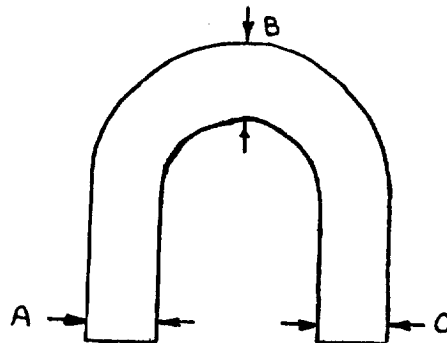
Appendix B

TABLE III

WALL THICKNESS SURVEY: AS - FORMED TUBE CONDITION\*

TUBE SPECIMEN	THICKNESS (INCH)		
	A	B	C
1-1	0.0120	0.0120	0.0120
2-1	0.0120	0.0120	0.0124
3-1	0.0120	0.0120	0.0120
4-1	0.0124	0.0122	0.0120
4A-7	0.0116	0.0122	0.0120
5A-0	0.0116	0.0116	0.0116

\* Thickness measurements taken at areas shown in sketch.



Appendix B

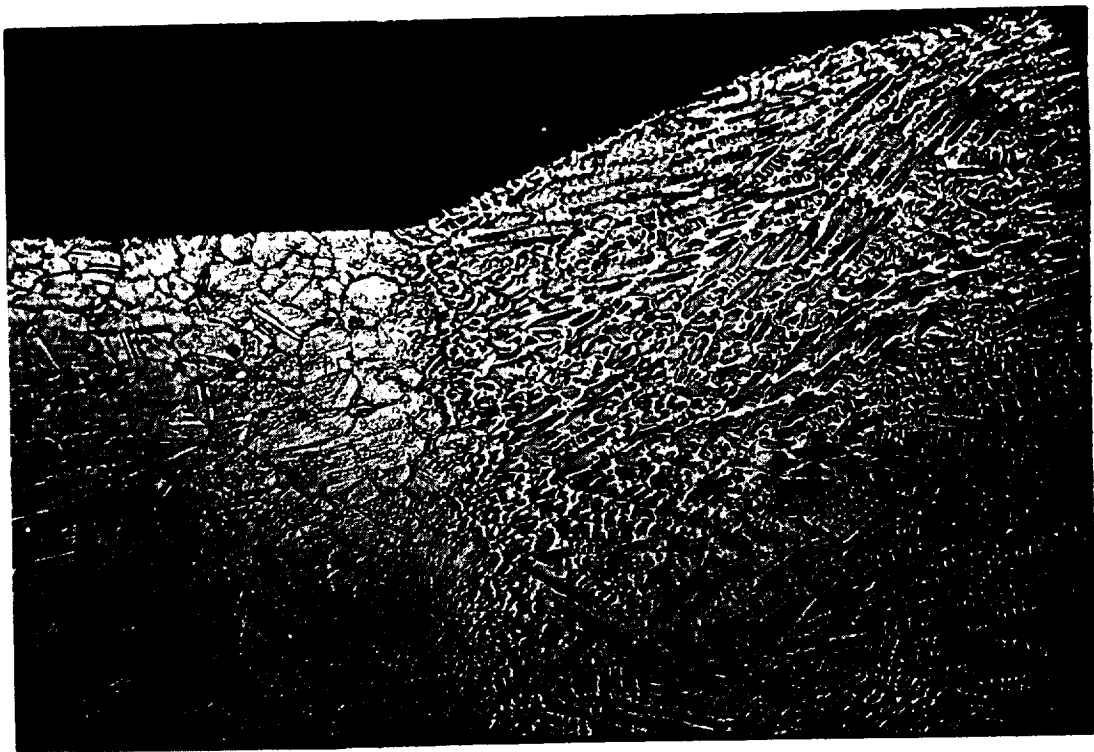
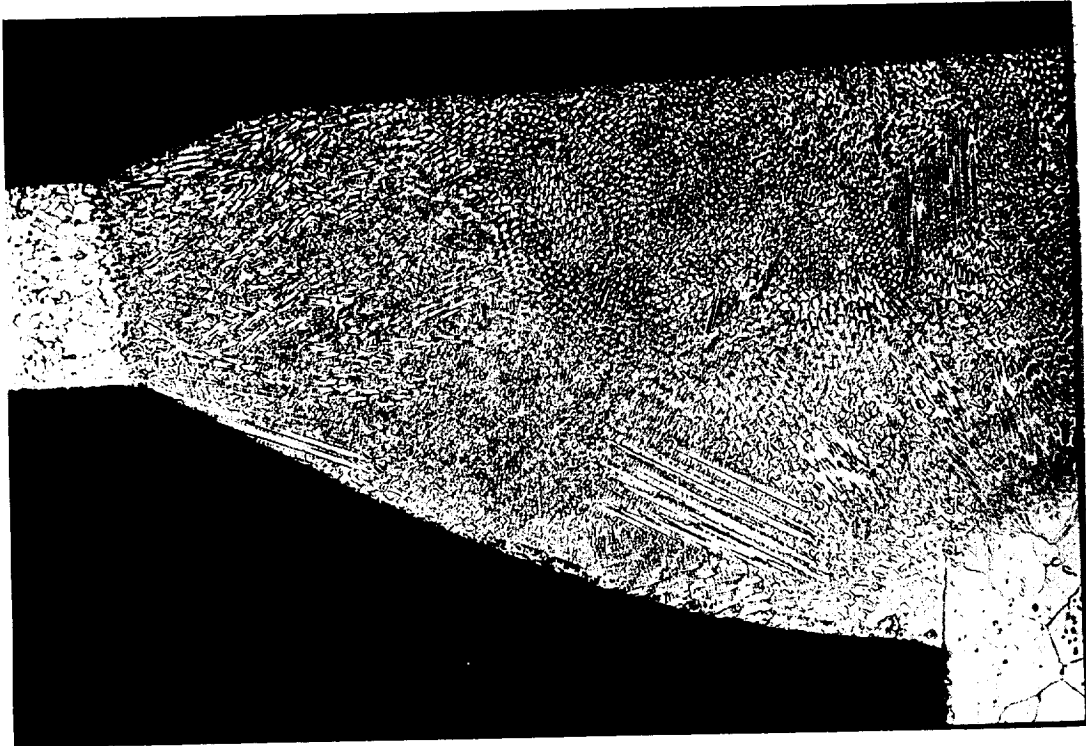


Figure 4 - Microstructure of welded end cap section 6-1 in as-formed condition.  
Etchant: 10% Oxalic, Electrolytic

Mag: 100X upper  
250X lower

Appendix B

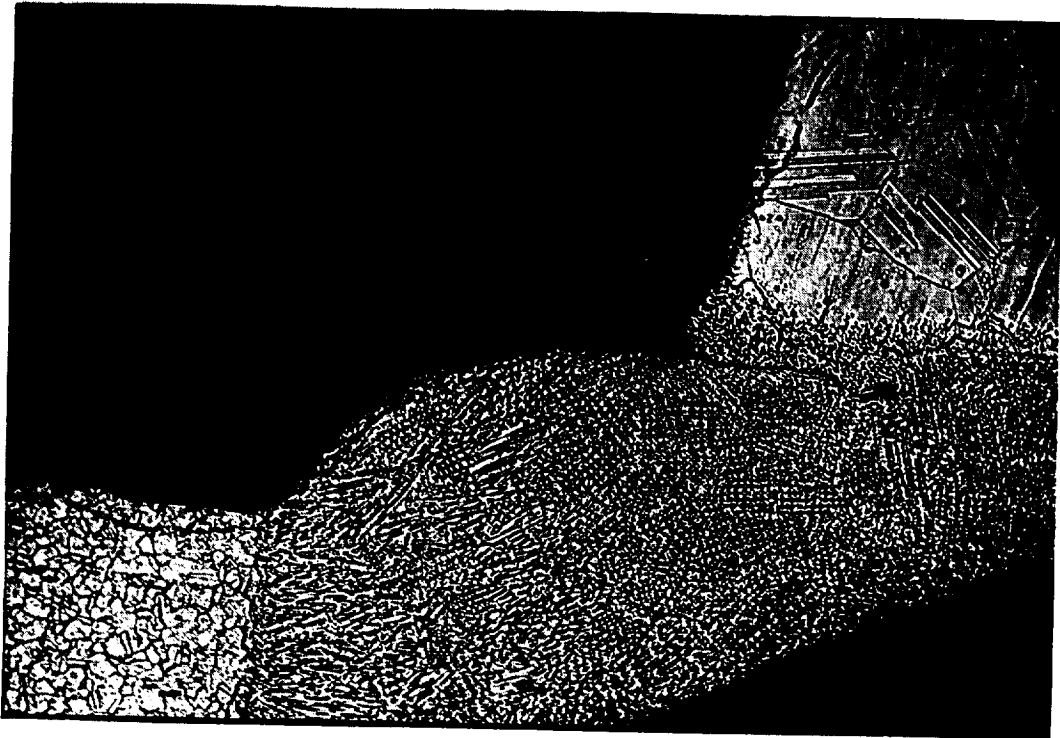


FIGURE 5 - Microstructure of welded end cap section 7-1 in as-formed condition.

Etchant: 10% Oxalic, Electrolytic

Mag: Upper 100X  
Lower 250X

## Appendix B

of metal oxide entrapment at the inner weld area. The oxide entrapment prevented a sound weld being formed during solidification of the weld metal. The discontinuity is not visible externally.

### 2. Phase B - Study of the Effect of a Simulated Braze Cycle on the As-Formed Tube

#### a. Microstructure Examination

Microstructure of the coolant tube sections is shown in Figure 6. The predominant grain size was ASTM No. 7. The grain size ranged from ASTM No. 6 to 8. As compared to the as-formed tube (Figure 2), the braze cycle exposed tube contained a greater amount of the carbide ( $M_6C$ ) precipitate in the matrix and especially at the grain boundaries. The somewhat reduced amount of twinning in the grains indicates an annealing effect.

#### b. Microhardness Survey

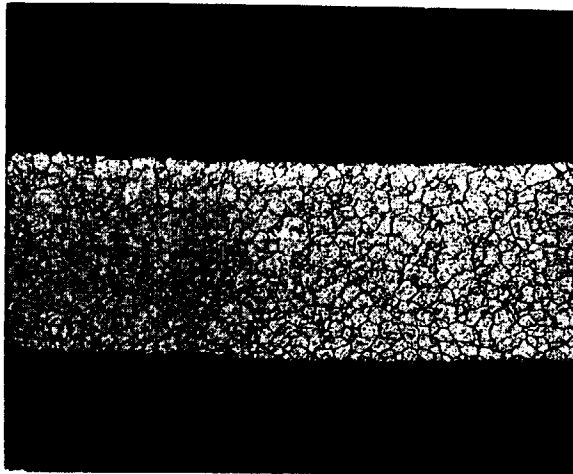
Microhardness survey results are listed in Table IV. Significant findings are listed below:

(a) The simulated braze cycle caused an increase in the hardness of the leg area due to carbide precipitation.

(b) The simulated braze cycle served as a partial stress-relief to reduce the hardness of the crown areas of the tube. Compare hardness results of Tube Sample 4A-7 (as-formed condition) and those of Tube Sample 4A-2 (simulated braze cycle condition).

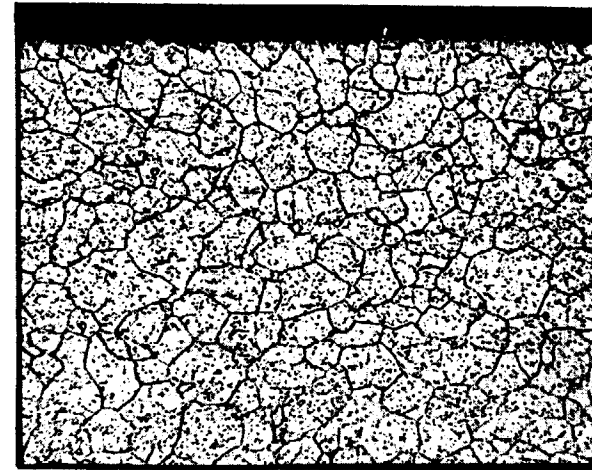
#### c. Microstructure Examination of Two Welded End-Caps (Samples 6-1 and 7-1)

Microstructures are shown in Figures 7 and 8. Both Samples 6-1 (forward end) and 7-1 (aft end) exhibited a sound weld joint. The metal oxide entrapment condition noted previously was an isolated case.



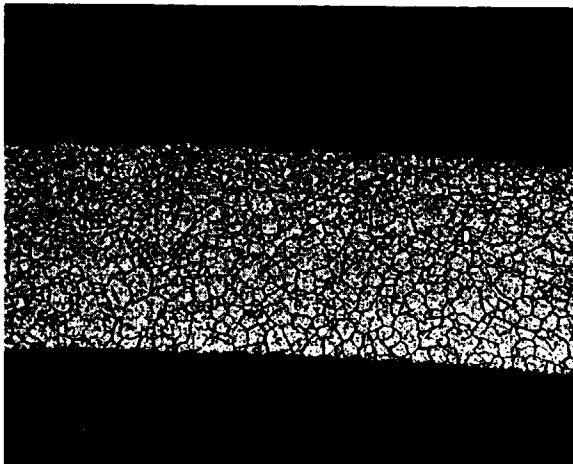
Tube Section 1-2

100X



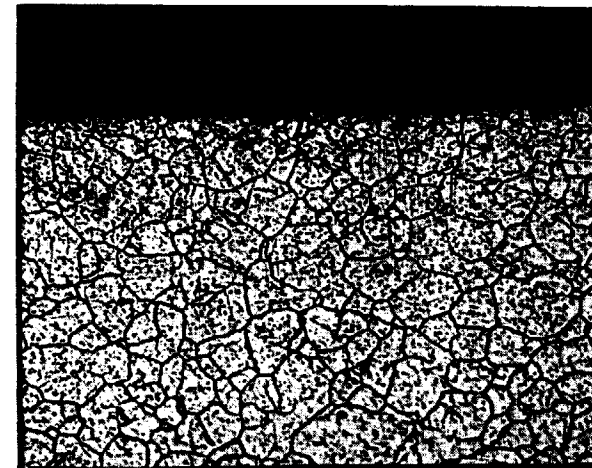
Tube Section 1-2

250X



Tube Section 2-2

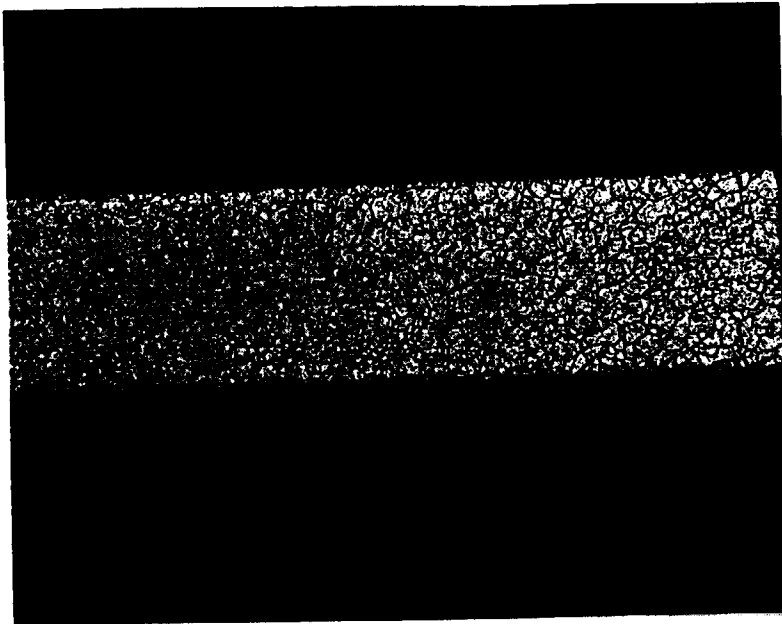
100X



Tube Section 2-2

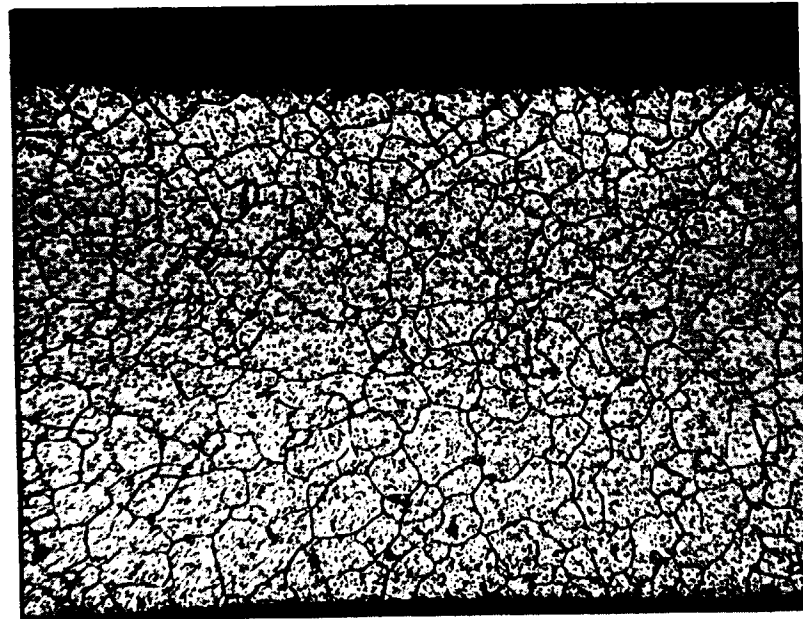
250X

Figure 6A - Microstructure of tube sections after simulated braze cycle  
Etchant 10% Oxalic, Electrolytic



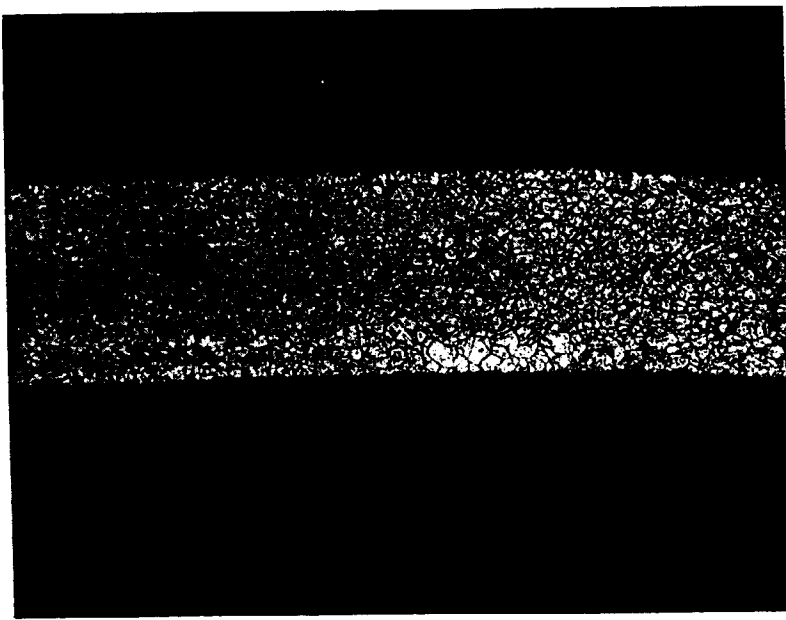
Tube section 3-2

100X



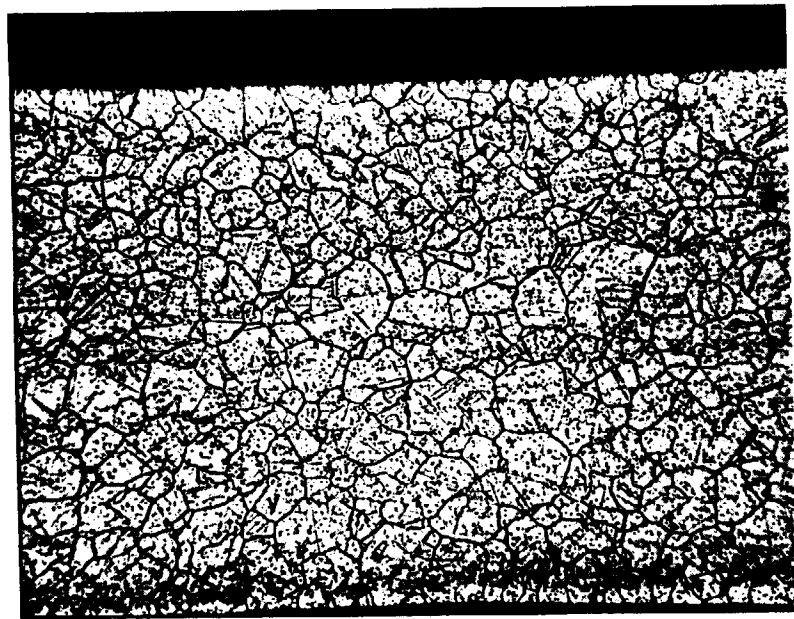
Tube Section 3-2

250X



Tube Section 4-2

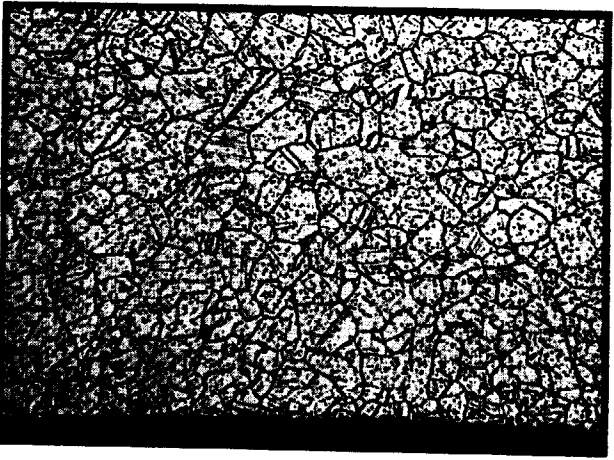
100X



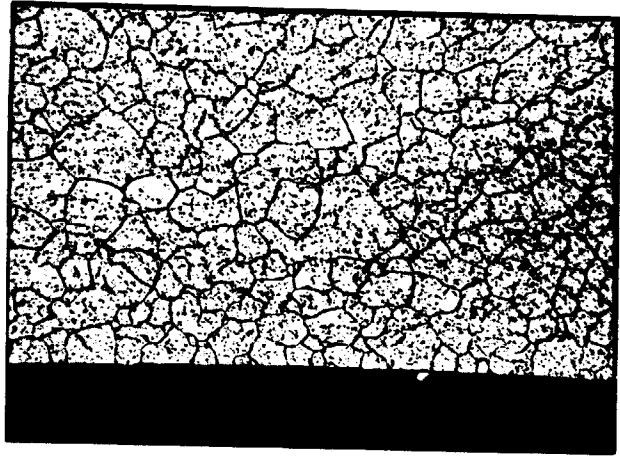
Tube Section 4-2

250X

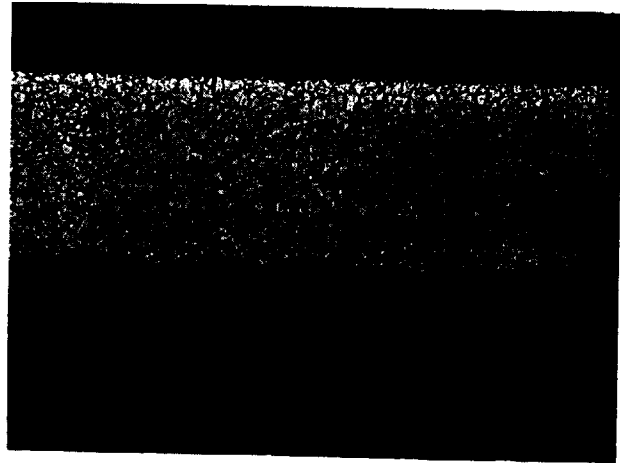
Figure 6B - Microstructure of tube sections after simulated braze cycles.  
Etchant: 10% Oxalic, Electrolytic



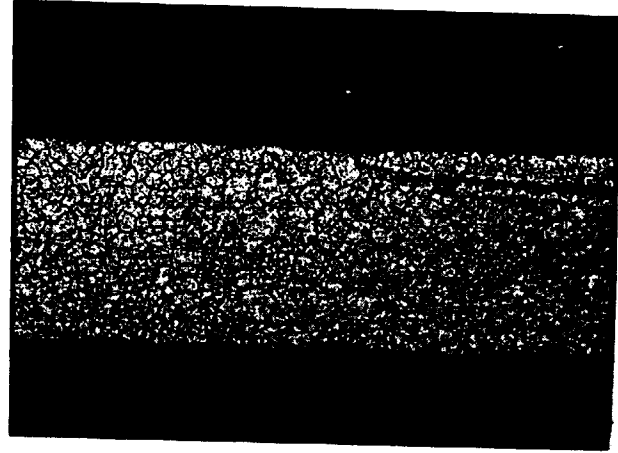
Tube Section 4A-2  
250X



Tube Section 5A-2  
250X



Tube Section 4A-2  
100X



Tube Section 5A-2  
100X

Figure 6C - Microstructure of tube sections after simulated braze cycles.  
Etchant: 10% Oxalic, Electrolytic



## Appendix B

TABLE IV

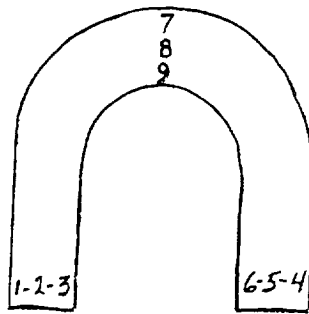
MICRO - HARDNESS SURVEY: SIMULATED BRAZE CYCLE ON AS - FORMED TUBE

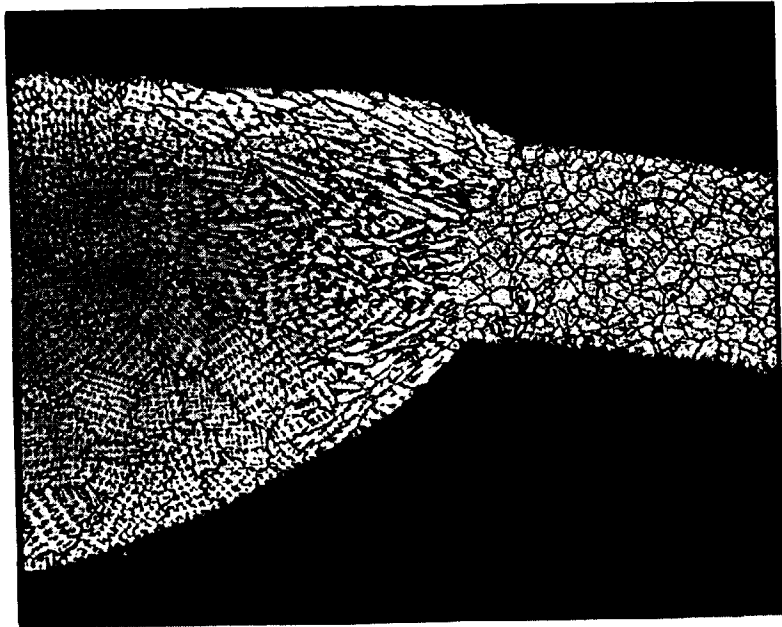
<u>TUBE SPECIMEN</u>	<u>KNOOP HARDNESS</u>	<u>ROCKWELL HARDNESS (CONVERTED)</u>
1-2	$\frac{1}{252}, \frac{2}{266}, \frac{3}{232}$ (leg)	$\frac{1}{R_c 20}, \frac{2}{R_c 23}, \frac{3}{R_B 95}$
	$\frac{4}{248}, \frac{5}{255}, \frac{6}{244}$ (leg)	$\frac{4}{R_B 99}, \frac{5}{R_c 21}, \frac{6}{R_B 99}$
	$\frac{7}{236}, \frac{8}{240}, \frac{9}{240}$ (crown)	$\frac{7}{R_B 97}, \frac{8}{95}, \frac{9}{93}$
2-2	$\frac{1}{287}, \frac{2}{264}, \frac{3}{254}$ (leg)	$\frac{1}{R_c 26.5}, \frac{2}{R_c 23}, \frac{3}{R_c 21}$
	$\frac{4}{305}, \frac{5}{277}, \frac{6}{325}$ (leg)	$\frac{4}{R_c 29}, \frac{5}{R_c 25}, \frac{6}{R_c 32}$
	$\frac{7}{257}, \frac{8}{261}, \frac{9}{265}$ (crown)	$\frac{7}{R_c 21}, \frac{8}{R_c 22}, \frac{9}{R_c 23}$
3-2	$\frac{1}{232}, \frac{2}{238}, \frac{3}{226}$ (leg)	$\frac{1}{R_B 96.5}, \frac{2}{97.5}, \frac{3}{95}$
	$\frac{4}{244}, \frac{5}{238}, \frac{6}{246}$ (leg)	$\frac{4}{R_B 99}, \frac{5}{97.5}, \frac{6}{99}$
	$\frac{7}{251}, \frac{8}{233}, \frac{9}{225}$ (crown)	$\frac{7}{R_c 20}, \frac{8}{R_B 95.5}, \frac{9}{95}$
4-2	$\frac{1}{244}, \frac{2}{247}, \frac{3}{247}$ (leg)	$\frac{1}{R_B 99}, \frac{2}{99}, \frac{3}{99}$
	$\frac{4}{249}, \frac{5}{220}, \frac{6}{261}$ (leg)	$\frac{4}{R_B 99}, \frac{5}{94}, \frac{6}{R_c 22}$
	$\frac{7}{250}, \frac{8}{248}, \frac{9}{238}$ (crown)	$\frac{7}{R_c 20}, \frac{8}{R_B 99}, \frac{9}{97.5}$
4A-2	$\frac{1}{238}, \frac{2}{254}, \frac{3}{233}$ (leg)	$\frac{1}{R_B 97.5}, \frac{2}{R_c 21}, \frac{3}{R_B 96.5}$
	$\frac{4}{245}, \frac{5}{227}, \frac{6}{238}$ (leg)	$\frac{4}{R_B 99}, \frac{5}{95}, \frac{6}{97.5}$
	$\frac{7}{248}, \frac{8}{244}, \frac{9}{220}$ (crown)	$\frac{7}{R_B 99}, \frac{8}{93.5}, \frac{9}{94}$

Appendix B

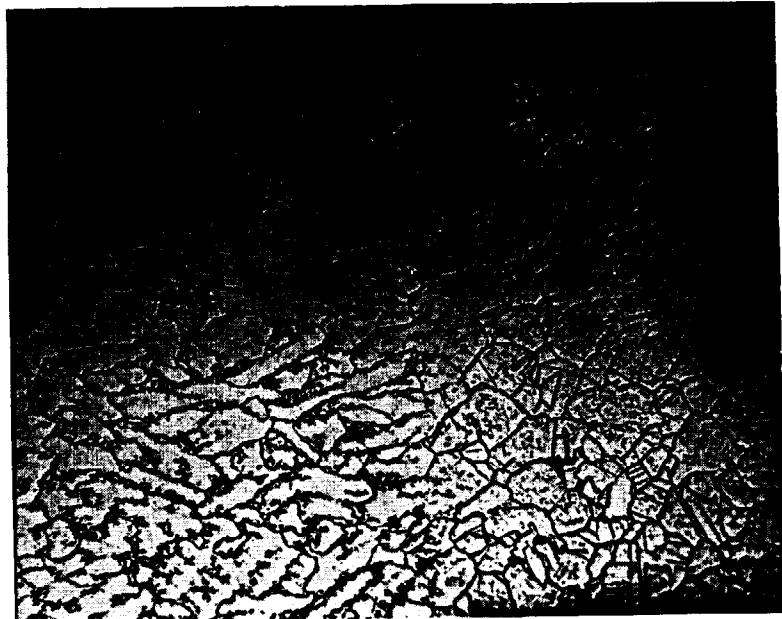
TABLE IV (cont.)

<u>TUBE SPECIMEN</u>	<u>KNOOP HARDNESS</u>	<u>ROCKWELL HARDNESS (CONVERTED)</u>
5A-2	$\frac{1}{242}, \frac{2}{248}, \frac{3}{250}$ (leg)	$\frac{1}{R_B 98}, \frac{2}{99}, \frac{3}{99}$
	$\frac{4}{268}, \frac{5}{220}, \frac{6}{222}$ (leg)	$\frac{4}{R_C 23}, \frac{5}{R_B 94}, \frac{6}{94}$
	$\frac{7}{290}, \frac{8}{221}, \frac{9}{274}$ (crown)	$\frac{7}{R_C 27}, \frac{8}{R_B 94}, \frac{9}{R_C 24}$



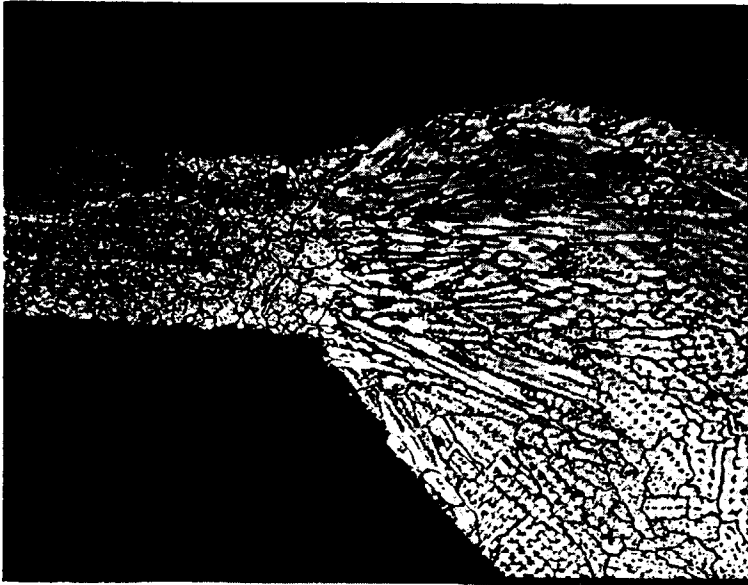


100X

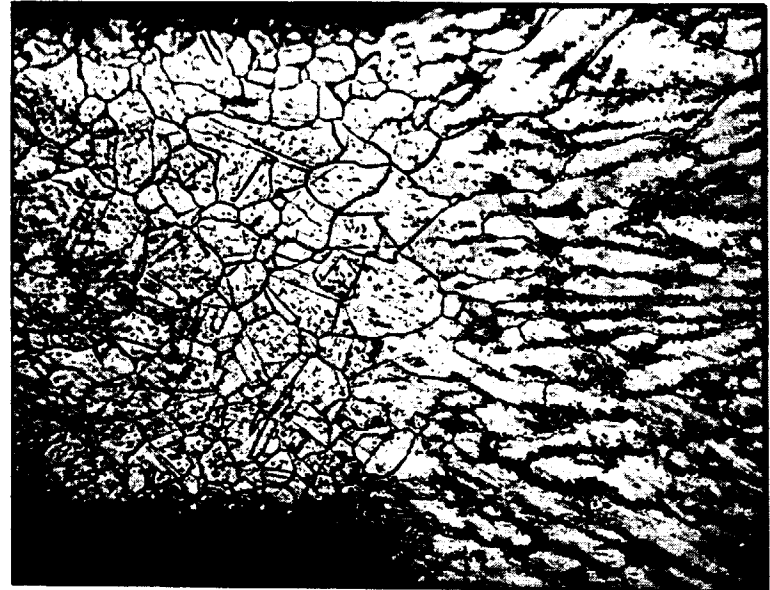


250X

Figure 7 - Microstructure of welded end cap section 6-2 after simulated braze cycle.  
Etchant: 10% Oxalic, Electrolytic



100X



250X

Figure 8 - Microstructure of welded end cap section 7-2 after simulated braze cycle.  
Etchant: 10% Oxalic, Electrolytic

## Appendix B

### d. Wall Thickness Survey on Coolant Tube

Wall thickness survey results are listed in Table V. Thicknesses ranged from 0.0114-inch to 0.0128-inch.

### 3. Phase C - Study of the Effect of an Annealing Cycle and Annealing Plus Simulated Braze Cycle on the As-Formed Tube

#### a. Effect of Annealing Cycles on Tube Dimensions

The "H" and "ID" dimensions of the U-tube samples before and after the 1925°F/5 minute and 1925°F/15 minute anneals are shown in Figure 9. The annealing cycles caused no significant change in the tube dimensions. The only major difference was noted in one ID dimension (Specimen 3-4) wherein the maximum variation was about 0.011-inch.

#### b. Microstructure

Microstructures of the coolant tube sections are shown in Figure 10. Significant observations are listed below:

The annealed and annealed plus brazed cycle treated samples contained a smaller amount of the precipitated carbide phase ( $M_6C$ ) at the grain boundaries than the direct braze cycle treated samples. Compare Figures 6 and 10.

There was no significant grain size difference among the annealed, the brazed, the annealed plus simulated brazed cycle, and the as-formed tube samples. Compare Figures 2, 6, and 10.

Almost complete removal of grain twinning has occurred.

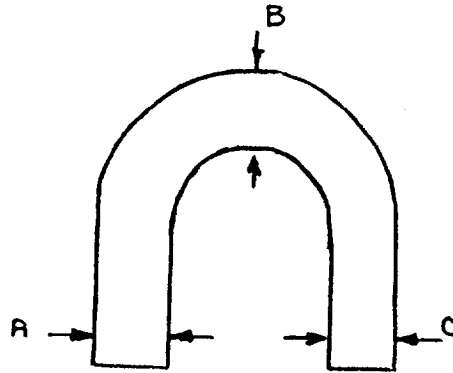
Appendix B

TABLE V

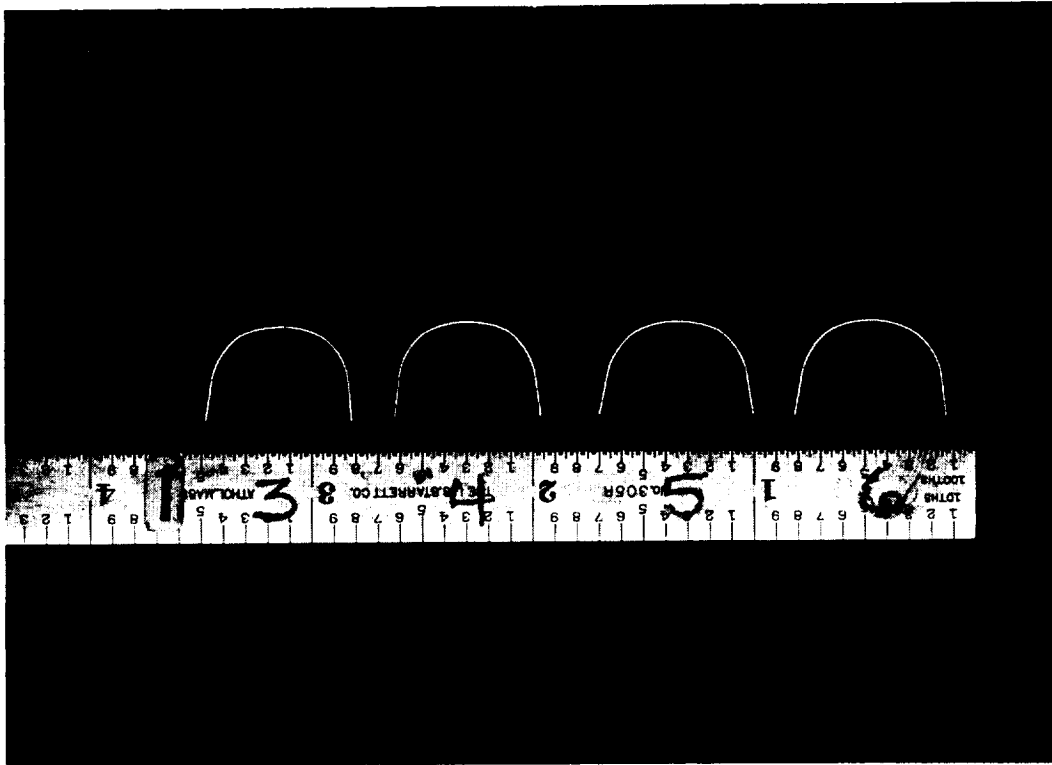
WALL THICKNESS SURVEY: AS - FORMED TUBE + SIMULATED BRAZE CYCLE CONDITION\*

TUBE SPECIMEN	THICKNESS (INCH)		
	A	B	C
1-2	0.0128	0.0120	0.0124
2-2	0.0122	0.0120	0.0126
3-2	0.0120	0.0122	0.0126
4-2	0.0120	0.0120	0.0124
4A-2	0.0116	0.0120	0.0118
5A-2	0.0120	0.0124	0.0114

\*Thickness measurements taken at areas shown in sketch.



Appendix B



<u>SPECIMEN</u>	<u>ANNEAL CYCLE</u>	<u>MEASUREMENT BEFORE</u>		<u>MEASUREMENT AFTER</u>	
		H	ID	H	ID
1-3	1925°F/5 min.	0.430	0.656	0.430	0.656
1-4	1925°F/5 min.	0.431	0.658	0.430	0.657
1-5	1925°F/5 min.	0.425	0.693	0.427	0.693
1-6	1925°F/5 min.	0.428	0.675	0.428	0.674

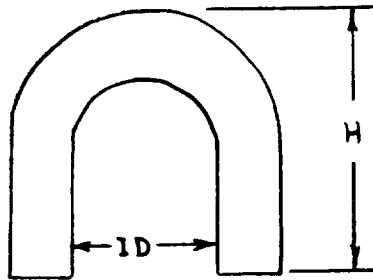
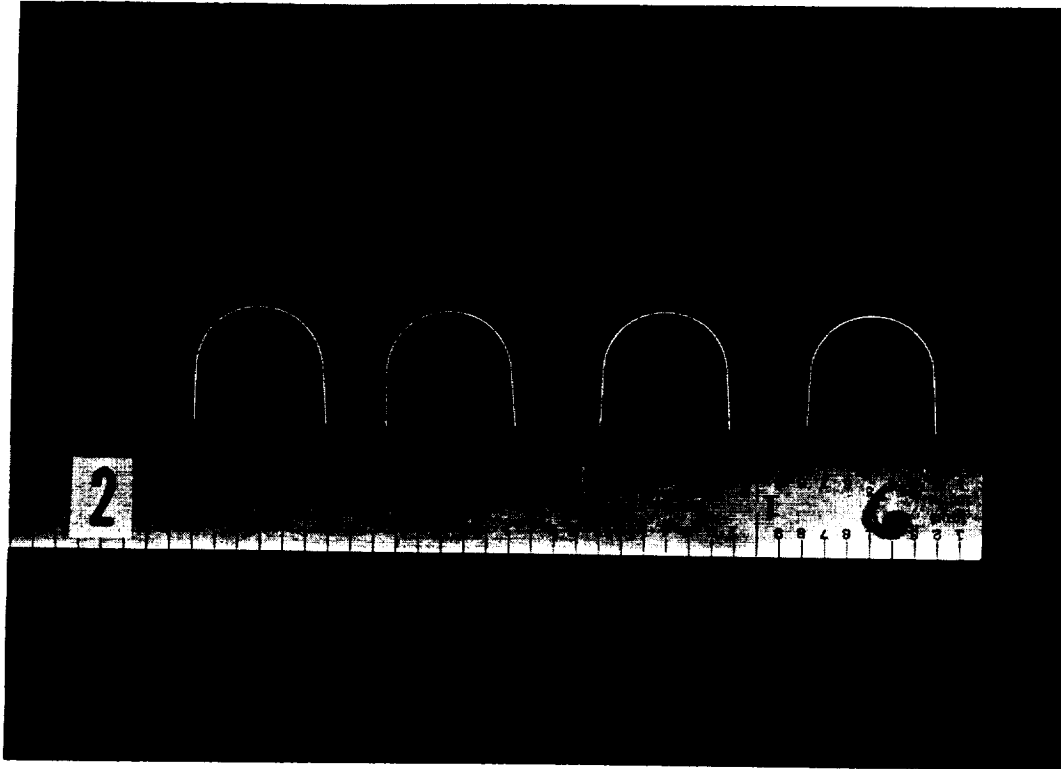


FIGURE 9A - EFFECT OF ANNEALING CYCLES ON TUBE DIMENSIONS (CROSS SECTION LOCATION).

Appendix B



<u>SPECIMEN</u>	<u>ANNEAL CYCLE</u>	MEASUREMENT BEFORE		MEASUREMENT AFTER	
		<u>H</u>	<u>ID</u>	<u>H</u>	<u>ID</u>
2-3	1925°F/5 min.	0.508	0.582	0.510	0.577
2-4	1925°F/5 min.	0.516	0.570	0.516	0.569
2-5	1925°F/5 min.	0.516	0.570	0.517	0.569
2-6	1925°F/5 min.	0.512	0.572	0.514	0.567

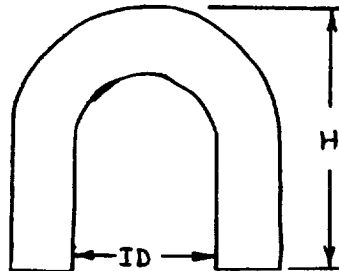
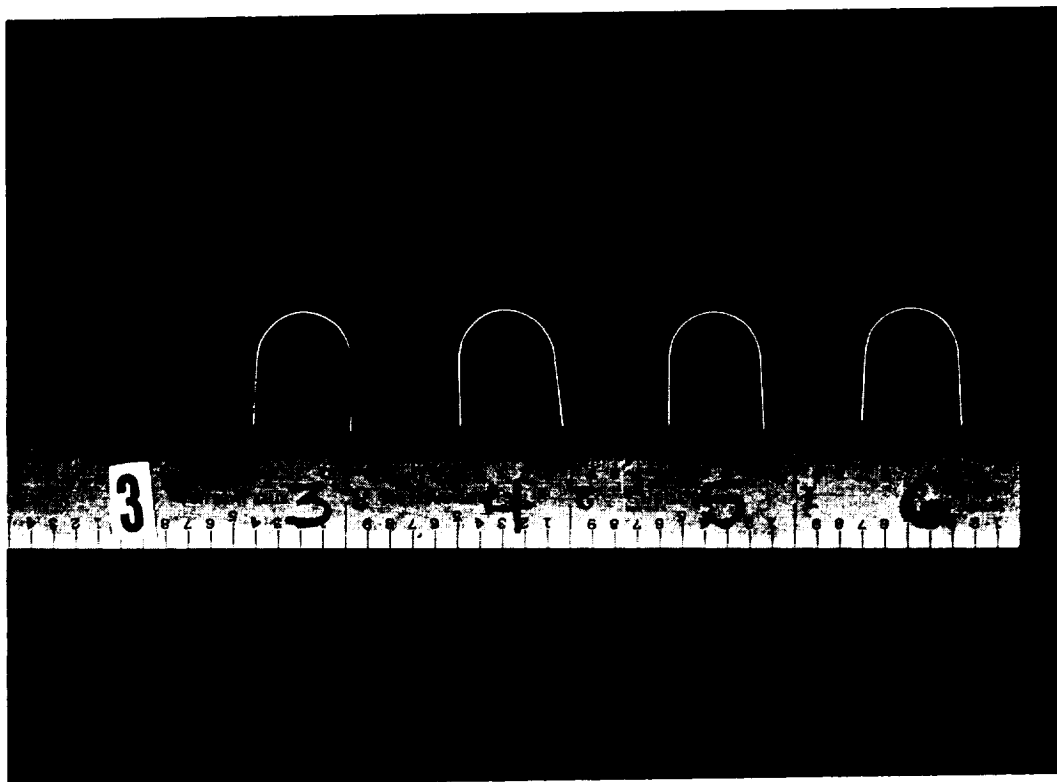


FIGURE 9B - EFFECT OF ANNEALING CYCLES ON TUBE DIMENSIONS (CROSS SECTION LOCATION)



Appendix B



SPECIMEN	ANNEAL CYCLE	<u>MEASUREMENT</u> <u>BEFORE</u>		<u>MEASUREMENT</u> <u>AFTER</u>	
		<u>H</u>	<u>ID</u>	<u>H</u>	<u>ID</u>
3-3	1925°F/5 min.	0.519	0.432	0.519	0.433
3-4	1925°F/5 min.	0.519	0.420	0.518	0.431
3-5	1925°F/5 min.	0.516	0.415	0.516	0.419
3-6	1925°F/5 min.	0.512	0.430	0.512	0.431

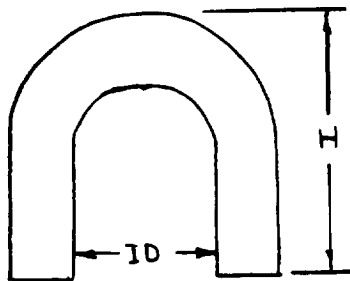
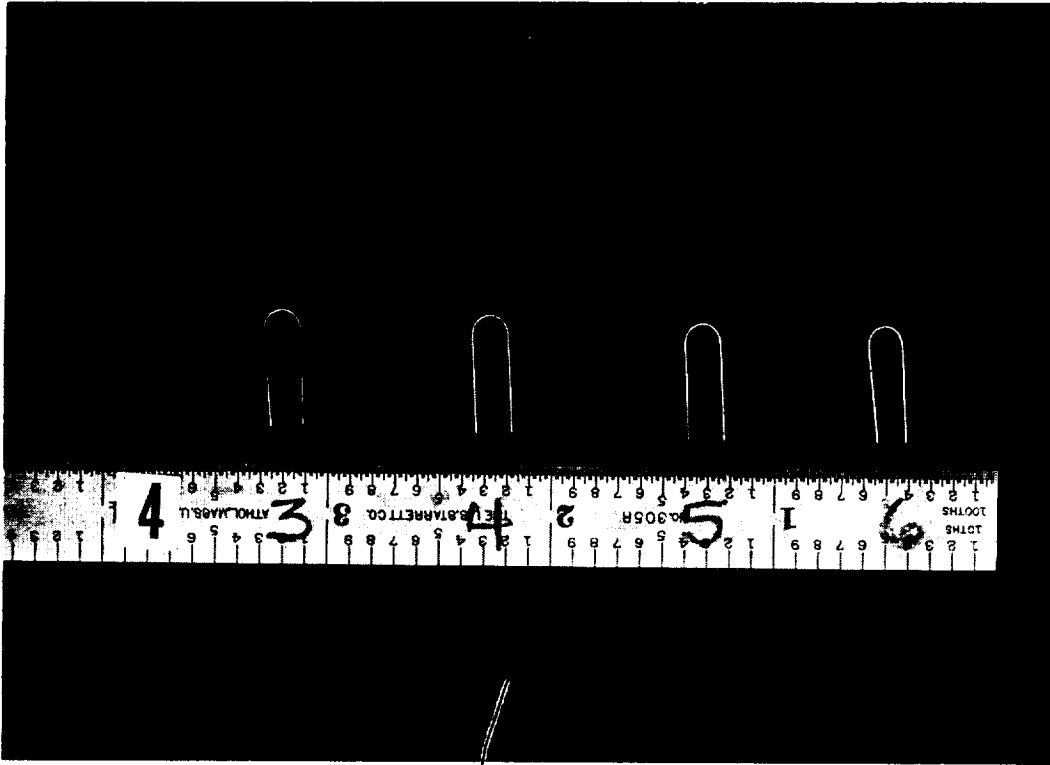


FIGURE 9C - EFFECT OF ANNEALING CYCLES ON TUBE DIMENSIONS (CROSS SECTION LOCATION).

Appendix B



SPECIMEN	ANNEAL CYCLE	MEASUREMENT BEFORE		MEASUREMENT AFTER	
		H	ID	H	ID
4-3	1925°F/5 min.	0.520	0.153	0.520	0.146
4-4	1925°F/5 min.	0.523	0.160	0.524	0.160
4-5	1925°F/5 min.	0.527	0.148	0.528	0.148
4-6	1925°F/5 min.	0.528	0.107	0.529	0.108

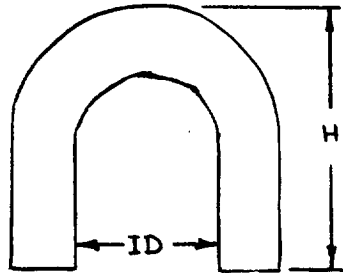
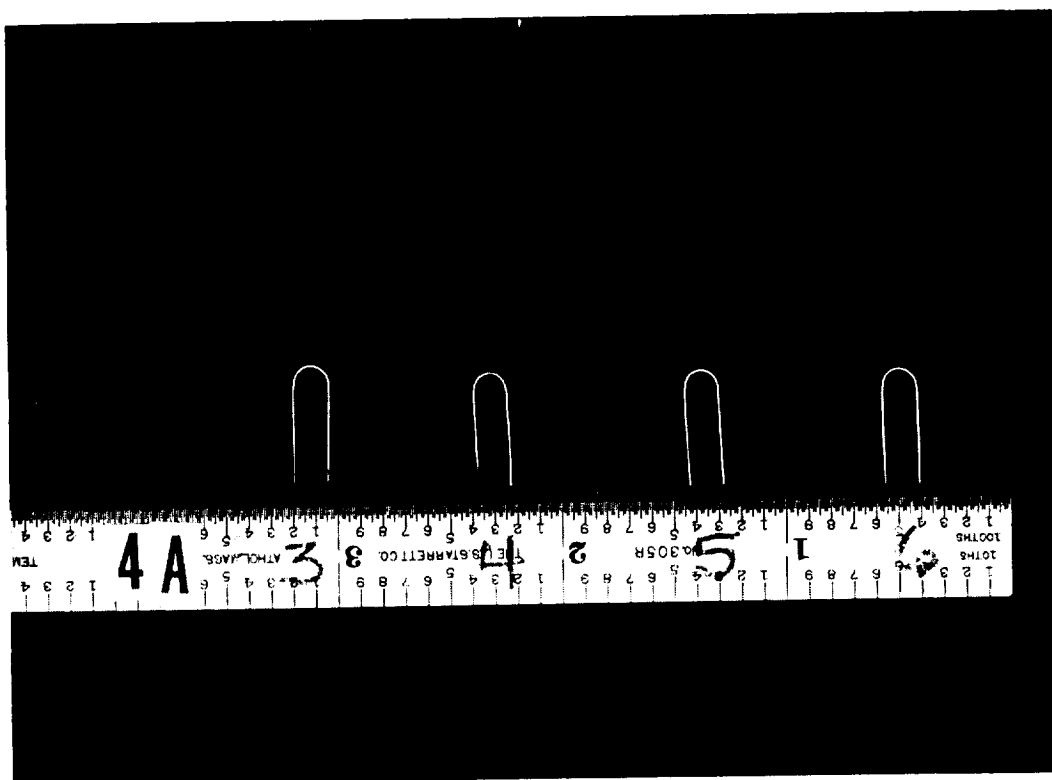


FIGURE 9D - EFFECT OF ANNEALING CYCLES ON TUBE DIMENSIONS (CROSS SECTION LOCATION).

Appendix B



<u>SPECIMEN</u>	<u>ANNEAL CYCLE</u>	<u>MEASUREMENT BEFORE</u>		<u>MEASUREMENT AFTER</u>	
		<u>H</u>	<u>ID</u>	<u>H</u>	<u>ID</u>
4A-3	1925°F/5 min.	0.525	0.150	0.526	0.148
4A-4	1925°F/5 min.	0.518	0.135	0.519	0.135
4A-5	1925°F/5 min.	0.523	0.149	0.524	0.150
4A-6	1925°F/5 min.	0.525	0.146	0.526	0.146

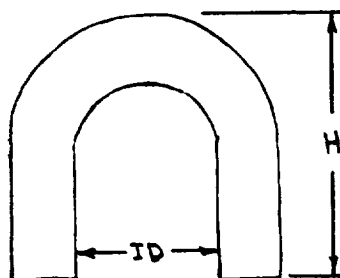
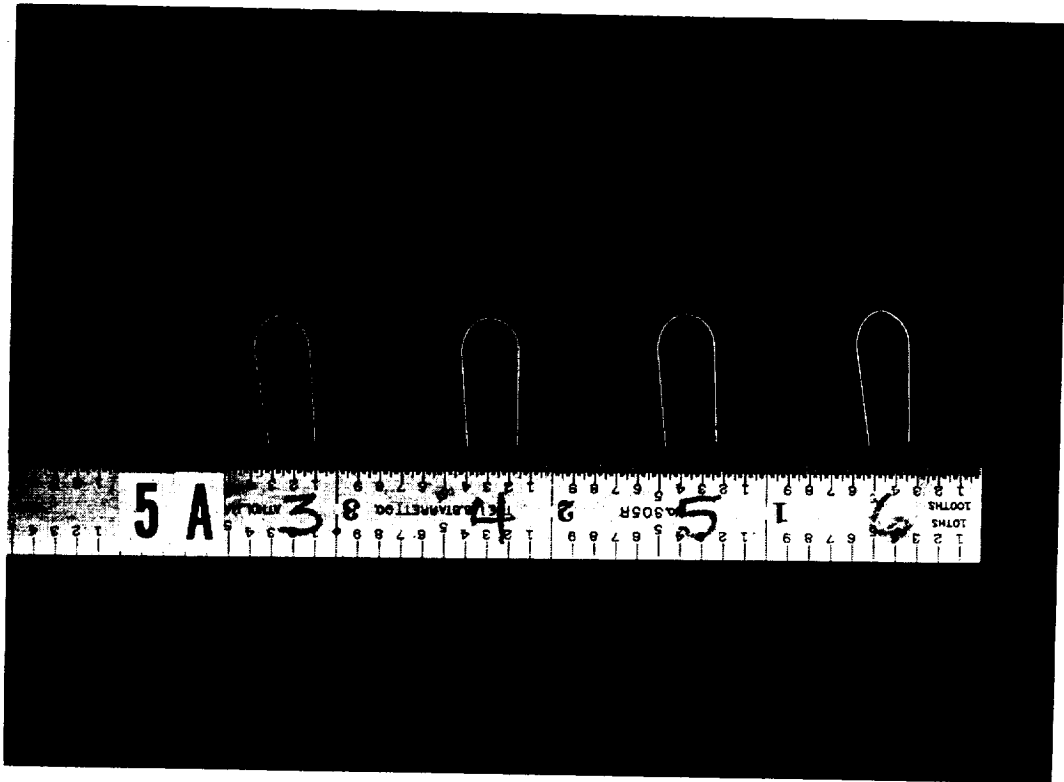


FIGURE 9E - EFFECT OF ANNEALING CYCLES ON TUBE DIMENSIONS (CROSS SECTION LOCATION).

Appendix B



<u>SPECIMEN</u>	<u>ANNEAL CYCLE</u>	<u>MEASUREMENT BEFORE</u>		<u>MEASUREMENT AFTER</u>	
		<u>H</u>	<u>ID</u>	<u>H</u>	<u>ID</u>
5A-3	1925°F/5 min.	0.600	0.210	0.600	0.208
5A-4	1925°F/5 min.	0.606	0.225	0.606	0.224
5A-5	1925°F/5 min.	0.608	0.225	0.610	0.225
5A-6	1925°F/5 min.	0.618	0.193	0.618	0.187

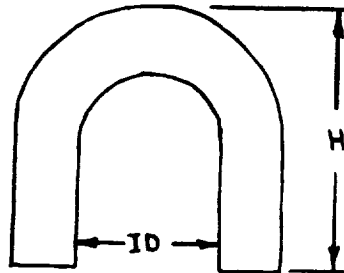
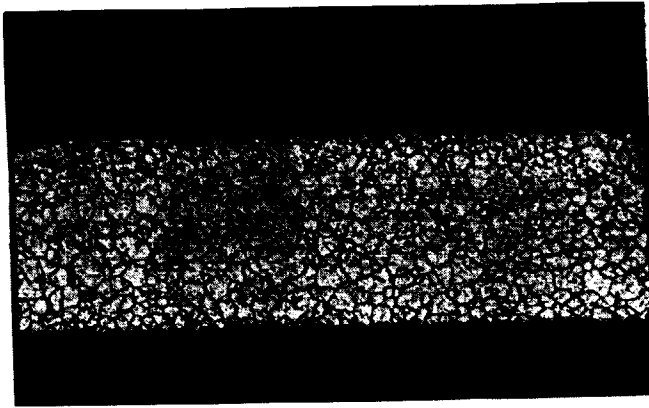
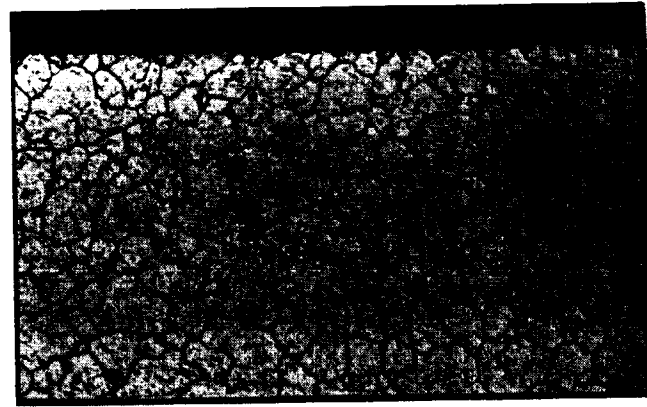


FIGURE 9F - EFFECT OF ANNEALING CYCLES ON TUBE DIMENSIONS (CROSS SECTION LOCATION).



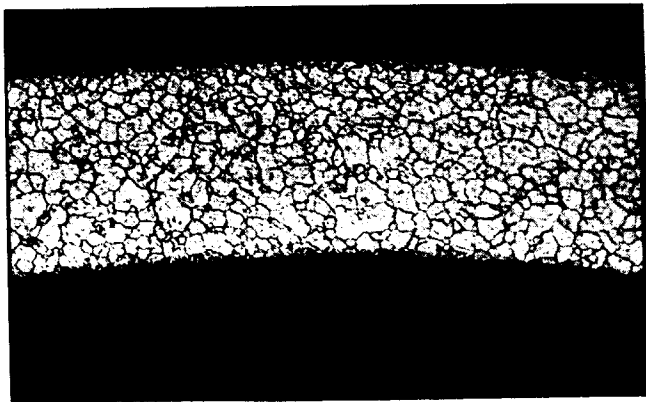
Tube Section 1-3  
Annealed 5 min @ 1925°F

100X



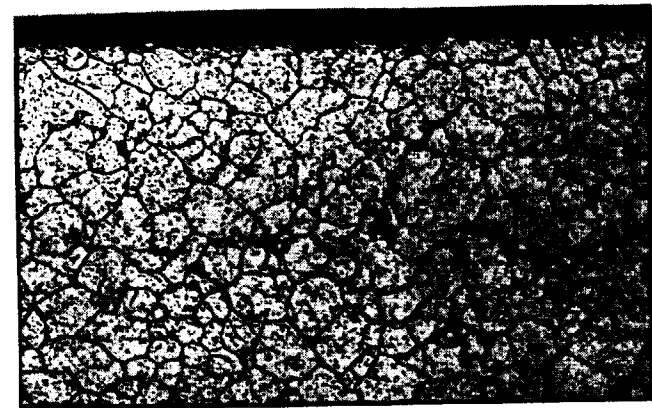
Tube Section  
Annealed 5 min @ 1925°F

250X



Tube Section 1-  
Annealed 5 min @ 1925°F + Braze Cycle

100X

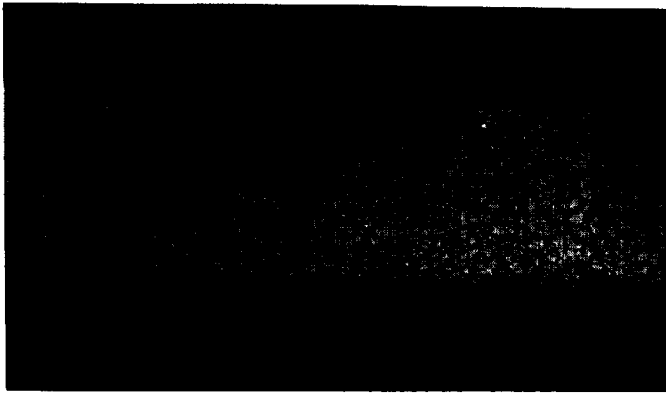


Tube Section 1-4  
Annealed 5 min @ 1925°F + Braze Cycle

250X

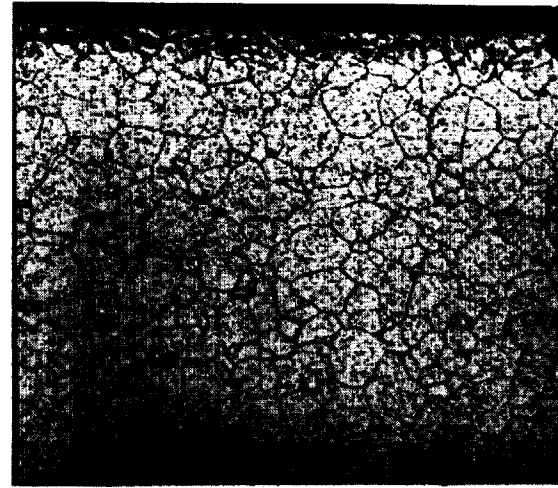
FIGURE 10A - Microstructure of tube sections 1-3 and 1-4 in the annealed and annealed plus simulated braze conditions.

Etchant: 10% Oxalic, Electrolytic



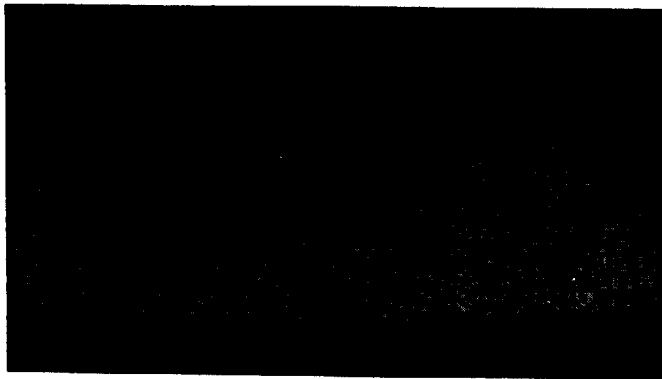
Tube Section 1-5  
Annealed 15 min @ 1925°F

100X



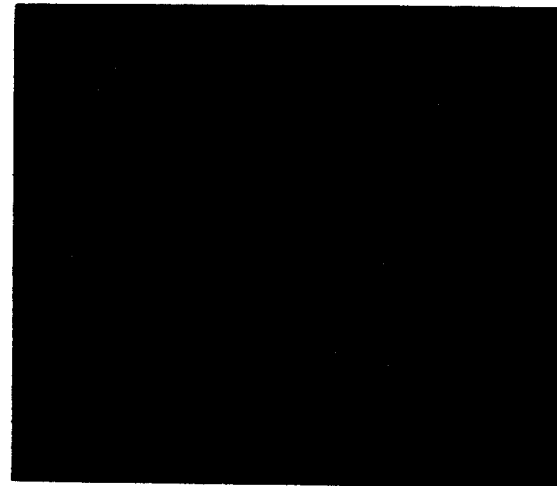
Tube Section 1-5

250X



Tube Section 1-6  
Annealed 15 min @ 1925°F + Braze Cycle

100X

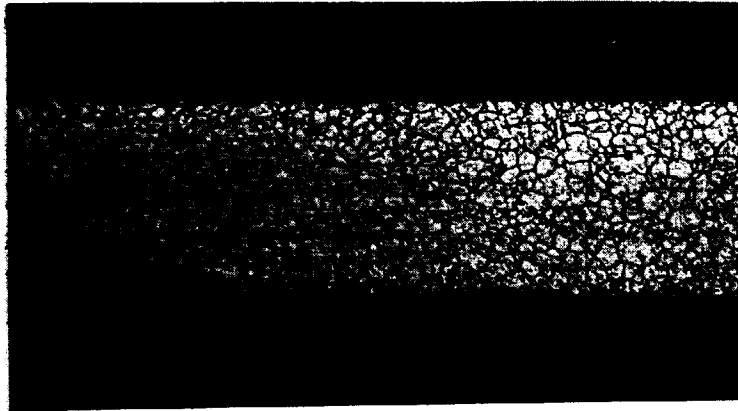


Tube Section 1-6

250X

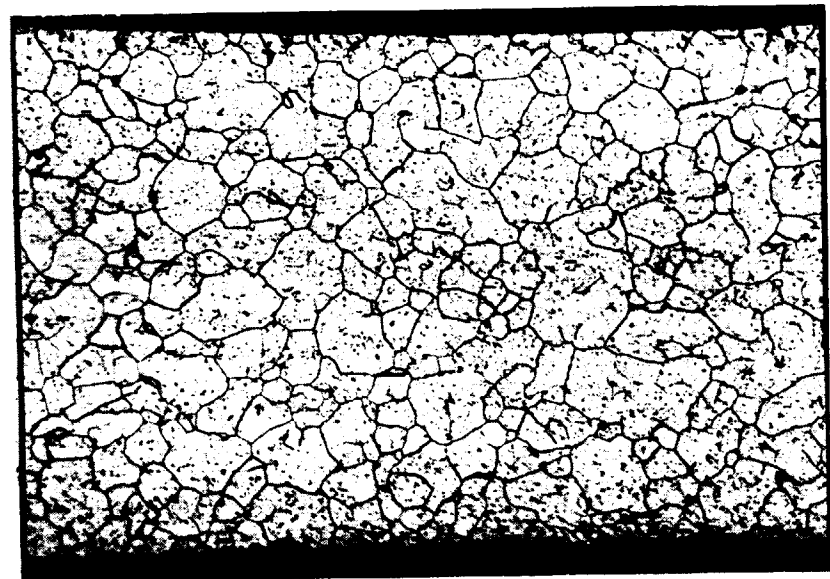
FIGURE 10B - Microstructure of tube sections 1-5 and 1-6 in the annealed and annealed plus simulated braze conditions.

Etchant: 10% Oxalic, Electrolytic



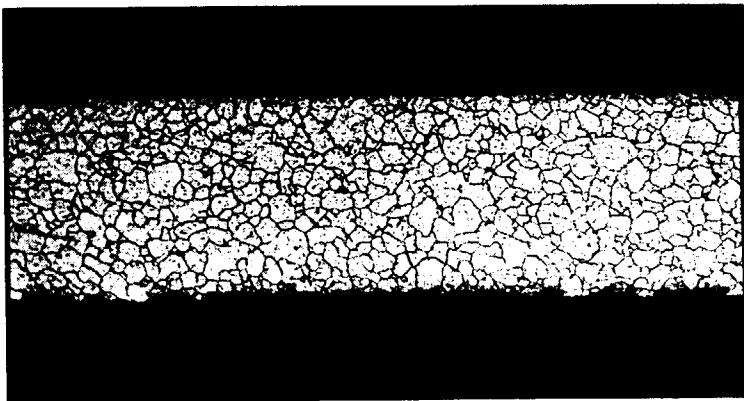
Tube Section 4-3  
Annealed 5 min @ 1925°F

100X



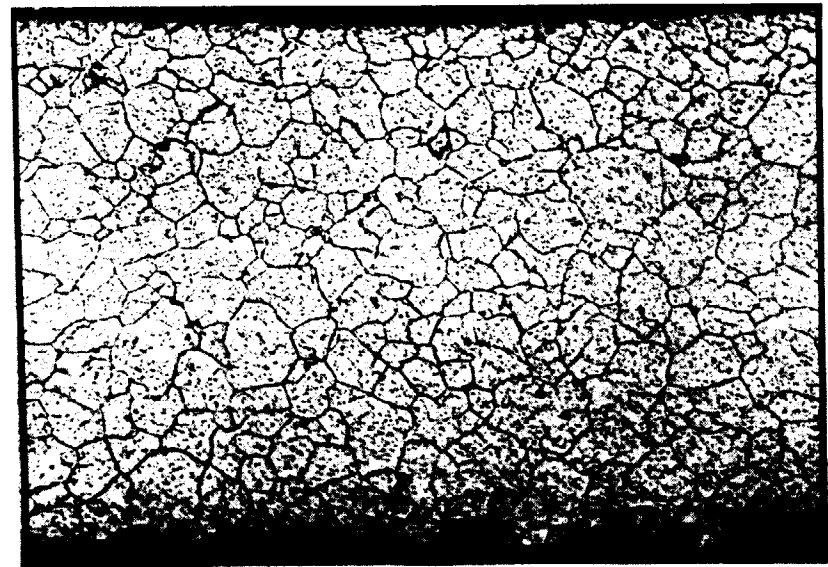
Tube Section 4-3

250X



Tube Section 4-4  
Annealed 5 min @ 1925°F + Braze Cycle

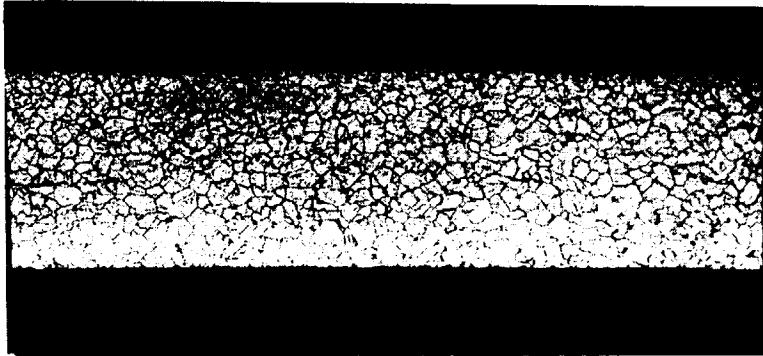
100X



Tube Section 4-4

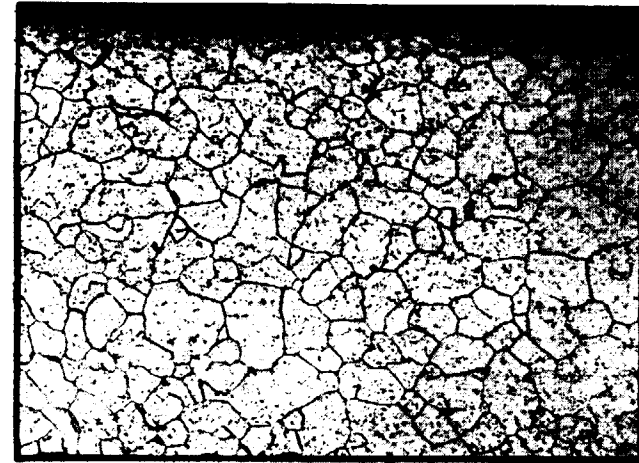
250X

Figure 10C - Microstructure of tube sections 4-3 and 4-4 in the annealed and annealed plus simulated braze conditions.  
Etchant: 10% Oxalic, Electrolytic



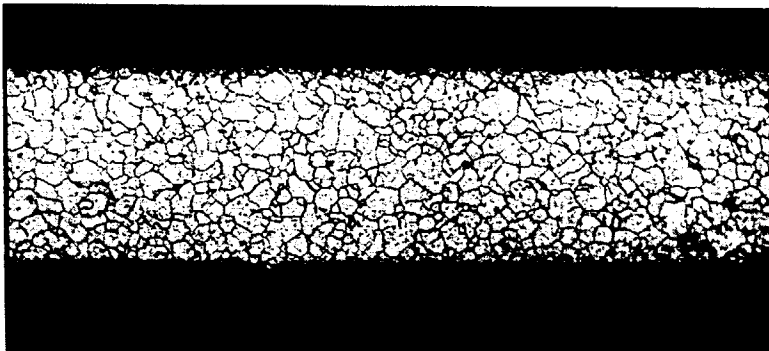
Tube Section 4-5  
Annealed 15 min @ 1925°F

100X



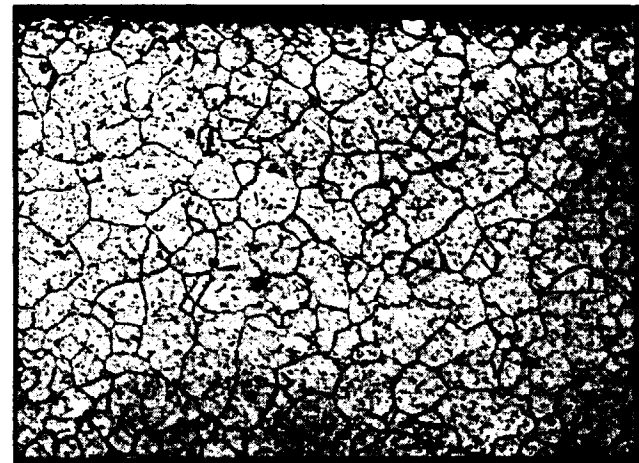
Tube Section 4-5

250X



Tube Section 4-6  
Annealed 15 min @ 1925°F + Braze Cycle

100X



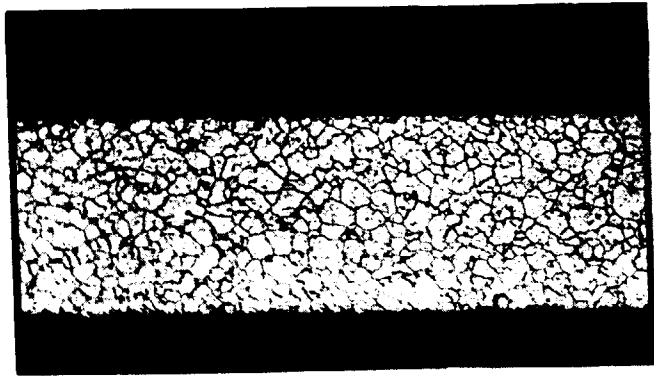
Tube Section 4-6

250X

Figure 10D - Microstructure of tube sections 4-5 and 4-6 in the annealed and annealed plus simulated braze conditions.

Etchant: 10% Oxalic, Electrolytic





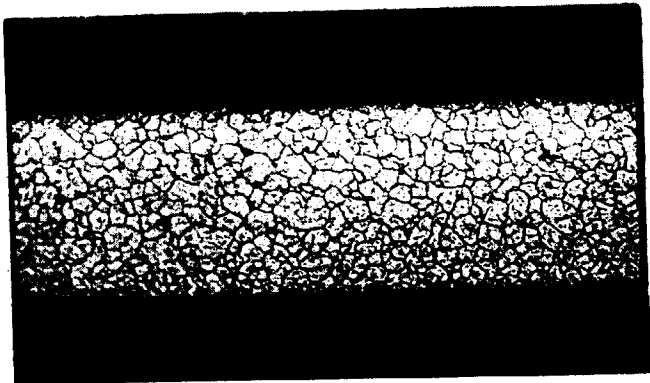
Tube Section 5A-3  
Annealed 5 min @ 1925°F

100X



Tube Section 5A-3  
Annealed 5 min @ 1925°F

250X



Tube Section 5A-4  
Annealed 5 min @ 1925°F + Braze Cycle

100X

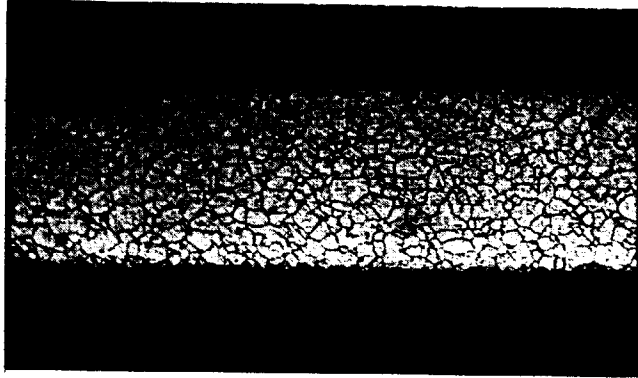


Tube Section 5A-4  
Annealed 5 min @ 1925°F + Braze Cycle

250X

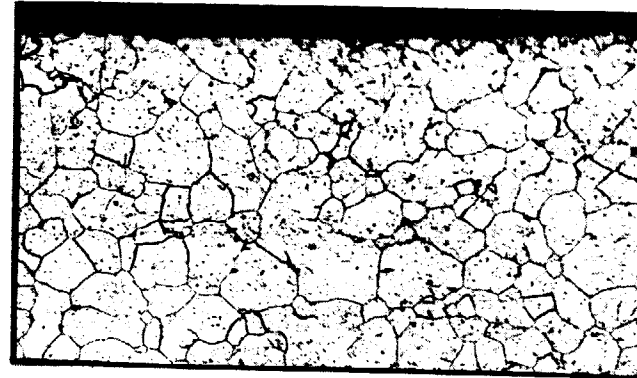
Figure 10E - Microstructure of tube sections 5A-3 and 5A-4 in the annealed and annealed plus simulated braze conditions.

Etchant: 10% Oxalic, Electrolytic



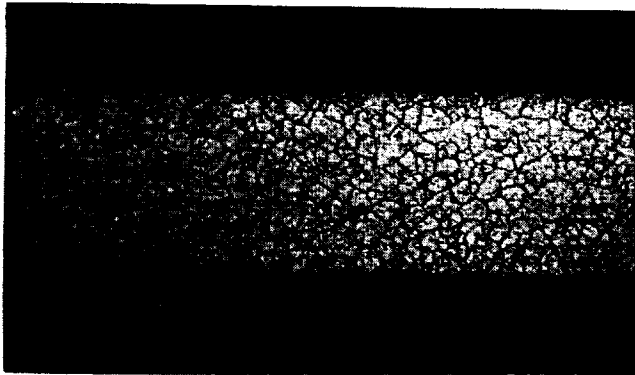
Tube Section 5A-5  
Annealed 15 min @ 1925°F

100X



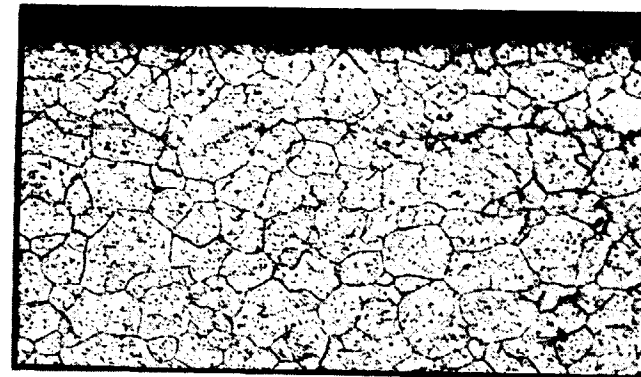
Tube Section 5A-5  
Annealed 15 min @ 1925°F

250X



Tube Section 5A-6  
Annealed 15 min @ 1925°F + Braze Cycle

100X



Tube Section 5A-6  
Annealed 15 min @ 1925°F + Braze Cycle

250X

Figure 10F - Microstructure of tube sections 5A-5 and 5A-6 in the annealed and annealed plus simulated braze conditions.  
Etchant: 10% Oxalic, Electrolytic

## Appendix B

### c. Hardness Survey

Hardness survey results are listed in Tables VI through IX. Significant findings are listed below:

As compared to the tube samples in the as-formed condition (Table I), the 1925°F/5 minute annealed and 1925°F/15 minute annealed tube samples had higher hardness.

As compared to the tube samples in the simulated brazed condition (Table IV), the 1925°F/5 minute annealed and 1925°F/15 minute annealed tube samples had slightly higher hardness.

No significant hardness differences were noted at the crown and leg areas of tube samples which had been subjected to the anneal cycles. The anneal cycles served to promote uniformity of hardness (equalization) by stress relief with a concomitant increase in hardness by a precipitation age hardening reaction.

#### 4. Hardness Results Summary

The average Knoop microhardness values for the various tube locations and for the leg and crown areas are summarized in Table X. In addition to the changes in hardness with the thermal cycle and location in the tube, the variation in total spread of the hardness values is also apparent from these data. Notice that the great variation in the as-formed crown areas, 102 Knoop, reduced to a more consistent value after the thermal treatments. The narrow spread for the original stock is reflected also in the as-formed leg values, but following the thermal treatments the leg hardness variation increased to within the approximate same spread limits as the heat treated crown values. The effects of the braze cycle and the 1925°F treatments produced a stress relieved material that responded to precipitation quite uniformly.

## Appendix B

TABLE VI

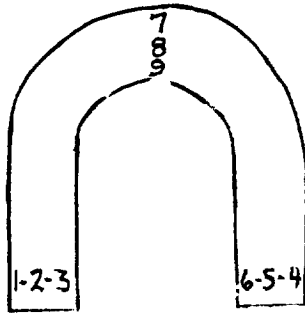
MICRO - HARDNESS SURVEY: 1925°F/5 MIN. ANNEAL ON AS - FORMED TUBE

<u>TEST SPECIMEN</u>	<u>KNOOP HARDNESS</u>	<u>ROCKWELL HARDNESS (CONVERTED)</u>
1-3	$\frac{1}{254}, \frac{2}{251}, \frac{3}{252}$ (leg)	$\frac{1}{R_c 21}, \frac{2}{20}, \frac{3}{20}$
	$\frac{4}{268}, \frac{5}{251}, \frac{6}{252}$ (leg)	$\frac{4}{R_c 23}, \frac{5}{20}, \frac{6}{20}$
	$\frac{7}{258}, \frac{8}{258}, \frac{9}{263}$ (crown)	$\frac{7}{R_c 21.5}, \frac{8}{21.5}, \frac{9}{22.5}$
2-3	$\frac{1}{268}, \frac{2}{297}, \frac{3}{268}$ (leg)	$\frac{1}{R_c 23}, \frac{2}{28}, \frac{3}{23}$
	$\frac{4}{290}, \frac{5}{249}, \frac{6}{287}$ (leg)	$\frac{4}{R_c 27}, \frac{5}{R_B 99}, \frac{6}{R_c 27}$
	$\frac{7}{256}, \frac{8}{278}, \frac{9}{263}$ (crown)	$\frac{7}{R_c 21}, \frac{8}{25}, \frac{9}{22.5}$
3-3	$\frac{1}{251}, \frac{2}{251}, \frac{3}{253}$ (leg)	$\frac{1}{R_c 20}, \frac{2}{20}, \frac{3}{20.5}$
	$\frac{4}{249}, \frac{5}{248}, \frac{6}{257}$ (leg)	$\frac{4}{R_B 99}, \frac{5}{R_B 99}, \frac{6}{R_c 21}$
	$\frac{7}{273}, \frac{8}{254}, \frac{9}{252}$ (crown)	$\frac{7}{R_c 24}, \frac{8}{21}, \frac{9}{20.5}$
4-3	$\frac{1}{263}, \frac{2}{254}, \frac{3}{261}$ (leg)	$\frac{1}{R_c 22.5}, \frac{2}{21}, \frac{3}{22}$
	$\frac{4}{254}, \frac{5}{256}, \frac{6}{266}$ (leg)	$\frac{4}{R_c 21}, \frac{5}{21}, \frac{6}{23}$
	$\frac{7}{288}, \frac{8}{296}, \frac{9}{272}$ (crown)	$\frac{7}{R_c 26.5}, \frac{8}{28}, \frac{9}{24}$
4A-3	$\frac{1}{256}, \frac{2}{278}, \frac{3}{284}$ (leg)	$\frac{1}{R_c 21}, \frac{2}{25}, \frac{3}{26}$
	$\frac{4}{278}, \frac{5}{268}, \frac{6}{258}$ (leg)	$\frac{4}{R_c 25}, \frac{5}{23}, \frac{6}{21.5}$
	$\frac{7}{273}, \frac{8}{263}, \frac{9}{282}$ (crown)	$\frac{7}{R_c 24}, \frac{8}{22.5}, \frac{9}{26}$

Appendix B

TABLE VI (cont.)

<u>TUBE SPECIMEN</u>	<u>KNOOP HARDNESS</u>	<u>ROCKWELL HARDNESS (CONVERTED)</u>
5A-3	$\frac{1}{245}, \frac{2}{238}, \frac{3}{244}$ (leg)	$\frac{1}{R_B 99}, \frac{2}{97.5}, \frac{3}{98.5}$
	$\frac{4}{248}, \frac{5}{248}, \frac{6}{248}$ (leg)	$\frac{4}{R_B 99}, \frac{5}{99}, \frac{6}{99}$
	$\frac{7}{253}, \frac{8}{252}, \frac{9}{256}$ (crown)	$\frac{7}{R_c 20.5}, \frac{8}{20}, \frac{9}{21}$



## Appendix B

TABLE VII

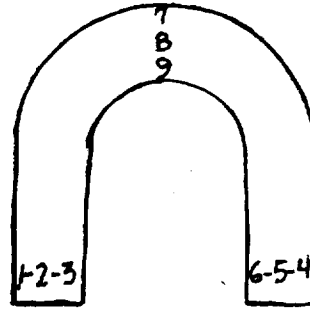
MICRO - HARDNESS SURVEY: 1925°F/5 MIN. ANNEAL + SIMULATED BRAZE CYCLE ON AS-FORMED TUBE

<u>TUBE SPECIMEN</u>	<u>KNOOP HARDNESS</u>	<u>ROCKWELL HARDNESS (CONVERTED)</u>
1-4	$\frac{1}{284}, \frac{2}{278}, \frac{3}{266}$ (leg)	$\frac{1}{R_c 26}, \frac{2}{25}, \frac{3}{23}$
	$\frac{4}{260}, \frac{5}{253}, \frac{6}{279}$ (leg)	$\frac{4}{R_c 22}, \frac{5}{20.5}, \frac{6}{25}$
	$\frac{7}{279}, \frac{8}{247}, \frac{9}{272}$ (crown)	$\frac{7}{R_c 25}, \frac{8}{R_B 99}, \frac{9}{24}$
2-4	$\frac{1}{286}, \frac{2}{275}, \frac{3}{286}$ (leg)	$\frac{1}{R_c 26}, \frac{2}{24.5}, \frac{3}{26}$
	$\frac{4}{278}, \frac{5}{293}, \frac{6}{290}$ (leg)	$\frac{4}{R_c 25}, \frac{5}{27.5}, \frac{6}{27}$
	$\frac{7}{269}, \frac{8}{270}, \frac{9}{269}$ (crown)	$\frac{7}{R_c 23.5}, \frac{8}{24}, \frac{9}{23.5}$
3-4	$\frac{1}{270}, \frac{2}{257}, \frac{3}{257}$ (leg)	$\frac{1}{R_c 24}, \frac{2}{21}, \frac{3}{21}$
	$\frac{4}{268}, \frac{5}{270}, \frac{6}{260}$ (leg)	$\frac{4}{R_c 23}, \frac{5}{24}, \frac{6}{22}$
	$\frac{7}{268}, \frac{8}{268}, \frac{9}{257}$ (crown)	$\frac{7}{R_c 23}, \frac{8}{23}, \frac{9}{21}$
4-4	$\frac{1}{245}, \frac{2}{279}, \frac{3}{261}$ (leg)	$\frac{1}{R_B 99}, \frac{2}{R_c 25}, \frac{3}{22}$
	$\frac{4}{263}, \frac{5}{284}, \frac{6}{252}$ (leg)	$\frac{4}{R_c 22.5}, \frac{5}{26}, \frac{6}{20}$
	$\frac{7}{248}, \frac{8}{279}, \frac{9}{291}$ (crown)	$\frac{7}{R_B 99}, \frac{8}{R_c 25}, \frac{9}{27}$
4A-4	$\frac{1}{275}, \frac{2}{258}, \frac{3}{263}$ (leg)	$\frac{1}{R_c 24.5}, \frac{2}{21.5}, \frac{3}{22.5}$
	$\frac{4}{276}, \frac{5}{285}, \frac{6}{297}$ (leg)	$\frac{4}{R_c 25}, \frac{5}{26}, \frac{6}{28}$
	$\frac{7}{297}, \frac{8}{284}, \frac{9}{273}$ (crown)	$\frac{7}{R_c 28}, \frac{8}{26}, \frac{9}{24}$

Appendix B

TABLE VII (cont.)

<u>TUBE SPECIMEN</u>	<u>KNOOP HARDNESS</u>	<u>ROCKWELL HARDNESS (CONVERTED)</u>
5A-4	$\frac{1}{248}, \frac{2}{256}, \frac{3}{243}$	$\frac{1}{R_B 99}, \frac{2}{R_C 21}, \frac{3}{R_B 98.5}$
	$\frac{4}{242}, \frac{5}{254}, \frac{6}{236}$ (leg)	$\frac{4}{R_B 98}, \frac{5}{R_C 21}, \frac{6}{R_B 97}$
	$\frac{7}{279}, \frac{8}{252}, \frac{9}{282}$ (crown)	$\frac{7}{R_C 25}, \frac{8}{20}, \frac{9}{25.5}$



## Appendix B

TABLE VIII

MICRO - HARDNESS SURVEY: 1925°F/15 MIN. ANNEAL ON AS - FORMED TUBE

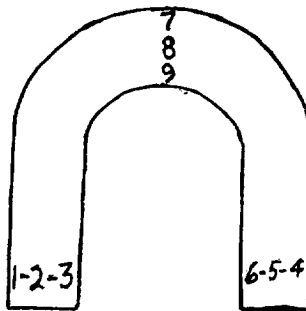
<u>TUBE SPECIMEN</u>	<u>KNOOP HARDNESS</u>	<u>ROCKWELL HARDNESS (CONVERTED)</u>
1-5	$\frac{1}{244}, \frac{2}{249}, \frac{3}{236}$ (leg)	$\frac{1}{R_B 99}, \frac{2}{R_B 99}, \frac{3}{R_B 97}$
	$\frac{4}{257}, \frac{5}{238}, \frac{6}{243}$ (leg)	$\frac{4}{R_C 21}, \frac{5}{R_B 97.5}, \frac{6}{R_B 98.5}$
	$\frac{7}{243}, \frac{8}{251}, \frac{9}{258}$ (crown)	$\frac{7}{R_B 98.5}, \frac{8}{R_B 99}, \frac{9}{R_C 21.5}$
2-5	$\frac{1}{276}, \frac{2}{262}, \frac{3}{286}$ (leg)	$\frac{1}{R_C 24.5}, \frac{2}{22}, \frac{3}{26}$
	$\frac{4}{290}, \frac{5}{281}, \frac{6}{272}$ (leg)	$\frac{4}{R_C 27}, \frac{5}{25.5}, \frac{6}{24}$
	$\frac{7}{262}, \frac{8}{249}, \frac{9}{252}$ (crown)	$\frac{7}{R_C 22.5}, \frac{8}{R_B 99}, \frac{9}{R_C 20}$
3-5	$\frac{1}{261}, \frac{2}{252}, \frac{3}{281}$ (leg)	$\frac{1}{R_C 22}, \frac{2}{20}, \frac{3}{25}$
	$\frac{4}{253}, \frac{5}{253}, \frac{6}{258}$ (leg)	$\frac{4}{R_C 20.5}, \frac{5}{20.5}, \frac{6}{21.5}$
	$\frac{7}{275}, \frac{8}{258}, \frac{9}{266}$ (crown)	$\frac{7}{R_C 24.5}, \frac{8}{21.5}, \frac{9}{23}$
4-5	$\frac{1}{257}, \frac{2}{276}, \frac{3}{286}$ (leg)	$\frac{1}{R_C 21}, \frac{2}{24.5}, \frac{3}{26}$
	$\frac{4}{266}, \frac{5}{268}, \frac{6}{268}$ (leg)	$\frac{4}{R_C 23}, \frac{5}{23}, \frac{6}{23}$
	$\frac{7}{268}, \frac{8}{281}, \frac{9}{272}$ (crown)	$\frac{7}{R_C 23}, \frac{8}{25.5}, \frac{9}{24}$
4A-5	$\frac{1}{261}, \frac{2}{261}, \frac{3}{261}$ (leg)	$\frac{1}{R_C 22}, \frac{2}{22}, \frac{3}{22}$
	$\frac{4}{256}, \frac{5}{256}, \frac{6}{260}$ (leg)	$\frac{4}{R_C 21}, \frac{5}{21}, \frac{6}{22}$
	$\frac{7}{263}, \frac{8}{262}, \frac{9}{285}$ (crown)	$\frac{7}{R_C 22.5}, \frac{8}{22}, \frac{9}{26}$



Appendix B

TABLE VIII (cont.)

<u>TUBE SPECIMEN</u>	<u>KNOOP HARDNESS</u>	<u>ROCKWELL HARDNESS (CONVERTED)</u>
5A-5	$\frac{1}{252}, \frac{2}{251}, \frac{3}{261}$ (leg)	$\frac{1}{R_c 20.5}, \frac{2}{20}, \frac{3}{22}$
	$\frac{4}{251}, \frac{5}{251}, \frac{6}{242}$ (leg)	$\frac{4}{R_c 20.5}, \frac{5}{20}, \frac{6}{R_B 98}$
	$\frac{7}{254}, \frac{8}{244}, \frac{9}{268}$ (crown)	$\frac{7}{R_c 21}, \frac{8}{R_B 99}, \frac{9}{R_c 23}$



## Appendix B

TABLE IX

MICRO-HARDNESS SURVEY: 1925°F/15 MIN. ANNEAL + SIMULATED BRAZE CYCLE ON AS-FORMED TUBE

<u>TUBE SPECIMEN</u>	<u>KNOOP HARDNESS</u>	<u>ROCKWELL HARDNESS (CONVERTED)</u>
1-6	$\frac{1}{266}, \frac{2}{248}, \frac{3}{260}$ (leg)	$\frac{1}{R_c 23}, \frac{2}{R_B 99}, \frac{3}{R_c 22}$
	$\frac{4}{247}, \frac{5}{254}, \frac{6}{266}$ (leg)	$\frac{4}{R_B 99}, \frac{5}{R_c 21}, \frac{6}{23}$
	$\frac{7}{266}, \frac{8}{266}, \frac{9}{266}$ (crown)	$\frac{7}{R_c 23}, \frac{8}{23}, \frac{9}{23}$
2-6	$\frac{1}{256}, \frac{2}{266}, \frac{3}{295}$ (leg)	$\frac{1}{R_c 21}, \frac{2}{23}, \frac{3}{27.5}$
	$\frac{4}{297}, \frac{5}{296}, \frac{6}{296}$ (leg)	$\frac{4}{R_c 28}, \frac{5}{28}, \frac{6}{28}$
	$\frac{7}{269}, \frac{8}{269}, \frac{9}{278}$ (crown)	$\frac{7}{R_c 23.5}, \frac{8}{23.5}, \frac{9}{25}$
3-6	$\frac{1}{266}, \frac{2}{254}, \frac{3}{265}$ (leg)	$\frac{1}{R_c 23}, \frac{2}{21}, \frac{3}{23}$
	$\frac{4}{265}, \frac{5}{265}, \frac{6}{265}$ (leg)	$\frac{4}{R_c 23}, \frac{5}{23}, \frac{6}{23}$
	$\frac{7}{275}, \frac{8}{263}, \frac{9}{268}$ (crown)	$\frac{7}{R_c 24.5}, \frac{8}{22.5}, \frac{9}{23}$
4-6	$\frac{1}{269}, \frac{2}{263}, \frac{3}{254}$ (leg)	$\frac{1}{R_c 23.5}, \frac{2}{22.5}, \frac{3}{21}$
	$\frac{4}{268}, \frac{5}{266}, \frac{6}{286}$ (leg)	$\frac{4}{R_c 23}, \frac{5}{23}, \frac{6}{26}$
	$\frac{7}{273}, \frac{8}{296}, \frac{9}{313}$ (crown)	$\frac{7}{R_c 24}, \frac{8}{28}, \frac{9}{30}$
4A-6	$\frac{1}{276}, \frac{2}{276}, \frac{3}{278}$ (leg)	$\frac{1}{R_c 25}, \frac{2}{25}, \frac{3}{25}$
	$\frac{4}{281}, \frac{5}{269}, \frac{6}{278}$ (leg)	$\frac{4}{R_c 25.5}, \frac{5}{23.5}, \frac{6}{25}$
	$\frac{7}{284}, \frac{8}{272}, \frac{9}{286}$ (crown)	$\frac{7}{R_c 26}, \frac{8}{24}, \frac{9}{26}$

Appendix B

TABLE IX (cont.)

<u>TUBE SPECIMENS</u>	<u>KNOOP HARDNESS</u>	<u>ROCKWELL HARDNESS (CONVERTED)</u>
5A-6	$\frac{1}{257}, \frac{2}{233}, \frac{3}{256}$ (leg)	$\frac{1}{R_c 21}, \frac{2}{R_B 96.5}, \frac{3}{R_c 21}$
	$\frac{4}{254}, \frac{5}{254}, \frac{6}{256}$ (leg)	$\frac{4}{R_c 21}, \frac{5}{21}, \frac{6}{21}$
	$\frac{7}{278}, \frac{8}{261}, \frac{9}{291}$ (crown)	$\frac{7}{R_c 25}, \frac{8}{22}, \frac{9}{27}$

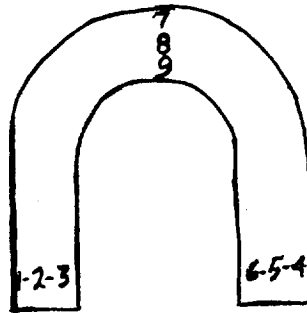


TABLE X

AVERAGE MICROHARDNESS (KNOOP) COMPARISONS ON HASTELLOY X COOLANT TUBE

SAMPLE LOC.	AS FORMED		AS FORMED +		AS FORMED +		AS FORMED +		AS FORMED +		AS FORMED +	
	LEG	CROWN	BRAZE LEG	CYCLE CROWN	5 MIN @ 1925°F LEG	5 MIN @ 1925°F CROWN	5 MIN @ 1925°F LEG	5 MIN @ 1925°F CROWN	15 MIN @ 1925°F LEG	15 MIN @ 1925°F CROWN	BRAZE LEG	CYCLE CROWN
1	230	251	250	239	255	260	270	266	245	251	257	266
2	231	272	285	261	276	266	285	269	278	254	284	272
3	229	204	237	236	252	260	264	264	260	266	263	269
4	233	274	245	246	259	285	264	273	270	274	268	294
4A	223	306	239	237	270	273	276	265	259	270	276	261
5	221	284	242	232	245	254	247	271	252	255	252	277
AVERAGE	228	265	250	242	260	266	268	268	261	262	267	273
SPREAD-TOTAL	12	102	48	25	31	31	38	9	33	23	32	35
PLUS	5	41	35	19	16	19	17	5	17	12	17	23
MINUS	7	61	13	10	15	12	21	4	16	11	15	12

ORIGINAL MATERIAL (AGC-90057):  $236 \pm \frac{5}{6}$

48

Appendix B

## C. DISCUSSION

This investigation has shown that a hardness increase occurred after the various thermal cycles. These results are compatible with the general property trends found by Comprelli and Wolf, Reference (1), who found substantial increases in the strength (or hardness) with exposures at 1050°F; the increase of hardness was accompanied by a decrease in ductility. The hardness increase has been observed also by Kaufmann, Reference (2), and corroborated by Wagoner, Reference (3). The increase in hardness is attributed to precipitation producing a strengthened matrix. Phase  $M_6C$  is believed to be the major precipitate conferring increased hardness, however, the existence of other phases,  $M_{23}C_6$ , Laves phase, and Mu phase cannot be discounted. In the case of annealing, further contribution to strengthening is believed to be due to solutioning of grain boundary carbides and subsequent reprecipitation within the matrix.

III. CONCLUSIONS

The hardness of Hastelloy X is increased by cycles of brazing, annealing, or annealing plus brazing. Brazing and annealing at the designated temperatures, does not promote grain growth. Brazing and annealing plus brazing promote carbide precipitation while annealing prior to brazing reduced the amount of carbides at grain boundaries. The annealing cycle had no effect on tube dimensions. A stress equalizing is achieved in cold-worked Hastelloy X by the anneal and anneal plus simulated braze cycles.

IV. RECOMMENDATIONS

Study the microstructures of the treated samples by electron microscopy to determine the morphology of the precipitated carbides and the primary phase segregates.

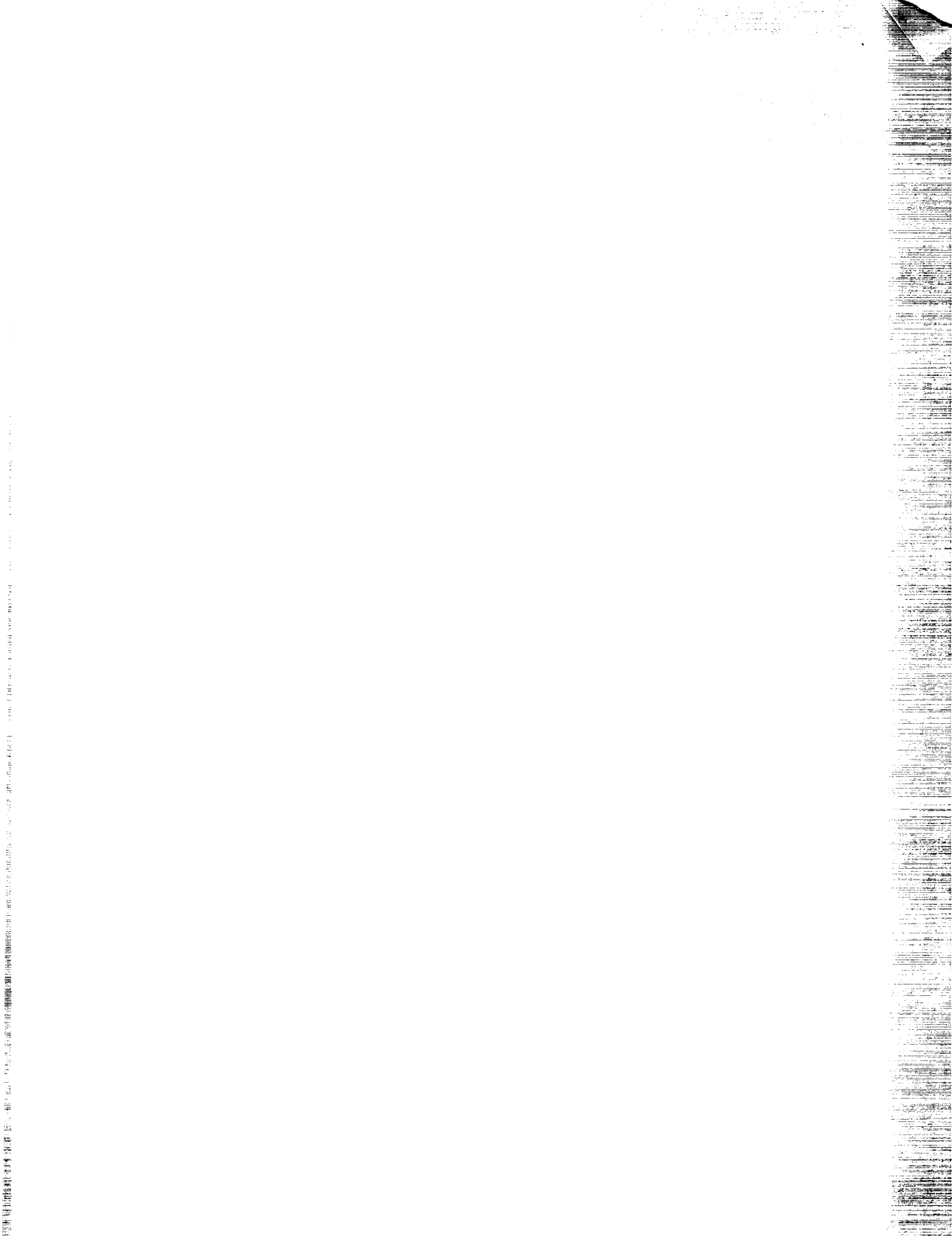
## Appendix B

### V. REFERENCES

- (1) Metals Engineering Quarterly, November 1965, Stability of High-Nickel Alloys in Superheated Steam, F. A. Comprelli and V. E. Wolff.
- (2) Thomson Engineering Laboratory Report R62SE17, November 1963, General Electric Co., Phase Studies - Miscellaneous Alloys, M. Kaufmann.
- (3) E. L. Wagoner, Physical Metallurgy and Mechanical Properties of Hastelloy Alloy X, Haynes Stellite Publication, June 23, 1961.

APPENDIX C

TORUS DISSIMILAR METAL WELDING EVALUATION





I. SUMMARY

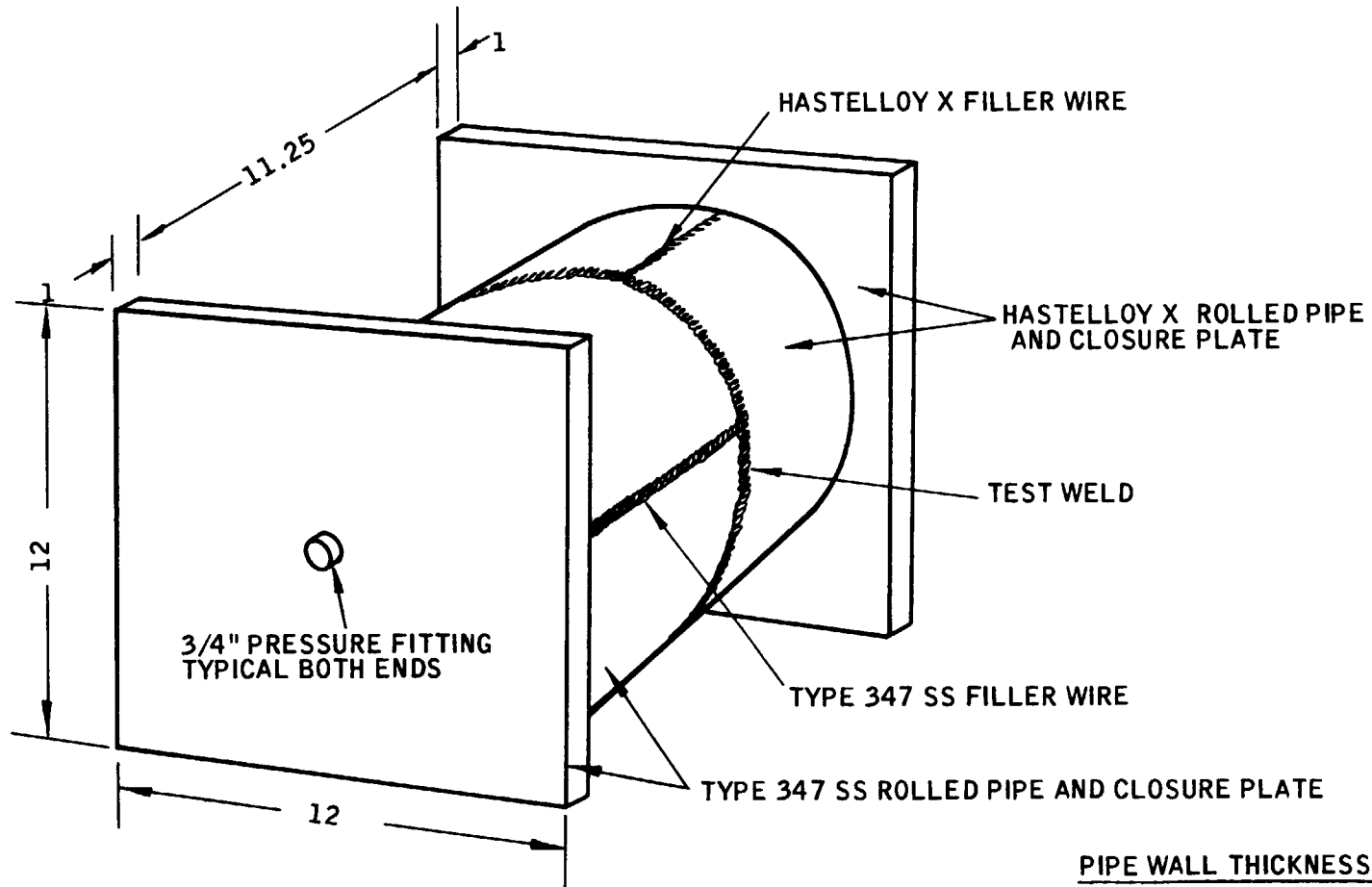
Hastelloy W or Inconel A filler wire may be used satisfactorily when joining Type 347 SS to Hastelloy X material. Both filler materials produced welds with ultimate strength at room temperatures greater than that of the Type 347 SS parent material. However, the Hastelloy W filler wire provided far better flow and wetting characteristics and a more favorable microstructure than did the Inconel A, and is, therefore, recommended for use on the subject Torus Weldment.

II. TECHNICAL DISCUSSION

A. PROCEDURE

Evaluation of the two filler materials was accomplished by welding a total of six pressure vessels, the design of which is shown in Figure 1. The center girth welds of the vessels were intended to simulate the Torus inlet and inlet adaptor weldment of the Phoebus Nozzle, which joins Type 347 SS to Hastelloy X material. Three of the six vessels were girth-welded using Inconel A as a filler wire while the remaining three were joined with Hastelloy W wire. In each instance, one of the three was welded manually, while the remaining two were welded automatically. This was done to provide assurance that both welding procedures would be satisfactory. All welds were made by the tungsten inert arc process. Welding conditions for the automatic and manual welds are shown in Table I. The joint preparation for the girth welds consisted of a 90-degree included angle, with a 0.060-inch root face.

Mechanical testing was performed by submitting four of the six vessels to proof pressure, one to burst pressure and by sectioning the remaining two into tensile and metallographic specimens. Shown in Table II are the chemical analyses of all materials involved.



<u>PIPE WALL THICKNESS &amp; DIA</u>	
HASTELLOY X	0.260
TYPE 347 SS	0.287
INSIDE DIAMETER	7-15/16

NOTE: ALL DIMENSIONS IN INCHES

Fig. 1  
Test Pressure Vessel Design

TABLE I

WELDING CONDITIONS FOR SIX TEST WELDS

<u>Vessel No.</u>	<u>Pass</u>	<u>Procedure</u>	<u>Amps</u>	<u>Volts</u>	<u>Welding Speed</u>	<u>Wire Feed Rate</u>	<u>Wire Dia.</u>	<u>Wire Type</u>	<u>Cover Gas + Flow</u>	<u>Backup Gas</u>	<u>Comments</u>
1	1	Automatic	240	8.5	6 IPM	20 IPM	.060	Hast "W"	A/30CFH	A/25CFH	Penetration Complete
	2	---	---	---	---	25 IPM	---	---	---	---	Excessive Penetration
	3	---	200	9.0	---	30 IPM	---	---	---	---	---
	4	---	200	9.0	---	20 IPM	---	---	---	---	---
	5	---	190	9.0	10 IPM	20 IPM	---	---	---	---	---
	6	---	190	9.0	10 IPM	20 IPM	---	---	---	---	---
2	1	Automatic	240	8.5	6 IPM	25 IPM	.060	Hast "W"	A/30CFH	A/25CFH	Penetration Complete
	2 thru 5	---	190	8.5	10 IPM	25 IPM	---	---	---	---	---
3	1	Automatic	240	8.0	6 IPM	20 IPM	.045	Inc. "A"	A/30CFH	A/25CFH	Penetration Complete
	2	---	---	8.5	---	25 IPM	---	---	---	---	Poor Wetting
	3	---	200	9.0	---	30 IPM	---	---	---	---	Poor Wetting
	4	---	200	9.0	---	20 IPM	---	---	---	---	---
	5	---	190	9.0	---	20 IPM	---	---	---	---	---
	6	---	190	9.0	---	20 IPM	---	---	---	---	---
4	1	Automatic	240	8.0	6 IPM	40 IPM	---	---	---	---	Penetration Complete
	2	---	230	8.0	---	50 IPM	---	---	---	---	Poor Wetting
	3	---	230	8.0	---	50 IPM	---	---	---	---	Using

Test Vessels No's. 3 and 5 were welded manually using Inconel "A" and Hastelloy "W" as filler wire, and argon as an inert gas. The welds were completed with five passes each.

TABLE II

CHEMICAL ANALYSIS OF MATERIALS USED IN TEST VESSELS

<u>C</u>	<u>Mn</u>	<u>P</u>	<u>S</u>	<u>Si</u>	<u>W</u>	<u>Cu</u>	<u>Cr</u>	<u>Ni</u>	<u>Mo</u>	<u>Cb/Ta</u>	<u>Al/Ti</u>	<u>Co</u>	<u>B</u>	<u>Va</u>	<u>Fe</u>
<u>Roll and Welded 8-In. Type 374 SS Pipe</u>															
.051	1.5	.026	.013	.61	--	.20	17.65	10.87	.39	.87	--	--	--	--	--
<u>Roll and Welded 8-In. Hastelloy X Pipe and 1-In.-Thick Closure Plate</u>															
0.05/0.15	1.0 max	.020 max	.015 max	1.0 max	.20/1.0	.35 max	20.5/23.0	Bal	8.0/10.0	--	.50 max	.50/2.5	.001 max	0.5 max	17.0/20.0
<u>1-In.-Thick Type 347 SS Closure Plate</u>															
.060	1.56	.023	.010	.42	--	--	18.0	9.6	--	.76	--	--	--	--	--
<u>Hastelloy X Filler Wire for 1-In.-Dia Hastelloy X Pipe Longitudinal Welds</u>															
.10	.42	.016	.010	.28	.87	.05	21.8	Bal	9.54	--	.09	2.16	.001	.04	17.5
<u>*Inconel A Filler Wire for Test Girth Welds</u>															
.10 max	2.0/2.75	--	.015 max	.35 max	--	.50 max	14.0/17.0	67.0 min	--	--	Ti 2.5/3.5	--	--	--	10.0 max
<u>*Hastelloy W Filler Wire for Test Girth Welds</u>															
.12 max	1.00 max	.040 max	.030 max	--	--	--	4.0/6.0	Bal	23.0/26.0	--	--	2.5 max	--	.60 max	4.0/7.0

\*Per Aerospace Material Specifications

Appendix C

## Appendix C

### B. WELDING

Automatic welding progressed much more favorably with the Hastelloy W filler wire than with Inconel A. Both wires showed the characteristic poor wetting ability that is synonymous with nickel-base, high-temperature materials. Also, both materials had what appeared to be islands of tight adhering oxides on the surface of the solidified weld bead. These "islands" also were apparent, floating on the surface of the weld melt. The Inconel A material had a tendency to "rope" during welding which required severe grinding at the edges of each pass to avoid cold shuts. No significant difference was noted in the flow characteristics of the two materials during manual welding.

Some difficulty was encountered in interpreting radiographs of the welds, due to the different densities of the materials involved. For example, the radiograph of one weld was interpreted as having almost complete lack of penetration, when, actually, considerable grinding was required to remove the excessive melt-through. Scattered porosity was noted in all of the welds, ranging in amounts from medium to light, but no attempt was made to make weld repairs.

Distortion in the form of "sinking" occurred in all welds. In some instances, the diameter at the weld was reduced by as much as 0.125 inch due to the effect of distortion. This condition can be corrected by proper internal fixturing.

### C. TEST RESULTS

One of the four vessels was tested to burst pressure (Vessel No. 2). This vessel, automatically welded with Hastelloy W filler wire, failed at an internal pressure of 5800 psi. Failure occurred in the girth weld in the form of a small crack. Internal pressure caused the vessel to bulge and permanently increased the diameter at the center by approximately 1-1/2 inches. Although the pressure attained exerted a hoop loading in the order of 80 ksi on the

## Appendix C

Type 347 SS (comparable to the ultimate strength of this material), the actual failure was triggered by a combination of grinding grooves and a stress riser due to weld distortion (sinking). As mentioned earlier in this report, welding stresses caused the girth weld to "sink" (decrease in diameter by as much as 0.125 inch). The "sink" resulted in a stress riser at this point, which was further aggravated by deep grind marks caused during the removal of excessive weld crown. Figure 2 shows the I.D. section of the girth weld in which the failure occurred; note the grind marks. The fracture surface is shown in Figure 3 with the typical sunburst pattern on the I.D. at the point of initiation. In Figure 4, the surface of the I.D. weld is shown adjacent to the point of failure at a higher magnification. Note the start of fissures in the grind marks. Without these failure-initiating fissures, the vessel may have sustained a slightly higher pressure.

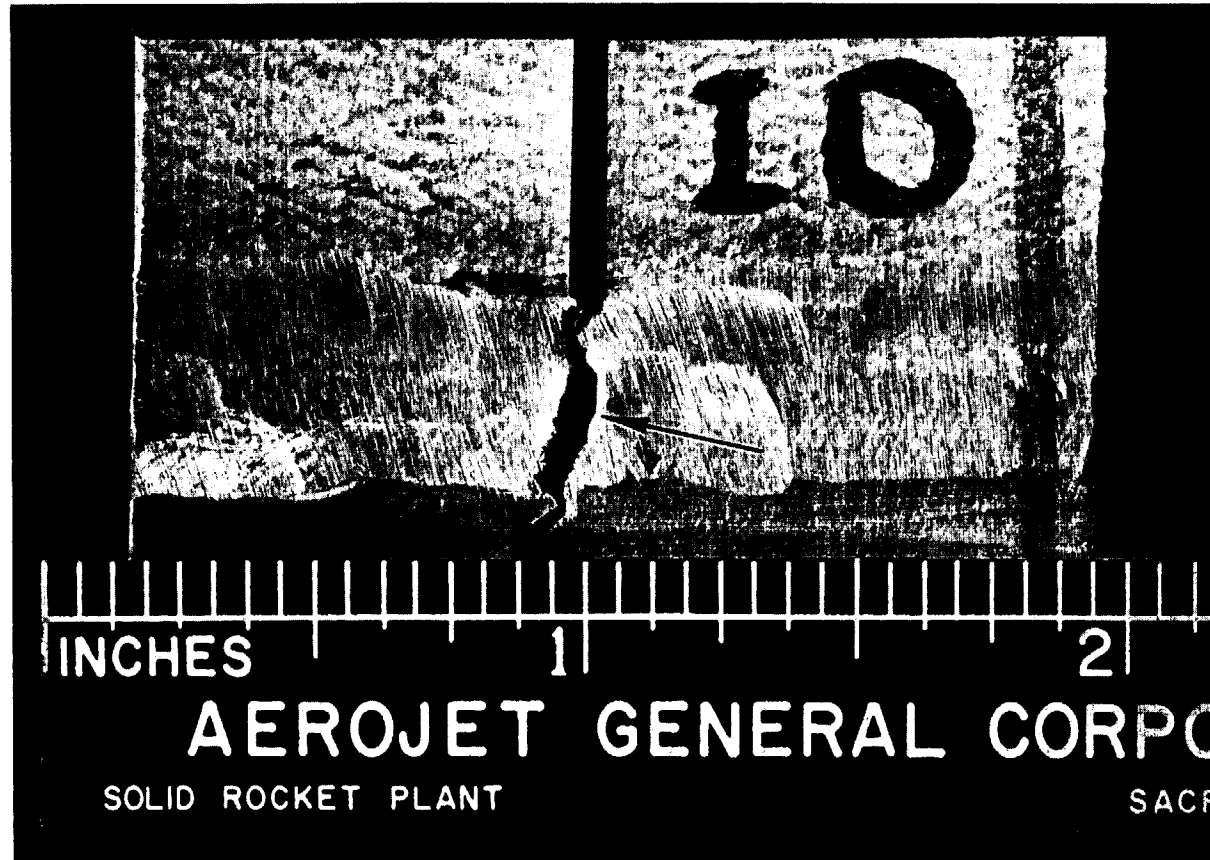
The three remaining vessels (Nos. 3, 4 and 5) satisfactorily passed proof testing at an internal pressure of 1450 psi.

Tensile testing was performed on specimens taken from the center girth weld of two (Nos. 1 and 6) of the six vessels, one of which was welded with Hastelloy W and the other with Inconel A filler wire. Three transverse weld tensile tests were made on each of the two welded joints. In all instances, the specimens failed in the parent metal of the Type 347 SS, well away from the weld or heat-affected zone. Table III shows the tensile properties of the specimens tested.

Samples from each of the two welded joints (Inconel A and Hastelloy W) were examined metallographically. The photomicrographs in Figure 5, which compare the cast weld structure of Inconel A with that of Hastelloy W, indicate that both structures are similar in that each displays coring or segregation common to nickel base alloy materials. Figure 6, a different area of the same Inconel A weld mount, shows a micro-crack. No cracking was observed in the Hastelloy W weld. The significance of the dark area at the interface of the

Fig. 2

Surface of Weld Inside Diameter  
Where Failure Occurred on Vessel No. 2



7

Appendix C

Appendix C

Fig. 3

Fracture Surface  
Showing Point of Initiation (Vessel No. 2) on O.D.

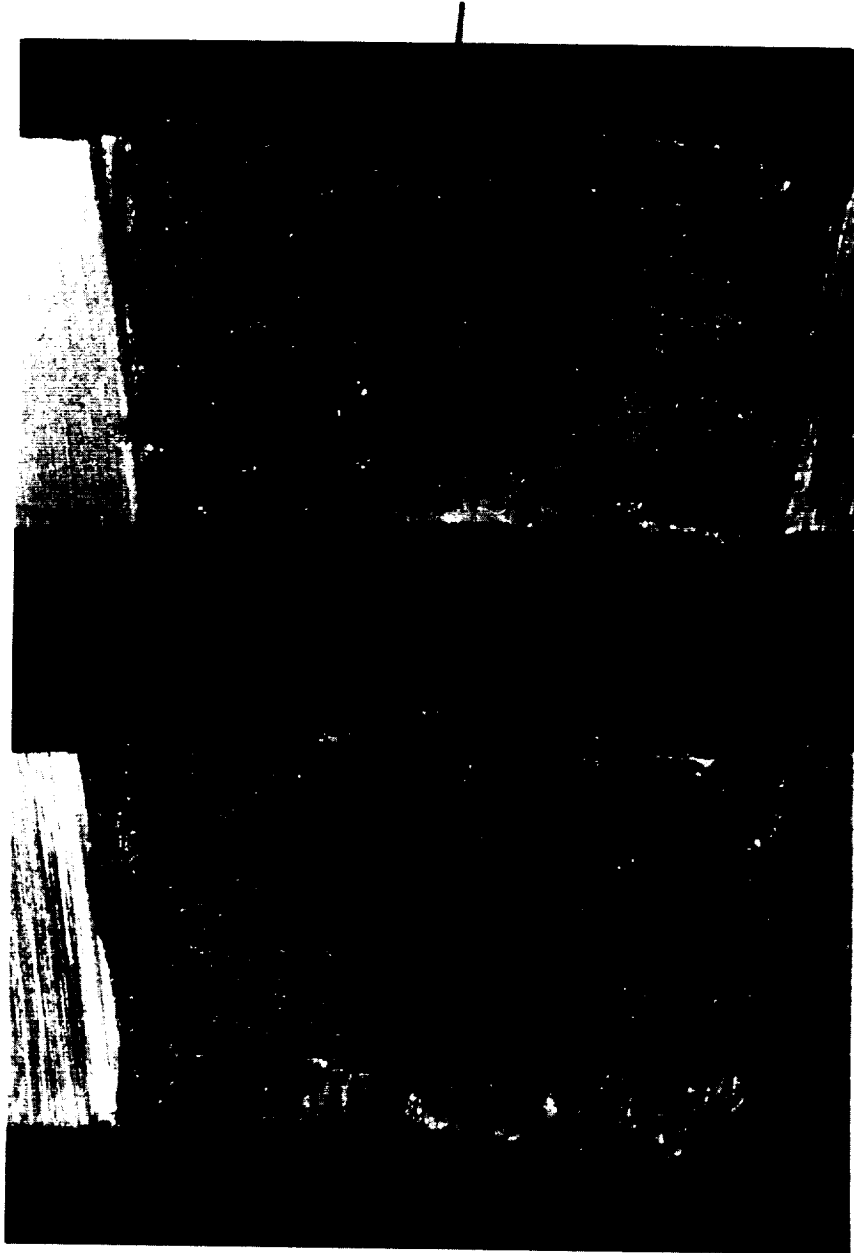
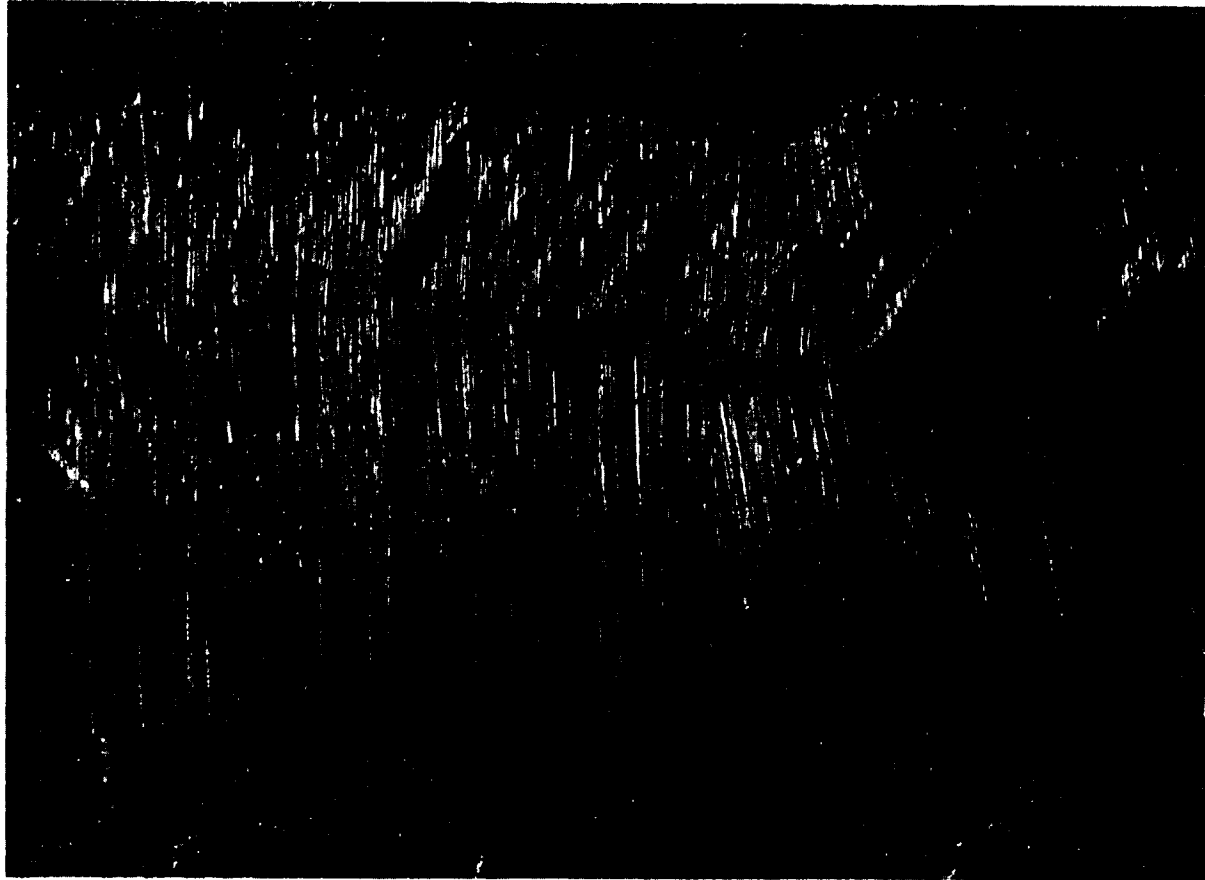




Fig. 4

Surface of Weld Inside Diameter  
Showing Fissures in Grinding Grooves



9

Appendix C

TABLE III

TRANSVERSE WELD TENSILE PROPERTIES OF HASTELLOY X WELDED TO TYPE 347 SS  
WITH INCONEL A AND HASTELLOY W FILLER WIRE

Inconel A Filler Wire

Spec. No.	Ult. Strength Ksi	Yield Strength Ksi	Elong. % 2"	R/A	Location of Failure
1	90.2	51.1	38.5	64.7	In 347 SS
2	91.3	51.1	40.0	64.4	Parent Metal, out of Heat affected
3	91.8	50.0	40.5	63.4	zone

Hastelloy W Filler Wire

1	89.7	48.2	38.5	66.0	In 347 SS
2	89.9	51.7	40.0	66.5	Parent Metal, out of Heat affected
3	89.4	50.6	--	63.3	zone

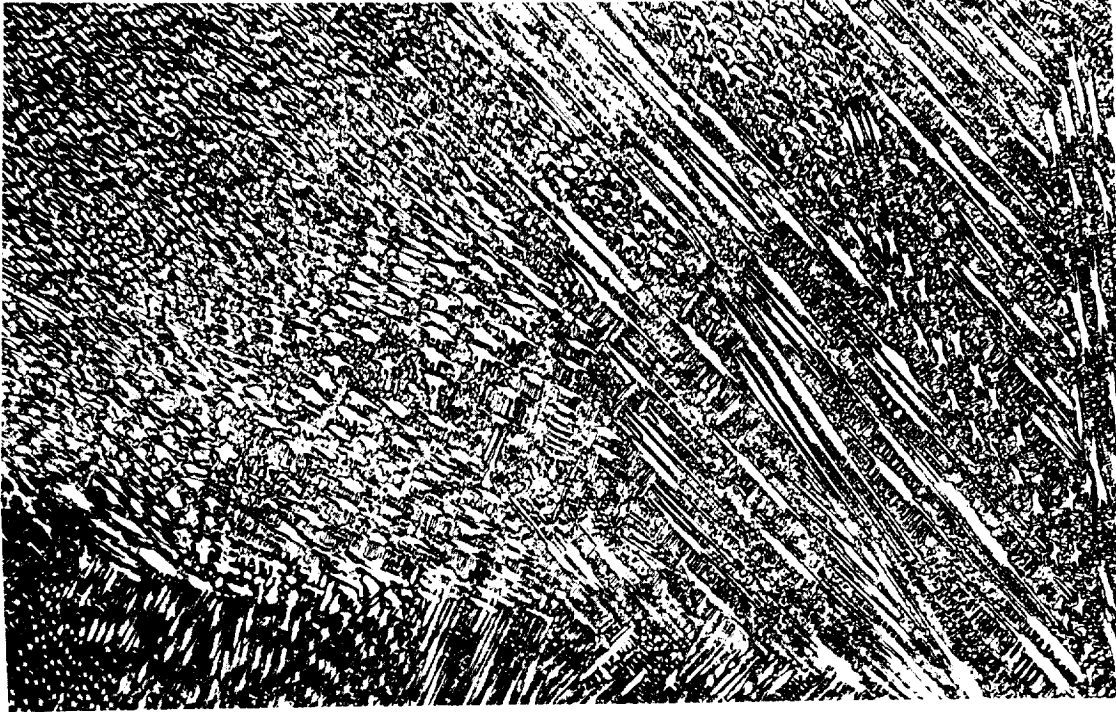
10

Appendix C

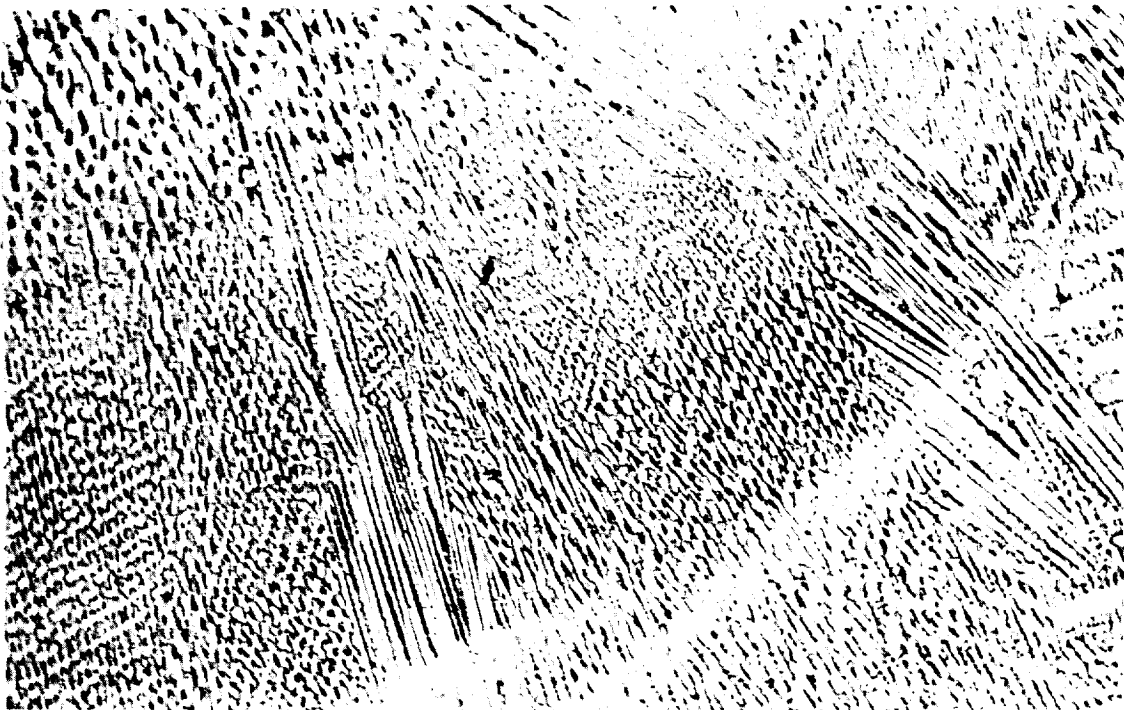
Appendix C

Fig. 5

Weld Cast Structure of Hastelloy "W" and Inconel "A" Filler Wire



Hastelloy "W" 100X Oxalic Etch

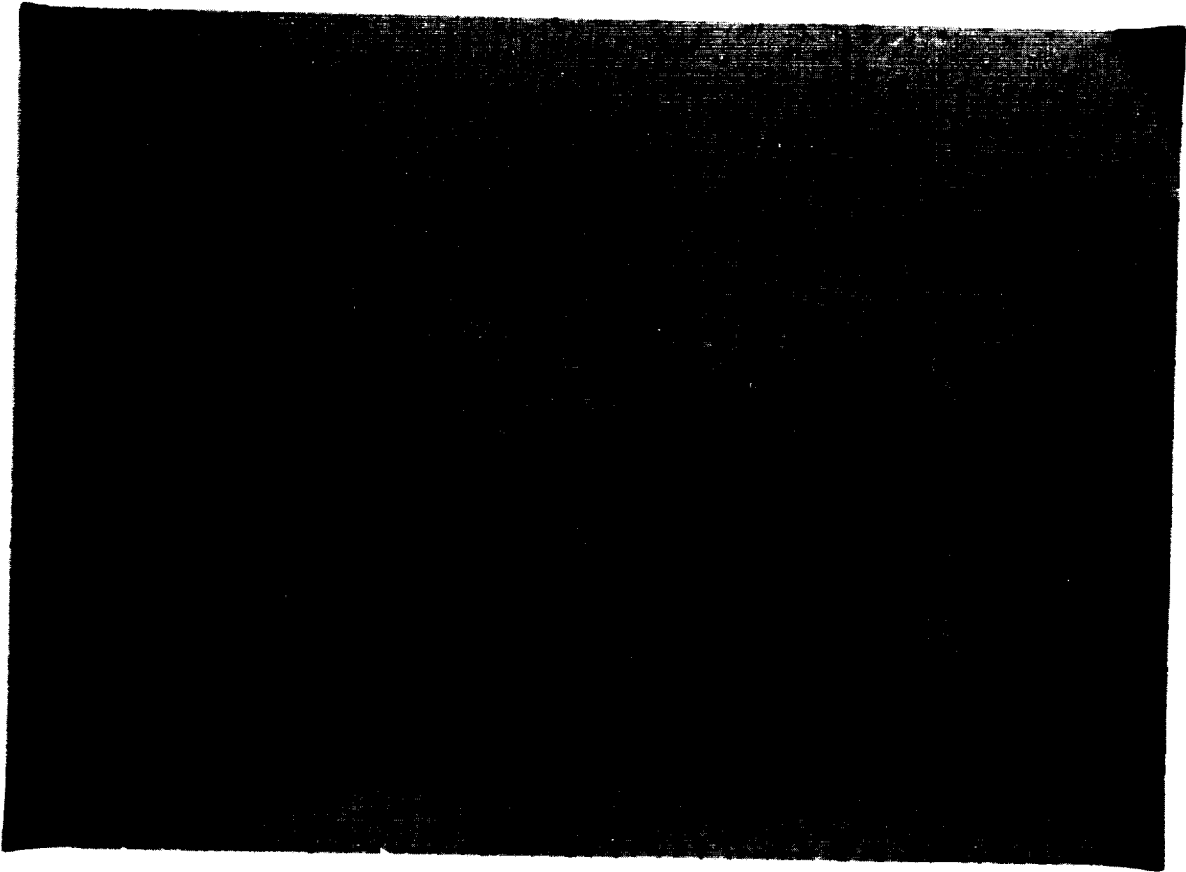


Inconel "A" 100X Oxalic Etch

Appendix C

Fig. 6

Micro Crack In Inconel "A" Weld Deposit



250X Oxalic Etch

## Appendix C

347 parent metal and the Inconel A weld deposit shown in Figure 7 is not clearly understood. This structure does not appear at the Inconel A and Hastelloy X interfaces shown in Figure 8.

Hardness surveys were made across welds representative of both the Inconel A and Hastelloy W deposits. These surveys are plotted in Figures 9 and 10. Both weld deposits show a slight increase in hardness at the interface of the cast structure and the parent materials. There appears to be no significant difference in hardness between the two weld deposits. Again, the darkly etched areas at the root and interface of the Inconel A weld deposit may be seen.

### D. CONCLUSIONS AND RECOMMENDATIONS

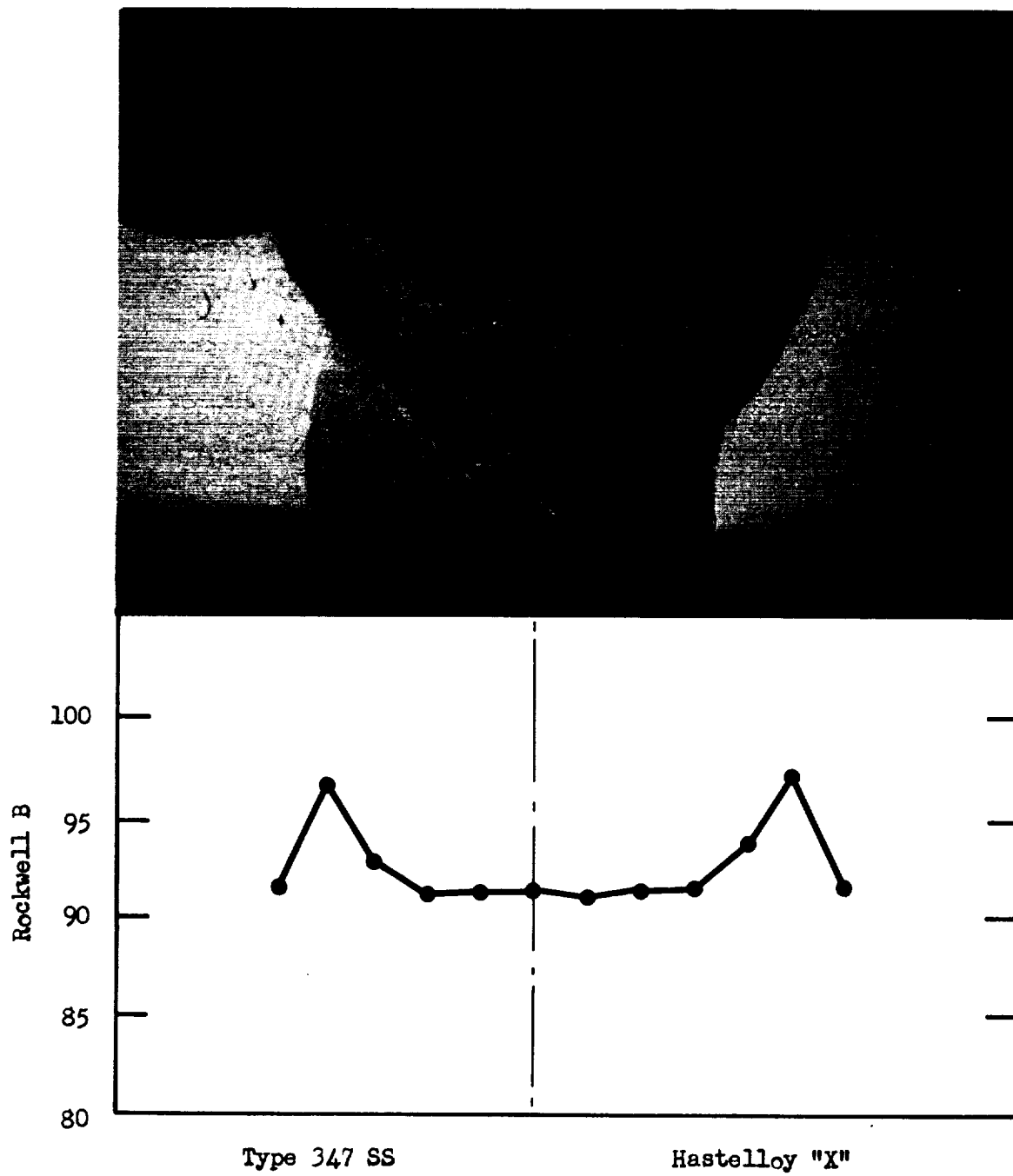
The superior welding characteristics, and microstructure of the weld produced with Hastelloy W filler wire, compared to that of the Inconel A material, indicates that Hastelloy W should be used for joining the Torus Inlet and Inlet Adaptor of the Phoebus Nozzle. This choice is further borne out by the excellent burst results of the pressure vessel tested.

In light of the fact that Inconel A is recommended for joining dissimilar metals, it would be of academic interest to perform further studies of the microstructure found at the interface of the Inconel A weld and the Type 347 SS parent metal.

Appendix C

Fig. 9

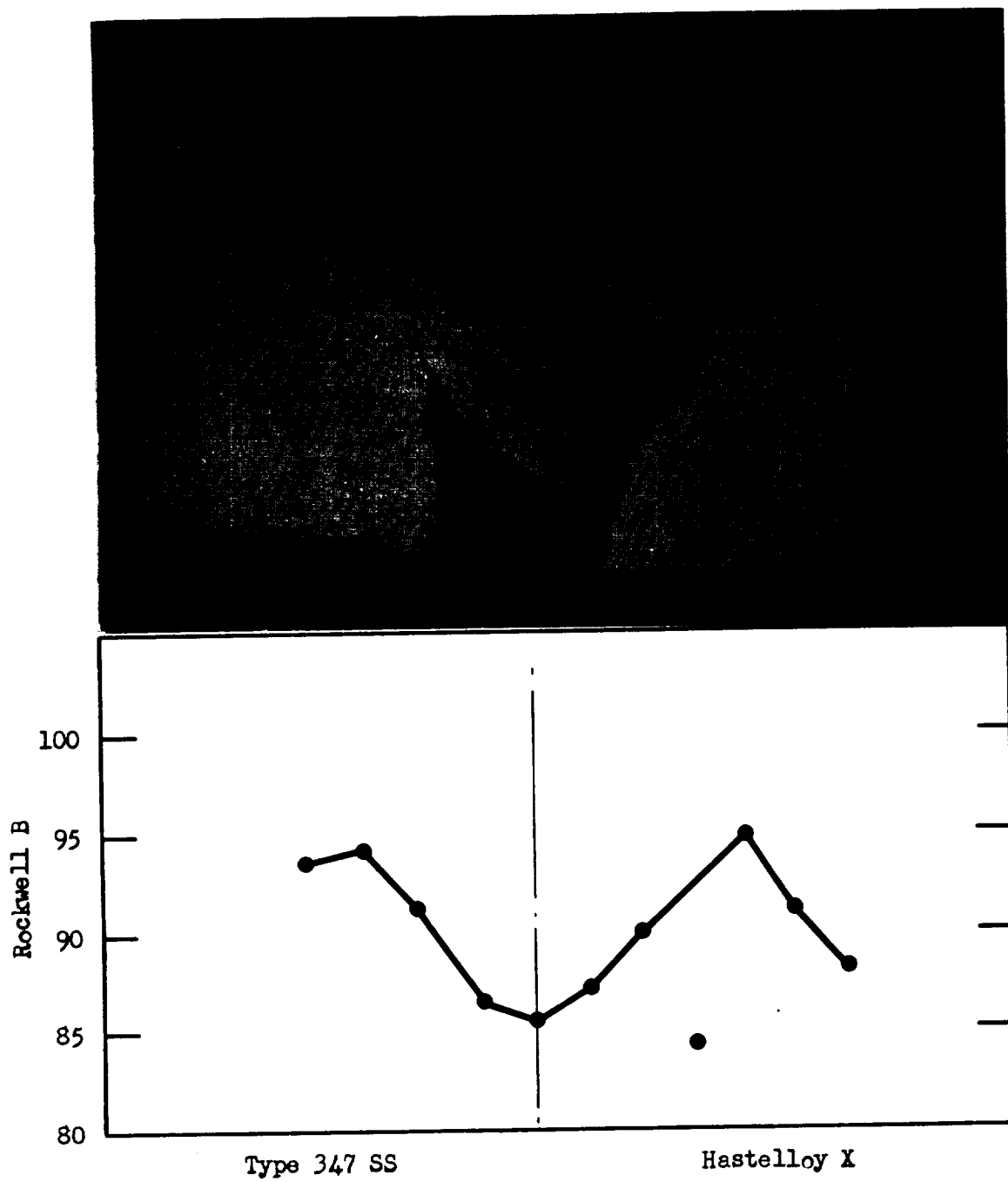
Hardness Survey Across Hastelloy "W" Weld Deposit



Appendix C

Fig. 10

Hardness Survey Across Inconel "A" Weld Deposit







APPENDIX D

TO INVESTIGATE THE CAPABILITY OF HASTELLOY X TUBING TO WITHSTAND  
THERMAL CYCLING BETWEEN 1600°F AND CRYOGENIC TEMPERATURE



I. SUMMARY

Two samples of Hastelloy X tubing, 0.190 in. diameter with 0.020 in. wall thickness were thermally cycled between 1600°F and cryogenic temperatures. Tube sample No. 1 underwent 20 cycles without failure but localized pitting was noted approximately 1 in. above the base electrode. Tube sample No. 2 withstood 20 cycles without failure and no pitting was noted.

A metallurgical analysis of the Hastelloy X tube sample No. 1 indicated extensive recrystallization and an unidentified constituent in the areas of the surface pits. It was determined that the unidentified constituent experienced melting at the test temperatures and indirectly caused the material to spall. The unidentified constituent was not analyzed in this study due to insufficient time. Its presence is attributed to contamination in processing.

II. INVESTIGATION AND RESULTS

A. HISTORY

A Heat Transfer Test HT-3-115 was conducted on annealed Hastelloy X tubing 0.190 in. O.D. x .020 in. wall, reduced by grinding from 0.250 in. outside diameter by .049 in. wall. The test results were reported in FSC 66-146, 28 March 1966. The Hastelloy X tubing was cycled 18 times from an outside wall diameter temperature of -326°F to a surface temperature ranging from 1360 to 1490°F. The tube cracked during test. Additional tests were scheduled to establish whether or not the tube failure was attributable to processing and was a common occurrence or if it was due to faulty material handling in test or manufacture.

## Appendix D

Two tubular test sections of Hastelloy X welded and drawn tubing (0.190 in. O.D. x 0.020 in. wall) were thermally cycled 20 times between a wall temperature of 1600°F and cryogenic temperatures. The results of these tests are discussed in this report.

### B. MATERIAL

Hastelloy X welded tube material for three thermal cycle test specimens was inspected and metallurgically analyzed; test sections were then fabricated for testing. The tube material quality was as follows:

Chemistry:	Boron analysis not available; otherwise meets requirements of AGC-90057.
Structure:	Uniform grain size less than ASTM 8 with scattered, small primary phase; grain size slightly coarser on O.D. No evidence of weld.
NDT:	No outer surface defects and I.D. defects are less than 0.001 in. deep.
Source:	Tube Methods Inc.
Type and Size:	Welded and drawn, 0.190 in. O.D. x 0.020 in. wall

### C. TESTING

#### 1. Procedure

The test sections were fabricated by brazing copper electrodes onto 12.0 in. lengths of tubing using NIORO alloy (shims and powder) at a furnace temperature of 1810-1825°F in a hydrogen atmosphere. The electrodes were 1.00 in. O.D. x 1.25 in. long copper rods drilled to receive the 0.190 in. dia tube, and brazed on the tube 7.00 in. apart. Some joint voids were present and additional powder was used to seal the copper-to-Hastelloy X joint on the second cycle at 1775°F to 1800°F. A third cycle at 1750°F to 1775°F was also conducted to duplicate the required three-cycle operation for the Phoebus nozzle. Cooling, following the initial braze cycle from the braze temperature,

## Appendix D

was equivalent to an air cool. The cooling rate was 100°F per hour for the second and third cycles. A fourth tube without copper electrodes was also processed with the three thermal cycling specimens. Tensile test results of this specimen are compared with those of 0.012 in. strip stock as follows:

	<u>Tube</u>	<u>0.012 in. Strip Average</u>
UTS (ksi)	118.3	108.0
YS (ksi)	55.2	50.0
Elong. (%)	22.0	25.0

The results compare favorably with strip stock tested during the design properties program. The slightly higher tube strength reflects the lower annealing temperature commonly used in processing strip and tubing compared to the full 2150°F anneal originally employed on the 0.012 in. strip. Figures 1 and 2 exhibit the microstructure of the tubing in the as-received and braze cycled conditions. The structures are essentially the same with the exception of an increase in visible primary phase in the brazed sample resulting from the thermal treatment.

The test sections were instrumented with four thermocouples and voltage taps restricted to the last three inches of the heated length, leaving the first four inches clear of any foreign material. Analysis of the wall temperature profile for this test section predicts that when the thermocouples located at axial distances of 5 in. and 6 in. read 1200°F, an outer wall temperature of 1600°F should occur approximately 2.0 in. from the inlet electrode. This 1600°F maximum outer wall temperature will be maintained for each cycle. The nominal heat flux will be 18 Btu/in.<sup>2</sup>-sec with a drop of approximately 400°F through the wall.

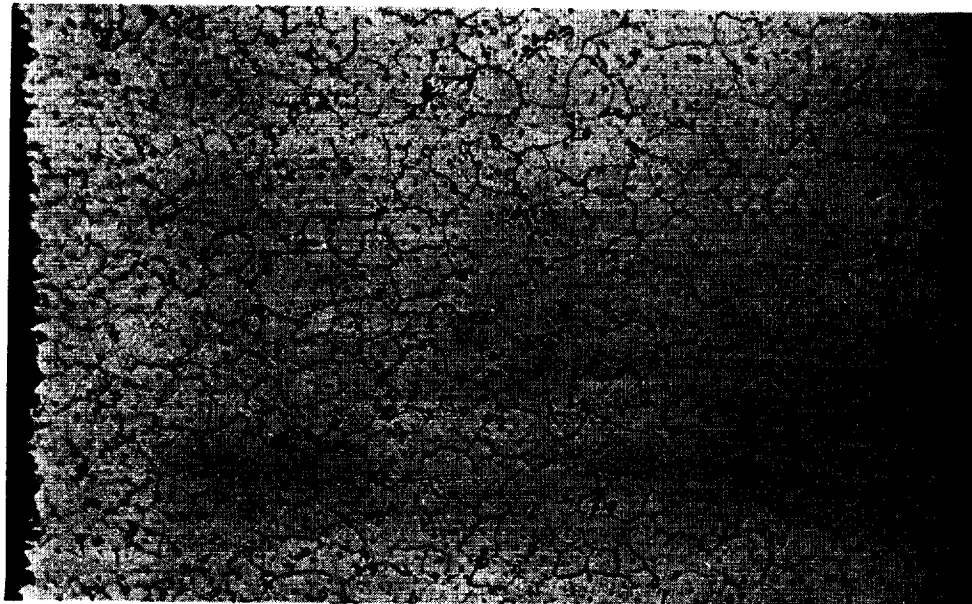
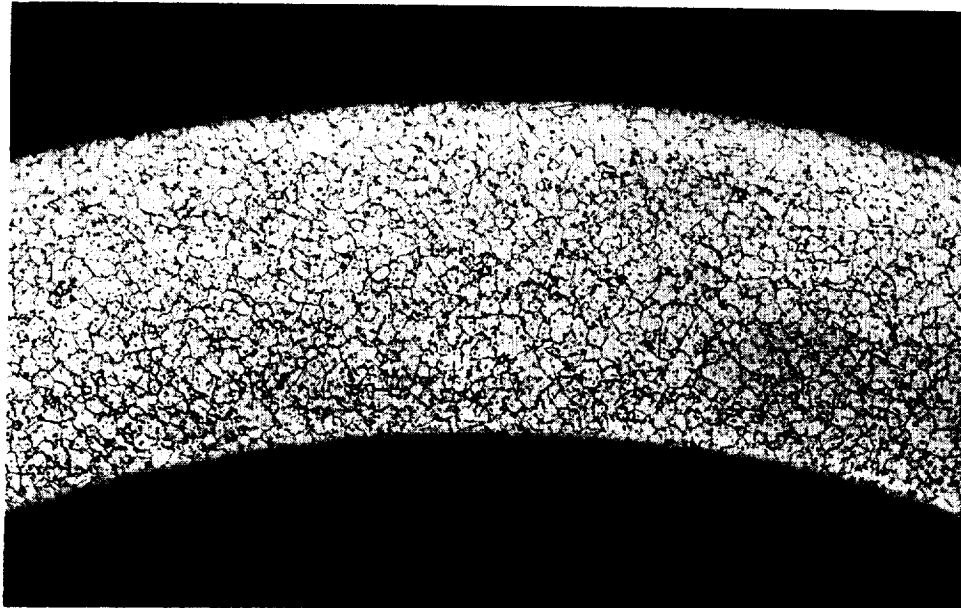
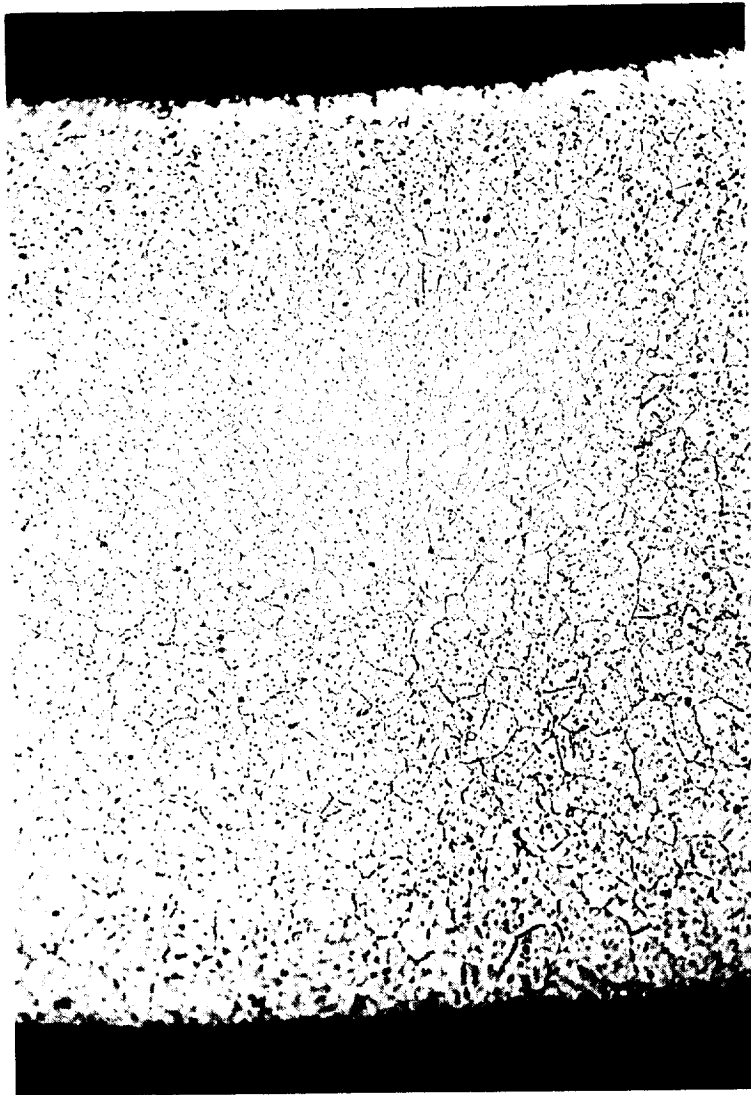


FIGURE 1. Photomicrographs of Hastelloy X tubing cross-section at 100X (top), 250X (bottom) showing the microstructure typical of the as-received condition. ASTM grain size 8.  
Etchant: Inco

FIGURE 2. Photomicrograph of Hastelloy X tube cross-section at 250X depicting typical microstructure caused by stimulated braze cycle. ASTM grain size 8 to 9. Etchant: Oxalic



Appendix D

2. Observation

The Hastelloy X tube was examined visually and dye penetrant inspected after every fourth cycle. The daily inspection reports for Samples 1 and 2 are as listed below:

<u>Sample 1</u>		
0 cycles	<u>Visual</u>	No marks or defects noted.
	<u>Penetrant</u>	No indications noted.
4 cycles	<u>Visual</u>	No marks or defects noted. Tubing distorted in bending approximately 1 in. above base electrode.
	<u>Penetrant</u>	Dye indication noted approximately 3/4 in. above base electrode. Dye indication removed by recleaning tube.
8 cycles	<u>Visual</u>	Two rough spots approximately 1/8 in. diameter noted 3/4 in. and 1 in. above base electrode.
	<u>Penetrant</u>	Same as visual.
12 cycles	<u>Visual</u>	Three rough spots approximately 1/8 in. diameter noted 3/4 in. to 1 in. above base electrodes. Faint linear (axial) indications noted to left of spots.
	<u>Penetrant</u>	Same as visual.
16 cycles	<u>Visual</u>	Same as 12 cycles only the rough spots enlarged.
	<u>Penetrant</u>	Same as above only linear indications more positive.
20 cycles	<u>Visual</u>	Defects cover wide area 3/4 in. to 1 in. above base electrode. All defects are on one side of tube. Three small razor edge protrusions noted above top pitting site.
	<u>Penetrant</u>	Dye penetrant indications are dispersed over defect area noted in visual examination and are less predominant. Slight indication noted 180° from major defect area.



## Appendix D

<u>Sample 2</u>		
0 cycles	<u>Visual</u>	Spotting of tube surface with dust-like particles of braze alloy. Indications are random and are less than 1/64 in. in any direction.
	<u>Penetrant</u>	No indications.
0-12 cycles	<u>Visual</u>	No indications. Spotting due to braze alloy still evident. Slight bending at mid-section of tube.
	<u>Penetrant</u>	No indications.
16-20 cycles	<u>Visual</u>	No indications. Spotting due to braze alloy still evident. Bending has changed configuration to that similar to Sample 1, approximately 1 in. from base electrode.
	<u>Penetrant</u>	No indications.

### D. DISCUSSION

#### 1. Visual Evaluation

The test runs of Samples No. 1 and 2 were identical in procedure. Figure 3 shows a test specimen in the thermal cycling fixture.

Hastelloy X tube Sample No. 1 experienced bending in the lower portion of the test area. The deformation occurring approximately 1 in. above the base electrode, was due to the restricted thermal expansion of the tube. Figure 4 shows the bend position and angle of deflection as measured on a 10 square to the inch grid. The shape of Sample No. 1 is identical to that of Sample No. 2 after the final test cycle. The change in bend configuration of the No. 2 tube during test is explained as a matter of probability. Some deflection and straightening occurs with each thermal cycle because of the restraint imposed by the test system. The ability of a tube to return to a given configuration after each cycle is due only to the weakened condition of the tube in that plane as a result of prior straining and the temperature.

## Appendix D

Figure 5 (top) is a close up of the defects noted on Sample No. 1. The left side of the photo is that portion of the tube nearest the base electrode. Note the shallow pit defects (center) and the more pronounced textured pit (left). The pit on the left was the most recent, occurring on the twelfth cycle. The general smoothing of the pit surfaces accounted for the less pronounced dye penetrant indications recorded on the final inspection than on earlier inspections of the sample (bottom). It is difficult to determine from inspection of the tubes during testing if the defects were mechanical due to bending or if they were an advanced state of corrosion accelerated by the strain and thermal energy induced at the bend. It is to be noted however that they were localized at the maximum bend strain surface and 180° away.

No surface defects were noted on Sample No. 2 but bending was recorded to have occurred in two locations at different times as compared to one bend which experienced repeated cycling in Sample No. 1. Although test procedures were the same, it is apparent that the stress fields were not.

### 2. Microexamination

The Hastelloy X tube, Sample No. 1 was sectioned for metallurgical analysis in various sectors on the defect area. The tube at the defect area had increased slightly in diameter from 0.190 in. to 0.197 in. and had experienced a reduction in wall thickness from 0.020 in. to 0.018 in. The dimensional change was not uniform overall due to the presence of surface pitting, approximately 0.002 in. deep. The diametral expansion was possibly due to the combined result of the compressive and bending forces exerted on the tube in thermal expansion.

Figure 6 shows the microstructure of the Hastelloy X Sample No. 1 as sectioned through a surface pit and of the area 180° away at the same level. It is noted that the internal diameter of the tube is significantly

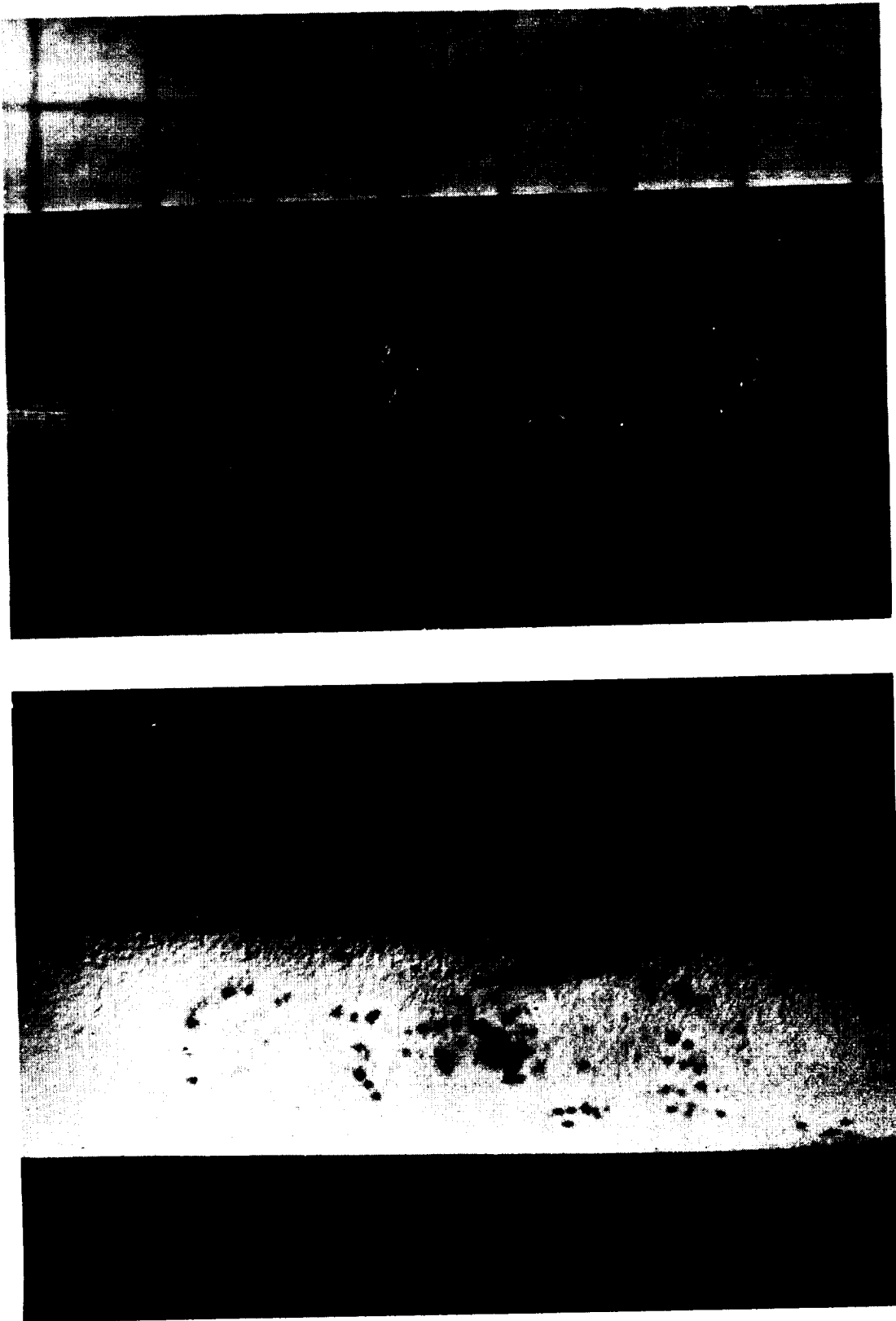


FIGURE 5. Photographs at approximately ten magnifications showing size and appearance of surface defects incurred on Hastelloy X tubing during thermal cycling. Top photograph shows visual appearance of surface pits; bottom, shows defects as detected by dye penetrant inspection.

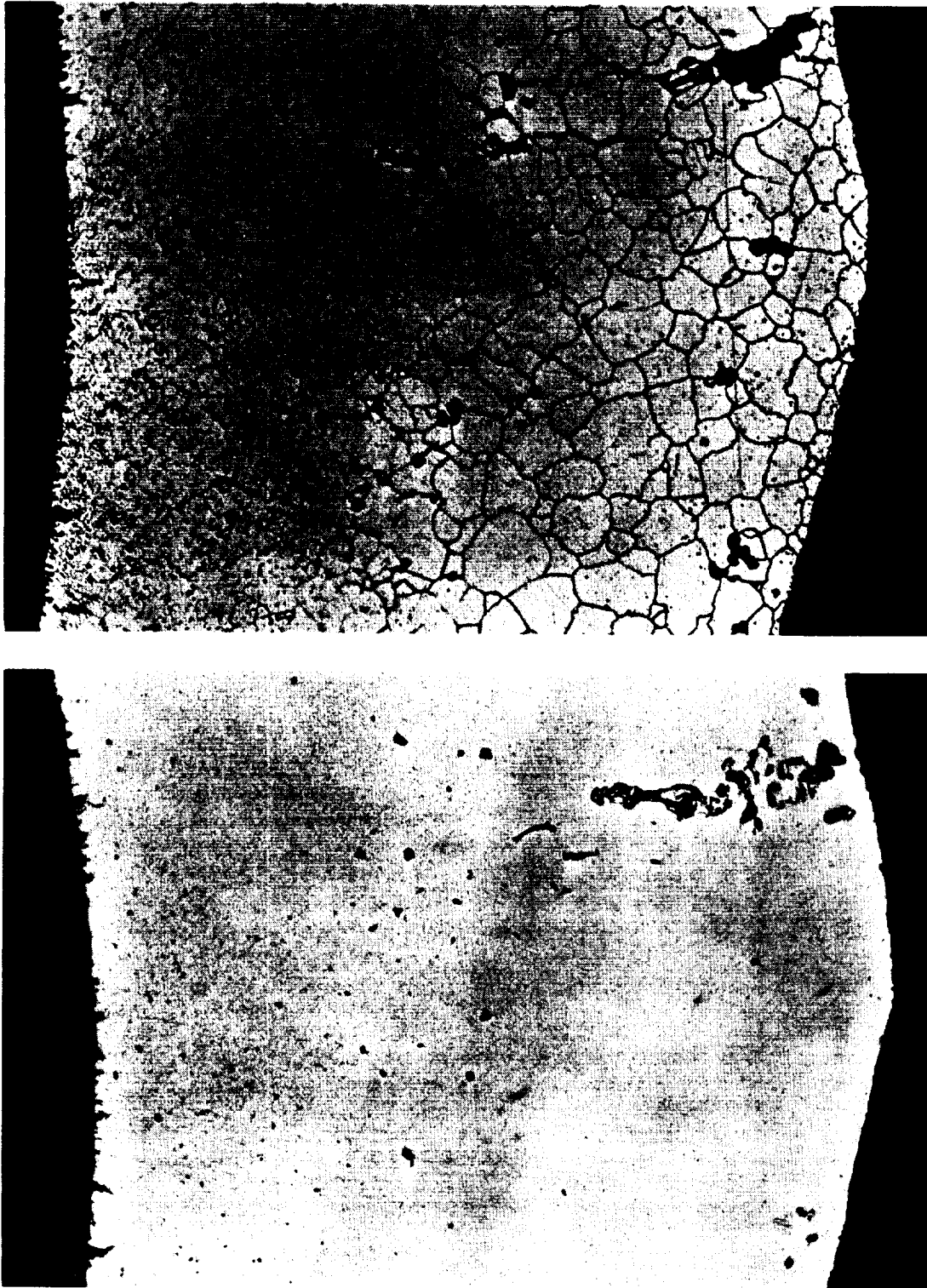


FIGURE 7. Photomicrographs of an edge of a surface defect on Hastelloy X tubing, Sample No. 1, in the etched and unetched condition. Note the unidentified second phase present at sites of porosity. Also note the extent of grain growth between the ID and OD portions of the tube cross-section.  
Etchant: Oxalic

Magnification: 250X



FIGURE 8. Photomicrograph at 250 magnifications, of Hastelloy X tube, Sample No. 1, O.D. unetched exhibiting cavity formed at areas of unidentified second phase.

III. CONCLUSIONS

The Hastelloy X tubing successfully underwent thermal cycling under the prescribed conditions. Surface pitting was noted on one of two samples tested. The pitting was attributed to the combined effects of grain growth and melting or vaporization of an unidentified constituent. The source of the unidentified constituent could not be determined in this analysis, but is most likely due to manufacturing procedures. Minor I.D. cracking was noted but was not considered detrimental.

IV. RECOMMENDATIONS

The unidentified constituent noted in the Hastelloy X tubing is a potential problem area for high temperature applications of the material and consequently should be identified. Once identified it can be traced to its origin and eliminated.



APPENDIX E

THERMAL FATIGUE ANALYSIS OF A CRYOGENICALLY COOLED ROCKET NOZZLE

A. E. Carden,\* D. G. Harman, and E. A. Franco-Ferreira  
Metals and Ceramics Division  
Oak Ridge National Laboratory  
Oak Ridge, Tennessee

Research sponsored by the U.S. Atomic Energy Commission under Contract with the Union Carbide Corporation. Work performed at the Oak Ridge National Laboratory under Interagency Agreement SNC-17 to AEC-NASA Space Nuclear Propulsion Office, Cleveland Extension.

---

\*Summer participant from the University of Alabama.





I. INTRODUCTION

Most interplanetary mission profiles require a source of primary thrust which can be throttled and cycled on and off a large number of times during a given journey. One attractive propulsion scheme for a mission of this type is the nuclear rocket presently under development in the Rover Program.

In essence, a nuclear rocket is a cryogenically cooled exhaust nozzle coupled to a reactor which acts as a heat source for the propellant. The configuration of the exhaust nozzle is typical of most regeneratively cooled nozzles. That is, the interior surface of the nozzle, which is in contact with the hot propellant gas, is made up of a multiplicity of suitably shaped, thin-walled tubes which are bonded to each other. The cryogenic coolant passes through the insides of these tubes, thereby preventing them from melting. In many cases it is necessary, in order to provide greater strength to resist high chamber pressures, to bond a relatively heavy reinforcement jacket to those portions of the tubes which make up the outer surface of the nozzle. A schematic diagram of a typical cross section of such a configuration is shown in Figure 1.

It is apparent that, in a nozzle of the type described above, there will be a very large  $\Delta T$  between the tube crowns on the hot gas side and those portions of the tubes bonded to each other and to the jacket. The  $\Delta T$ 's experienced in normal modes of operation are capable of producing calculated thermal strains of as much as 2%. Due to the restraint provided by the jacket, it is likely that a significant portion of the longitudinal thermal strain will be converted into mechanical deformation of the tube crowns. Thus, under conditions of cyclic nozzle operation, it may be possible to induce low-cycle thermal fatigue failures in the tubes.

It is not economically feasible to use full-scale nozzle hardware to analyze experimentally the behavior described above. Consequently, there is an incentive to devise a scale-model type of test which is capable of evaluating

Appendix E

I. INTRODUCTION

Most interplanetary mission profiles require a source of primary thrust which can be throttled and cycled on and off a large number of times during a given journey. One attractive propulsion scheme for a mission of this type is the nuclear rocket presently under development in the Rover Program.

In essence, a nuclear rocket is a cryogenically cooled exhaust nozzle coupled to a reactor which acts as a heat source for the propellant. The configuration of the exhaust nozzle is typical of most regeneratively cooled nozzles. That is, the interior surface of the nozzle, which is in contact with the hot propellant gas, is made up of a multiplicity of suitably shaped, thin-walled tubes which are bonded to each other. The cryogenic coolant passes through the insides of these tubes, thereby preventing them from melting. In many cases it is necessary, in order to provide greater strength to resist high chamber pressures, to bond a relatively heavy reinforcement jacket to those portions of the tubes which make up the outer surface of the nozzle. A schematic diagram of a typical cross section of such a configuration is shown in Figure 1.

It is apparent that, in a nozzle of the type described above, there will be a very large  $\Delta T$  between the tube crowns on the hot gas side and those portions of the tubes bonded to each other and to the jacket. The  $\Delta T$ 's experienced in normal modes of operation are capable of producing calculated thermal strains of as much as 2%. Due to the restraint provided by the jacket, it is likely that a significant portion of the longitudinal thermal strain will be converted into mechanical deformation of the tube crowns. Thus, under conditions of cyclic nozzle operation, it may be possible to induce low-cycle thermal fatigue failures in the tubes.

It is not economically feasible to use full-scale nozzle hardware to analyze experimentally the behavior described above. Consequently, there is an incentive to devise a scale-model type of test which is capable of evaluating

ORNL-DWG 66-11586

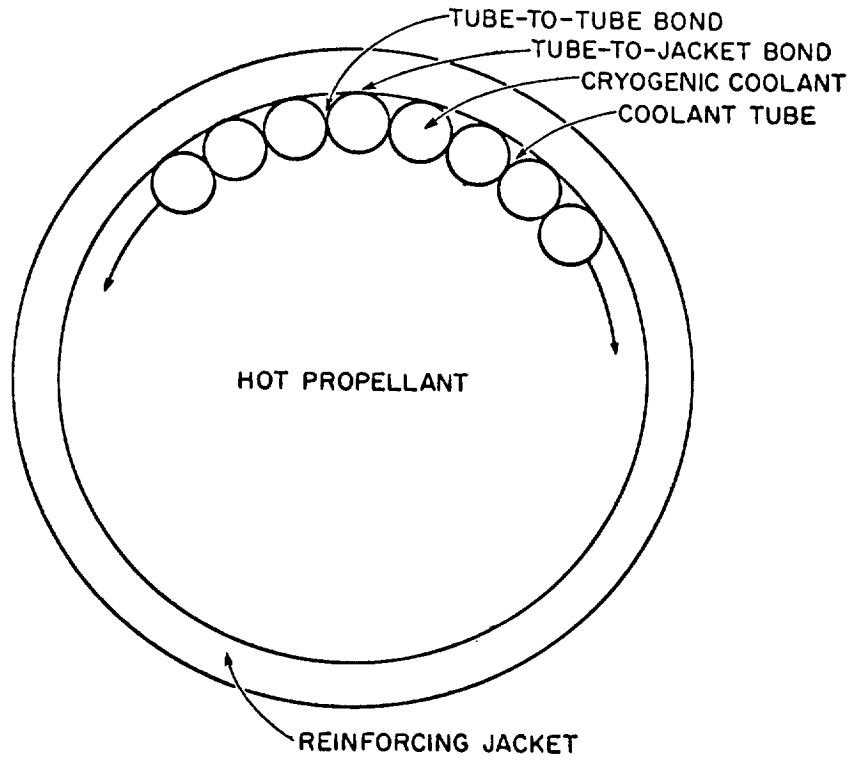


Fig. 1. Typical Cross Section of a Cryogenically-Cooled Rocket Nozzle.

## Appendix E

the effects of all the important parameters which are operative in an actual nozzle. In the case of thermal cycling stresses, as discussed here, the important considerations include (a) the temperature distribution, (b) the physical and mechanical properties of the nozzle material, (c) the operating environment, (d) the geometry of the nozzle elements, and (3) the loading conditions.

This paper describes the thermal cycle testing of specimens which were designed to simulate and evaluate the conditions existing in a nozzle of the general configuration shown in Figure 1. The test results are related to important fabrication and operating parameters. An effort is also made to relate the results to a range of nozzle operating conditions.

### II. SPECIMEN PREPARATION

Each test specimen consisted of a planar array of six thin-walled Hastelloy X tubes brazed to each other and to a thick Hastelloy X base plate. The tubes were 1/2-in. dia with a 0.012-in. wall and the base plate was 4 in. wide, 10 in. long, and 7/8 in. thick. A schematic diagram of the specimen is shown in Figure 2. Both ends of each tube were plugged. Entry and exit ports for the coolant were drilled through the base plate and into the tubes near opposite ends of each specimen.

Each specimen was instrumented with numerous thermocouples to provide temperature distribution data. These thermocouples were Chromel-P-Alumel with a wire diameter of 0.010 in. They were resistance welded to the tube crowns and to the base plate at various locations. For each thermocouple, the individual wires were welded to the specimen a short distance apart so that a portion of the specimen itself would be included in the junction. The thermocouple locations and attachment procedure were carefully controlled and reproduced for each test.

ORNL-DWG 66-11587

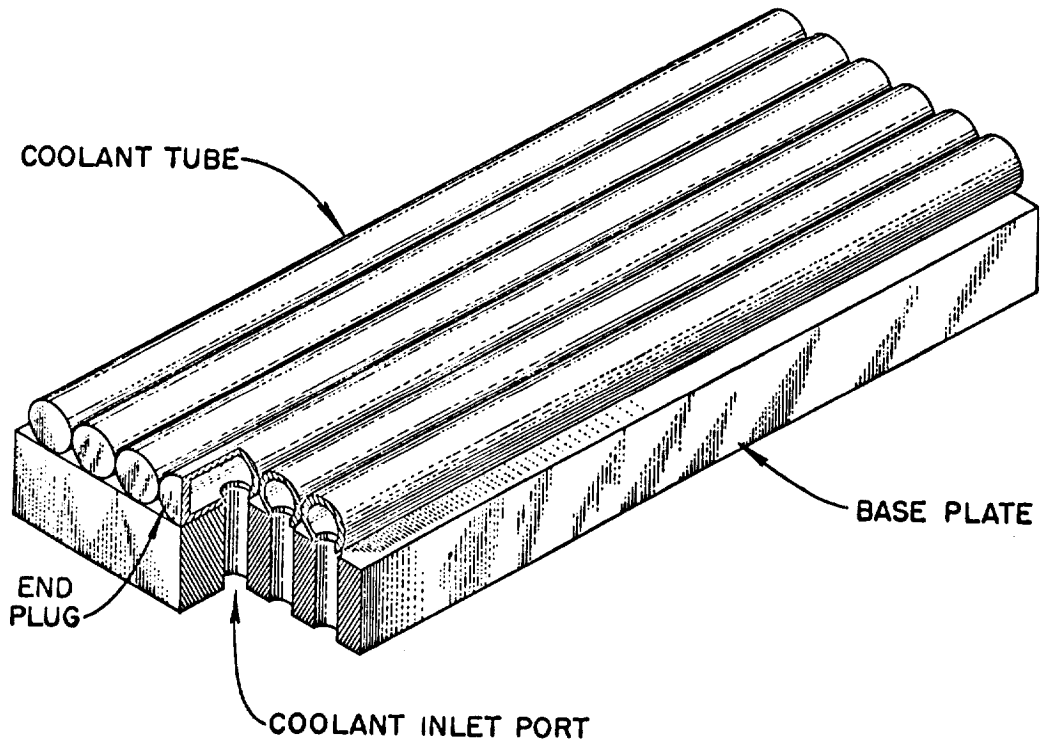


Fig. 2. Thermal Cycle Test Specimen. Baseplate is about 4-in. wide, 10-in. long, and 7/8-in. thick. Coolant tubes are 1/2-in. diam with a 0.012-in. wall.

## Appendix E

The heat source used in these experiments was a quartz lamp radiant furnace. It was positioned parallel to, and approximately 1/2 in. above, the tube crowns. The furnace had a lamp area of 8 in. by 2-1/2 in. and an electrical power input to the lamps of 13.2 kw. This produced a measured heat flux at the specimen surface of approximately 700 w/in.<sup>2</sup>. An overall view of the test setup, with the furnace tilted up to expose the lamps, is shown in Figure 3.

The specimen base plate was kept at or near the coolant temperature by bolting it to a massive copper heat sink. As evident in Figure 3, this heat sink was contained in a pan which enabled it to remain completely submerged in coolant during the test.

Coolant flow was introduced into the insides of the tubes through a copper manifold, shown at the left end of the specimen in Figure 3. This manifold was positioned beneath the surface of the coolant in the pan to maintain a constant temperature for the flow of tube coolant.

### III. TESTING PROCEDURE

In all tests, LN<sub>2</sub> was used as the coolant. The pan shown in Figure 3 was maintained full of LN<sub>2</sub> for the duration of each test. A separate source of LN<sub>2</sub> was connected to the tube coolant inlet manifold. The LN<sub>2</sub> flow which cooled the tubes was allowed to exhaust directly into the pan at atmospheric pressure. Provisions were made to maintain an argon atmosphere over the tube surfaces to protect them from excessive oxidation.

A test run for a given specimen was characterized by thermally cycling the tube crowns from LN<sub>2</sub> temperature to an elevated temperature and back to LN<sub>2</sub> temperature. A number of identical cycles were reproduced until tube failure occurred.



## Appendix E

A complete thermal cycle proceeded as follows: (1) The heat sink and base plate were held at or near  $LN_2$  temperature; (2) the tubes were cooled to  $LN_2$  temperature by their internal coolant flow; (3) the quartz lamp furnace was turned on and the tube crowns brought to the specified peak temperature and held for a predetermined length of time (hold times of 15 sec and 5 min were studied); coolant flow through the tubes was maintained during this step; (4) the furnace was turned off and the entire specimen was cooled to  $LN_2$  temperature.

A typical test thermal cycle, as traced by a strip-chart recorder connected to the specimen thermocouples, is shown in Figure 4. This particular cycle was for the 5-min hold time.

During test equipment checkout runs using mockup specimens, it was noticed that small dents in the tubes of the mockup specimens acted as geometric instabilities and led to premature failure. Since the existence of small tube dents as fabrication defects cannot be ignored, it was decided to include a study of their effects in this program. Controlled dents were therefore made in some of the specimen tube crowns. This was done using a 1/4-in.-dia cylindrical indenter with its longitudinal axis parallel to the plane of the specimen base plate, but at a  $90^\circ$  angle to the longitudinal axes of the tubes. Dents were made to depths of 0.005, 0.010, and 0.020 in.

A closeup view of the tube crown surfaces of one of the specimens prior to testing is shown in Figure 5. Both smooth and pre-dented (with two controlled dents 0.020 in. deep) tubes, as well as the attachment points of six monitor thermocouples, are shown. The various parameters studied in the entire series of tests are listed in Table I.

### IV. TEST RESULTS

The results of all the tests are detailed in Table I. For undented tubes, local creep buckling in the form of ripples occurred in the tube crowns

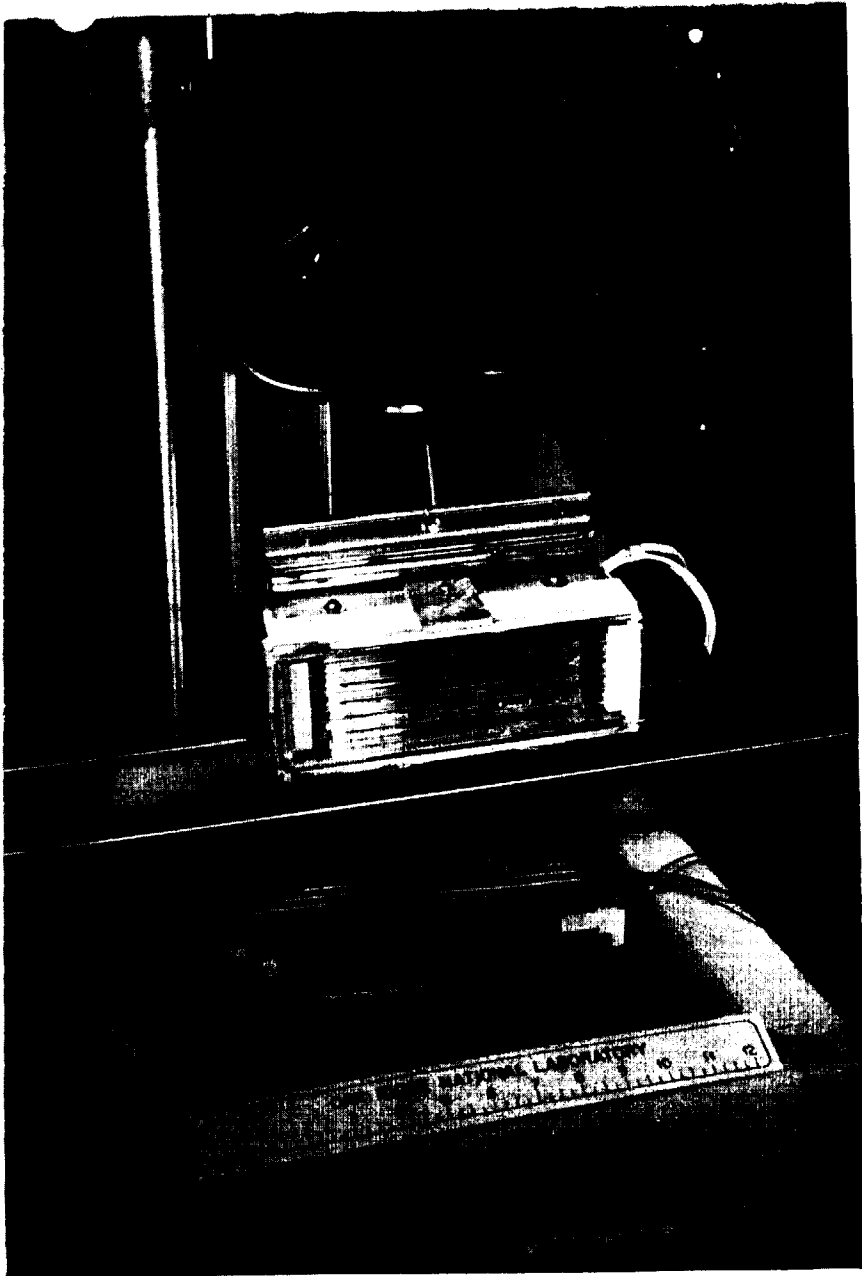


Fig. 3. Overall View of Thermal Test Setup.

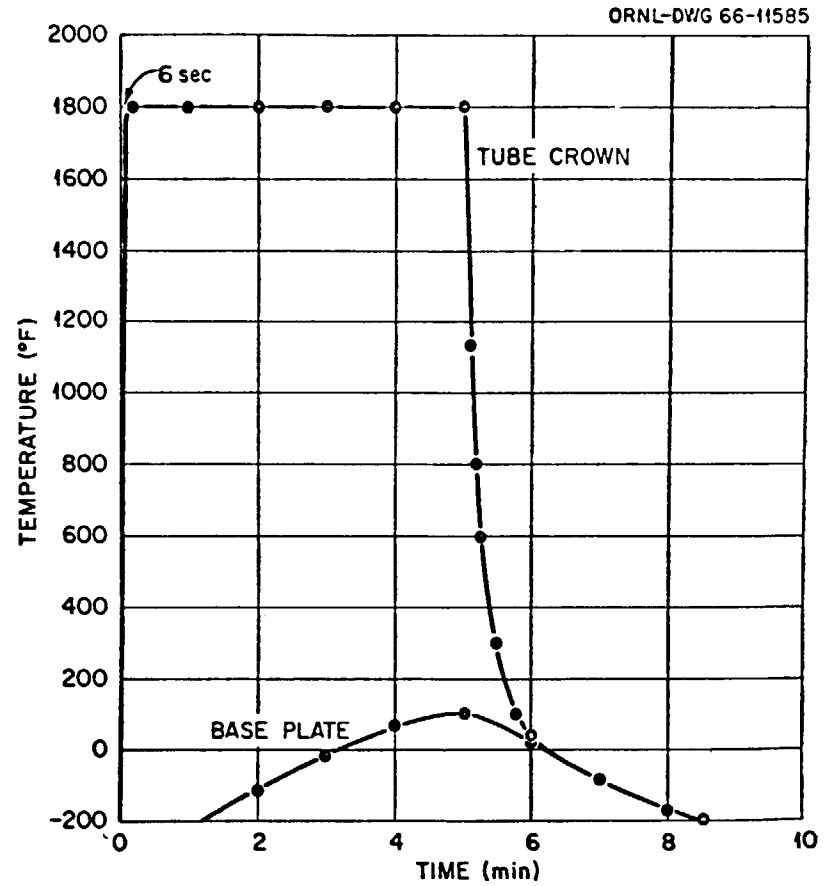


Fig. 4. Typical Test Cycle Showing Tube Crown and Baseplate Temperatures.

## Appendix E

TABLE I  
THERMAL CYCLE DATA<sup>a</sup>

Specimen Number	Temperature, °F		Hold Time at Temperature Maximum	Tube Condition	Number of Thermal Cycles to Failure		
	Maximum	Minimum			First Visible Wrinkling	First Visible Crack	Crack Through Wall
x-1	1800	-200	5 min	Smooth	14	41	50
x-2	1800	-200	15 sec	Smooth	30	70	80
x-3	1900	-200	5 min	Smooth	11	32	42
				20-mil dent <sup>b</sup>		18	22
				20-mil dent <sup>b</sup>		21	26
x-4	1800	-200	5 min	Smooth	14	49	57
				Small sharp dent <sup>c</sup>		25	33
				Medium deep dent <sup>c</sup>		39	49
				Large shallow dent <sup>c</sup>		56	d
				20-mil dent <sup>b</sup>		19	28
				20-mil dent <sup>b</sup>		22	30
				20-mil dent <sup>b</sup>		25	33
				10-mil dent <sup>b</sup>		25	35
				5-mil dent <sup>b</sup>		d	d
				x-5		1600	-200
20-mil dent <sup>b</sup>	23	35					
20-mil dent <sup>b</sup>	25	38					

<sup>a</sup>Tube crown heating time from -200°F to temperature maximum was approximately 5 sec/cycle.

<sup>b</sup>Depth of controlled dent made in top of tube crown with a 1/4-in.-dia indenter.

<sup>c</sup>Description of dents in as-received specimen.

<sup>d</sup>No failure.

## Appendix E

in approximately 15 to 30 cycles, depending on hold time. The ripples stabilized in location but increased in amplitude as the cycling progressed. Failure was always associated with a ripple and normally occurred in a valley rather than on a peak. Failure was defined as a crack through the tube wall capable of passing LN<sub>2</sub>.

In the case of dented tubes, the dent locations can be considered to be "prerippled" sites. During cycling, the dents deepened while the adjacent smooth tubing developed ripples. The deepening dents invariably were responsible for premature failure. The presence of these deleterious dents appears to reduce tube life, as compared with that for a smooth tube, by a factor of 1/3 to 1/2. However, there does seem to be a threshold value of dent severity below which damage does not occur. For example, the 0.005-in.-deep controlled dent and the so-called "large shallow" as-received dent had no effect on tube life.

The appearance of the specimen pictured in Figure 5 at the 22-cycle point in its test is shown in Figure 6. Failure has occurred at both of the 0.020-in.-deep controlled dents and the ripples are well established in the originally smooth tube surfaces. Figure 7 shows the specimen at the test termination point of 42 cycles. Both the cracked dents and the ripples have continued to deepen. The tube shown at the bottom of Figure 7, which was originally smooth, has also failed at a ripple location which suddenly became unstable and grew considerably deeper than its neighbors. This general behavior was typical of all the specimens tested.

### V. ANALYSIS OF RESULTS

An effort was made to relate the data obtained in these tests to existing fatigue data. A survey of literature revealed only a small amount of such data<sup>(1)</sup> for Hastelloy X, and it was for isothermal strain fatigue. It was

---

(1) M. B. Reynolds, Strain-Cycle Phenomena in Thin-Wall Tubing, GEAP-4462 (Jan. 30, 1964).

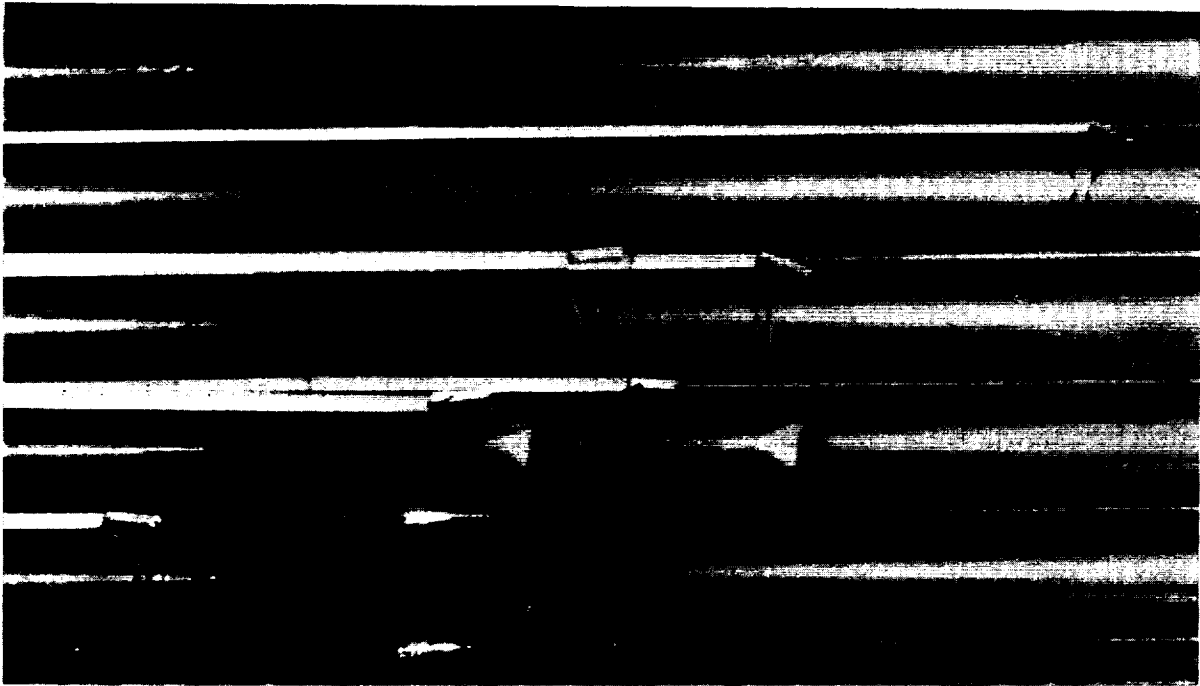


Fig. 5. Pretest Specimen. Note thermocouple locations and two 0.020-in.-deep controlled dents made with 1/4-in.-diam indenter.

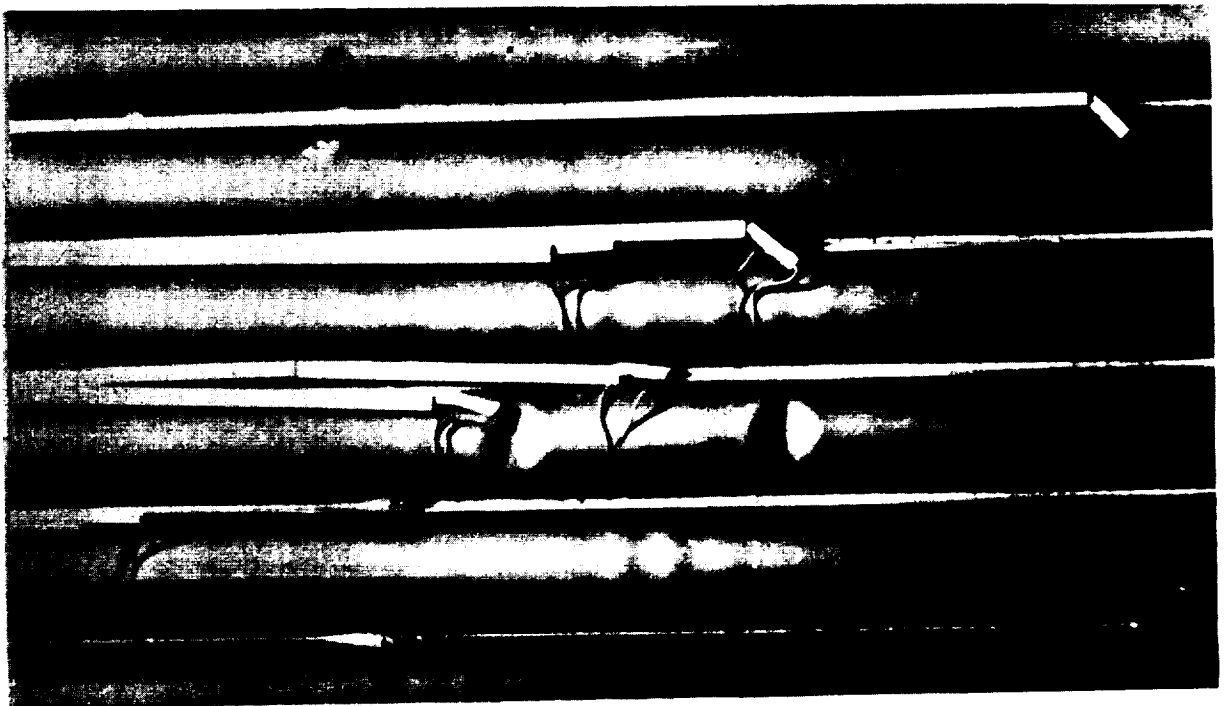


Fig. 6. Appearance of Specimen after 22 Cycles. Note failures at both dent locations and wrinkling in the remainder of the tubing.

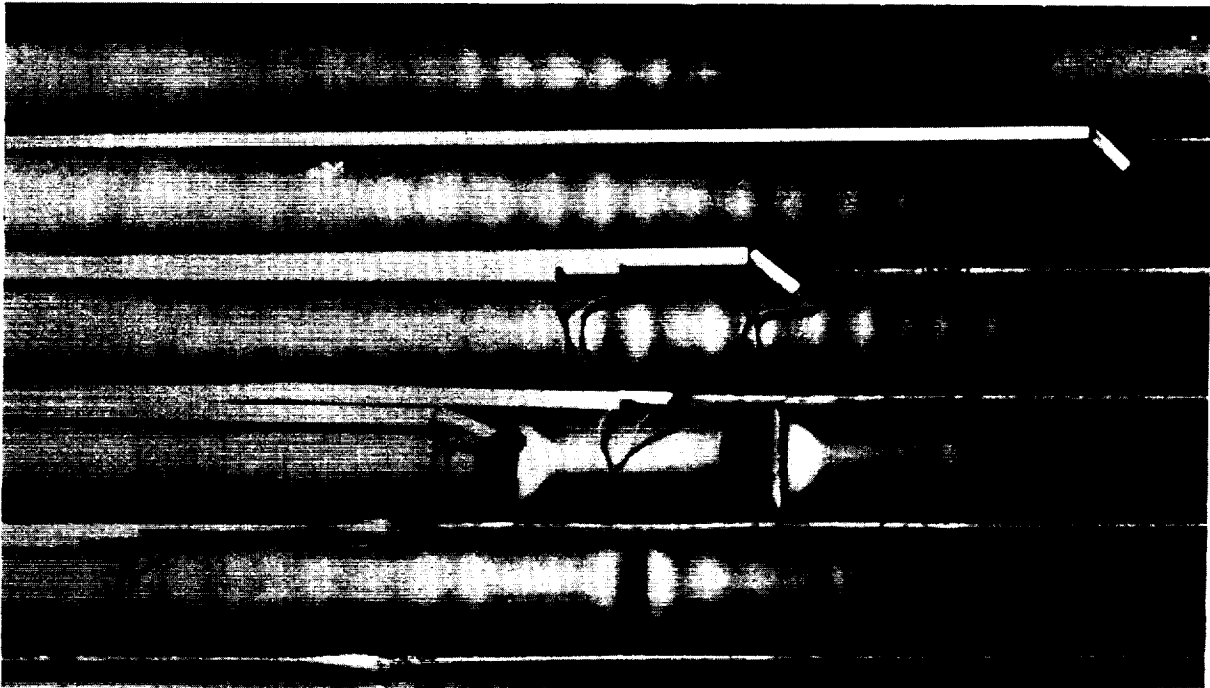


Fig. 7. Appearance of Specimen after 42 Cycles. Note failure of an originally smooth tube at a wrinkle location.

not possible to obtain a good correlation between this and our thermal fatigue data. However, appropriate information,<sup>(2)</sup> obtained by thermal cycle testing of tubular specimens, was available for a similar alloy, Hastelloy N. This was used for correlations with our test results.

The Hastelloy N thermal fatigue data is plotted as  $\Delta T$  (thermal cycle test temperature range) versus  $N_f$  (number of cycles to failure) in Figure 8. The curve is for a constraint factor ( $F$ ) of unity. This constraint factor is defined as the ratio of actual mechanical deformation in the specimen to the total available thermal strain ( $\alpha\Delta T$ ) calculated from the thermal cycle. Figure 9 shows a family of thermal fatigue curves for Hastelloy N, plotted for three different constraint factors. The curve for  $F = 1$  is a repetition of the curve shown in Figure 8, while the curves for  $F = 1.2$  and  $F = 1.5$  are derived by calculation from the  $F = 1$  curve.

An analysis of the geometry of the specimens used in these tests indicated that the tube crowns were under very effective constraint. In fact, it appeared reasonable to consider the constraint factor for a smooth-tubed specimen to be on the order of unity. Variables such as longer hold times and dented tubes were expected to increase the constraint factor.

The data generated by these tests have been superimposed on the family of curves of Figure 9. This is shown in Figure 10. The data for the 15-sec hold time and the  $F = 1$  curve correlate quite well. The data for the longer hold time of 5 min indicate that the effective constraint factor has been increased to the order of  $F = 1.2$ . It is felt that this is due primarily to stress relaxation of the tube crowns which can occur under the conditions of time and temperature studied. The results for the dented tubes show constraint factors in the vicinity of  $F = 1.5$  due to the strain concentrating effects of the dents.

---

(2) A. E. Carden, "Thermal Fatigue of a Nickel-Base Alloy," J. Basic Eng. Trans. ASME, Ser. D 87, 237-244 (1965).



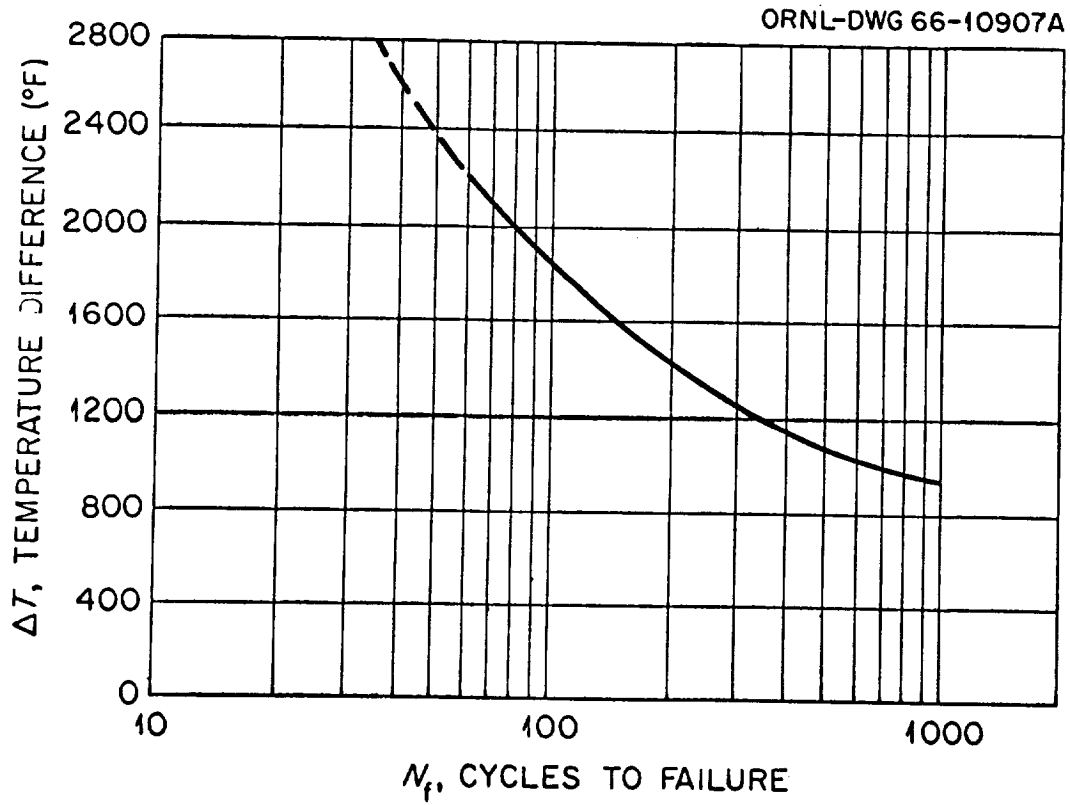


Fig. 8. Thermal Cycle Fatigue of Hastelloy N for a Constraint Factor of Unity. Data from Trans ASME [D], 237-244 (1965).

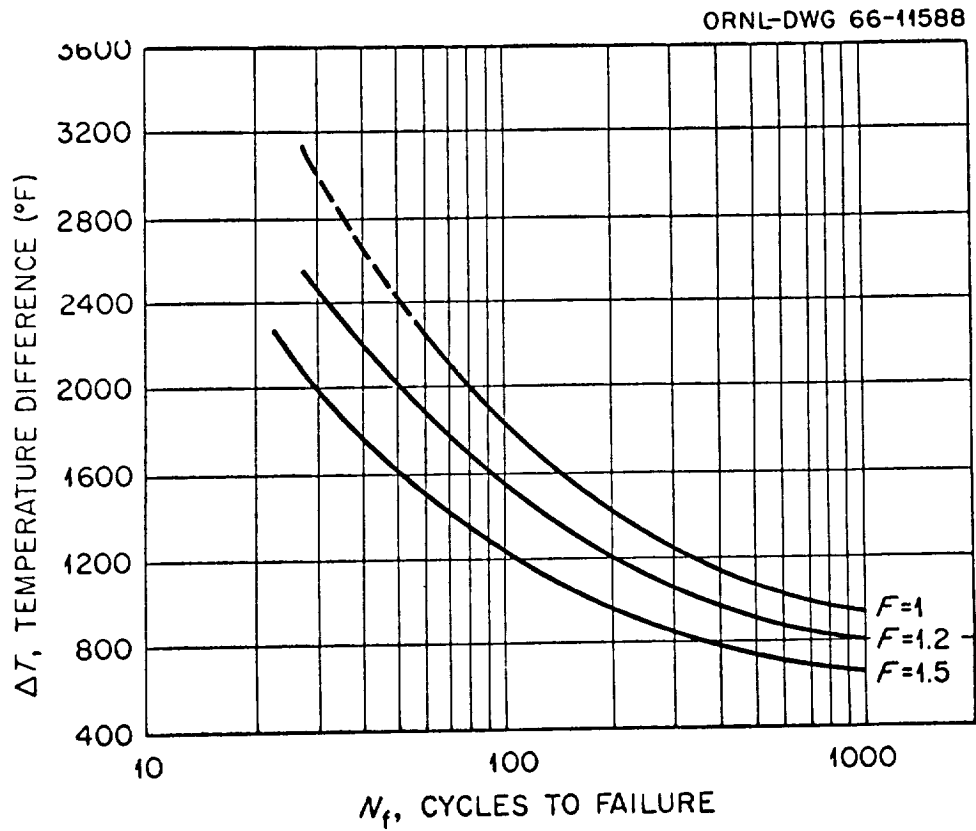


Fig. 9. Thermal Cycle Fatigue of Hastelloy N for Constraint Factors of 1, 1.2, and 1.5. The higher constraint curves are calculated from the  $F = 1$  curve.

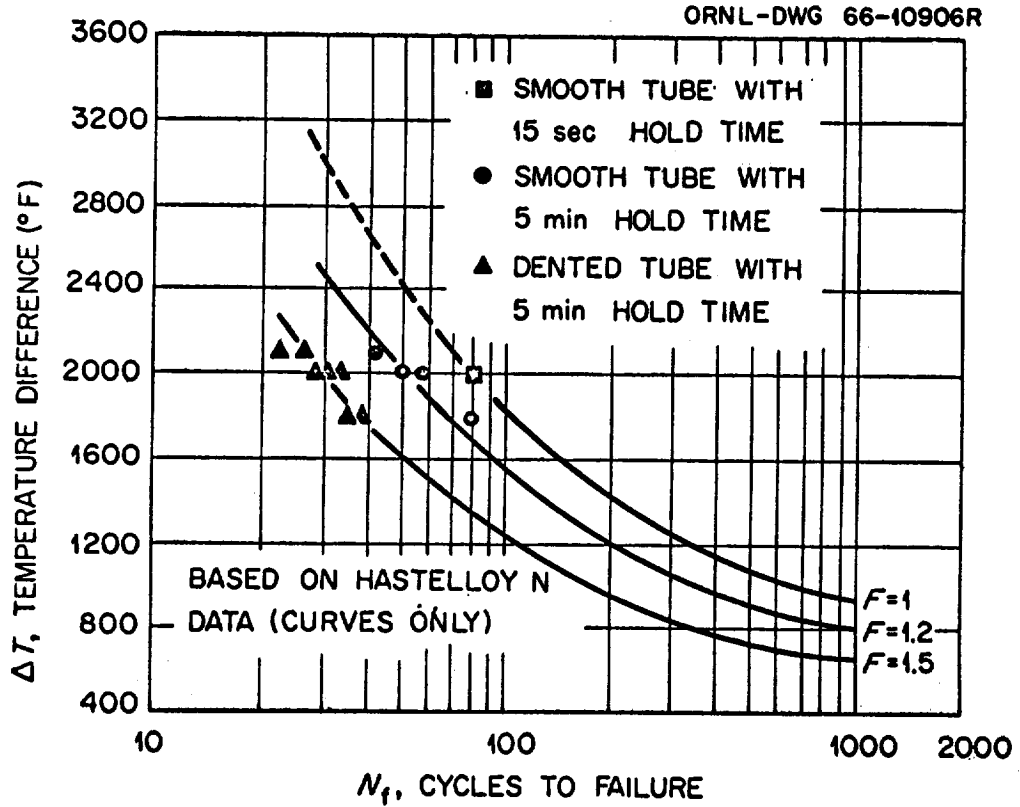


Fig. 10. Thermal Cycle Data for Hastelloy X Thin-Wall Tube Bundles Cycled Between  $-200^{\circ}\text{F}$  and  $1600$ ,  $1800$ , and  $1900^{\circ}\text{F}$ . Hastelloy N constraint curves are shown for comparison. Failure is defined as a crack through tube wall capable of passing liquid nitrogen.

## Appendix E

It appears from this correlation that the techniques used for the determination of the Hastelloy N data are appropriate to the thermal fatigue problems in regeneratively cooled rocket nozzles. Therefore, work is presently under way to obtain similar data for Hastelloy X. This data will be associated with the points plotted in Fig. 10. It should then be possible to extrapolate accurately the data obtained in the tests reported here to a wide range of nozzle operating conditions. Additional tests will be performed to investigate the effects of internal pressure on the fatigue life of the tubes.

### VI. CONCLUSIONS

1. Thermal fatigue can be a serious problem for the coolant tubes of regeneratively cooled rocket nozzles.
2. A laboratory test has been devised which provides thermal conditions similar to those seen in service. This test has been capable of producing tube failure in substantially less than 100 thermal cycles. Thus, the principles of similitude and modeling appear to be appropriate for the examination or determination of low-cycle fatigue characteristics of large complex structures.
3. Increasing high-temperature hold times, up to 5 min, and dents in the tubes appreciably curtail the fatigue life.

### VII. ACKNOWLEDGEMENTS

The authors are indebted to B. C. Williams, who conducted the tests, to C. K. Thomas for assistance in preparing the test facility, and to J. R. Weir for helpful suggestions during the course of the work.

